

**Adaptations in physiological and neuronal function during
diet-induced obesity**

by

© Lisa Zoey Fang

A Thesis submitted to the School of Graduate Studies in partial fulfillment of the
requirements for the degree of

Doctor of Philosophy

Department of BioMedical Sciences (Neurosciences), Faculty of Medicine

Memorial University of Newfoundland and Labrador

February 2024

St. John's, Newfoundland and Labrador

Abstract

Obesity significantly increases the risk of developing chronic conditions including type II diabetes, cardiovascular disease, and some cancers. The rate of obesity has tripled globally since 1975, which is in part due to the sudden prevalence and overconsumption of palatable high-fat diets (HFDs). Obesity profoundly perturbs the neural control of energy balance, affecting diverse cell types within the hypothalamus. However, an incomplete understanding of how HFD impacts the regulation of energy balance hinders our ability to more effectively treat obesity.

In this thesis, I describe the physiological and neuronal response to HFD feeding in rodents. We identified that HFD exposure elevates the body weight set point, which is initially driven by a transient hyperphagia. This hyperphagia coincides with increased excitatory transmission to lateral hypothalamic orexin (ORX) neurons, which regulate acute food intake. This suggests that ORX neurons may be involved in the initial hyperphagia, implicating them in the development of obesity. As HFD prolongs, body weight gain slows and reaches a new steady state regardless of age at the start, duration of feeding, or palatability of the diet. This sustained weight coincides with increased synaptic contacts to melanin-concentrating hormone (MCH) neurons, which promote weight gain and food intake, likely contributing to the maintenance of obesity.

The molecular mechanism underlying the establishment of a new set point remains elusive. During HFD feeding, the presence of a chronic low-grade

hypothalamic inflammation exacerbates weight gain, therefore we reasoned that inflammatory factors could modulate appetite-promoting neurons to maintain a new set point. We found that the inflammatory mediator prostaglandin E₂ (PGE₂) activate MCH neurons via its EP2 receptor (EP2R). Suppressing PGE₂-EP2R on MCH neurons partially protects against excess weight gain and fat accumulation in the liver during HFD feeding. This mechanism could contribute to the maintenance of an elevated body weight set point in during diet-induced obesity.

Without long-term treatment options in face of the increasing rates of obesity, we are in desperate need of novel interventions. In the future, we hope that targeting EP2R on MCH neurons can lower body weight set point and aid in combatting obesity.

General Summary

The rate of obesity has dramatically increased over the past few decades, leaving a third of the world overweight or obese. This is partially due to the availability of high-fat diets (HFDs), which are often eaten in excess. Our body weight is controlled by the brain – in particular by the hypothalamus. Within the hypothalamus, different cells coordinate how much food we eat and how much energy we expend. However, eating a HFD can change the natural activity of these cells, which may contribute to the development of obesity. Two cell types, orexin (ORX) and melanin-concentrating hormone (MCH) neurons, are known to promote appetite, and may be impacted by HFD. Understanding how these cells change in response to HFD and how they in turn impact weight gain may be important in developing new treatments for obesity in the future.

We fed rodents a HFD, which caused an initial period of rapid weight gain that eventually slowed as body weight reached a new stable level. The initial rapid weight gain was due to a brief period of overeating HFD, which coincided with ORX neurons being more active. This could mean that an increase in ORX neuron activity promotes overeating in the development of obesity. During the period where rodents gain and maintain significant weight, MCH neurons became more active. This may mean that MCH neurons drive weight gain that is important in maintaining obesity.

We next sought how MCH neurons become activated. During obesity, the brain becomes inflamed, therefore we wondered whether inflammation could be

activating MCH neurons. We found that prostaglandin E₂, (PGE₂) an inflammatory molecule, activated MCH neurons, which was responsible for weight gain and fatty liver disease in mice.

In conclusion, we found that changes to ORX and MCH neuron activity are behind the development and maintenance of obesity, respectively. We also identified PGE₂ signalling on MCH neurons to contribute to obesity, therefore, we hope this aids in progressing new obesity treatments in the future.

Acknowledgements

First, I would like to sincerely thank my supervisor **Dr. Michiru Hirasawa**. You have molded me into the scientist and the person that I am today. I will forever be grateful for your guidance, brilliance, and patience. I am also thankful for the many Hirasawa lab members over the past years. In particular, **Victoria Linehan**, who taught me (and continues to teach me) so much, and who I consider one of my best friends to this day. As well, thank you to current lab members **Mohammed Sohel Chowdhury**, **Damilola Adekunle**, **Deogratias Riwa**, and **Shona Campbell** for making it easy to spend so much time in the lab.

I am thankful to the many staff and faculty in the Faculty of Medicine – especially **Dr. Jackie Vanderluit**, **Dr. Craig Moore**, and **Dr. Ann Dorward** for always making time for me. As well, I am grateful to my committee members **Dr. Sherri Christian** and **Dr. Matt Parsons**. Thank you for enduring my 3 hour-long committee meetings, for the lively discussions, and innumerable reference letters over the years.

I would like to additionally express my gratitude to **Dr. Matt Parsons** – thank you for LP, G&Ts, and for teaching me how to see the positives in my (many) failures. As well, thank you to the Parsons lab for tolerating me as your honorary member.

Over the course of my PhD, I have been incredibly lucky to have so many people in my corner. Thank you **Abhinaba Ghosh**, **Ben Rogers**, **Firoozeh Nafar**, **Jess Barron**, **Jocelyn Adundo**, **Katie Fifield**, **Kyle Brymer**, **Rob**

Flemmer, Rochelle Benoit, and Vishaal Rajani – graduate school is easier with good company. An extra special thank you to **Christie Costello** and **Gaylene Russell McEvoy** for the late-night writing sessions, and for saying yes to all my antics – no matter how spontaneous. As well, to **Sam Carew** and **Stephanie Blandford** for the many therapeutic lunch dates and countless pep talks. To my dear friends **Alicia Morry, Anna Swain, Ashton Banfield, Bret Kenny, Denis Adundo,** and **Josué Lilly Vidal,** thank you for being there for me no matter how much time has passed, or how much distance there is. Lastly, to **Dylan Galloway** and **Mochi,** thank you for believing in me and for being strong when I could not be.

I was fortunate to embark on a 4-month stint to perform research abroad at Washington University in St. Louis. I am grateful to **Dr. Meaghan Creed** for hosting and mentoring me, as well as to **Dr. Alexxai Kravitz** for supporting me. Thank you also to the members of the Creed and Kravitz labs, especially **Jess Tooley, Justin Wang, Yu-Hsuan Chang,** and **Yvan Vachez,** for your friendship.

Finally, to my parents, **Xing Su Fang** and **Wei Qun Fang,** thank you for teaching me resilience and perseverance, and to my little sister, **Carmen Fang,** for reminding me to be brave. These are qualities that have served me well in graduate school, and will continue to serve me well in my academic career.

Table of Contents

Abstract.....	ii
General Summary	iv
Acknowledgements	vi
Table of Contents	viii
List of Figures	xiii
List of Tables	xvi
List of Abbreviations	xvii
List of Publications.....	xxiii
Co-Authorship Statement.....	xxiv
Chapter 1 – General introduction and overview	1
1.1. <i>Obesity and the current state of treatment</i>	2
1.1.1. <i>Epidemiology</i>	2
1.1.2. <i>Contributors to present day obesity</i>	2
1.1.3. <i>Treatment</i>	3
1.2. <i>Energy balance</i>	4
1.2.1. <i>Homeostatic vs hedonic control of food intake</i>	4
1.2.2. <i>Energy expenditure</i>	5
1.3. <i>High-fat diet induced obesity: pathogenesis and mechanisms</i>	6
1.3.1. <i>Fat accumulation</i>	6
1.3.2. <i>Inflammation</i>	6
1.3.2.1. <i>Systemic inflammation</i>	7
1.3.2.2. <i>Neuroinflammation</i>	8
1.3.3. <i>Leptin and insulin resistance</i>	9
1.4. <i>Control of energy balance</i>	11

1.4.1.	<i>Hypothalamic control of energy balance</i>	11
1.4.1.1.	<i>Overview</i>	11
1.4.1.2.	<i>Arcuate nucleus (ARC)</i>	14
1.4.1.3.	<i>Paraventricular nucleus of the hypothalamus</i>	15
1.4.1.4.	<i>Lateral hypothalamus</i>	16
1.4.2.	<i>Extrahypothalamic control of feeding</i>	17
1.4.3.	<i>Neuroplastic changes during obesity</i>	18
1.5.	<i>The lateral hypothalamus</i>	19
1.5.1.	<i>Defining the role of the lateral hypothalamus</i>	19
1.5.2.	<i>Refining the role of the lateral hypothalamus</i>	20
1.5.3.	<i>MCH neurons</i>	20
1.5.3.1.	<i>Other roles of MCH</i>	22
1.5.4.	<i>Orexin neurons</i>	23
1.5.4.1.	<i>Other roles of ORX</i>	24
1.6.	<i>Thesis objectives and overview</i>	25
Chapter 2 – High-fat diet-induced elevation of body weight set point in male mice		
.....		28
2.1.	<i>Introduction</i>	29
2.2.	<i>Materials and Methods</i>	30
2.2.1.	<i>Animals</i>	30
2.2.2.	<i>Data analysis</i>	33
2.3.	<i>Results</i>	33
2.4.	<i>Discussion</i>	63
2.5.	<i>Conclusions</i>	67
Chapter 3 – Prostaglandin E ₂ activates melanin-concentrating hormone neurons		
to drive diet-induced obesity		69
3.1.	<i>Introduction</i>	70
3.2.	<i>Materials and Methods</i>	71
3.2.1.	<i>Animals</i>	71
3.2.2.	<i>In-vitro electrophysiology</i>	73

3.2.3.	<i>Drugs</i>	74
3.2.4.	<i>Identification of MCH and ORX neurons</i>	74
3.2.5.	<i>Double immunohistochemistry</i>	78
3.2.6.	<i>Adipose and liver histology and analysis</i>	78
3.2.7.	<i>Data analysis</i>	79
3.3.	<i>Results</i>	79
3.3.1.	<i>High-Fat Diet Depolarizes MCH Neurons</i>	79
3.3.2.	<i>WD Inhibits Na⁺/K⁺-ATPase in MCH Neurons</i>	88
3.3.3.	<i>PGE₂ Mediates WD-Induced MCH Activation</i>	93
3.3.4.	<i>PGE₂-EP2R Signalling in MCH Neurons Promotes Diet-Induced Obesity in Male Mice</i>	101
3.3.5.	<i>PGE₂-EP2R Signaling in MCH Neurons Modestly Contributes to Diet-Induced Obesity in Female Mice</i>	112
3.4.	<i>Discussion</i>	117
Chapter 4 – High-fat diet induces time-dependent synaptic plasticity of the lateral hypothalamus		120
4.1.	<i>Introduction</i>	121
4.2.	<i>Methods</i>	123
4.2.1.	<i>Animals</i>	123
4.2.2.	<i>Electrophysiology</i>	124
4.2.3.	<i>Identification of ORX and MCH neurons</i>	125
4.2.4.	<i>Double immunohistochemistry</i>	126
4.2.5.	<i>Confocal imaging and analysis</i>	127
4.2.6.	<i>Data analysis</i>	127
4.3.	<i>Results</i>	128

4.3.1.	<i>Orexin neurons</i>	129
4.3.2.	<i>Melanin-concentrating hormone neurons</i>	134
4.4.	<i>Discussion</i>	139
4.5.	<i>Conclusion</i>	144
Chapter 5 –	Summary and discussion	146
5.1.	<i>Summary of main findings</i>	147
5.2.	<i>Discussion</i>	149
5.2.1.	<i>Reversal of obesity</i>	149
5.2.2.	<i>The search for a molecular/cellular correlate of set point</i>	150
5.2.3.	<i>Timeline of obesity development vs maintenance</i>	150
5.2.4.	<i>Sex differences in obesity</i>	152
5.2.5.	<i>Inflammation – cause vs result?</i>	153
5.2.6.	<i>Circuit-level considerations</i>	154
5.2.7.	<i>Putative upstream targets</i>	155
5.2.8.	<i>Downstream targets of MCH and ORX</i>	156
5.2.9.	<i>Cell-level considerations</i>	157
5.2.9.1.	<i>Cell specificity</i>	157
5.2.9.2.	<i>MCH neuron subpopulations</i>	159
5.2.9.3.	<i>ORX neuron subpopulations</i>	160
5.2.10.	<i>Perspective on obesity treatment and prevention</i>	161
5.2.10.1.	<i>Anti-inflammatory pharmacotherapies</i>	161
5.2.10.2.	<i>Dietary intervention and supplementation</i>	162
5.2.10.3.	<i>Deep brain stimulation</i>	162
5.2.10.4.	<i>Development of novel therapies</i>	163
5.2.11.	<i>Limitations and challenges</i>	164
5.2.11.1.	<i>Diet</i>	164
5.3.	<i>Conclusion</i>	167
References	169
Appendices	217

7.1.	<i>Supplementary material for Chapter 2</i>	217
7.2.	<i>Supplementary material for Chapter 3</i>	230
7.3.	<i>Ethics clearance</i>	245
7.4.	<i>Copyright permissions</i>	247
7.5.	<i>Diet composition information</i>	250

List of Figures

Figure 1.1 Overview of the hypothalamic control of energy balance.....	12
Figure 2.1. Time-dependent effect of dietary fat on energy balance.....	35
Figure 2.2. HFD-fed mice defend a consistent BW level regardless of type of HFD, feeding duration or starting age.....	38
Figure 2.3. Acute effects of 45FD and WD exposure.....	41
Figure 2.4. Fasting-induced homeostatic response is intact in HFD-fed mice.....	43
Figure 2.5. Dieting lowers the defended body weight.....	46
Figure 2.6. Chronic exposure to high-fat/high-sugar diet disrupts body weight regulation.....	49
Figure 2.7. Prolonged WD elevates the floor of the homeostatic set point.....	52
Figure 2.8. Effect of diet cycling on body weight control in HFD-induced obesity.....	56
Figure 2.9. Effect of diet cycling on body weight control in 45FD-induced obesity	58
Figure 2.10. Comparison of diet cycling and single dieting.....	61
Figure 3.1. Electrophysiological characterization of MCH and ORX neurons.....	76
Figure 3.2. Chronic Western Diet (WD) feeding induces a persistent activation of MCH neurons.....	81
Figure 3.3. Time-dependent WD-induced changes in excitability of MCH neurons.	83
Figure 3.4. The effect of WD on action potential waveform properties of MCH neurons in rats.....	85

Figure 3.5. Body weight and food intake.	86
Figure 3.6. WD downregulates Na ⁺ /K ⁺ -ATPase in MCH neurons.	89
Figure 3.7. WD reduces the Na ⁺ /K ⁺ -ATPase activity of MCH neurons.	91
Figure 3.8. PGE2 bidirectionally modulates the activity of MCH neurons through distinct receptor subtypes.	95
Figure 3.9. PGE2-EP2R-mediated inhibition of Na ⁺ /K ⁺ -ATPase underlies WD- induced depolarization of MCH neurons.	98
Figure 3.10. WD induces PGE2 signaling to depolarize MCH neurons.	100
Figure 3.11. Confirmation of EP2R deletion in MCH neurons of MCH-EP2R KO mice.	103
Figure 3.12. Extrahypothalamic Cre-expressing cells are insensitive to EP2R agonist	105
Figure 3.13. PGE2-EP2R signalling in MCH neurons exacerbates diet-induced obesity and liver steatosis in male mice.	108
Figure 3.14. Organ profile of male f/f and KO mice after chow or WD feeding. .	111
Figure 3.15. PGE2-EP2R signalling in MCH neurons modestly contributes to diet- induced obesity in female mice.	113
Figure 3.16. Organ profile of female f/f and KO mice after chow or WD feeding.	116
Figure 4.1. Acute HFD feeding induces an increase in spontaneous excitatory transmission to ORX neurons.	130
Figure 4.2. HFD does not influence the number of excitatory synapses to ORX neuron somata.	133

Figure 4.3. Chronic HFD persistently increases excitatory transmission to MCH neurons.....	135
Figure 4.4. HFD induces a delayed increase in the number of excitatory synaptic contacts to MCH neurons.....	137
Figure 4.5. Net change in synaptic properties of adult ORX and MCH neurons over the course of HFD feeding	143
Figure 5.1. Summary figure depicting the time course of ORX and MCH neuron activation with body weight and food intake changes.	148
Figure 5.2. ORX neurons express EP2R.....	158

List of Tables

Table 2.1. Diet macronutrient composition	32
Table 3.1. Diet macronutrient composition	72
Table 5.1. Fatty acid composition of WD and 45FD.....	166
Supplementary Table 7.1. Statistics for Figures 2.1 – 2.10	217
Supplementary Table 7.2. Statistics for Figures 3.2 – 3.16	230

List of Abbreviations

α -MSH	alpha-melanocyte-stimulating hormone
10FD	10% fat diet
25FD	25% fat diet
45FD	45% fat diet
60FD	60% fat diet
Aceta	Acetaminophen
ACSF	Artificial cerebrospinal fluid
AgRP	Agouti-related protein
AHP	Afterhypolarizing potential
ANOVA	Analysis of variance
AP	Action potential
ARC	Arcuate nucleus
BAT	Brown adipose tissue
BBB	Blood-brain barrier
BMI	Body mass index
BNST	Bed nucleus of the stria terminalis
But	Butaprost
BW	Body weight
CART	Cocaine and amphetamine regulated transcript
CCK	Cholecystokinin

CCL2	C-C motif chemokine ligand 2
CGRP	Calcitonin gene-related peptide
CNS	Central nervous system
Ctrl	Control
COX	Cyclooxygenase
COX1	Cyclooxygenase 1
COX2	Cyclooxygenase 2
D-AP5	D-2-Amino-5 phosphopentanoic acid
D1-MSN	Dopamine receptor 1-expressing medium spiny neuron
D2-MSN	Dopamine receptor 2-expressing medium spiny neuron
DAPI	4',6-diamidino-2-phenylindole
DBS	Deep brain stimulation
DIO	Diet-induced obesity
DMH	Dorsomedial hypothalamus
DNQX	6,7-Dinitroquinoxaline-2,3-dione
DYN	Dynorphin
EP1R	Prostaglandin E ₂ receptor 1
EP2R	Prostaglandin E ₂ receptor 2
EP3R	Prostaglandin E ₂ receptor 3
EP4R	Prostaglandin E ₂ receptor 4
EP2Rf/+	Mice that contain one floxed prostaglandin E ₂ receptor 2 allele

EP2Rf/f	Mice that contain two floxed prostaglandin E2 receptor 2 alleles
f/f	Flox/flox
GABA	Gamma-aminobutyric acid
GLP1R	Glucagon-like peptide 1 receptor
GPCR	G-protein-coupled receptor
H&E	Hematoxylin and eosin
HFD	High-fat diet
HFMS	High fat/moderate sucrose diet
Iba1	Ionized calcium binding adaptor molecule 1
IgG	Immunoglobulin G
IKK β	Inhibitor of nuclear factor kappa-B kinase subunit beta
IL1 β	Interleukin 1 beta
INDO	Indomethacin
KO	Knockout
LC	Locus coeruleus
LFD	Low-fat diet
LFHS	Low fat/high sucrose diet
LH	Lateral hypothalamus
LHb	Lateral habenula
IOFC	Lateral orbitofrontal cortex
LPS	Lipopolysaccharide

LS	Lateral septum
LTD	Long-term depression
MBH	Mediobasal hypothalamus
MC3R	Melanocortin 3 receptor
MC4R	Melanocortin 4 receptor
MCH	Melanin-concentrating hormone
MCH ^{Cre} ; EP2R ^{ff}	Mice that lack the prostaglandin E ₂ receptor 2 from melanin-concentrating hormone neurons
MCHR1	Melanin-concentrating hormone receptor 1
MCHR2	Melanin-concentrating hormone receptor 2
mEPSC	Miniature excitatory postsynaptic current
MRI	Magnetic resonance imaging
MRN	Medullary raphe nucleus
MSN	Medium spiny neuron
NAc	Nucleus accumbens
NAFLD	Non-alcoholic fatty liver disease
NEI	Neuropeptide EI
NF κ B	Nuclear factor kappa B
NGE	Neuropeptide GE
NMDA	N-methyl-D-aspartate
NMDG	N-methyl-D-glucamine
NPY	Neuropeptide Y

NSAID	Non-steroidal anti-inflammatory drug
NTS	Nucleus tractus solitarius/nucleus of the solitary tract
ORX	Orexin
ORXA	Orexin-A
ORXB	Orexin-B
OX1R	Orexin-1 receptor
OX2R	Orexin-2 receptor
OXT	Oxytocin
PBN	Parabrachial nucleus
PBS	Phosphate-buffered saline
PFA	Paraformaldehyde
PFC	Prefrontal cortex
PGE ₂	Prostaglandin E ₂
PGF ₂ α	Prostaglandin F ₂ alpha
PGI ₂	Prostacyclin
PKA	Protein kinase A
pLC	Pre-locus coeruleus
POMC	Proopiomelanocortin
PVN	Paraventricular nucleus
REM	Rapid eye movement
RM ANOVA	Repeated measures analysis of variance
RMP	Resting membrane potential

S.E.M	Standard error of the mean
SFA	Saturated fatty acid
SOCS3	Suppressor of cytokine signalling 3
TLR4	Toll-like receptor 4
TMN	Tuberomammillary nucleus
TNF α	Tumor necrosis factor-alpha
TWD	Total Western Diet
USA	United States of America
Vglut2	Vesicular glutamate transporter 2
Vglut3	Vesicular glutamate transporter 3
VH	Ventral hippocampus
VMH	Ventromedial hypothalamus
VTA	Ventral tegmental area
WAT	White adipose tissue
WD	Western Diet
ZI	Zona incerta

List of Publications

1. **Lisa Z. Fang**, Victoria Linehan, Maria Licursi, Christian O. Alberto, Jacob L. Power, Matthew P. Parsons, & Michiru Hirasawa. Prostaglandin E2 activates melanin-concentrating hormone neurons to drive obesity (2023). *Proceedings of the National Academy of Sciences of the United States of America*. doi: <https://doi.org/10.1073/pnas.2302809120>. ***Included as Chapter 3**
2. **Lisa Z. Fang** & Meaghan C. Creed. Updating the striatal-pallidal wiring diagram (2023). Accepted at *Nature Neuroscience*.
3. **Lisa Z. Fang**, Josué A. Lily Vidal, Oishi Hawlader, & Michiru Hirasawa. High-fat diet-induced elevation of body weight set point in male mice (2023). *Obesity*. doi: DOI: 10.1002/oby.23650. ***Included as Chapter 2**
4. Victoria Linehan#, **Lisa Z. Fang**#, Matthew P. Parsons, & Michiru Hirasawa. High-fat diet induces time-dependent synaptic plasticity of the lateral hypothalamus. (2020). *Molecular Metabolism*. doi: <https://doi.org/10.1016/j.molmet.2020.100977>. #denotes equal contribution; ***Included as Chapter 4**
5. Victoria Linehan, **Lisa Z. Fang**, & Michiru Hirasawa. Short-term high-fat diet primes excitatory synapses for long-term depression in orexin neurons (2018). *The Journal of Physiology*. doi: <https://doi.org/10.1113/JP275177>

Co-Authorship Statement

I, Lisa Z. Fang, in collaboration with my supervisor, Michiru Hirasawa, designed, performed, and analyzed all experiments presented herein and wrote all portions of this thesis unless specified below. Essential contributions to this thesis were provided by collaborators as listed below.

In Chapter 2, Josué A. Lily Vidal, Christian O. Alberto, Maria Licursi, Oishi Hawlader, Todd Rowe, and Tinotenda Muyaka contributed to weighing mice and food in all figures. In Chapter 3, Victoria Linehan contributed to data collection in Figures 1B-G, 2C-G, and 4A, D, F. Sherri Bowes contributed to data collection in Figure 1B. Maria Licursi bred and genotyped all animals used in Figures 5 and 6. Jacob L. Power contributed to data analysis in Figures 5N-O and 6N-O. Matthew Parsons and Christian Alberto contributed to data collection in Figures 1F-G. Nick Newhook and Mohammed Sohel Chowdhury aided in weighing and feeding mice, contributing to Figures 5D-F and 6D-F. In Chapter 4, Victoria Linehan contributed to data collection in Figures 1 and 3.

Chapter 1 – General introduction and overview

1.1. Obesity and the current state of treatment

1.1.1. Epidemiology

Rates of obesity have increased to epidemic proportions across the world, with a staggering third of the global population being overweight or obese.

Obesity is a major risk factor for many non-communicable diseases including cardiovascular disease, type II diabetes, and some cancers, which are amongst the leading causes of death in the world¹. As rates of obesity escalate, the risk of developing these diseases would escalate in parallel.

In 2017, close to 5 million global deaths were attributed to high body mass index (BMI), which is mirrored by the 147 million global years lost due to disability or premature death² representing a significant global burden of disease. Not only this, but obesity has a significant impact on the global economy, such that medical care for overweight and obesity will account for almost 3% of the global gross domestic product by 2035³. Therefore, obesity presents a significant encumbrance on the state of health and economy globally.

1.1.2. Contributors to present day obesity

Obesity is the product of genetic and environmental factors, however, an environmental shift due to globalization has likely kickstarted the epidemic.

Although the rapid advancements in technology, economic growth, and cultural spread across the world has vastly improved the quality of life for many, it also accelerated the spread of obesity⁴. This acceleration is driven by the sudden availability and overconsumption of diets that are high in fat, sugar, and salt⁵, a shift towards decreased physical activity due to a rise in personal and public

transportation⁶⁻⁸, less physically-demanding occupations^{6,9}, increased sedentary leisurely activities¹⁰⁻¹⁴, and poor sleep¹⁵⁻¹⁷.

1.1.3. *Treatment*

The first line treatment for obesity is still reducing caloric consumption and increasing physical activity. Popular methods include eating a low-calorie diet or a very-low calorie diet, as well as incorporating exercise programs such as high intensity interval training or aerobic exercise, which all have been associated with weight loss and fat reduction^{18,19}. However, major lifestyle changes such as these are difficult to adhere to, making sustained weight loss challenging, and could result in yo-yo dieting/weight cycling²⁰⁻²².

Several new pharmacotherapies have been made available in recent years with variable success. The most promising of the new wave of pharmacological treatments are analogues for gut-derived satiety factors that boast an impressive 15% - 20% weight loss after 68-72 months in clinical trials²³. However, higher doses of these drugs are not well tolerated, limiting their therapeutic potential^{24,25}. Also, as withdrawal from these drugs results in rapid weight regain²⁶, patients must continuously take these drugs, which may present challenges due to supply chain issues²⁷ or financial barriers²⁸. Also, these drugs are typically recommended for those with a BMI ≥ 30 , or a BMI ≥ 27 with at least one existing weight-related condition^{23,29}, making it unavailable to some.

Other treatments include bariatric surgery or weight loss devices implanted in the stomach, which are highly invasive procedures and can be costly.

Generally, surgical treatment of obesity is more effective than non-surgical options, with increased weight loss and maintenance of weight lost^{30,31}. On the other hand, bariatric surgery is associated with a greater risk of complications³². Like the pharmacotherapies described above, surgical treatments are typically reserved for those with a BMI ≥ 40 , or a BMI ≥ 35 with at least one existing weight-related condition³⁰, limiting its availability.

With mortality rates increasing significantly for individuals who are overweight or obese³³, and treatment options that are far from ideal, we are in desperate need of novel therapeutic targets.

1.2. *Energy balance*

To identify potential therapeutic targets, we must first understand how body weight is regulated. Generally, our body weight is maintained by the balance between how much energy we intake (food intake) and how much we expend (energy expenditure). This is coordinated by complex processes intercalated by the brain and the body, which are subject to dysregulation during obesity.

1.2.1. *Homeostatic vs hedonic control of food intake*

Broadly speaking, food intake can be divided into two main components: homeostatic and hedonic. Homeostatic feeding satisfies basic metabolic demands³⁴. If homeostatic feeding were the only type of feeding present, then one would imagine a relatively static, unchanging body weight. This is the basis

behind a body weight “set point”, which is defined as the target physiological value that the body attempts to maintain through modifications to energy intake and expenditure³⁵.

Hedonic feeding occurs even in the absence of hunger, resulting in the overconsumption of calories beyond homeostatic demands³⁴. Hedonic eating is thought to be the chief driver of excess weight gain and obesity development³⁶. As such, mechanisms underlying hedonic control are suggested to be augmented during this time³⁷. Using functional neuroimaging, studies have shown that humans with obesity have persistent activation of reward-related brain areas after a meal compared to those that were of healthy weight³⁸. Likewise, diet-induced obese animals have altered reward circuitry systems^{39–41}.

1.2.2. Energy expenditure

A reduction in energy expenditure can also facilitate weight gain. Although it appears that some components of energy expenditure, such as diet-induced thermogenesis and resting energy expenditure, increase during obesity to account for the increase in weight burden^{42,43}, there are no detectable changes in total energy expenditure between individuals with obesity and healthy weight individuals⁴³. This may seem insignificant, however, an increased intake beyond metabolic need without a concomitant increase in energy expenditure may compound over time to support excess fat accrual. As well, individuals with obesity spend significantly more time sedentary than healthy weight individuals^{44,45}. Together, these factors may contribute to obesity.

1.3. High-fat diet induced obesity: pathogenesis and mechanisms

Obesity is a pervasive condition that impacts the whole body and multiple organ systems, priming them for dysfunction and disease. At the center of diet-induced obesity (DIO) is overnutrition, particularly of palatable foods high in fat, which becomes a catalyst for excess weight gain and adiposity. In this section, we examine how dietary fat drives obesity pathology, and the mechanisms underscoring these changes.

1.3.1. Fat accumulation

In response to overnutrition, fat cells (adipocytes) increase in number (hyperplasia) and in size (hypertrophy)⁴⁶. The adipose tissue expandability hypothesis posits that white adipose tissue (WAT) depots have a defined limit of expansion, and once this limit is reached, excess lipid is stored in non-adipose tissue organs such as the liver, kidneys, and heart, which creates a cacophony of problems⁴⁷. For example, this ectopic fat accumulation can increase the risk of cardiovascular events due to arterial stiffness⁴⁸, as well as hasten the development of cardiac hypertrophy⁴⁹, and non-alcoholic fatty liver disease (NAFLD)⁵⁰. In addition to its role in energy storage, WAT are also involved in inflammation that instigate obesity pathology during overnutrition, which is highlighted below.

1.3.2. Inflammation

Obesity-induced inflammation is observed systemically as well as centrally. Marked by immune cell recruitment and activation, and secretion of proinflammatory factors, such as tumor necrosis factor alpha (TNF α), interleukin

1 beta (IL-1 β), and chemokine (C-C motif) ligand 2 (CCL2), this chronic inflammation is perhaps the crux of dysfunction in many organs, including the WAT, liver, muscles, gut, and brain⁵¹.

1.3.2.1. *Systemic inflammation*

Although it is not known where systemic inflammation originates, it is thought that changes at the level of the gut and WAT are amongst the first to occur in response to HFD⁵². HFD alters the composition of gut microbiota, skewing the diversity, which has been associated with weight gain in mice and in humans^{53–55}. Changes in gut microbiota can increase intestinal permeability and subsequent release of lipopolysaccharide (LPS) – a component of gram-negative bacterial cell walls – into circulation. LPS then binds to toll-like receptor 4 (TLR4) on macrophages, potentially triggering proinflammatory cytokine release⁵⁶ and propagating systemic inflammation.

Saturated fatty acids (SFAs), found in abundance in HFDs, also activate TLR4^{57,58}, triggering a proinflammatory response. Recently, evidence suggests that SFAs are not bona fide agonists and that TLR4 priming of macrophages is needed for SFA-induced alterations in lipid metabolism and ER stress⁵⁹. This could mean that TLR4s act as “coincidence detectors” during obesity, requiring the presence of circulating LPS and SFAs.

Another site of early HFD-induced action is the WAT. Considered an endocrine organ due to its ability to release unique cytokines (adipokines), WAT is a prime source for inflammation⁶⁰. Macrophages residing within WAT are

abundant and take on an activated state during HFD feeding, releasing proinflammatory factors in excess. Prolonged inflammatory states ultimately contribute to and result in the wealth of adipocyte death seen during obesity^{60,61}. This cell death and clearance of dead adipocytes attracts an inordinate number of proinflammatory macrophages, which then secrete more cytokines, chemokines, and toxic factors⁶².

1.3.2.2. *Neuroinflammation*

HFD induces a persistent, low-grade neuroinflammation in the brain⁶³ that is characterized by gliosis, infiltration of peripheral immune cells, and increased proinflammatory factors such as nuclear factor kappa B (NF- κ B), TNF α , IL1 β , and cyclooxygenase 2 (COX2)⁶⁴, reminiscent of peripheral inflammation.

Chronic HFD consumption and obesity are associated with an increase in the permeability of the blood-brain barrier (BBB), contributing to the inflammatory milieu in the brain by exposing it to peripheral proinflammatory molecules⁶⁴, and infiltrating immune cells^{65,66}.

A landmark study established that HFD not only induces hypothalamic inflammation, but this inflammation can in turn promote the development of obesity. Indeed, deletion of hypothalamic inhibitor of nuclear factor kappa-B kinase subunit beta (IKK β), an enzyme upstream of the proinflammatory transcription factor NF- κ B, was protective against DIO in mice⁶⁷. Due to the early and persistent presence of gliosis in the hypothalamus in response to HFD feeding⁶⁸, other studies expanded this finding to show that depleting microglia or

restraining inflammatory signalling in microglia or astrocytes is sufficient to reduce weight gain during DIO^{65,69}. Magnetic resonance imaging (MRI) studies have provided evidence of the translatable nature of these findings, as gliosis has been observed in the mediobasal hypothalamus (MBH) of humans with obesity⁶⁸. However, there are mixed results on whether body mass reduction can reverse MBH gliosis^{70,71}.

Despite the focus on glia in DIO-related neuroinflammation, neurons are the ultimate effectors of behavior and physiology, and are also affected by HFD. HFD induces neuronal cell death in the hypothalamus⁷², and satiety-promoting neurons appear to be particularly sensitive to degeneration⁶⁸, which would favor positive energy balance. Selective deletion of IKK β /NF- κ B from appetite-promoting agouti-related protein (AgRP) neurons in DIO mice preserved central insulin and leptin signalling, which is lost during obesity, and protected against excess weight gain and hyperphagia⁶⁷.

Inflammatory factors can act as potent regulators of neuronal activity^{73–75}. Their effect on neurons, however, has almost exclusively been explored under the pretense of high-grade inflammation, such as infection or chronic inflammatory conditions⁷⁶. This leaves the burning question of what happens during low-grade inflammation.

1.3.3. *Leptin and insulin resistance*

Leptin and insulin are peripherally produced hormones that regulate energy homeostasis. Leptin is a cytokine secreted from adipocytes that signals

the availability of energy as stored fat⁷⁷, while insulin is released from the pancreas postprandially to promote glucose uptake in various organs⁷⁸.

Aside from their important actions in the periphery, both leptin and insulin can be transported across the BBB to impart critical central effects^{79,80}. Through its action on energy balance neurons, leptin is a potent appetite suppressant⁸¹, and insulin is critical to the regulation of whole-body glucose homeostasis – suppressing hepatic glucose production and increasing glucose uptake into organs to overall decrease blood glucose levels after a meal⁸². During obesity, central resistance to leptin and insulin occurs and their physiological function on appetite and glucose production is attenuated despite hyperleptinemia and hyperinsulinemia^{77,83}. This is detrimental, as this can exacerbate the obese state and lead to the development of type II diabetes^{83,84}.

Inflammation has been identified as a major factor contributing to local leptin and insulin resistance^{85–87}. In response to inflammation, proteins modulating cytokine signaling become upregulated⁸⁸, such as suppressor of cytokine signalling 3 (SOCS3). SOCS3 potently inhibits leptin and insulin receptor signalling, and deletion of SOCS3 from satiety-promoting proopiomelanocortin (POMC) neurons restores insulin and leptin sensitivity, and protected mice against HFD-induced weight gain⁸⁹. Despite this, it remains unknown whether HFD-induced inflammatory factors can modulate the activity of appetite-related neurons directly, influencing energy balance.

1.4. Control of energy balance

Our brains govern the balance between energy intake and energy expenditure. Many different regions in the forebrain and hindbrain are important to this process, with the hypothalamus chief in the orchestration of energy balance. Here, we review a simplified framework of energy balance control, starting with the hypothalamus.

1.4.1. Hypothalamic control of energy balance

1.4.1.1. Overview

The hypothalamus is a small, but evolutionarily conserved structure that contains several distinct nuclei critical in maintaining energy balance, including the paraventricular nucleus (PVN), lateral hypothalamus (LH), dorsomedial hypothalamus (DMH), ventromedial hypothalamus (VMH), and arcuate nucleus (ARC). Here we will focus our discussion on the ARC, PVN, and LH (Figure 1.1).

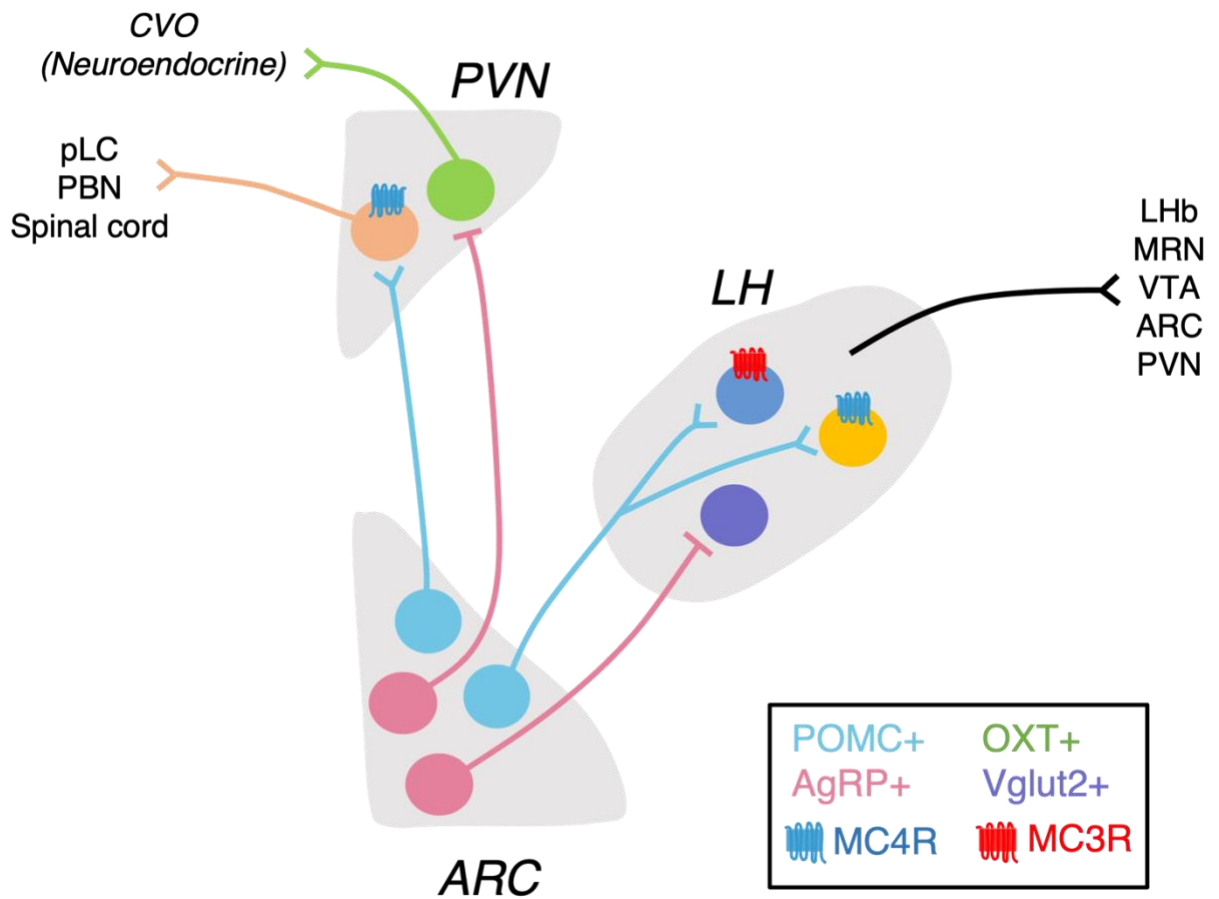


Figure 1.1 Overview of the hypothalamic control of energy balance.

Arcuate nucleus (ARC) populations agouti-related protein (AgRP) and proopiomelanocortin (POMC) neurons, project to diverse cell types in the lateral hypothalamus (LH) and paraventricular nucleus (PVN) to coordinate energy balance. AgRP and POMC neurons exert their effects through a melanocortin-dependent and -independent manner.

Abbreviations: MC3R (melanocortin 3 receptor); MC4R (melanocortin 4 receptor); OXT (oxytocin); Vglut2 (vesicular glutamate transporter 2); CVO (circumventricular organ); pLC (pre-locus coeruleus); PBN (parabrachial

nucleus); LHb (lateral habenula); MRN (medullary raphe nucleus); VTA (ventral tegmental area).

1.4.1.2. *Arcuate nucleus (ARC)*

Localized in the MBH next to the median eminence, a circumventricular organ with highly fenestrated capillaries, the ARC is perfectly poised to receive and integrate signals regarding energy status from the periphery. As such, the ARC contains “first order” cells in the energy balance relay, acting as an interface point for substrates of metabolic status⁹⁰.

The ARC is comprised of two molecularly distinct cell types that function in tandem but antagonistically to each other. The orexigenic AgRP^{91–93} and anorexigenic POMC⁹⁴ neurons are outfitted with receptors for many feeding-related hormones⁹⁵, dominating homeostatic control over energy balance. AgRP neurons contain co-transmitters that modulate distinct facets of energy balance. While AgRP itself promotes sustained food intake, neuropeptide Y (NPY), another orexigenic peptide, plays a role in acute feeding and glucose regulation⁹⁶, and gamma-aminobutyric acid (GABA) restrains energy expenditure⁹⁷. On the other hand, alpha-melanocyte-stimulating hormone (α -MSH), a product of POMC primarily suppresses food intake and increases basal metabolic rate⁹⁸, while its co-transmitter, cocaine- and amphetamine-regulated transcript (CART), enhances energy expenditure and physical activity⁹⁹.

These cells have common projection targets, including hypothalamic regions such as the paraventricular nucleus (PVN) and lateral hypothalamus (LH), where they synapse on so-called “second order” effector neurons. AgRP and POMC neurons impart their effects through the melanocortin 4 receptor

(MC4R) on target cells, whereby α -MSH and AgRP act as an agonist and an inverse agonist, respectively¹⁰⁰.

1.4.1.3. *Paraventricular nucleus of the hypothalamus*

In the PVN, MC4R-expressing cells (PVN^{MC4R}) integrate the dense inputs from AgRP and POMC neurons. Loss of MC4R in the PVN causes profound obesity in mice and humans^{101,102}, while stimulation of PVN^{MC4R} potently suppresses food intake¹⁰³. This occurs even during simultaneous AgRP neuron stimulation¹⁰³, highlighting satiety-promoting α -MSH's dominance at MC4R. While PVN^{MC4R} are known to be critical for satiety, feeding may be partially regulated by MC4R-independent mechanisms as dual stimulation of AgRP \rightarrow PVN^{MC4R} terminals and PVN^{MC4R} cell bodies does not completely attenuate feeding. AgRP neurons have been found to inhibit oxytocin (OXT)-expressing cells in the PVN to induce feeding¹⁰⁴, however, whether OXT cells can reliably evoke feeding remains contentious^{103,105,106}. This may in part be explained by the neurochemical heterogeneity of OXT neurons¹⁰⁷ and will require further investigations in the future.

More recently, several other MC4R-lacking neurons in the PVN have been identified to be involved in feeding, demonstrating that this area is not autonomously regulated by α -MSH and AgRP, and that there is complexity in the feeding schema of the PVN.

Lastly, pre-autonomic neurons in the PVN can modulate energy expenditure and suppress appetite through projections to the pre-locus coeruleus (pLC), the parabrachial nucleus (PBN), as well as the spinal cord^{103,108,109}.

1.4.1.4. *Lateral hypothalamus*

The LH also receives dense innervation from the ARC. AgRP→LH stimulation is sufficient to promote eating¹¹⁰, however, like in the PVN, this is MC4R-independent¹⁰³. AgRP neurons inhibit LH cells that express vesicular glutamate transporter 2 (Vglut2; LH^{Vglut2}), enhancing sweet taste preference¹¹¹, possibly increasing palatability. Coincidentally, activation of LH^{Vglut2} cells suppresses feeding, even in hungry mice¹¹².

Reports of MC4R signalling in the LH are mixed, as some see an anorectic effect¹¹³, while others report no effect on feeding at all¹¹⁴. Approximately 75% of MC4R colocalize with neurotensin-expressing neurons in the LH¹¹⁵, which are known to suppress food intake and increase locomotor activity¹¹⁶, consistent with the actions of POMC neurons. Interestingly, α -MSH also binds to melanocortin 3 receptors (MC3R), and activation of LH MC3R-expressing cells drives locomotor activity¹¹⁷.

The downstream effectors of the LH are diverse, as cells project broadly throughout the brain. Connections to the lateral habenula (LHb)¹¹⁸, ventral tegmental area (VTA)^{119,120}, medullary raphe nucleus (MRN)¹²¹, as well as the ARC^{122,123} and PVN¹²⁴ likely regulate diverse energy balance behaviors. Notably, LH melanin-concentrating hormone (MCH) neurons project directly to cerebral

ventricles¹²⁵ where CSF can deliver the MCH peptide to distal brain regions. This would enable widespread MCH-mediated control of areas that are not direct synaptic targets of these neurons.

1.4.2. Extrahypothalamic control of feeding

Various external factors can modulate feeding in spite of metabolic demand, such as food scarcity or abundance, and predator threat. The nucleus accumbens (NAc) is a basal forebrain structure known for its role in reward and coordinates motivated feeding in response to such factors¹²⁶. Medium spiny neurons (MSNs) comprise the main cell type here, expressing either the dopamine D1 receptor (D1-MSN) or the D2 receptor (D2-MSN). A divergent role for these two subpopulations in energy balance has been identified, such that activation of D1-MSNs suppresses feeding, likely through its connection to the LH, while D2-MSNs promote feeding^{126,127}.

Another basal forebrain structure, the lateral septum (LS), has recently emerged as a regulator of energy balance, as inhibition of this area strongly promotes feeding¹²⁸. Moreover, the LS is a common downstream target for the PVN and LH. Stimulation of PVN MC4R terminals in the LS reduces feeding¹²⁹, while LH^{Vglut2} inputs modulate palatability¹¹¹.

In the brainstem, stimulation of calcitonin gene-related peptide (CGRP)-expressing neurons in the parabrachial nucleus (PBN) has a profound anorectic effect in rodents, and mediates cancer-induced anorexia and malaise¹³⁰. A recent study also established a role for these neurons in the physiological regulation of feeding, such that AgRP neurons inhibit CGRP neurons to delay satiation and

meal termination¹³¹. The PBN also receives input from the PVN¹³² and the LH¹³³ that control energy balance behaviors, cementing its role in illness-related and homeostatic suppression of feeding.

The nucleus tractus solitarius (NTS) in the brainstem is a primary integrative site for vagal afferents, relaying visceral information to other brain areas¹³⁴. Distinct subpopulations of catecholaminergic neurons in the NTS have been found to oppositely influence food intake. Direct vagal projections to epinephrine-expressing cells promote feeding, possibly mediated by connection to the ARC, while norepinephrine-expressing cells in the same area suppress feeding, likely through PBN connections^{135–137}.

As current research continues to unveil previously unknown brain regions and circuits that are involved in energy balance regulation, we move towards a complete understanding of energy homeostasis.

1.4.3. Neuroplastic changes during obesity

HFD is known to profoundly affect neuronal function, impeding normal physiological function. Generally, in response to HFD feeding, hypothalamic neurons seem to be tuned to increase energy intake and promote obesity.

HFD can also induce neuroplastic changes extrahypothalamically, such as in the NAc and prefrontal cortex (PFC), which can increase motivation for palatable foods⁴⁰, and impair decision making^{138,139}, respectively.

In the ARC, AgRP and POMC neurons exhibit fewer excitatory and inhibitory synaptic contacts, respectively, after 3 months of HFD consumption^{140,141}, ultimately increasing anorectic drive. In contrast, HFD

differentially modulates AgRP^{142,143} and POMC neuron excitability^{144,145} to favor positive energy balance. The functional consequence of this divergence in synaptic and intrinsic plasticity is not known. Another orexigenic ARC cell population, pronociceptin neurons, is excited after HFD consumption¹⁴⁶, promoting palatable food intake.

Meanwhile in the LHA, anorexigenic Vglut2+ neurons are inhibited by HFD¹⁴⁷, which would result in feeding. Furthermore, we previously showed that excitatory synapses to orexin (ORX) neurons undergo long-term depression (LTD) after acute, but not chronic, HFD¹⁴⁸. Given the orexigenic role of ORX neurons, this LTD may be a counterregulatory response to prevent overeating, which is lost as HFD prolongs.

1.5. *The lateral hypothalamus*

1.5.1. *Defining the role of the lateral hypothalamus*

Early lesion and stimulation studies in rodents pioneered our understanding of the role of the LHA and demonstrated its great diversity in function. The first LHA lesion study was performed by Anand & Brobeck (1951) who reported pronounced aphagia in rats, earning this area the distinction of being the “feeding center” of the brain¹⁴⁹. Many others since have performed these lesions and recapitulated this striking effect – with observances of somnolence¹⁵⁰, severe aphagia, adipsia, and weight loss, which ultimately led to death^{151,152}.

These lesion studies have limitations, like non-specific ablation of cell bodies and processes that resulted in severing of the nigrostriatal bundle, which

confounded the aphagia phenotype^{153,154} as rats became immobile. However, when the ascending dopaminergic system is spared, hypophagia still resulted, providing strong evidence that the LH is indeed a “feeding center”¹⁵⁵.

1.5.2. Refining the role of the lateral hypothalamus

With the advent of more sophisticated techniques, we can begin to refine the many roles ascribed to the LH, with a precision that allows for projection- and cell type-specificity. The highly diverse roles of the LH are paralleled only by the equally diverse neurochemical phenotypes, projection targets, and receptor expression – undoubtedly important in casting broad influence over the brain. Therefore, I will limit the discussion to the two major neuropeptidergic cell types of the LH – MCH and ORX neurons.

1.5.3. MCH neurons

The neuropeptide MCH is contained within neurons that are predominantly restricted to the LH and the adjacent zona incerta. MCH is derived from its precursor prepro-MCH, which has other cleavage products including neuropeptides EI (NEI) and GE (NGE)¹⁵⁶. NEI has been shown to modulate grooming and locomotor activity¹⁵⁷, while little is known regarding the function of NGE.

MCH neurons are indisputably important in energy balance, promoting weight gain by increasing food intake and concomitantly decreasing energy expenditure. These effects have been recapitulated consistently over time and with more sophisticated techniques in both rats and mice^{158–161}. Suppressing

MCH action either by genetic deletion or cell ablation results in leanness, decreased adiposity, increased brown adipose tissue (BAT) activity, and reduced triglyceride levels in the liver^{162,163}.

In target regions, MCH exerts its effect through the MCH receptor 1 (MCHR1) in all mammals, while MCH receptor 2 (MCHR2) is functional in humans and some mammals, but notably not rodents¹⁶⁴. This is important as most of the studies highlighted are performed in rodents, and may not entirely reflect the function of MCH in humans. MCHR1 is a G-protein-coupled receptor (GPCR) that couples to Gi/o or Gq proteins¹⁶⁵. It is distributed widely throughout the central nervous system (CNS)¹⁶⁶, such as in other hypothalamic areas¹⁶⁷ and the NAc¹⁶⁸, which may underlie energy intake, also the brainstem¹⁰⁸ and motor cortex¹⁶⁹, which may mediate energy expenditure. Expression in other areas¹⁶⁶ likely regulate other facets of MCH neuron function. Of note, the Gq protein-coupled MCHR2 has a similar expression pattern to MCHR1¹⁷⁰, and artificially co-expressing MCHR2 in the same cells that express MCHR1 in mice, protects against DIO¹⁷¹. This suggests that MCHR2 attenuates MCHR1 function. However, it is not known whether cells do co-express MCHR1 and MCHR2 in humans, and it is possible that the resultant energy outcome would differ contingent on their differential expression on various cell types.

MCH neurons are host to other neuropeptide transmitters, and classical fast neurotransmitters including CART, nesfatin1, GABA and glutamate^{172–174}. As many of the energy balance effects have been recapitulated in MCHR1 null animals, the MCH peptide seems to play a principal role. However, effects on

glucose homeostasis and anxiety may be independent of the MCH peptide^{175,176}, and future studies will be needed to delineate the role of other transmitters.

Lastly, MCH neuron activity can be dynamically modulated by neurotransmitters such as serotonin, norepinephrine, and dopamine^{177,178}, as well as neuropeptides nociceptin¹⁷⁹, dynorphin (DYN)¹⁸⁰, OXT, and vasopressin¹⁸¹. Also, MCH neurons are glucose-¹⁸² and insulin-sensitive¹⁸³, and although they do not express the leptin receptor, MCH expression seems to be regulated by leptin^{184,185}.

1.5.3.1. *Other roles of MCH*

MCH is multifunctional and has roles in sleep/wake regulation, memory, and mood. Firstly, activation of MCH neurons promotes sleep in rodents, which is underscored by an extension of rapid eye movement (REM) sleep^{186,187}, and stabilizes non-rapid eye movement (NREM) sleep¹⁸⁸. Coordination of sleep may be mediated by MCH innervation of the locus coeruleus (LC) and tuberomammillary nucleus (TMN)¹⁸⁹. Through dense innervations to the dorsal hippocampus (DH), MCH neurons also play a role in memory. Although, the exact role remains contentious, as some report that MCH promotes memory^{190,191} while others suggest it promotes forgetting¹⁹². On the other hand, connections to the ventral hippocampus (VH) have been shown to regulate impulsivity¹⁹³. Lastly, the MCH system promotes anxiety-¹⁹⁴ and depressive-like behaviors¹⁹⁵, possibly through amygdalar connections.

1.5.4. Orexin neurons

Orexins (ORX), also known as hypocretin, are an orexigenic neuropeptide localized in the LH and perifornical areas¹⁹⁶. ORX neurons release peptides orexin-A (ORX-A) and orexin-B (ORX-B), which are cleaved from the same precursor prepro-orexin¹⁹⁷. They exert their effects by binding to Ox1 receptors (OX1R) and Ox2 receptors (OX2R), which are found throughout the brain, but are particularly dense in the LC and TMN, respectively¹⁹⁸. ORX-A and ORX-B have differential binding affinities, such that OX1R preferentially binds ORX-A while OX2R binds both ORX-A and ORX-B with similar affinities¹⁹⁷.

Due to their naming, it is logical to assume that ORX neurons are orexigenic, and indeed, central infusion of ORX reliably increases acute food intake^{199,200}, and ORX neuron ablation results in hypophagia²⁰¹. Despite this, the role of ORX neurons in energy balance is curious, as they also robustly increase energy expenditure. Genetic ablation of ORX neurons in mice results in late-onset obesity despite chronic undereating, suggesting their role in energy expenditure is dominant^{202,203}. Of note, patients with narcolepsy, caused by ORX deficit, tend to gain weight and have an increased incidence of obesity despite eating less²⁰⁴, which supports the notion that ORX primarily regulates energy expenditure. This increase in energy expenditure is a result of increased spontaneous locomotor activity, metabolism, thermogenesis, as well as arousal^{205–207}, which may be coordinated by hindbrain connections^{208,209}. However, the role of ORX neurons in feeding cannot be ignored. This increase in food intake may be a result of the increased locomotor activity and represent a

foraging behavior²¹⁰. On the other hand, ORX also modulates reward²¹¹ and motivated behavior^{212,213} through extensive connections to the NAc and VTA²¹⁴, which suggests a role in hedonic feeding, independent of locomotion.

Like MCH neurons, ORX neurons also utilize several co-transmitters, including glutamate and the endogenous opioid peptide dynorphin (DYN)¹⁷². In fact, there is almost a perfect overlap of ORX and DYN expression in the LH²¹⁵, and it was recently found that they can be packaged in the same synaptic vesicle²¹⁶.

Despite the harmonious co-packaging, ORX and DYN seem to have opposing functions in the same area^{216–218}. How neurons respond to the co-release of ORX and DYN is highly variable¹⁸⁰ and likely dependent upon the brain region, release dynamics of each neuropeptide, and receptor expression on the target cells (ORX1R, ORX2R for ORX and kappa opioid receptors 1 and 2 for DYN).

Modulated by many of the same factors as MCH neurons, ORX neuron activity is regulated by serotonin, dopamine, norepinephrine^{219–222}, cholecystokinin²²³, vasopressin²²⁴, and neurotensin²²⁵. These cells are sensitive to glucose^{182,226}, and ghrelin and leptin modulate their activity in opposing manners²¹⁹, likely indirectly, as localization of the corresponding receptors on ORX neurons is not described.

1.5.4.1. *Other roles of ORX*

ORX neurons play a cardinal role in arousal. Human narcolepsy, characterized by the involuntary loss of consciousness and daytime sleepiness, has been attributed to the loss ORX neurons^{227,228}. This is recapitulated in ORX-deficient mice that display narcolepsy-like symptoms and increases in REM sleep^{229,230}, which may be mediated by resultant dysfunction in the LC²³¹, TMN²³² or sublateralodorsal tegmental nucleus²³³. Also, ORX neurons are involved in stress-related behaviors²³⁴, and sympathetic responses are mediated through ORX signalling in the brainstem^{208,209}.

The many roles of MCH and ORX neurons are bestowed by a diversity of co-transmitters, projection targets, and receptor expression patterns, which all contribute to enacting such dynamic modulation of behavior.

1.6. Thesis objectives and overview

It is clear that environmental factors, especially diet, impact our body weight regulation. This is highlighted by a study showing that immigrants living in the USA or Europe have an increased likelihood of exhibiting unhealthy dietary habits in comparison to those in their geographic origin²³⁵. Therefore, it is imperative to understand how HFDs influence body weight regulation. This will then guide our search for a neural correlate associated with HFD-induced perturbations in energy balance.

To this end, in Chapter 2, I investigate how diets high in dietary fat alter body weight regulation in male mice. We found that HFDs (>45%) elevate the body weight set point, which initially manifests as a transient overeating phase

followed by a steady state that is avidly defended. I argue that homeostatic mechanisms are intact under HFD conditions and try to maintain body weight at this new level, rather than being dysregulated by hedonic mechanisms, making weight loss difficult.

In Chapter 3, I begin to disentangle possible neural correlates for the elevated body weight set point. We investigate the role of neuroinflammation in the response of MCH and ORX neurons after HFD consumption. We found that only MCH neurons were persistently excited after prolonged HFD consumption, which was mediated through the inflammatory molecule prostaglandin E₂ (PGE₂). Importantly, conditional deletion of PGE₂ signaling in these cells protected male and female mice from DIO and fat accumulation.

To build on the previous chapter's findings, Chapter 4 investigates the synaptic changes that occur in MCH and ORX neurons after HFD consumption. We found a transient increase in excitatory transmission to ORX neurons coinciding with an early hyperphagia. On the other hand, MCH neurons display a delayed but persistent increase in excitatory drive over the course of feeding, which coincides with the HFD-induced intrinsic activation of MCH neurons seen in Chapter 3.

These results support the notion that ORX and MCH neurons have time-dependent complementary roles in energy balance regulation during HFD, which are likely part of the well-coordinated homeostatic response to an elevation in body weight set point. Together, this thesis attempts to identify the neural

underpinnings of an elevated set point, which is induced by eating diets that are high in fat.

Chapter 2 – High-fat diet-induced elevation of body weight set point in male mice

Adapted from

Lisa Z. Fang et al., High-fat diet-induced elevation of body weight set point in male mice. *Obesity* **31**, 1000-1010 (2023). doi: <https://doi.org/10.1002/oby.23650>

2.1. Introduction

Human and animal studies have previously postulated the concept of body weight (BW) set point, which is defined as the target physiological value that the body attempts to maintain ^{236,237}. The level of BW set point can change dynamically as seen during development, aging and pregnancy ²³⁸. Furthermore, it is well-documented that obese animals, including humans, avidly defend an elevated BW ^{239–241}. This is clearly manifested during intentional weight loss as resistance to losing weight or rebound weight gain ^{242–244}. Thus, obese animals have intact homeostatic mechanisms defending a BW higher than physiologically optimal levels.

In contrast, energy-dense, high-fat diets (HFD) are often consumed in excess of fulfilling physiological needs ²⁴⁵. This has led to the notion that palatable HFD elicits hedonic eating by overriding or dysregulating homeostatic controls that maintain energy balance ²⁴⁶. This assumes that upon exposure to HFD, the BW set point remains at the pre-HFD level while the hedonic mechanism escapes the homeostatic processes to drive hyperphagia.

The discrepancy between these two concepts may stem from the fact that in studies focused on the defense of a higher set point, homeostatic challenge is commonly applied to obese animals eating HFD, and resistance to weight loss is interpreted as intact homeostasis. Meanwhile, studies focused on HFD-induced hyperphagia do not use HFD as the background diet, and drastic increases in caloric consumption from HFD that is greater than the level of consumption of the baseline normal-fat diet are interpreted as dysregulated homeostasis. Thus, it

remains unclear whether and how the homeostatic set point is modulated during the entire course of HFD feeding. Is it the cumulative, secondary effect of a chronic calorie-dense diet that gradually elevates the set point? Alternatively, does HFD itself raise the set point, which in turn triggers a counter-regulatory response to facilitate BW gain to reach the new set point? To answer these questions, we fed mice with various HFD in different patterns and followed the changes in BW and food intake. Our results support the idea that HFD elevates the set point at which BW is defended, which is largely reversible upon removal of HFD. However, prolonged exposure to HFD blunts its reversibility, which is particularly pronounced with high-sugar HFD.

2.2. *Materials and Methods*

Animal procedures were approved by Memorial University's Institutional Animal Care Committee according to the guidelines of the Canadian Council on Animal Care (18-02-MH). To confirm reproducibility, experiments were performed in multiple cohorts over 6 years.

2.2.1. *Animals*

Male C57BL/6NCrl mice from Charles River (Saint Constant, Quebec, Canada) were housed individually or in groups of 2 or 3 in a temperature-controlled room ($23 \pm 1^\circ\text{C}$) on a 12h light-dark cycle (8:00 AM-8:00 PM lights on). Mice were acclimatized for a week prior to random assignment to various diets (Table 1). A standard chow was provided as the control diet or when mice were

not on purified diets (10-60FD, WD) as indicated in the Figures. Food and water were available *ad libitum* except for food deprivation study (below). Some groups switched diets during the experiment as indicated in the Results and Figures. Researchers were aware of mouse allocation to ensure provision of the correct diet.

BW and food intake were measured twice a week between 9:00 and 11:00 AM. For group-housed mice, average caloric intake for individual mice was calculated from total food intake per cage. Caloric efficiency was estimated by dividing BW gained by calories consumed (average caloric intake was used for group-housed). At the end of the feeding period, mice were sacrificed under 4% isoflurane anesthesia for organ dissection. The number of animals used is based on similar studies in the literature. No animals were excluded from the study.

Table 2.1. Diet macronutrient composition

Diet	Company	Catalogue#	Cal density kcal/g	Fat %	Protein %	Carbo-hydrate %	Sucrose %
Chow	LabDiet*	Prolab RMH 3000	3.20	14	26	60	n.a.
10FD	Research Diets**	D12450H	3.82	10	20	70	17.2
25FD	Research Diets	D11071701	4.19	25	20	55	17.2
45FD	Research Diets	D12451	4.73	45	20	35	17.2
60FD	Research Diets	D12492	5.24	60	20	20	6.9
WD	Research Diets	D12079B	4.70	40	17	43	29.4

* LabDiet (St. Louis, MO, USA)

** Research Diets Inc. (New Brunswick, NJ, USA)

2.2.2. Data analysis

Statistical analyses were performed using Prism 9 (GraphPad). Differences between groups over time were assessed using mixed-effects two-way or three-way repeated measures ANOVA with Sidak's multiple comparisons test. Following assessment of variance with Brown-Forsythe or F-test, and normality with Kolmogorov-Smirnov test, group comparisons were analyzed using one-way, two-way, or three-way ANOVA, Kruskal-Wallis test, two-tailed unpaired t-test, or Welch's t-test, as appropriate. When group comparisons found significance, *post-hoc* Tukey's or Dunn's multiple comparisons were performed. Correlation assessment used least squares linear regression analysis. Detailed statistical results are summarized in Supplementary Table 7.1 in the Appendix. Data are shown as mean \pm S.E.M. of the group and/or as scatter plots representing individual data. $p < 0.05$ was considered statistically different.

2.3. Results

To determine how dietary fat modulates BW regulation, male C57BL/6N mice were fed with purified diets with 10% to 60% fat (Fig. 2.1). A distinct fat content-dependent stratification was observed. Mice fed 10% or 25% fat diets (10FD, 25FD) maintained leanness with a similar rate of weight gain, caloric intake and efficiency (the ratio of BW gain to caloric intake) throughout the feeding period (Fig. 2.1A-D). Contrastingly, those fed 45% or 60% fat diets (45FD, 60FD) showed accelerated weight gain during the first 4 weeks, which gradually returned to baseline levels by week 10 (Fig. 2.1B). Caloric intake was higher in the 45FD and 60FD groups throughout the feeding period (Fig. 2.1C).

Accordingly, caloric efficiency was higher, indicative of reduced energy expenditure, in the 45FD and 60FD groups during the first 4 weeks of the respective diets (Fig. 2.1D). At week 12, significant differences were observed in the white adipose tissues in parallel with the BW change (Fig. 2.1E-G). Particularly, epididymal fat showed a dose-dependent increase, while other organs examined were not different (Fig. 2.1H-L). Therefore, diets high in fat initially induce rapid weight gain accompanied by higher caloric intake and efficiency. After this transition, BW reaches a steady state at a higher level maintained primarily by caloric intake.

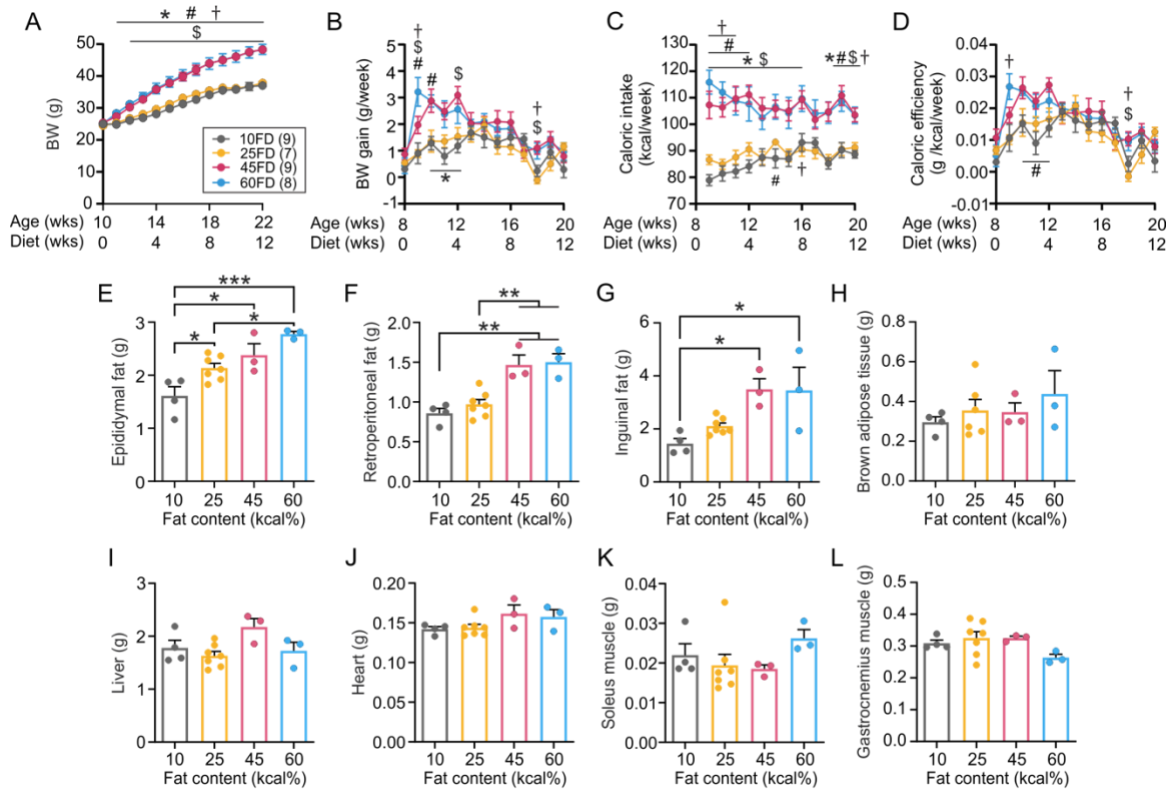


Figure 2.1. Time-dependent effect of dietary fat on energy balance

(A) Body weight (BW) of mice fed diets with various fat content showing an all-or-none response to high-fat diets (HFD). 45% and 60%-fat diet (45FD and 60FD, respectively) induce a consistently higher BW relative to diets with 10% and 25% fat (10FD and 25FD, respectively).

(B) Weekly BW change showing a transient acceleration in the HFD groups at first, which is not seen in low-fat groups.

(C) Weekly caloric intake.

(D) Caloric efficiency calculated as the ratio of weekly BW gain and caloric intake.

For panels A-D, * $p < 0.05$ for 10FD vs 45FD; # $p < 0.05$ for 10FD vs 60FD; \$ $p < 0.05$

for 25FD vs 45FD; † $p < 0.05$ for 25FD vs 60FD. Sidak's multiple comparisons test following two-way RM ANOVA. Number of mice in each group (n) is indicated in parentheses after group ID.

(E-L) Weight of various organs as indicated at the end of 12-week feeding.

* $p < 0.05$, ** $p < 0.01$, *** $p < 0.001$. Tukey's multiple comparisons test following one-way ANOVA (E-J, L) or Dunn's multiple comparisons test following Kruskal-Wallis test (K). n = 3-9 mice/group.

Details of statistical results can be found in Table 7.1 in the Appendix.

Next, we tested how the duration of HFD feeding and age affected BW regulation. Both juvenile- (4-week old; Juv-45FD) and adult 45FD (12-week old; Adult-45FD) mice gained significant weight compared to chow controls, regardless of the age HFD started (Fig. 2.2A). The rate of BW gain, caloric intake and efficiency of 45FD groups were initially greater than chow controls but returned to chow levels by the end of the feeding period (Fig. 2.2B-D). Interestingly, both 45FD groups settled at the same steady-state BW following a period of rapid weight gain (Fig. 2.2A). Thus, the degree of obesity is not correlated with the duration of HFD or exacerbated by HFD exposure from juvenile age.

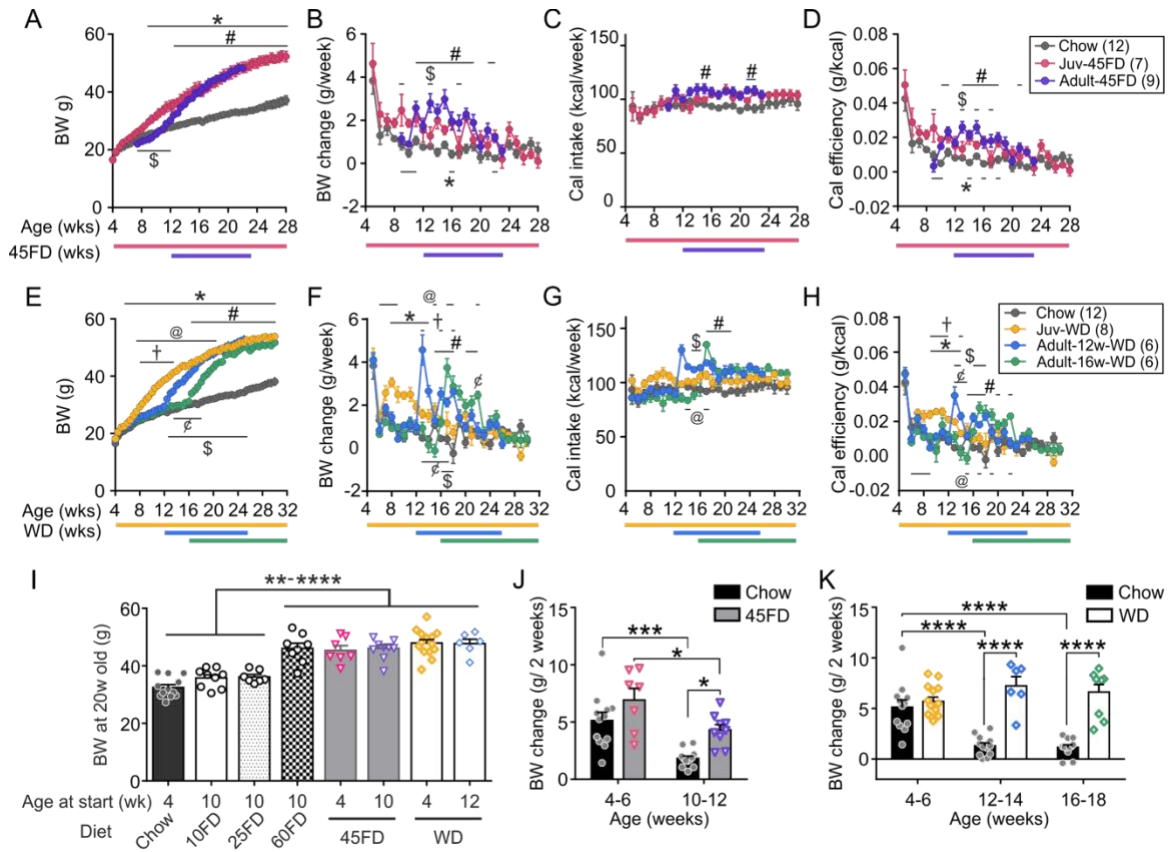


Figure 2.2. HFD-fed mice defend a consistent BW level regardless of type of HFD, feeding duration or starting age.

(A) BW of mice fed low-fat chow or 45FD. 45FD commenced at different ages and continued until the end of the feeding period.

For A-H, bars with corresponding colors below the graph indicate the HFD feeding period.

(B) Weekly BW change of mice in (A) showing that switching to 45FD initially increases the rate of BW gain, which eventually decays to the chow control level.

(C, D) Weekly caloric intake (C) and efficiency (D) of mice in (A).

For panels A-D, * $p < 0.05$ for chow vs Juv-45FD; # $p < 0.05$ for chow vs Adult-45FD; \$ $p < 0.05$ for Juv-45FD vs Adult-45FD. Sidak's multiple comparisons test following two-way RM ANOVA. n is indicated in parentheses after group ID.

(E) BW of mice fed chow or Western Diet (WD). WD commenced at different ages and continued until the end of the feeding period.

(F) Weekly BW change of mice in (E) showing that switching to WD transiently increases the rate of BW gain, which eventually decays to chow control levels.

(G, H) Weekly caloric intake (G) and efficiency (H) of mice shown in (E).

For panels E-H, * $p < 0.05$ for chow vs Juv-WD; # $p < 0.05$ for chow vs Adult-16w-WD; \$ $p < 0.05$ for chow vs Adult-12w-WD; @ $p < 0.05$ for Juv-WD vs Adult-16w-WD; † $p < 0.05$ for Juv-WD vs Adult-12w-WD; ¢ $p < 0.05$ for Adult-16w-WD vs Adult-12w-WD. Sidak's multiple comparisons test following two-way RM ANOVA. n in indicated in parentheses after group ID.

(I) BW of mice at 20 weeks of age. Displayed data correspond to groups from Figures 1 and 2.

** $p < 0.01$, *** $p < 0.001$, **** $p < 0.0001$. Tukey's multiple comparisons following one-way ANOVA. n = 7-14 mice/group

(J, K) BW change over a two-week period immediately following a switch to 45FD (J) or to WD (K) at different ages, along with that of age-matched chow-fed mice.

* $p < 0.05$, *** $p < 0.001$, **** $p < 0.0001$. Tukey's multiple comparisons following two-way ANOVA. n = 6-14 mice/group

As palatable diets are thought to override homeostatic mechanism to drive hedonic eating, we asked if a high-fat, high-sugar Western-style diet (WD), which mice prefer over 45FD (data not shown), would disrupt BW regulation. Upon switching to WD, 12- or 16-week-old adult groups (Adult-12w-WD; Adult-16w-WD) displayed a spike in caloric intake (Fig. 2.2G). Additionally, rapid weight gain and higher caloric efficiency was seen in the juvenile (4-week old; Juv-WD) and adult groups (Fig. 2.2E,F,H). Following this transition, all WD groups settled at the same BW level regardless of what age WD started (Fig. 2.2E), while the rate of BW change, caloric intake and efficiency returned to chow control levels (Fig. 2.2F-H). These results are like 45FD, albeit the presence of a spike in BW gain and caloric intake after the switch to WD, which may represent a hedonic response to palatable WD (Fig. 2.3A-C). Remarkably, all groups fed with HFD containing $\geq 40\%$ fat (60FD, 45FD, WD) had consistent BW when compared at a specific age (20-week old), despite the differences in the type of HFD, duration of feeding, or age at the beginning of the feeding period (Fig. 2.2I). Similarly, groups fed a diet with $\leq 25\%$ fat (chow, 10FD, 25FD) had a consistent BW, which was significantly lower than that of HFD groups (Fig. 2.2I). Thus, dietary fat appears to determine the level of defended BW.

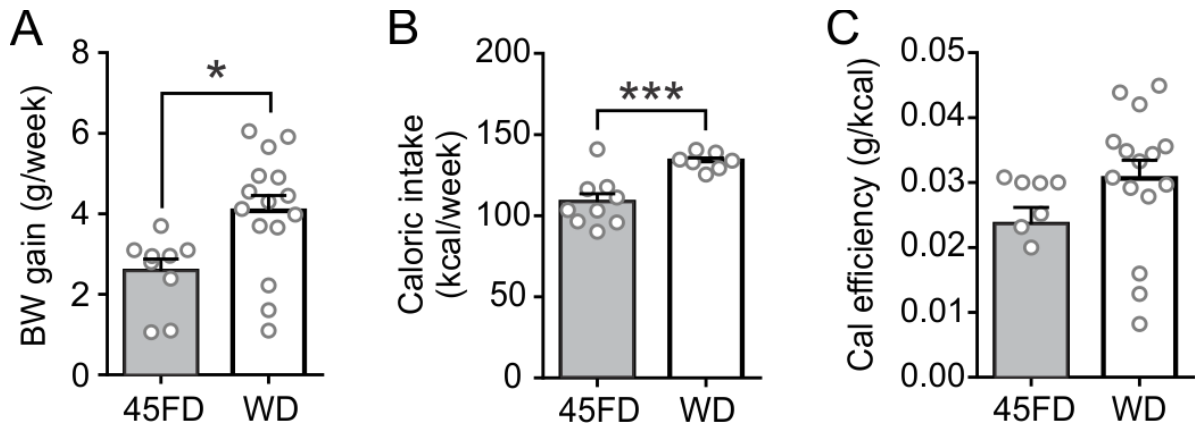


Figure 2.3. Acute effects of 45FD and WD exposure

(A-C) A comparison of the initial BW gain (A), caloric intake (B) and efficiency (C) of mice fed 45FD or WD after one week. Data displayed correspond to the adult groups in Figure 2.

* $p < 0.05$, *** $p < 0.001$. Unpaired two-tailed t-test or Welch's t-test. $n = 7-15$ mice/group.

To determine whether HFD-exposed mice can express normal homeostatic responses, they were challenged with an acute food deprivation. All mice lost significant weight after the 16-hour fasting period (5:00PM to 9:00AM). However, the weight lost during fasting was largely regained within a day of refeeding (Fig. 2.4A), such that the BW loss and gain was roughly equal in all groups (Fig. 2.4B). This indicates a counter-regulatory response to restore acute perturbations in energy balance, supporting the idea that homeostatic mechanisms are not dysregulated in diet-induced obese (DIO) animals; rather, diets high in fat elevate the defended level of BW.

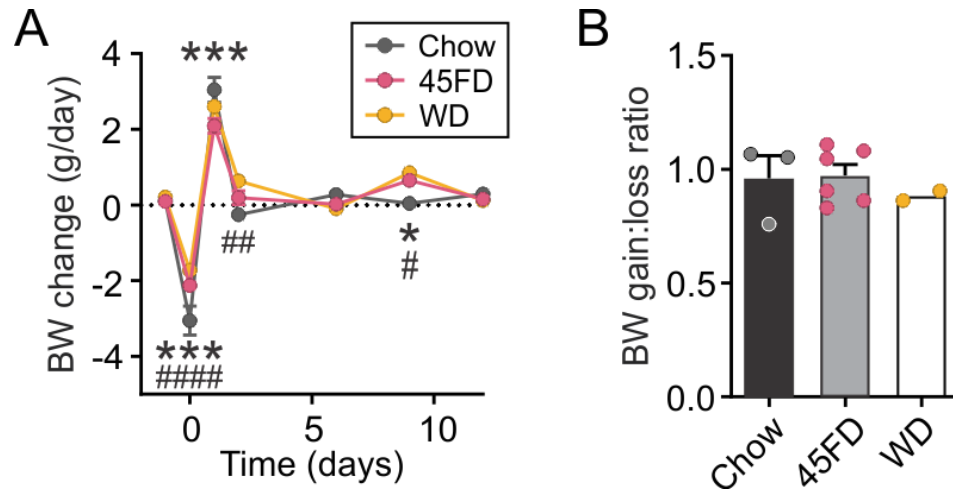


Figure 2.4. Fasting-induced homeostatic response is intact in HFD-fed mice

(A) Daily BW change of mice fed chow, 45FD, or WD before and after a 16-hour fast at time=0, followed by *ad libitum* refeeding of the diet they were fed prior to the fast.

* $p < 0.05$, *** $p < 0.001$ for chow vs 45FD; # $p < 0.05$, ## $p < 0.01$, #### $p < 0.0001$ for chow vs WD. Sidak's multiple comparisons following 2-way RM ANOVA.

(B) The ratio of BW loss to 24h-BW regain. After fasting, all groups display nearly symmetric weight regain within a day of refeeding.

n = 2-6 mice/group

While the fattening effect of HFD was seen in mice of various ages, there were some age-dependent differences in the initial response to HFD. After commencement of HFD, juvenile groups initially resisted excess weight gain and hyperphagia compared to the chow group (Fig. 2.2A-C,E-G,J,K). It was not until they reached adulthood (>8 weeks of age) that they started to gain weight more rapidly than chow controls. In contrast, adult mice that switched to HFD immediately started to overeat and gain excess BW. This age-dependent difference is due to a higher rate of weight gain and caloric efficiency in chow controls during youth (Fig. 2.2D,H,J,K). Thus, during the juvenile period, homeostatic processes for energy balance may be more tuned to developmental weight gain, which masks the response to energy-dense diet.

If BW set point can be elevated by HFD, it might also be lowered by low-fat diet (LFD). Previous studies have shown that switching from HFD to LFD results in transient hypophagia and rapid weight loss^{247,248}. This may reflect a reversal of the BW set point that was elevated by the preceding HFD. To confirm the effect of switching from an HFD to an LFD (dieting), mice were initially provided with 45FD and then switched to standard chow. To determine whether the duration of 45FD exposure affects the effectiveness of subsequent dieting, the 45FD feeding period was varied from 4 to 24 weeks (4 weeks: 4w45FD-diet; 8 weeks: 8w45FD-diet; 24 weeks: 24w45FD-diet).

All groups of mice fed 45FD, regardless of feeding duration, quickly lost weight upon switching to chow (Fig. 2.5A). This was characterized as a drastic reduction in the rate of BW change, caloric intake and efficiency at the start of

dieting, which gradually decayed to the level of chow controls (Fig. 2.5B-D). This acute hypophagia was attenuated by prolonged 45FD exposure (24 weeks; Fig. 2.5F). However, there was no significant difference in BW change or caloric efficiency between the groups (Fig. 2.5E,G). Interestingly, we found that a significant predictor of initial BW lost upon dieting (first week of chow feeding) was how heavy pre-dieting 45FD mice were compared to age-matched chow-fed controls i.e. the difference between putative BW set point of 45FD and chow groups (Fig. 2.5H). This is consistent with the idea that the main driving force for BW loss is the mismatch in the levels of BW set point between 45FD and chow.

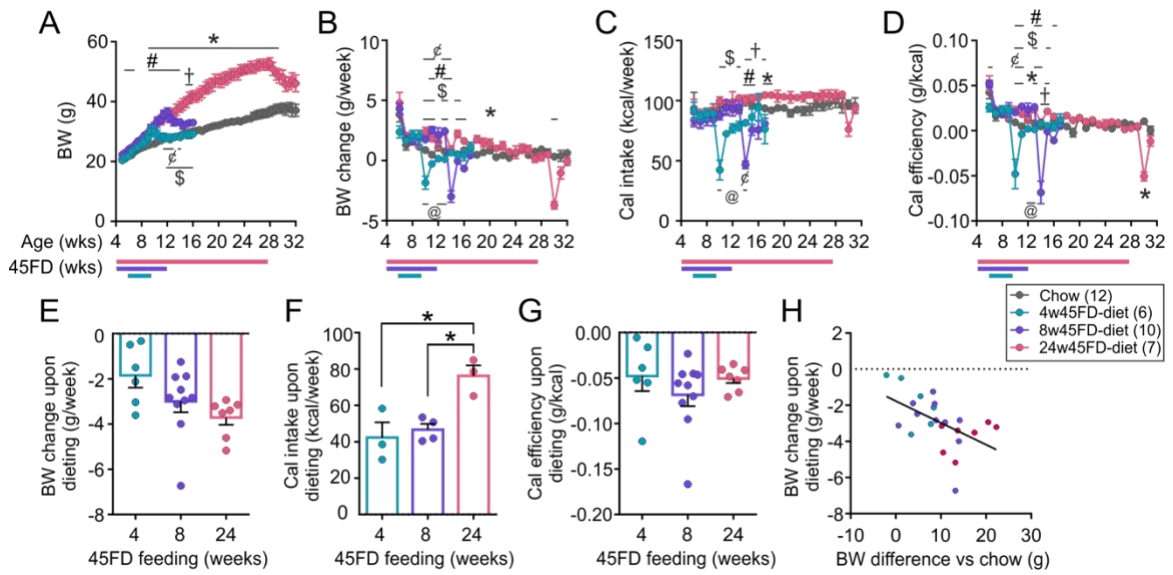


Figure 2.5. Diets lowers the defended body weight

(A) BW of mice fed 45FD for 4, 8 or 24 weeks and then switched to chow (4w45FD-, 8w45FD-, and 24w45FD-diet, respectively). Chow controls are shown for comparison.

(B) Weekly BW change of the mice in (A), showing that switching from 45FD to chow induces a transient BW loss, which recovers to chow control levels within a few weeks.

(C, D) Caloric intake (C) and efficiency (D) of mice shown in (A).

For panels A-D, * $p < 0.05$ for chow vs 24w45FD-diet; # $p < 0.05$ for chow vs 8w45FD-diet; @ $p < 0.05$ chow vs 4w45FD-diet; \$ $p < 0.05$ for 4w45FD-diet vs 24w45FD-diet; † $p < 0.05$ for 8w45FD-diet vs 24w45FD-diet; ¢ $p < 0.05$ for 8w45FD-diet vs 4w45FD-diet. Sidak's multiple comparisons following two-way RM ANOVA. n is indicated in parentheses after group ID.

(E-G) BW change (E), caloric intake (F), and efficiency (G) during the first week

upon switching to chow (dieting) after various durations of 45FD feeding.

* $p < 0.05$, Tukey's multiple comparisons following one-way ANOVA.

(H) Relationship between the initial BW change upon dieting (first week of chow consumption) and the difference between the pre-diet BW of 45FD-fed mice and the average BW of chow-fed control mice. Simple linear regression $R^2 = 0.2698$, $p < 0.05$.

For panels E-H, $n = 6-10$ mice/group

Since there were some differences detected in the effect of 45FD and WD on BW, we tested the effect of dieting after WD consumption. Mice were fed WD for 24 weeks (24wW-diet) or 8 weeks starting from 4 weeks of age (Juv-8wW-diet). As an age control, another group was matched to the age of the 24wW-diet group but only received WD for 8 weeks (Adult-8wW-diet). After WD feeding, all groups were switched to chow, resulting in rapid weight loss accompanied by a sharp decrease in caloric intake and efficiency, which decayed and eventually plateaued at control levels after several weeks (Fig. 2.6A-D). Weight loss was efficient in the Juv-8wW-diet group, while significantly attenuated in the 24wW-diet group (Fig. 2.6A,B,E). This was not due to age, as the Adult-8wW-diet group responded as efficiently as the Juv-8wW-diet group (Fig. 2.6A-G).

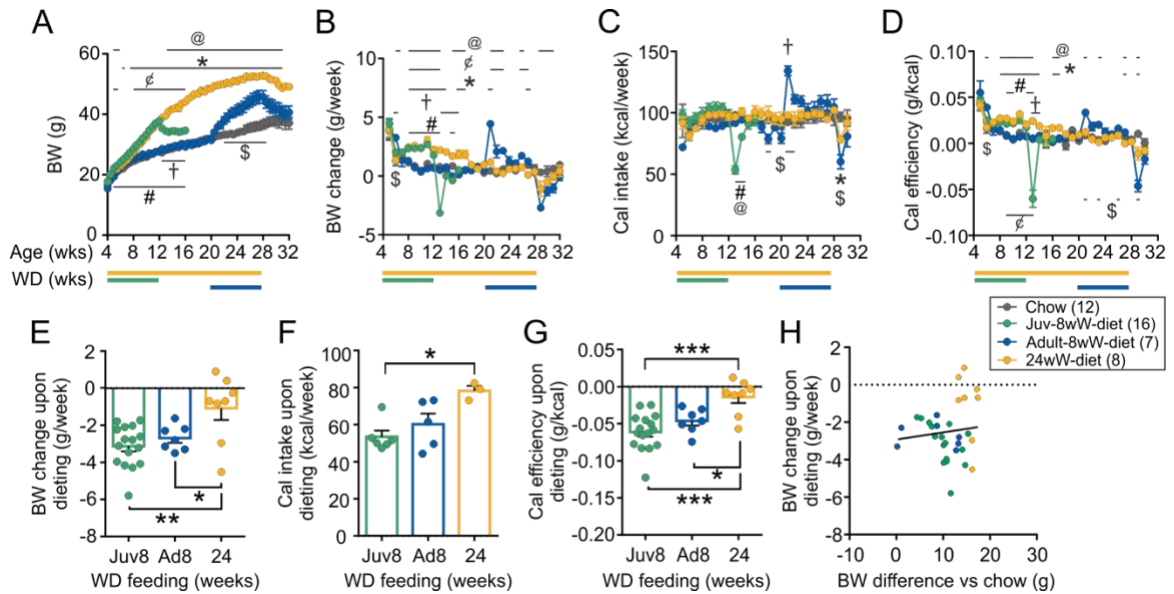


Figure 2.6. Chronic exposure to high-fat/high-sugar diet disrupts body weight regulation

(A) BW of mice fed WD for 8 or 24 weeks, and then switched to chow for 4 weeks. 8-week WD groups were either juvenile (Juv-8wW-diet) or adult (Adult-8wW-diet) at the start of WD period. 24wW-diet group was juvenile when WD started and ended WD concurrently as Adult-8wW-diet group. Chow controls are shown for comparison.

(B-D) Weekly BW gain (B), caloric intake (C) and efficiency (D) of mice shown in (A).

For panels A-D, * $p < 0.05$ for chow vs 24wW-diet; # $p < 0.05$ for chow vs Juv-8wW-diet; \$ $p < 0.05$ for chow vs Adult-8wW-diet; @ $p < 0.05$ for 24wW-diet vs Adult-8wW-diet; † $p < 0.05$ for 24wW-diet vs Juv-8wW-diet; ‡ $p < 0.05$ for Juv-8wW-diet vs Adult-8wW-diet. Sidak's multiple comparisons following two-way RM ANOVA. n is indicated in parentheses after group ID.

(E-G) BW change (E), caloric intake (F), and efficiency (G) during the first week upon switching to chow (dieting) after various durations of WD feeding.

* $p < 0.05$, ** $p < 0.01$, *** $p < 0.001$. Tukey's multiple comparisons following one-way ANOVA.

(H) Relationship between the initial BW change upon dieting (first week of chow consumption) and the difference between the pre-diet BW of WD-fed mice and the average BW of chow-fed control mice.

Simple linear regression $R^2 = 0.01228$, $p > 0.05$. For panels E-H, $n = 7-16$ mice/group

Unlike the 45FD dieting groups, the BW change upon dieting did not correlate with the difference in putative BW set point (i.e. pre-dieting BW) between WD- and age-matched chow-fed groups (Fig. 2.6H). Indeed, the slope of the regression lines between mice on the two HFDs were significantly different from one another (Fig. 2.7A). Upon further examination, the correlation was still present after 8 weeks of WD feeding (Juv-8wW-diet), as the slope of the regression line was similar to that of the 8w45FD-diet group (Fig. 2.7B). Meanwhile the slopes became significantly different after 24 weeks of feeding (Fig. 2.7C). Thus, the set point elevated by 45FD or WD is readily reversible by dieting, but this reversibility becomes dampened by chronic WD.

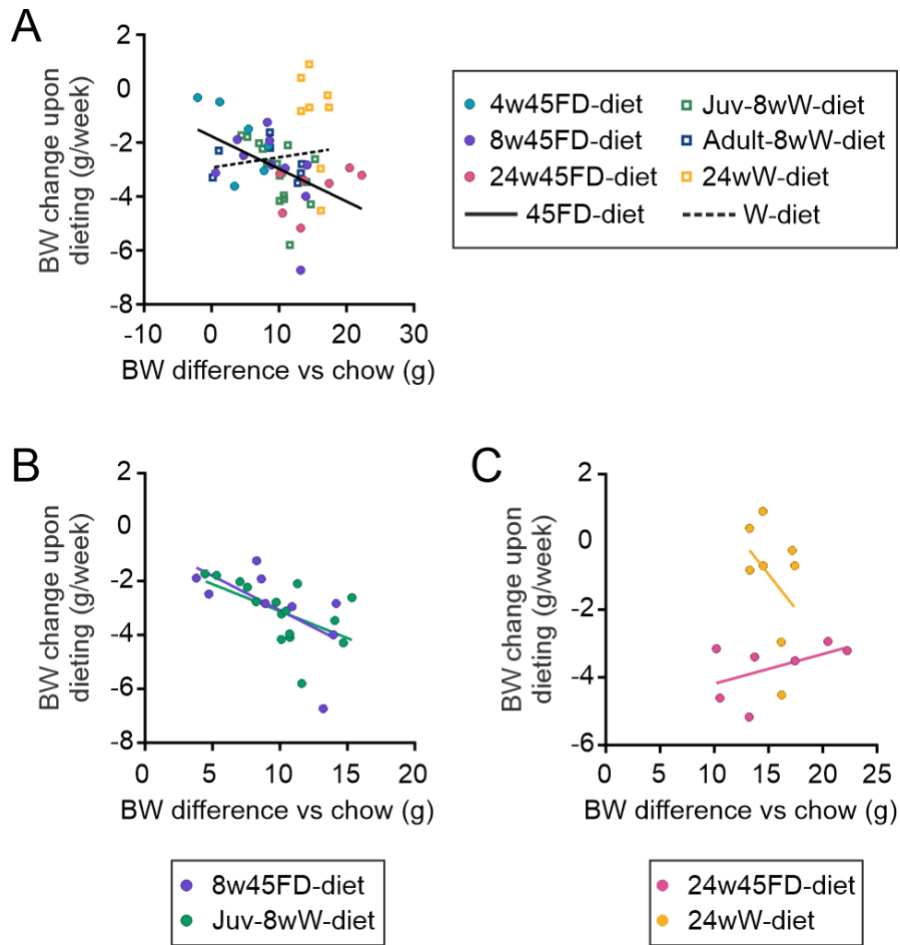


Figure 2.7. Prolonged WD elevates the floor of the homeostatic set point

Relationship between the BW change of HFD-fed mice after 1 week of dieting (switch from HFD to chow) and the difference in the pre-diet BW of HFD mice vs age-matched chow controls.

(A) Results shown in Figure 3H and 4H are reproduced for a direct comparison of the linear regression for mice fed different HFD (45FD vs. WD). n=6-16 mice/group.

(B) Results of mice fed for 8 weeks on 45FD or WD, starting at 3 weeks of age. n=9-16 mice/group.

(C) Results of mice fed for 24 weeks on 45FD or WD, starting at 3 weeks of age. n=7-8 mice/group.

Altogether, these results indicate that there is an interaction between BW set point and food environment, such that the level of defended BW is immediately elevated by HFD and lowered by LFD. Furthermore, the reversal of an elevated set point by LFD is influenced by the type and duration of preceding HFD.

These results led us to investigate what happens during yoyo dieting, where repeated attempts to lose weight through dieting result in cyclic weight loss and regain. To test this, mice were initially maintained on a HFD (45FD or WD) for 8 weeks, and then alternated between chow and HFD for a period of 4 weeks each for two additional cycles. We found that mice cycling between chow and 45FD (45FD-yoyo) showed a similar transient increase in weight gain, caloric intake and caloric efficiency at every chow-to-45FD switch (Fig. 2.8A-D; Fig. 2.9A-C). Caloric intake was increased only at the 2nd and 3rd switch to 45FD (Fig. 2.8C; Fig. 2.9B); this lack of change at the 1st switch may be due to the young age (4 weeks old) at which it occurred. Notably, there was no evidence of accelerated weight gain with repeated dieting cycles. In response to dieting (switch from 45FD to chow), mice lost an equivalent amount of weight at every chow cycle, and caloric intake and efficiency were also approximately the same between dieting cycles (Fig. 2.8A-D; Fig. 2.9D-F). When this alternating diet was tested with a more palatable WD (WD-yoyo), we observed a similar pattern, where BW change, caloric intake and efficiency were elevated after the 2nd and 3rd switches from chow to WD without acceleration with repeated cycles (Fig. 2.8E-H; Fig. 2.9G-I). In contrast to 45FD, however, subsequent switches from

WD to chow resulted in a significant attenuation of the initial BW lost, hypophagia and caloric efficiency with repeated cycles (Fig. 2.8E-H; Fig. 2.9J-L).

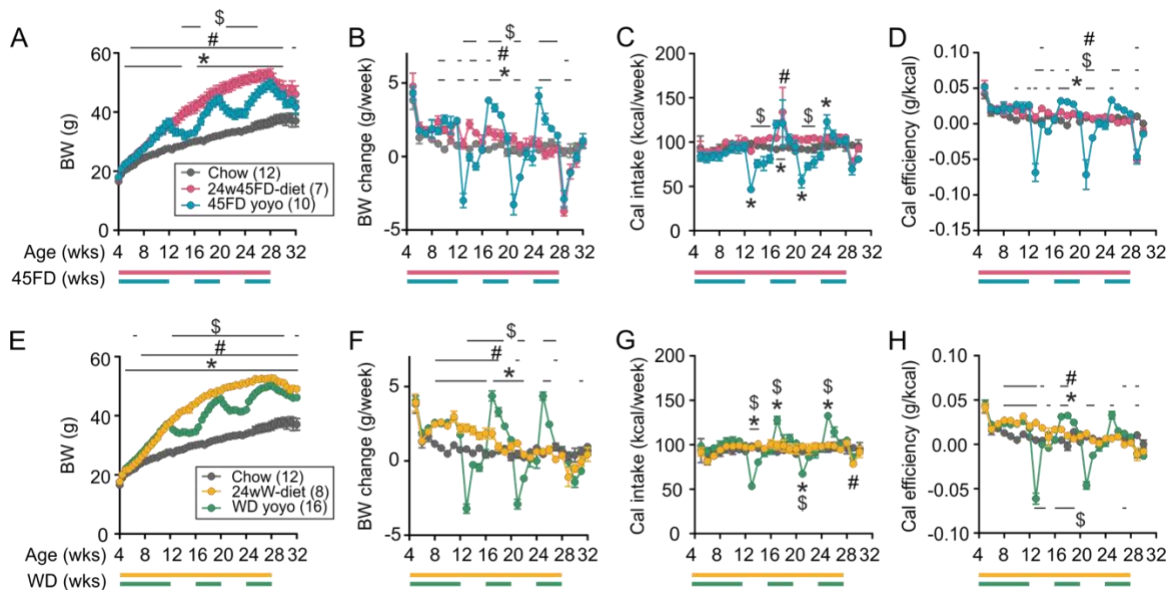


Figure 2.8. Effect of diet cycling on body weight control in HFD-induced obesity

(A-D) BW (A), weekly BW change (B), caloric intake (C) and efficiency (D) of mice fed an alternating diet of 45FD and chow (45FD yoyo). Chow control and a single diet group (24w45FD-diet; 24 weeks of 45FD then switched to chow) are shown for comparison. Bars with corresponding colors below the graph indicate the 45FD feeding period. * $p < 0.05$ for chow vs 45FD-yoyo; # $p < 0.05$ for chow vs 45FD-diet; \$ $p < 0.05$ for 45FD-diet vs 45FD-yoyo. Sidak's multiple comparisons following two-way RM ANOVA. n is indicated in parentheses after group ID.

(E-H) BW (E), weekly BW change (F), caloric intake (G) and efficiency (H) of mice fed an alternating diet of WD and chow (WD yoyo). Chow control and a single diet after 24 weeks of WD (24wWD-diet) are shown for comparison.

* $p < 0.05$ for chow vs WD-yoyo; # $p < 0.05$ for chow vs WD-diet; \$ $p < 0.05$ for WD-

diet vs WD-yoyo. Sidak's multiple comparisons following two-way RM ANOVA. n is indicated in parentheses after group ID

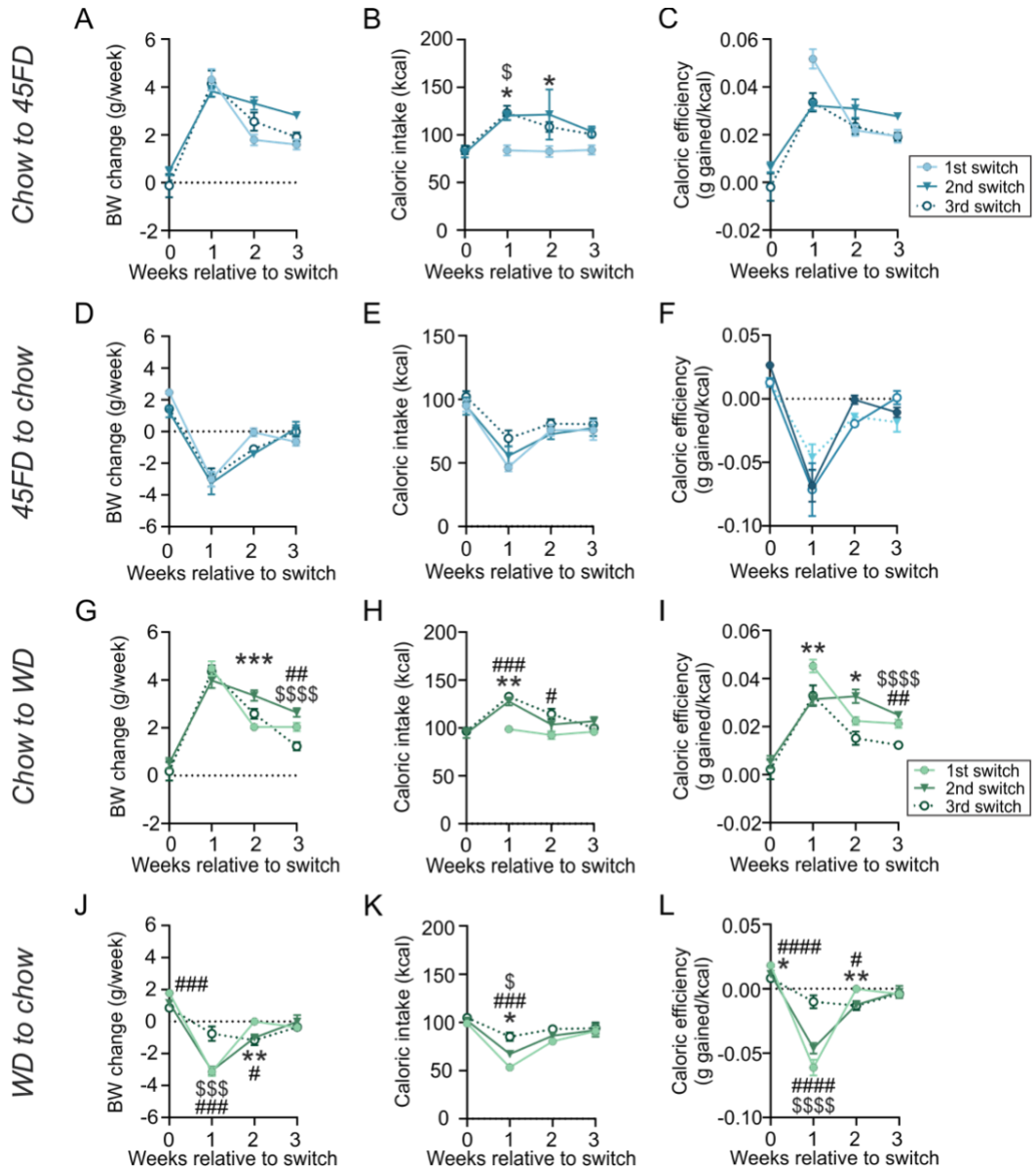


Figure 2.9. Effect of diet cycling on body weight control in 45FD-induced obesity

(A-F) Weekly BW change (A,D), caloric intake (B,E) and efficiency (C,F) before and after each diet switch. Diet switch occurred at week 0, from chow to 45FD (A-

C) or from 45FD to chow (D-F). Data displayed correspond to the 45FD-yoyo group in Figure 5. n=10 mice.

(G-L) Weekly BW change (G,J), caloric intake (H,K) and efficiency (I,L) before and after each diet switch. Diet switch occurred at week 0. Diet was switched from chow to WD (G-I) or from WD to chow (J-L).

Data displayed correspond to the WD-yoyo group in Figure 5.

*p<0.05, **p<0.01, ***p<0.001 for 1st switch vs 2nd switch; #p<0.05, ##p<0.01, ###p<0.001, ####p<0.0001 for 1st switch vs 3rd switch; \$p<0.05, \$\$\$, p<0.001, \$\$\$\$p<0.0001 for 2nd switch vs 3rd switch. Sidak's multiple comparisons test following two-way RM ANOVA. n=16 mice.

To determine how the history of dieting or type of diet influenced the efficacy of dieting, a direct comparison of the 3rd dieting period of the yoyo dieters and age-matched single dieters (24 weeks of HFD followed by a switch to chow) was performed. For both 45FD and WD, there were no apparent differences in the effect of yoyo and single dieting on caloric intake and efficiency (Fig. 2.8C-D, G-H). Overall, all groups displayed a significant BW reduction upon chow intervention (Fig. 2.10A). Nevertheless, there was a significant main effect of the type of dieting, with yoyo dieters being lighter than their single-dieting counterparts (Fig. 2.10A), although there were no significant differences in the weight lost over 4 weeks between the dieting groups (Fig. 2.10B). Moreover, there was a clear main effect of the type of HFD, where dieting was more effective after 45FD than after WD (Fig. 2.10A,B).

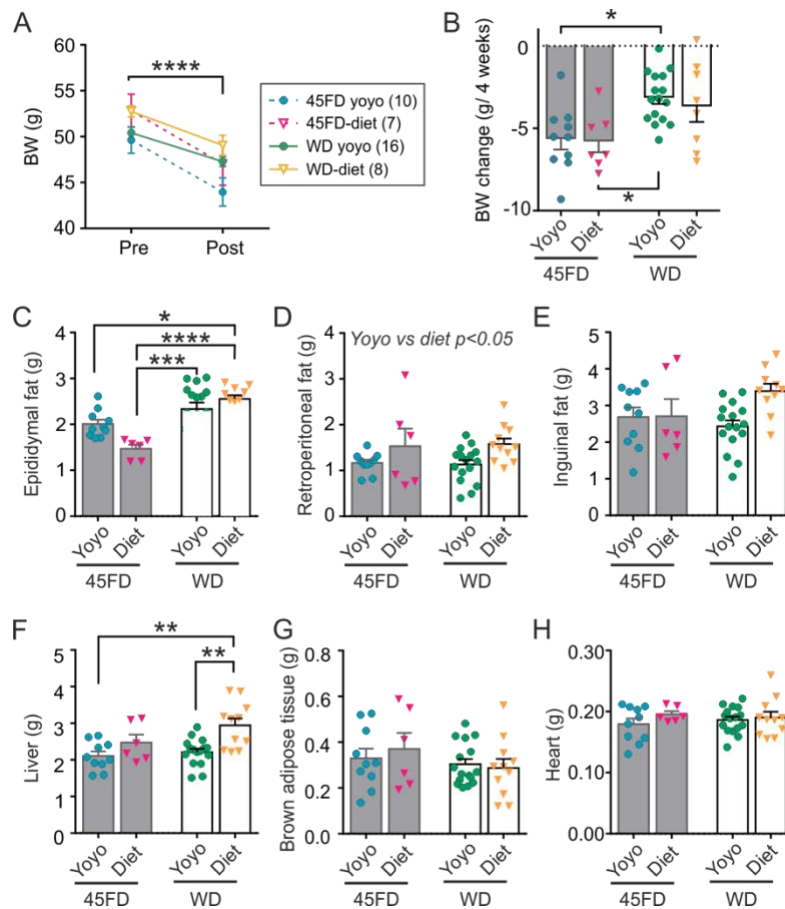


Figure 2.10. Comparison of diet cycling and single dieting

(A) Pre- and post-dieting BW of mice from diet cycling (45FD yoyo; WD yoyo) and single diet (45FD-diet; WD-diet) groups shown in Figure 5. Pre-dieting BW: at 28 weeks of age, just prior to the final switch from either 45FD or WD to chow (3rd switch for the yoyo groups); post-dieting BW: after 4 weeks on chow at 32 weeks of age. **** $p < 0.001$. Tukey's multiple comparisons following 3-way ANOVA. n is indicated in parentheses after group ID.

(B) Total BW change during the final 4-week dieting bout for the mice shown in A. * $p < 0.05$, Tukey's multiple comparisons following 2-way ANOVA. n = 7-16 mice/group.

(C-H) Weight of various organs after the feeding paradigm, as indicated. * $p < 0.05$, ** $p < 0.01$, *** $p < 0.001$, **** $p < 0.0001$. Tukey's multiple comparisons following 2way ANOVA. n = 6-16 mice/group

We also assessed dietary fat-sensitive organs to determine whether they were affected by the type of HFD or dieting method. The size of the epididymal fat pad was significantly affected by the type of HFD, with WD-fed mice having a greater fat mass after dietary intervention (Fig. 2.10C). On the other hand, the retroperitoneal fat pad and liver were more effectively reduced by yoyo dieting than single dieting (Fig. 2.10D,F). No significant differences were detected in other organs surveyed (Fig. 2.10E,G,H).

Together, these results indicate that both the type of HFD and the method of dieting are important factors. There is some benefit of yoyo dieting on the long-term regulation of BW. However, the benefit on organ weights is diminished depending on the type of HFD eaten.

2.4. *Discussion*

Our study found that diets with $\geq 40\%$ fat induce DIO while those with $\leq 25\%$ fat do not, which is consistent with a previous study showing that the threshold of dietary fat content for inducing excess weight gain is 25%²⁴⁹. However, 25FD is not without effect as the epididymal fat pad, one of the most obesity-responsive visceral adipose tissue²⁵⁰, showed a dose-dependent increase. We found that the major difference between the diets is the ability of HFD to immediately but transiently accelerate weight gain, caloric intake and efficiency upon commencement. Following this transition phase, these heightened energy balance measures gradually decay so as not to overshoot the eventual BW plateau. In our study, this pattern was remarkably consistent across

groups of adult mice fed HFD. Specifically, mice on diets with $\geq 40\%$ fat (45FD, 60FD, WD) displayed a similar steady-state BW respective of their age, despite the differences in fat content and palatability of these diets. Notably, the level of BW plateau was not affected by the duration of HFD or the age that HFD feeding started. Furthermore, the higher BW was well-defended against acute negative energy balance induced by fasting. These direct comparisons of diets with differential palatability, fat content and energy density, and feeding periods support the idea that BW is homeostatically regulated even under HFD conditions, when a higher set point is defended.

We have shown that high-fat, high-sucrose WD and high-fat, moderate-sucrose diets (45FD and 60FD) induce similar weight gain and energy expenditure, similar to some previous studies²⁵¹, while others have found 45FD and 60FD to be more obesogenic than WD^{252,253}. The reason for this discrepancy is unclear, but it is unlikely due to sub-strains of mouse models used. Our lab and Dr. Bodine's group²⁵³ obtained different results while using the NIH strain of C57BL/6 mice (C57BL/6N) from Charles River. However, in their study, BW difference between 45FD- and WD-fed mice was significant yet modest. It is possible that differences in housing conditions such as temperature and humidity could cause minor differences in experimental outcomes. It has also been shown that BW plateau of DIO mice can be further elevated by supplementing HFD with a liquid diet Ensure²⁴⁰. Nevertheless, once a steady-state was reached, the rate of BW gain in their HFD-fed mice with or without Ensure was identical. Thus, the BW set point may be altered in a graded fashion depending on the type of diet.

While the present study did not directly assess energy expenditure, previous studies found that energy expenditure is lowered during chronic HFD compared to chow^{240,251}. Thus, mice show a coordinated behavioral and metabolic response to alterations in dietary fat through concurrent changes in energy intake and expenditure, consistent with previous models²⁵⁴.

This elevation of the BW set point is reversible by switching from HFD back to LFD. This is strongly supported by the magnitude of initial weight lost upon a switch to chow being significantly correlated with the difference in putative BW set point defined by HFD and chow conditions. In other words, a diet switch creates a mismatch between the actual BW and BW set point for the respective diet, which is the driving force for BW changes. However, this reversal becomes more difficult as HFD feeding persists, especially with WD. This attenuation may be explained by many lasting changes that are induced by extended consumption of HFD, which may include, but are not limited to, adipose tissue expansion²⁵⁵, increased pancreatic islets²⁵¹, leptin and insulin resistance²⁵⁵, inflammation within the brain and peripheral organs⁶⁴, neuroplasticity in the energy balance and reward circuitries^{239,256,257}, and changes in the intestinal microbiome²⁵⁸. Thus, the history of HFD consumption could interact with energy homeostatic mechanism to result in the elevated floor of the homeostatic set point²⁴⁰.

While there is a stark similarity in the effect of different HFDs on long-term BW, differences between 45FD and WD also emerged through our study, despite similar fat contents (45% vs. 40%). A switch from chow to a HFD induced a transient hyperphagia, which was more pronounced with WD than 45FD. This

may reflect an inherent preference for the more palatable WD – a hedonic mechanism overriding the homeostatic mechanism. The subsequent decay in food intake seen in both 45FD and WD may be explained by HFD-induced reduced motivation for food reward ²⁵⁹. Furthermore, spontaneous hypophagia upon switching from HFD to chow may be due to negative contrast of the diets ²⁶⁰. However, these factors are unlikely to affect caloric intake over the course of several weeks ^{261,262}. Another notable difference between the two HFDs is in the weight loss effect of repeated dieting, which was severely attenuated with WD→chow cycling, but not in 45FD→chow cycling mice. This suggests that the type of HFD eaten prior to dieting affects the efficacy of dieting, which may be explained by different types of fats producing distinct hypothalamic inflammatory responses, whole body oxidative stress, and adiposity ^{252,263}. Moreover, the higher sucrose content of WD may play a role, as high-sucrose HFD has been shown to induce intense astrogliosis in the arcuate nucleus ²⁶⁴.

Our study suggests that diet cycling is better than not dieting at all for long-term BW regulation, consistent with previous reports ^{258,265}. Further, yoyo groups showed better organ weight profiles than single dieting groups, suggesting that diet cycling may have cumulative benefits on organ weights compared to single dieting. However, weight cycling has been associated with poorer metabolic profiles, cardiovascular health, abnormal eating patterns, and reduced locomotion in rodents and humans ^{266–271}. Thus, a lower BW and adiposity may not necessarily equate to better health.

2.5. Conclusions

Our study strongly suggests that dietary fat per se induces energy imbalance by increasing the defended BW, indicating that diets high in fat elevate the set point. One potential alternative to this idea is the presence of pre-existing set points for different food environments in each animal, which are revealed by different diets. This would explain the immediate response to diet switches and the strikingly consistent BW defended by mice on different HFD feeding regimens. Nonetheless, the difference between the actual BW and the set point is the driving force for the autonomic and behavioral responses that favor weight gain. Motivated, goal-oriented behaviors are part of compensatory responses to various homeostatic pressures^{272,273}, therefore, it is reasonable to assume this is also the case for energy homeostasis. That is, the reward mechanisms can be engaged to accelerate weight gain as part of a homeostatic response to an HFD-induced elevation in set point. This model can integrate homeostatic, hedonic and cognitive feedback mechanisms that regulate food intake and BW²⁷⁴. After the mismatch between the actual BW and the new set point is resolved, resulting DIO would be in a state of energy balance. While the new set point is reversible by LFD, this reversibility diminishes with chronic exposure to HFD, which could in part explain the commonly observed resistance to weight loss or post-dieting weight regain.

The current study used male C57BL/6N mice as a model and the results may not be entirely generalizable. For example, some rat studies showed little to no BW loss after switching from HFD to LFD²⁷⁵, while other studies showed rapid

weight loss in both rats and mice upon removal of HFD like our study ^{265,267,276}. Therefore, caution should be exercised to apply this concept to other strains or species, as BW regulation is undoubtedly under the influence of genetics and other variables. Individual variations observed in the human population underscore the diverse factors that affect BW. Moreover, mice in the present study were not given dietary choice, which is known to contribute to excess caloric intake [²⁷⁷ but see ²⁷⁸]. Nevertheless, human studies have shown that moving from a dietary specific region to one that contains a western-style diet alters the likelihood of being overweight ²⁷⁹, which may be associated with dietary change. Our animal model recapitulates such a shift in diet changing the BW set point. Thus, animal models are useful for mechanistic investigation of energy homeostasis under well-controlled environmental and genetic parameters, which enable us to draw direct conclusions. Our study supports a novel concept of BW regulation and offers a characterized animal model that could be useful for future investigations.

**Chapter 3 – Prostaglandin E₂ activates melanin-concentrating hormone
neurons to drive diet-induced obesity**

Adapted from

Lisa Z. Fang et al., Prostaglandin E₂ activates melanin-concentrating hormone
neurons to drive diet-induced obesity. *Proceedings of the National Academy of
Sciences of the United States of America* **120**, e2302809120 (2023). doi:
10.1073/pnas.2302809120

3.1. Introduction

High-fat diet (HFD) induces inflammation in the hypothalamus^{63,68,280}, which can in turn promote overeating and weight gain, creating a vicious feed-forward cycle underlying diet-induced obesity (DIO)^{67,281}. Curiously, hypothalamic inflammation is better known for causing sickness syndrome associated with disease states, including anorexia and weight loss²⁸². These physiological outcomes depend on the hypothalamus, which coordinates food intake and energy expenditure²⁸³. It remains unclear how the hypothalamic neural circuit senses local inflammation and produce opposing effects on energy balance, namely obesity and sickness-related weight loss.

Melanin-concentrating hormone (MCH) neurons are a key hypothalamic cell population that regulate energy balance. These neurons promote food intake, suppress energy expenditure, and play an integral role in obesity^{125,163,284}. In contrast, these cells are suppressed by inflammatory mediators, speculated to underlie inflammation-induced anorexia during sickness syndrome^{285,286}. However, it is unknown how MCH neurons respond to inflammation associated with obese states.

Prostaglandin E₂ (PGE₂) is a key inflammatory mediator that induces sickness syndrome through its action in the hypothalamus²⁸². Here, we provide evidence that hypothalamic PGE₂ also mediates DIO through modulation of MCH neurons. We found that HFD activates MCH neurons, which is mediated by endogenous PGE₂. Moreover, PGE₂ bidirectionally modulates MCH neurons in a concentration-dependent manner, which could explain how mild hypothalamic

inflammation promotes obesity while inflammatory disease states accompany weight loss. Importantly, disrupting PGE₂ signaling in MCH neurons ameliorates DIO and hepatic steatosis. Thus, the PGE₂ -MCH pathway acts as a direct conduit between the hypothalamic inflammatory milieu and the resultant energy outcome.

3.2. *Materials and Methods*

3.2.1. *Animals*

All animal procedures were approved by the Institutional Animal Care Committee under the guidelines of the Canadian Council on Animal Care. Male Sprague-Dawley rats and C57BL/6NCrl mice were from Charles River (Saint Constant, Quebec, Canada). MCH-Cre;EP2R^{f/+} and EP2R^{ff} mice were crossed to generate MCH-Cre;EP2R^{ff} and EP2R^{ff} mice. MCH-Cre mice were originally generated by Dr. Brad Lowell ²⁸⁷ (Beth Israel Deaconess Medical Center, USA) and kindly provided by Dr. Melissa Chee (Carleton University, Canada). EP2R^{f/+} mice were a gift from Dr. Katrin I. Andreasson ²⁸⁸(Stanford University, USA). Animals were housed in a temperature-controlled room (23°C) with lights on at 8AM-8PM. Food (Table 3.1) and water were available *ad libitum*.

Table 3.1. Diet macronutrient composition

Diet	Product name	Company	Macronutrient (kcal %)		
			Fat	Carbohydrates	Protein
Chow	Prolab RMH 3000	LabDiet*	14.377	26.126	59.497
WD	D12079B	Research Diets Inc**	40	43	17
HFMS	D12451	Research Diets Inc	45	35	20
LFHS	D12450B	Research Diets Inc	10	70	20

*LabDiet (St. Louis, MO, USA), **Research Diets Inc (New Brunswick, NJ, USA)

3.2.2. *In-vitro electrophysiology*

Animals were anesthetized with 4% isoflurane and the brain removed to generate 250- μ m slices using a vibratome (VT1000 S, Leica Microsystems) in cold artificial cerebrospinal fluid (ACSF; in mM: 126 NaCl, 2.5 KCl, 1.2 NaH₂PO₄, 1.2 MgCl₂, 2 CaCl₂, 18 NaHCO₃, and 2.5 glucose). Brain slices were incubated at 32-34°C in ACSF or a recovery solution (in mM: 93 N-methyl-D-glucamine (NMDG), 2.5 KCl, 1.2 NaH₂PO₄, 10 MgSO₄, 0.5 CaCl₂, 30 NaHCO₃, 20 HEPES, 25 glucose, 5 Na-ascorbate, 2 thiourea and 3 Na-pyruvate) for 30 min, then at room temperature. For K⁺-free ACSF, KCl was replaced with equimolar NaCl. All extracellular solutions were bubbled with 95% O₂/5% CO₂.

For whole-cell recording, brain slices were perfused with ACSF at 27-30°C, while large neurons within the lateral hypothalamus were identified using infrared-differential interference contrast (DM LFSA, Leica Microsystems). Glass recording electrodes were filled with internal solution (in mM: 123 K-gluconate, 2 MgCl₂, 1 KCl, 0.2 EGTA, 10 HEPES, 5 Na₂ATP, 0.3 NaGTP, 2.7 biocytin) except for high-internal Na⁺ experiments where 30 mM K-gluconate was replaced with equimolar Na-gluconate.

Data were recorded using Multiclamp 700B and pClamp 9.2/10.7 (Molecular Devices, Sunnyvale, CA, USA). Current clamp signals were filtered at 10 kHz, voltage clamp at 1 kHz, and digitized at 5-10 kHz. Measured membrane potentials were corrected for liquid junction potential (14.9 mV). For voltage ramp experiments, cells were ramped from -90 to -30 mV over 3 seconds.

3.2.3. *Drugs*

Brain slices were incubated with PGE₂ and the PGE₂ EP2 receptor agonist for at least 35 min, while EP receptor antagonists and cyclooxygenase (COX) inhibitors were applied for at least 50 min prior to recording. PGE₂ (Cat# 2296), PF 04418948 (EP2 receptor antagonist; Cat# 4818), L-798,106 (EP3 receptor antagonist; Cat# 11129), BGC 20-1531 (EP4 receptor antagonist; Cat# 5327), butaprost (EP2 receptor agonist; Cat# 13740), SC-560 (COX-1 inhibitor; Cat# 1550), and SC-236 (COX-2 inhibitor; Cat# 3919) were from Tocris Bioscience (Minneapolis, MN, USA). ONO-8711 (EP1 receptor antagonist; Cat# 14070) was from Cayman Chemicals (Ann Arbor, Michigan, USA). Acetaminophen (COX inhibitor; A7085) and H89 (PKA inhibitor; B1427) were from Sigma-Aldrich (Oakville, ON, CA).

The following drugs were perfused through the recording chamber: Ouabain octahydrate (Na⁺/K⁺-ATPase inhibitor; Cat# 03125) and picrotoxin (Cl⁻ channel blocker; P1675) from Sigma-Aldrich (Oakville, Ontario, CA). Tetrodotoxin (Na⁺ channel blocker; T-550) from Alomone Labs (Jerusalem, Israel). D-(-)-2-Amino-5-phosphonopentanoic acid (D-AP5; NMDA receptor antagonist; ab120003) from Abcam (Cambridge, MA, USA), and 6,7-Dinitroquinoxaline (DNQX; non-NMDA receptor antagonist; Cat# 0189) from Tocris Bioscience (Minneapolis, MN, USA).

3.2.4. *Identification of MCH and ORX neurons*

MCH and ORX neurons display distinct electrophysiological characteristics

in response to a series of 600-ms step currents (-200 to +200 pA), serving as highly accurate cell-type markers^{220,289} (Figure 3.1A). For a more thorough descriptions of characteristics, please see section 4.3.2. The neurochemical cell identity was confirmed by post-hoc immunohistochemistry on a subset of cells filled with biocytin during recording (Figure 3.1B).

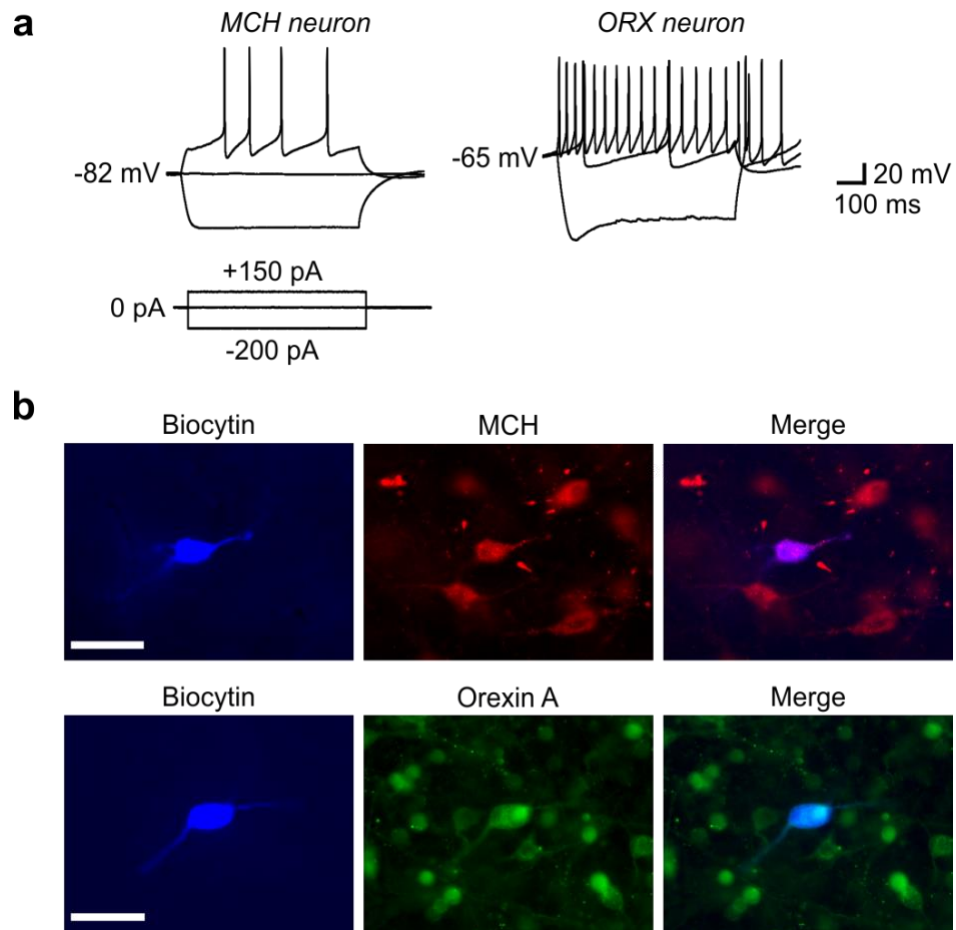


Figure 3.1. Electrophysiological characterization of MCH and ORX neurons.

(A) Representative traces from melanin-concentrating hormone (MCH) and orexin (ORX) neurons in response to positive and negative currents.

MCH neurons are not spontaneously active but fire action potentials upon positive current injections and show strong spike adaptation. Contrastingly, ORX neurons fire spontaneously and display less spike adaptation. ORX neurons also display an H-current and rebound depolarization following relief from hyperpolarization.

(B) Representative post-hoc immunohistochemistry for biocytin (blue), MCH (red), and orexin A (green) to confirm neuropeptide expression of recorded cells. Scale bar = 50 μ m. Cells are filled with biocytin during electrophysiological recording. After recording, brain slices were fixed in 10% formalin overnight, then incubated in goat anti-ORX-A IgG (1:2000; sc-8070, Santa Cruz Biotechnology, Dallas, TX, USA) and rabbit anti-MCH IgG (1:1000-2000; H-070-47, Phoenix Pharmaceuticals, Burlingame, CA, USA) for 3 days at 4°C, followed by appropriate secondary antibodies and AMCA-conjugated streptavidin (1:500; Jackson ImmunoResearch, West Grove, PA, USA) for 2h at room temperature or 1 day at 4°C. Colocalization of biocytin and ORX-A or MCH was observed using an epifluorescence microscope

3.2.5. *Double immunohistochemistry*

Rats were transcardially perfused with 4% paraformaldehyde under isoflurane anesthesia. Brains were post-fixed in paraformaldehyde overnight and sectioned on a cryostat. 16- μm sections underwent antigen retrieval in Na-citrate buffer (pH 6.0) before goat anti-promCH IgG (1:500, sc-14509, Santa Cruz Biotechnology, Dallas, TX, USA) and rabbit anti-EP2R IgG (1:500, 101750, Cayman Chemical, Ann Arbor, MI, USA) were applied overnight at 4°C. Next, Alexa 488-conjugated anti-goat IgG (1:500, A-11055, Invitrogen, Waltham, MA, USA) and Alexa 594-conjugated anti-rabbit IgG (1:500, A-21207, Invitrogen, Waltham, MA, USA) were applied for 2h at room temperature. Sections were imaged on an inverted fluorescence microscope (Axio Observer Z1 with Apotome 2, Carl Zeiss Ltd.). Brightness and contrast of images were adjusted using PaintShop Pro 2018 (Corel Corporation, Ottawa, Ontario, Canada).

3.2.6. *Adipose and liver histology and analysis*

White adipose and liver tissues were dissected after sacrifice and fixed in 10% neutral buffered formalin for at least 24h. Fixed tissues were paraffin-embedded, sectioned at 5- μm and H&E stained.

For adipocyte analysis, brightfield images of epididymal fat were acquired using inverted light microscope. The area of individual adipocytes was determined using ImageJ Adiposoft²⁹⁰ for >100 adipocytes per animal. Brightfield images of the liver were taken using an imaging reader (Cytation 5, BioTek, Winooski, VT, USA). Colorized images were converted to 8-bit before

applying a threshold to generate a binary image using ImageJ by an experimenter blind to the genotype. A morphometric particle analysis was performed in ImageJ to assess lipid droplet size²⁹¹. Prior to the analysis, a pilot study was conducted on hematoxylin and eosin (H&E)-stained liver histology images to determine an appropriate minimum particle size and circularity to detect lipid droplets by comparing the binary image to the original color brightfield image. All particles with circularity between 0.40-1.00 and size greater than 20 μm^2 were included. Large structures captured by automated detection that were not lipid droplets (e.g. central vein) were manually excluded. Total lipid area was determined as the percentage of the area analyzed (1.39 mm^2 per mouse).

3.2.7. Data analysis

The number of cells (n) and animals (N) for each experiment are indicated in Supplementary Table 7.2 in the Appendix. All data are represented as the mean \pm SEM. Two-tailed unpaired t-tests, one-way and two-way ANOVA were performed as appropriate using Prism 9 (GraphPad, San Diego, CA, USA) and $p < 0.05$ was considered significant. If ANOVA found significance, appropriate multiple comparison tests were performed.

3.3. Results

3.3.1. High-Fat Diet Depolarizes MCH Neurons

To test the effect of palatable HFD on MCH neurons, male rats were fed Western diet (WD) high in fat and sugar. This resulted in a significantly

depolarized resting membrane potential (RMP) of MCH neurons (Figures 3.2A-B), accompanied by increased firing, a shorter latency to first spike in response to driving currents, and lower threshold (Figures 3.2C-D, 3.3A-B, 3.4A-G). The excitatory effect became apparent at week 4, before the onset of accelerated weight gain, and persisted at least to week 11 (Figures 3.2B-D and 3.5A-B). Interestingly, this excitatory effect was reversible upon returning to chow for 4 weeks (Figure 3.2E), indicating that continued exposure to WD is needed to maintain MCH neurons in a depolarized state.

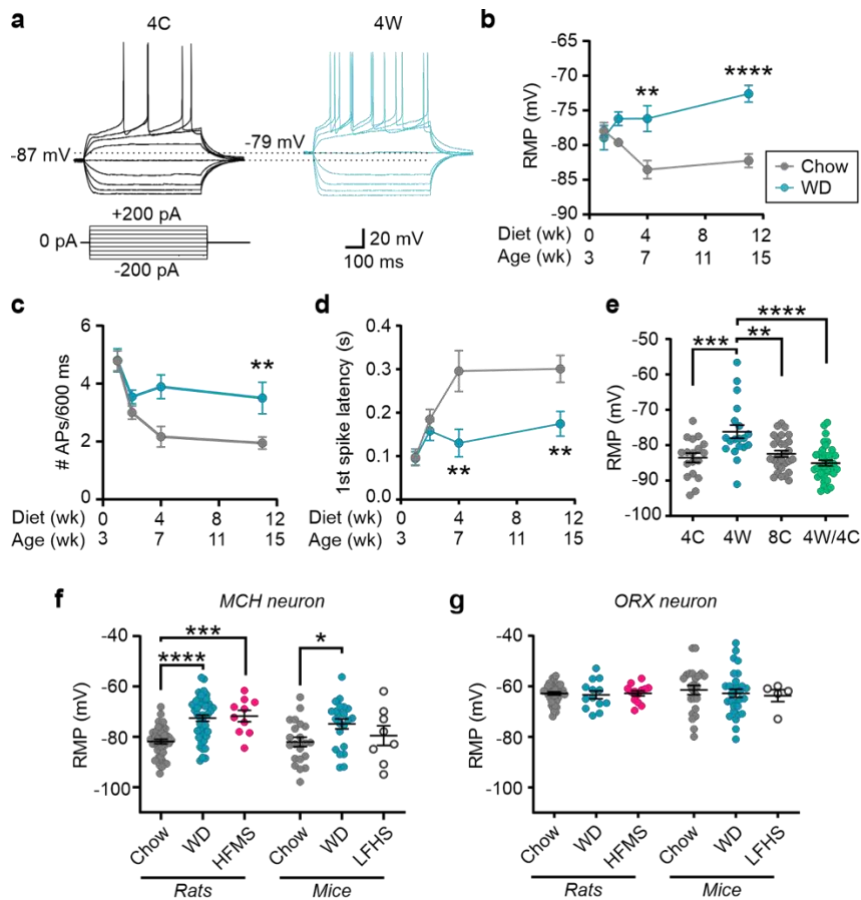


Figure 3.2. Chronic Western Diet (WD) feeding induces a persistent activation of MCH neurons.

(A) Representative traces of rat MCH neurons after 4 weeks of chow (4C) or WD (4W). **(B)** Time course of changes in RMP. **(C-D)** Time course of changes in action potentials fired (#APs) (C), and 1st spike latency (D) during a 600-ms, 100-pA driving current. **(E)** RMP of MCH neurons following various feeding paradigms. 8C: 8-week chow, 4W/4C: 4-week WD followed by 4-week chow. **(F to G)** RMP of MCH (F) and orexin (ORX) neurons (G) from animals fed various diets as indicated. HFMS: high fat/moderate sugar diet, LFHS: low-fat/high-sugar

diet. See Fig. 3.5 for body weight and food intake.

(B-D) Bonferroni multiple comparison, ** $p < 0.01$, **** $p < 0.0001$. (E-G) Tukey's multiple comparison, * $p < 0.05$, ** $p < 0.01$, *** $p < 0.001$, **** $p < 0.0001$.

Details of statistical results can be found in Table 7.2 in the Appendix.

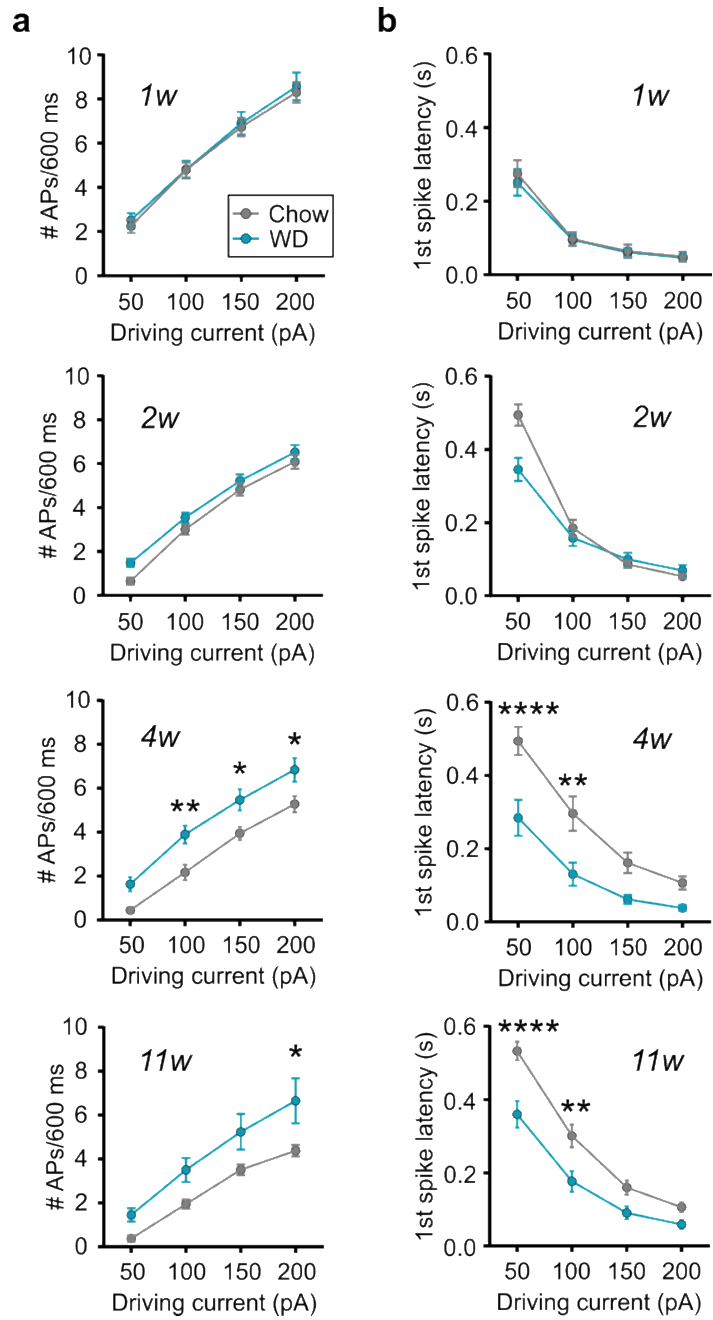


Figure 3.3. Time-dependent WD-induced changes in excitability of MCH neurons.

(A to B) Number of action potentials (APs; A) and 1st spike latency (B) elicited by 600-ms driving currents. Rats were fed chow or WD for 1 to 11 weeks (1w – 11w) as indicated.

Bonferroni multiple comparison: * $p < 0.05$, ** $p < 0.01$, *** $p < 0.0001$ chow vs WD.

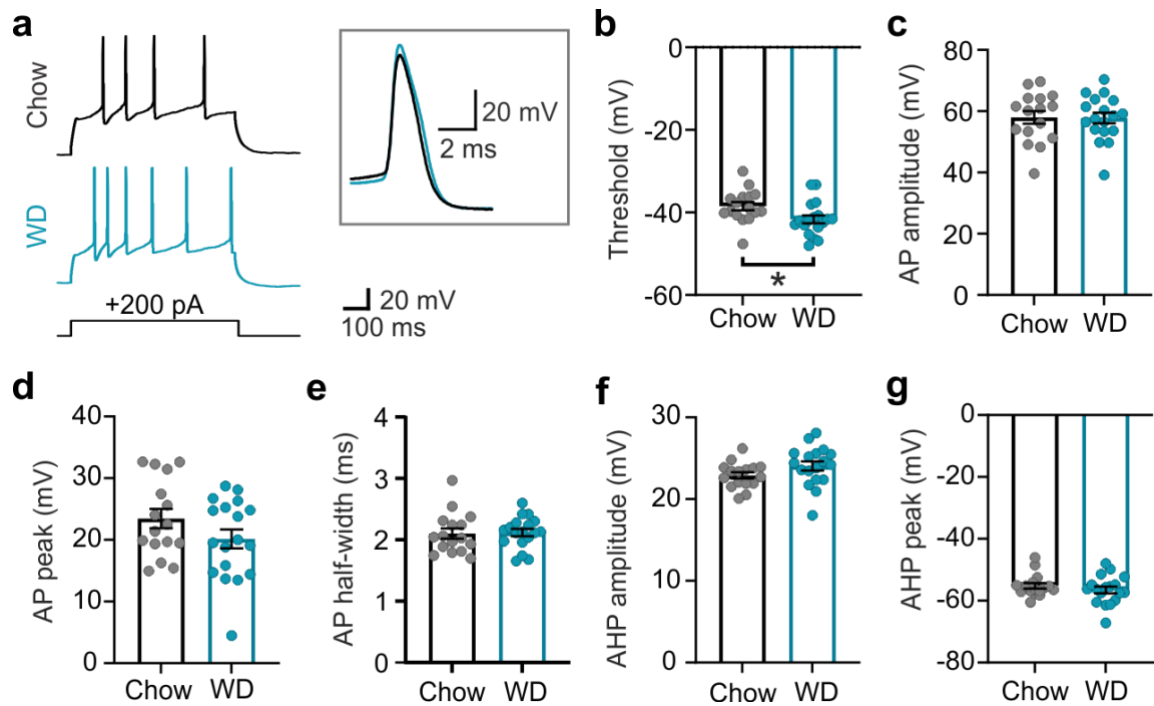


Figure 3.4. The effect of WD on action potential waveform properties of MCH neurons in rats.

(A) Representative current clamp traces from MCH neurons in response to 200-pA current injection in male rats fed chow or WD for 4 weeks. Inset: superimposed, expanded traces of action potentials (AP).

(B to G) Electrophysiological properties of MCH neurons from chow or WD-fed rats including threshold (B), AP amplitude (C), AP peak (D), AP half-width (E), afterhyperpolarizing potential (AHP) amplitude (F), and AHP peak (G). Two-tailed unpaired t-test * $p < 0.05$

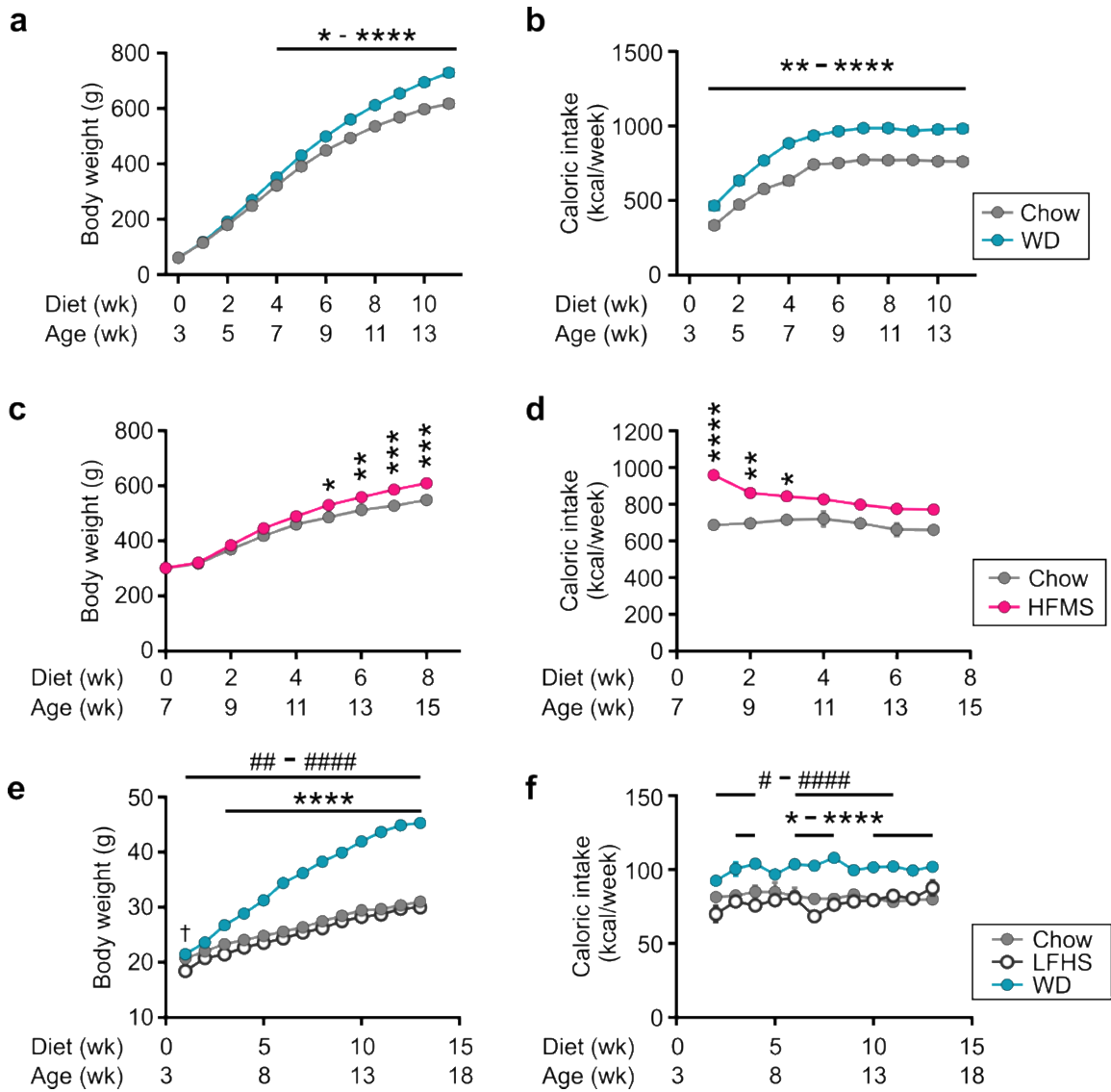


Figure 3.5. Body weight and food intake.

(A to B) Body weight (A) and caloric intake (B) of rats. WD: Western diet (high-fat/high-sugar). Bonferroni multiple comparison: * $p < 0.05$, ** $p < 0.01$, *** $p < 0.001$, **** $p < 0.0001$ chow vs WD.

(C to D) Body weight (C) and caloric intake (D) of rats. HFMS: high-fat/moderate sugar diet. Bonferroni multiple comparison: * $p < 0.05$, ** $p < 0.01$, *** $p < 0.001$, **** $p < 0.0001$ chow vs HFMS.

(E to F) Body weight (E) and caloric intake (F) of mice. LFHS: low-fat/high-sugar diet. Tukey's multiple comparison: * $p < 0.05$, ** $p < 0.01$, *** $p < 0.001$, **** $p < 0.0001$ WD vs chow; # $p < 0.05$, ## $p < 0.01$, ### $p < 0.001$, #### $p < 0.0001$ WD vs LFHS, † $p < 0.05$ chow vs LFHS.

All animals had access to food and water ad libitum. Rats were single housed. C57BL/6NCrl mice were housed in groups of 2-5/cage and total food intake per cage was divided by the number of mice to calculate average caloric intake.

The excitatory effect of WD was also observed in mice (Figure 3.2F). Both the weight gain and the MCH depolarization appear to be due to dietary fat, as a high fat/moderate sucrose (HFMS) diet was equally effective as WD at depolarizing MCH neurons, while a low fat/high sucrose (LFHS) diet was not (Figures 3.2F and 3.5C-F). Orexin neurons, another energy balance-related hypothalamic cell group, did not respond to any of the diets tested in rats and mice (Figure 3.2G). Together, these results indicate that MCH neurons are activated by chronic dietary fat consumption. This activation is selective to MCH neurons and conserved across species.

3.3.2. WD Inhibits Na^+/K^+ -ATPase in MCH Neurons

The effect of WD on RMP of MCH neurons appears to be cell-intrinsic, as it was insensitive to the voltage-gated Na^+ channel blocker tetrodotoxin (1 μ M) or a cocktail of synaptic blockers (50 μ M D-AP5, NMDA receptor antagonist; 10 μ M DNQX, AMPA/kainate receptor antagonist; 50 μ M picrotoxin, GABA_A receptor blocker) (Figure 3.6A). However, membrane resistance did not differ between chow and WD groups or correlate with RMP (Figures 3.7A-C). Thus, differential ion channel activity is unlikely to underlie the difference in RMP.

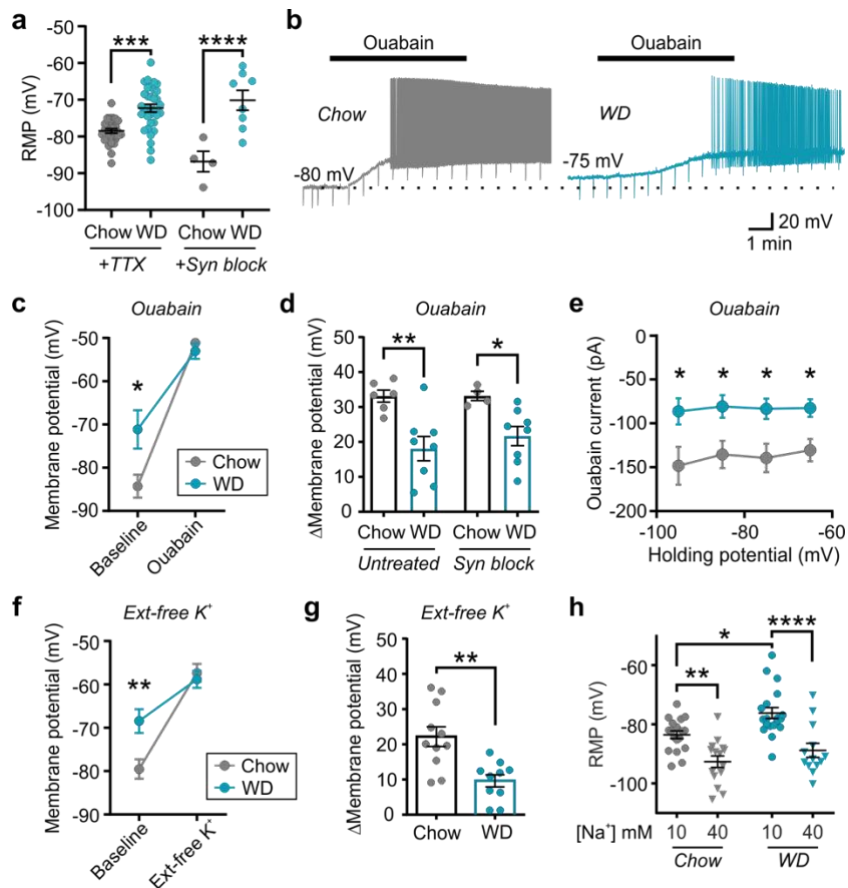


Figure 3.6. WD downregulates Na⁺/K⁺-ATPase in MCH neurons.

(A) RMP of rat MCH neurons in tetrodotoxin (TTX) or synaptic blockers (syn block). **(B)** Representative current clamp recording showing ouabain-induced depolarization. **(C)** Membrane potential before (baseline) and during 25 μ M ouabain. **(D)** Ouabain-induced change in membrane potential with or without synaptic blockers. **(E)** Voltage-current relationship of ouabain-induced current. **(F to G)** Membrane potential before (baseline) and during removal of extracellular K⁺ (Ext-free K⁺, F) and resultant change in membrane potential (G). **(H)** RMP of MCH neurons recorded with 10- or 40-mM intracellular Na⁺.

(A,C-F) Bonferroni multiple comparison: *p<0.05, **p<0.01, ***p<0.001,

**** $p < 0.0001$, chow vs WD. (G) two-tailed unpaired t-test: ** $p < 0.005$. (H) Tukey's multiple comparison: * $p < 0.05$, ** $p < 0.01$, **** $p < 0.0001$.

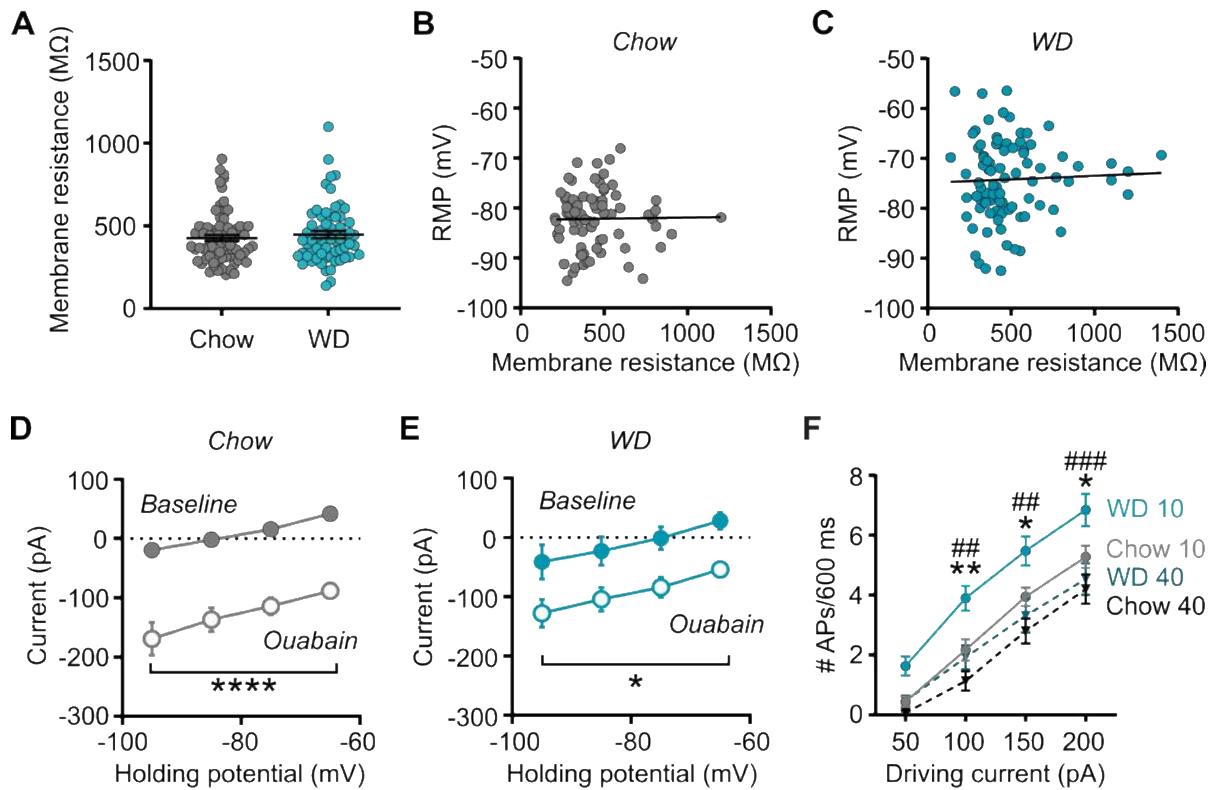


Figure 3.7. WD reduces the Na⁺/K⁺-ATPase activity of MCH neurons.

(A) Membrane resistance of rat MCH neurons under different diets.

(B to C) Correlation analyses between RMP and membrane resistance of MCH neurons under different diets as indicated. Least squares linear regression: chow

(B): $r^2=0.0002358$, $p=0.8946$; WD, (C): $r^2=0.001677$, $p=0.7048$.

(D to E) Voltage-current relationship of the ouabain-induced current in chow (D)

and WD-fed (E) rats. Bonferroni multiple comparison: * $p<0.05$, **** $p<0.0001$

baseline vs ouabain.

(F) Evoked APs recorded with 10- or 40-mM intracellular Na⁺. Tukey's multiple comparison: *p<0.05, **p<0.01 chow vs WD; ##p<0.01, ###p<0.001 WD 10 vs WD 40.

Other contributors to RMP are electrogenic transporters such as Na⁺/K⁺-ATPase. Inhibiting Na⁺/K⁺-ATPase with ouabain (25 μM) induced a significant depolarization of MCH neurons and abolished the difference in RMP between chow and WD groups (Figures 3.6B-D). This ouabain effect was insensitive to synaptic blockade (Figure 3.6D), voltage-independent within the range of membrane potentials tested (Figures 3.6E and 3.7D-E), and mimicked by eliminating extracellular K⁺, which also inhibits Na⁺/K⁺-ATPase activity²⁹² (Figures 3.6F-G). These are consistent with the characteristics of Na⁺/K⁺-ATPase currents, indicating their involvement in the WD-induced RMP depolarization.

If the reduction in the resting Na⁺/K⁺-ATPase activity is due to functional downregulation, intracellular Na⁺ should stimulate its activity and hyperpolarize the membrane²⁹³. Increasing intracellular Na⁺ from 10 to 40 mM significantly hyperpolarized MCH neurons and abolished the WD-induced differences in RMP and firing (Figures 3.6H and 3.7F). Thus, the majority of Na⁺/K⁺-ATPase expressed on MCH neurons are active at rest and contribute to the hyperpolarized RMP under chow conditions. WD functionally downregulates Na⁺/K⁺-ATPase, which can be re-activated by elevated intracellular Na⁺.

3.3.3. *PGE₂ Mediates WD-Induced MCH Activation*

HFD is known to upregulate inflammatory cytokines and prostanoids in the hypothalamus^{63,280}. Furthermore, PGE₂ has been shown to mediate the inhibitory effect of TNFα on hepatic Na⁺/K⁺-ATPase activity²⁹⁴. Thus, we speculated that

PGE₂ mediates the WD-induced Na⁺/K⁺-ATPase inhibition in MCH neurons. If so, PGE₂ should mimic the excitatory effect of WD. To test this, we applied various concentrations of PGE₂ (10 pM – 100 μM) on MCH neurons from chow-fed rats. Surprisingly, this revealed a bidirectional effect where lower concentrations excited, while higher concentrations inhibited MCH neurons (Figures 3.8A-B). To determine how PGE₂ induces these opposing effects, specific antagonists for PGE₂ receptor EP1R (ONO-8711, 1 μM), EP2R (PF04418948, 1 μM), EP3R (L-798,106, 1 μM) and EP4R (BGC20-1531, 1 μM) were tested. We found that the EP3R antagonist blocked the inhibitory effect of 10 μM PGE₂ (Figures 3.8C-D). In contrast, the EP2R antagonist abolished the excitatory effect of 100 pM PGE₂, and an EP2R agonist (butaprost, 1 μM) depolarized MCH neurons (Figures 3.8E-F). Moreover, double immunofluorescence labeling showed colocalization of EP2R with MCH neurons (Figure 3.8G). These results indicate that PGE₂ can mimic WD and directly depolarize MCH neurons through EP2R.

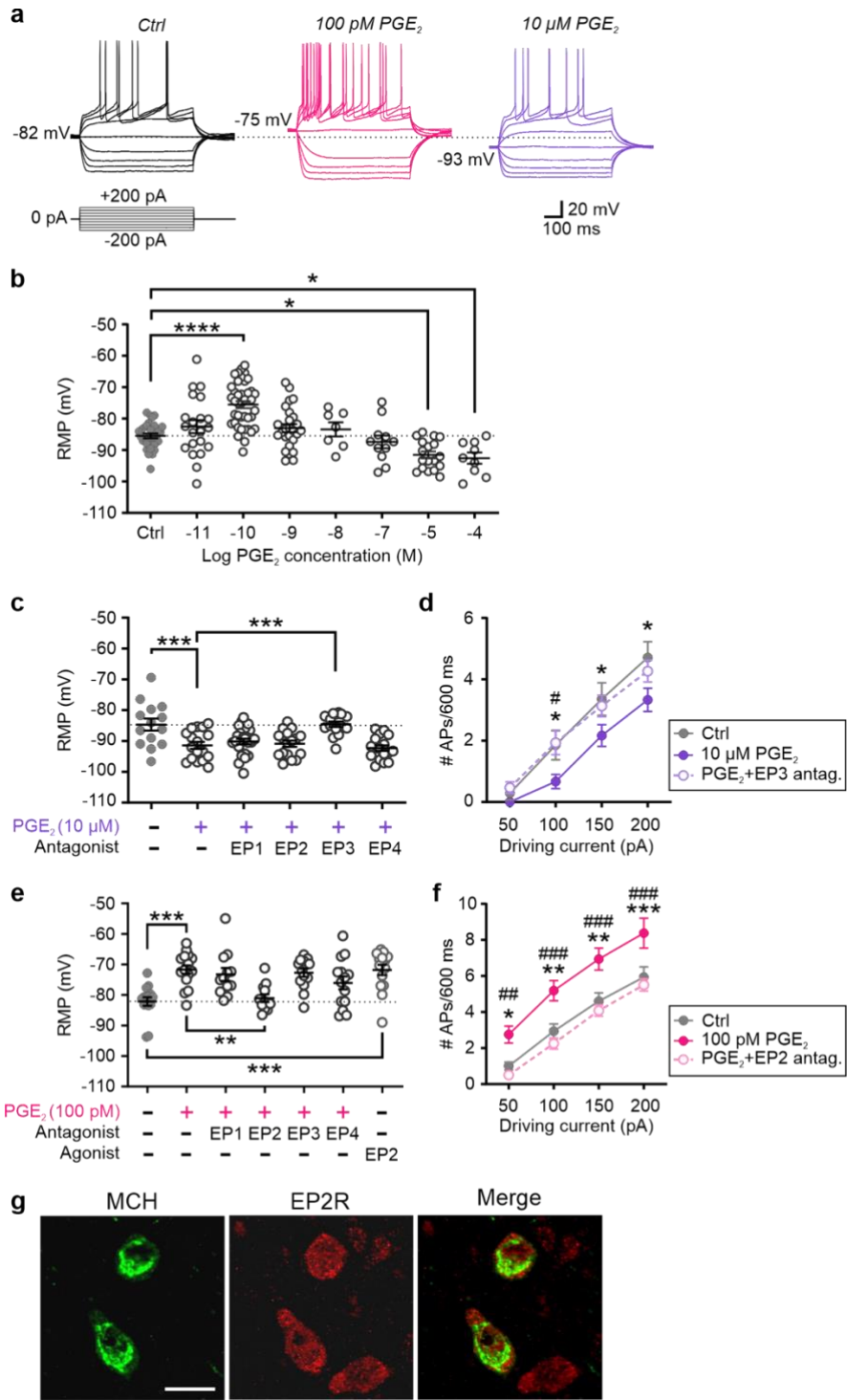


Figure 3.8. PGE₂ bidirectionally modulates the activity of MCH neurons through distinct receptor subtypes.

(A) Representative traces of MCH neurons from chow-fed rat, untreated control (Ctrl) or treated with PGE₂. **(B)** RMP of MCH neurons from chow-fed rats treated with various concentrations of PGE₂ or left untreated (Ctrl). For (B), (C) and (E), dotted horizontal lines denote the mean of untreated control. **(C)** Effect of 10 μM PGE₂ on RMP with or without EP receptor antagonists. **(D)** Evoked APs with 10 μM PGE₂ alone or with EP3R antagonist L-798,106. **(E)** Effect of 100 pM PGE₂ on RMP with or without EP receptor antagonists. **(F)** Evoked APs with 100 pM PGE₂ alone or with EP2R antagonist PF04418948. **(G)** Representative double immunofluorescence images of MCH (green) and EP2R (red) expression in the lateral hypothalamus. Scale bar = 20 μm

(B-C, E) Dunnett's multiple comparisons: *p<0.05, **p<0.01, ***p<0.001, ****p<0.0001 vs Ctrl (left-most column). (D) Dunnett's multiple comparison: *p<0.05, Ctrl vs 10 μM PGE₂; #p<0.05, PGE₂ vs PGE₂+EP3 antagonist. (F) Dunnett's multiple comparison: *p<0.05, **p<0.01, ***p<0.001, Ctrl vs 100 pM PGE₂; ##p<0.01, ###p<0.001, PGE₂ vs PGE₂+EP2 antagonist.

Cyclooxygenase (COX) is a critical enzyme for prostanoid synthesis and may be induced by WD to produce endogenous PGE₂. A non-selective COX inhibitor (acetaminophen, 50 μM) had no effect on chow controls but reversed the effect of WD on RMP and the ouabain-induced depolarization of MCH neurons (Figures 3.9A, C-D). Furthermore, a COX-2 inhibitor (SC-236, 1 μM) blocked the WD-induced depolarization, while a COX-1 inhibitor (SC-560, 5 μM) did not, indicating that WD upregulates the inducible isoform COX-2 (Figure 3.9A). Applying a COX inhibitor indomethacin throughout the brain dissection procedure did not prevent the WD-induced depolarization of MCH neurons (Figure 3.10A), confirming that COX activation is not due to the trauma caused by tissue dissection. These results show that sustained production of endogenous prostanoids is necessary for the persistent depolarization of MCH neurons by WD.

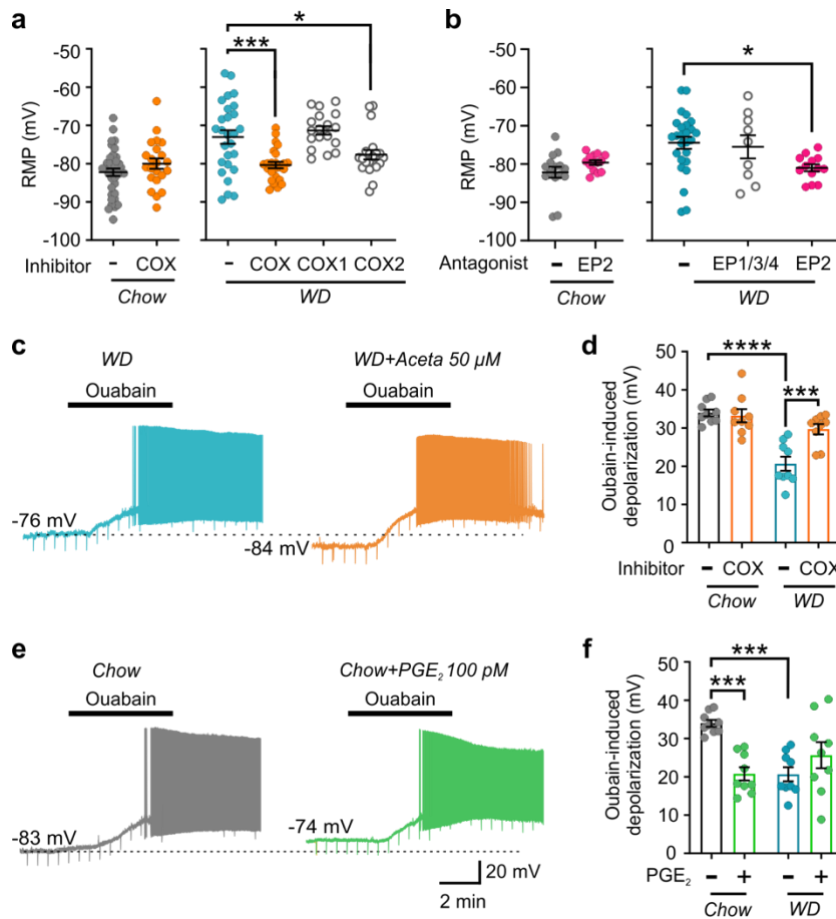


Figure 3.9. PGE₂-EP₂R-mediated inhibition of Na⁺/K⁺-ATPase underlies WD-induced depolarization of MCH neurons.

(A) Effect of COX inhibitors on RMP of MCH neurons. **(B)** Effect of EP receptor antagonists on RMP of MCH neurons. EP_{1/3/4}: a cocktail of EP₁, EP₃ and EP₄ receptor antagonists. **(C)** Representative current clamp traces from WD-fed rat MCH neurons. Aceta: acetaminophen. **(D)** Effect of COX inhibitor acetaminophen on the ouabain-induced membrane depolarization. **(E)** Representative current clamp traces from chow-fed rat MCH neurons. **(F)** Effect of 100 pM PGE₂ on the ouabain-induced change in membrane potential of MCH neurons.

(A-B) Dunnett's multiple comparison: * $p < 0.05$, *** $p < 0.001$ vs WD with no inhibitor

(-). (D, F) Tukey's multiple comparison: *** $p < 0.001$, **** $p < 0.0001$.

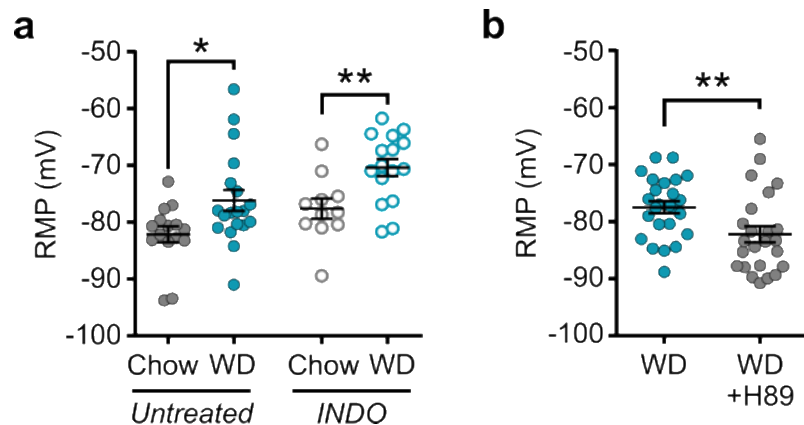


Figure 3.10. WD induces PGE2 signaling to depolarize MCH neurons.

(A) RMP of MCH neurons in rat brain slices, which were generated in the absence (untreated) or presence of the COX inhibitor indomethacin (INDO, 30 μ M) throughout the dissection and slicing. INDO does not prevent the WD-induced RMP depolarization, suggesting that the induction of COX is not due to the trauma of brain dissection.

Bonferroni multiple comparison: * $p < 0.05$, ** $p < 0.01$.

INDO from Sigma-Aldrich (Cat# I7378, Ann Arbor, Michigan, USA) or Tocris Biosciences (Cat# 1708; Minneapolis, MN, USA) was dissolved in saline and intracardially perfused through rats prior to brain sampling under isoflurane anesthesia. Furthermore, INDO was added to ACSF during brain slicing on a vibratome.

(B) PKA inhibitor H89 (10 μ M) hyperpolarizes RMP of MCH neurons from WD-fed rats. Two-tailed unpaired t-test, ** $p < 0.01$

If PGE₂ is the primary endogenous prostanoid induced by WD, it is likely to act through EP2R, which were found to mediate its excitatory effect. Indeed, the EP2R antagonist reversed the WD-induced depolarization of MCH neurons, while other EP receptor antagonists had no effect (Figure 3.9B). Contrastingly, the EP2R antagonist alone had no effect on chow controls (Figure 3.9B). Together with the lack of effect of COX inhibition in chow controls, this suggests that there is no significant PGE₂ production during low-fat diet consumption in the local environment of MCH neurons. 100 pM PGE₂ and WD individually inhibited the ouabain-induced depolarization to the same level, and their effects were not additive, indicating that both PGE₂ and WD act through Na⁺/K⁺-ATPase (Figures 3.9E-F). The WD effect is mediated by protein kinase A (PKA), a downstream effector of EP2R, as a PKA inhibitor H89 reversed the WD-induced depolarization (Figure 3.10B). These results indicate that EP2R signaling activated by WD-induced PGE₂ is responsible for the functional downregulation of Na⁺/K⁺-ATPase and consequent depolarization of MCH neurons.

3.3.4. PGE₂-EP2R Signalling in MCH Neurons Promotes Diet-Induced Obesity in Male Mice

To explore the functional role of EP2R on MCH neurons in energy balance, mice that lacked EP2R in MCH neurons were generated (MCH^{Cre/+};EP2R^{ff}). This knockout (KO) model was validated using an EP2R agonist (butaprost; 1 μM), which increased the excitability of wild type MCH

neurons but not KO MCH cells from male mice (Figures 3.11A-C).

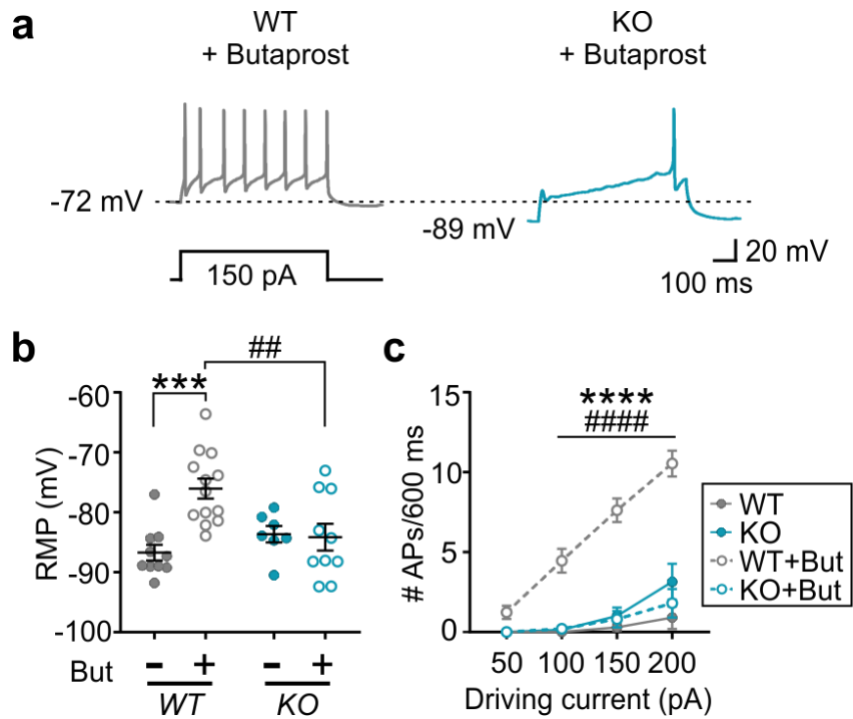


Figure 3.11. Confirmation of EP2R deletion in MCH neurons of MCH-EP2R KO mice.

(A) Representative traces from MCH neurons from wild type (WT) and MCH^{Cre};EP2R^{ff} (KO) mice. EP2R agonist butaprost stimulates WT but not KO neurons.

(B to C) Effect of butaprost (But) on RMP (B) and evoked APs (C) of MCH neurons in WT and KO mice. Butaprost activates WT neurons but not KO neurons.

Tukey's multiple comparison:

*** $p < 0.001$, **** $p < 0.0001$ WT no treatment vs WT+But;

$p < 0.01$, ##### $p < 0.0001$ WT vs KO

Although MCH-immunopositive neurons are confined to the hypothalamus, Cre-reporter mice (MCH Cre-tdTomato) showed sparse tdTomato expression in MCH-immunonegative neurons in the septal area. Importantly, butaprost did not alter their excitability (Figure 3.12A-C). Thus, these extrahypothalamic neurons are unlikely to significantly contribute to the KO phenotype.

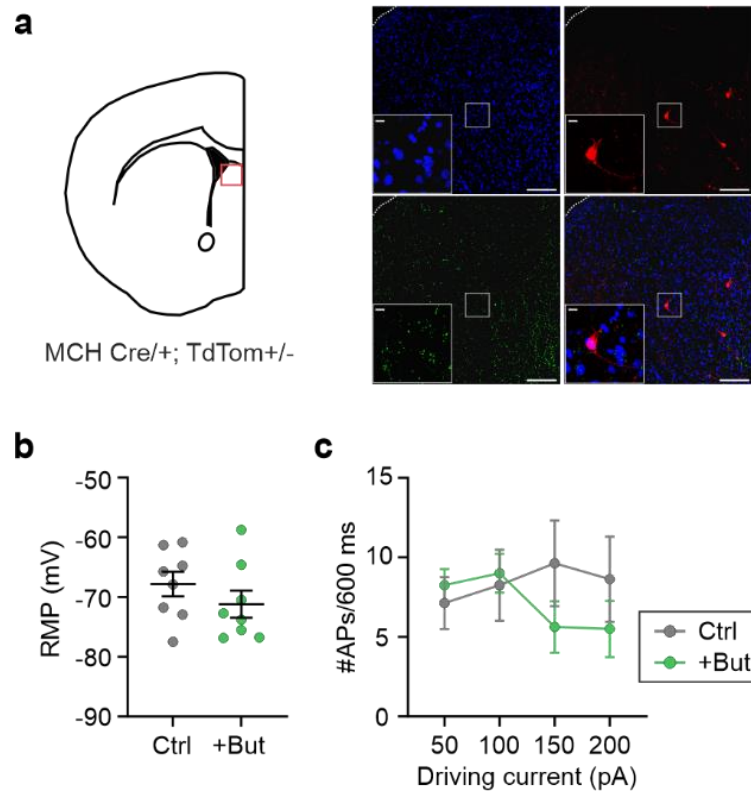


Figure 3.12. Extrahypothalamic Cre-expressing cells are insensitive to EP2R agonist

(A, left) Schematic depicting the approximate location of TdTom-positive cells (red box) pictured in the immunofluorescence images (right).

(A, right) Representative confocal fluorescence images showing the presence of Cre-dependent tdTomato-positive cells driven by the MCH promoter (red) in the lateral septal area using 4',6-diamidino-2-phenylindole (DAPI; blue) as a counterstain. Note the distinct lack of immunostaining of proMCH (green) in tdTomato-positive cells in this area. Scale bar = 100 μ m; inset scale bar = 10 μ m.

(B to C) RMP (B) and evoked APs (C) of extrahypothalamic Cre-expressing cells in the absence (Ctrl) or presence of butaprost (+But). Butaprost has no significant effect on the excitability of these cells.

Using the KO model, we assessed the effect of diet on MCH neuron excitability. RMP of MCH neurons was comparable between chow-fed male KO mice and littermate controls (EP2R^{f/f}, hereinafter known as f/f). Conversely, WD feeding depolarized f/f MCH neurons but not KO neurons (Figures 3.13A-C). These results confirm a critical role of EP2R in the WD-induced activation of MCH neurons.

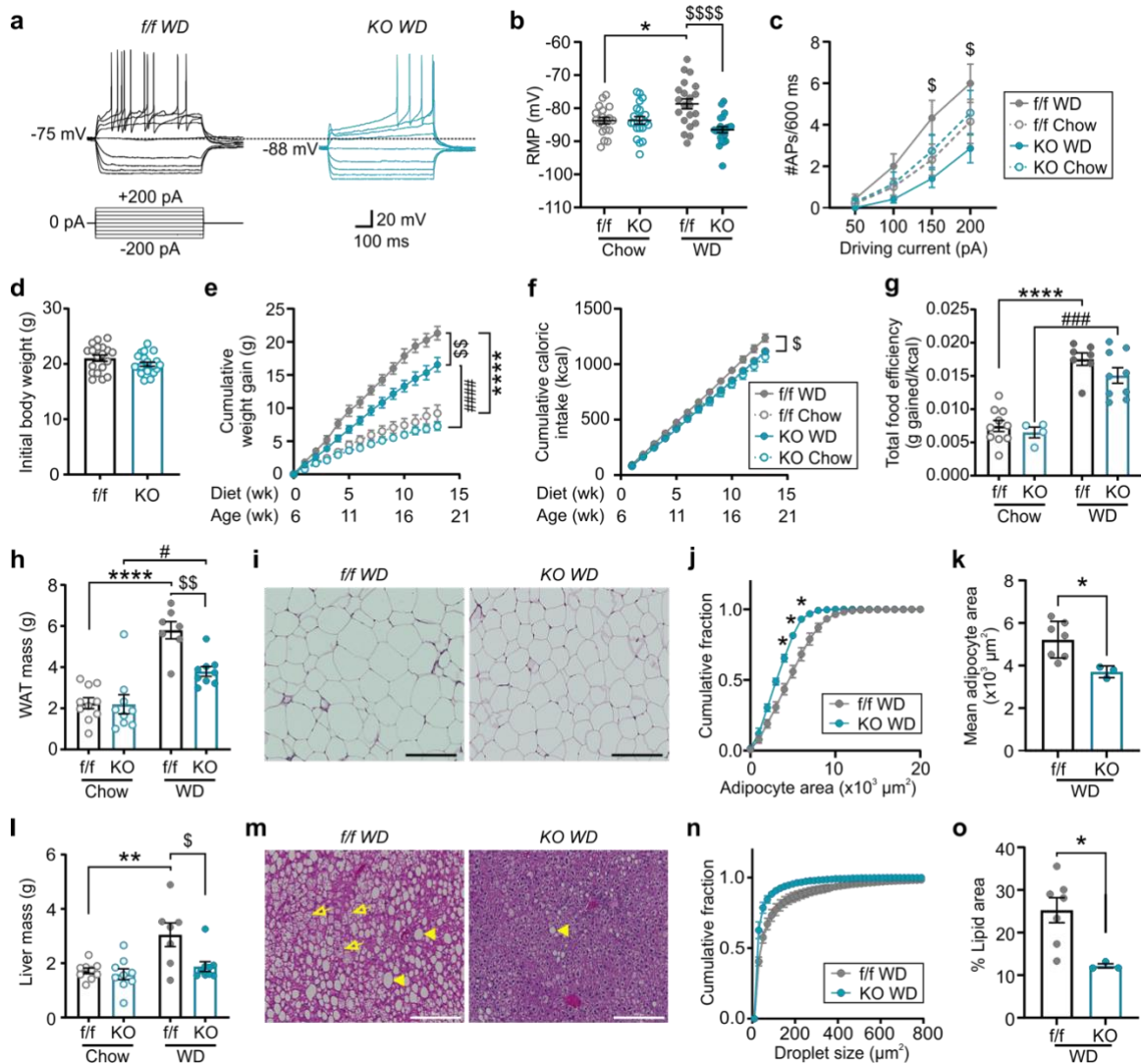


Figure 3.13. PGE2-EP2R signalling in MCH neurons exacerbates diet-induced obesity and liver steatosis in male mice.

(A) Representative traces of MCH neurons from WD-fed male *f/f* or *KO* mice. **(B)** RMP of MCH neurons after 13-week chow or WD. **(C)** Evoked APs from cells shown in (B). **(D)** Baseline body weight at 6 weeks of age. **(E-F)** Body weight (E) and cumulative caloric intake (F) during feeding period. **(G)** Food efficiency calculated as total weight gained per calorie consumed during 13-week feeding.

(H) White adipose tissue (WAT) mass (sum of epididymal, inguinal and retroperitoneal pads) after 13-week feeding. **(I)** Representative H&E-stained adipocytes from epididymal fat pads. **(J to K)** Cumulative distribution (J) and mean adipocyte area (K). **(L)** Liver mass after 13-week feeding. **(M)** Representative H&E-stained images of the liver. Arrowheads: macrosteatosis; Open arrows: microsteatosis. **(N to O)** Cumulative distribution of liver lipid droplet size (N) and percent lipid area (O).

(B-C, E-G, H, L) Tukey's multiple comparison: * $p < 0.05$, ** $p < 0.01$, **** $p < 0.0001$ f/f-chow vs f/f-WD; \$ $p < 0.05$, \$\$ $p < 0.01$, \$\$\$ $p < 0.0001$ f/f-WD vs KO-WD; # $p < 0.05$, ### $p < 0.001$, #### $p < 0.0001$ KO-chow vs KO-WD. (J) Bonferroni multiple comparison test: * $p < 0.05$. (K, O) Two-tailed unpaired t-test * $p < 0.05$. (I, M) Scale bar = 200 μm .

KO and *f/f* mice displayed similar body weight (BW) at baseline (6 weeks old) and throughout chow feeding (Figure 3.13D-E). When fed with WD, *f/f* mice developed DIO, whereas KO mice gained much less BW (Figure 3.13E). This is likely due to a greater WD intake and not energy expenditure as estimated by food efficiency (weight gained per calorie consumed) by *f/f* mice (Figures 3.13F-G). Upon completion of feeding, both WD-fed *f/f* and KO mice had more adiposity than chow-fed counterparts, although WD-KO had less than WD-*f/f* mice, indicating that EP2R deletion is partially protective (Figures 3.13H and 3.14A-C). This difference in fat mass between the WD-fed groups was at least in part due to a smaller adipocyte size (Figure 3.13I-K). KO mice were also largely protected from WD-induced hepatosteatosis (Figures 3.13L-O). Other organs showed no discernible differences due to EP2R deletion, except lean muscle mass, which was smaller only in WD-KO (Figure 3.14D-G). In all, our data suggest that EP2R-mediated activation of MCH neurons contributes to DIO, adiposity, and hepatosteatosis.

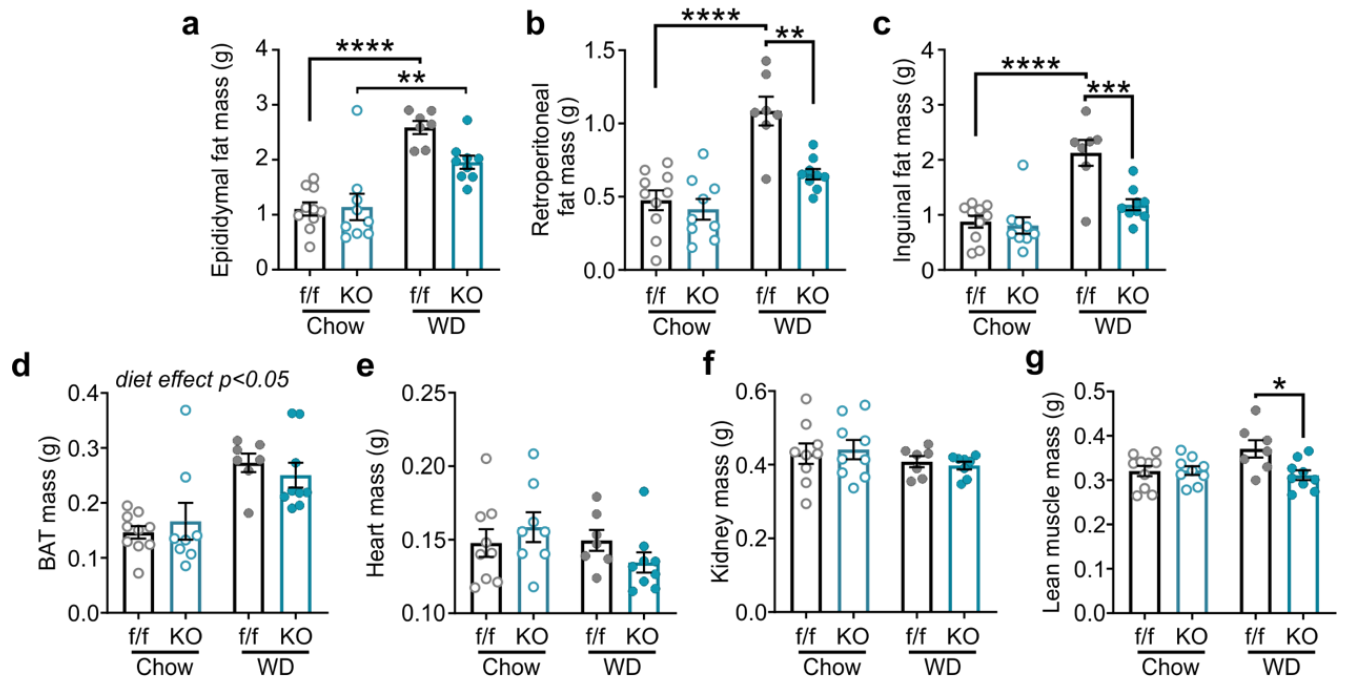


Figure 3.14. Organ profile of male f/f and KO mice after chow or WD feeding.

(A to G) Weight of various organs from male control (f/f) and MCH-EP2R KO mice (KO) following 13-week chow or WD, including epididymal fat (A), retroperitoneal fat (B), inguinal fat (C), brown adipose tissue (BAT; D), heart (E), kidneys (F), and lean muscle mass (G).

Tukey's multiple comparison: * $p < 0.05$, ** $p < 0.01$, *** $p < 0.001$, **** $p < 0.0001$.

3.3.5. PGE₂-EP2R Signaling in MCH Neurons Modestly Contributes to Diet-Induced Obesity in Female Mice

To determine whether EP2R signaling in MCH neurons similarly contributes to obesity in female mice, the effect of WD on the excitability of MCH neurons was assessed. This revealed a main effect of diet on RMP without significant difference between specific groups by multiple comparisons (Figures 3.15A-B). Furthermore, no difference in AP firing was found between groups (Figure 3.15C). These results suggest that the excitatory effect of WD on RMP does not involve EP2R in females, or perhaps is attenuated without the contribution of EP2R.

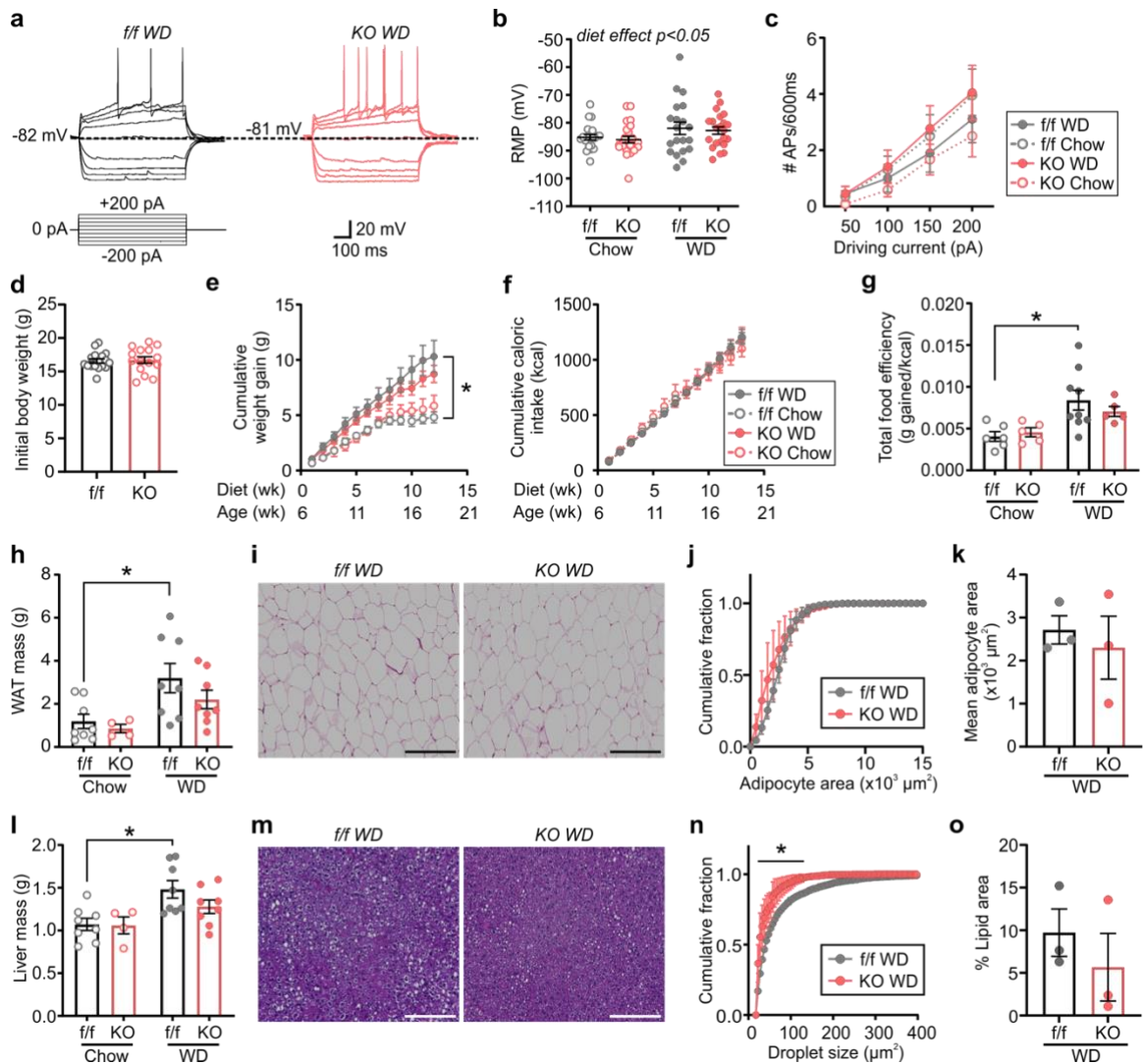


Figure 3.15. PGE2-EP2R signaling in MCH neurons modestly contributes to diet-induced obesity in female mice.

(A) Representative traces of MCH neurons from WD-fed female *f/f* or *KO* mice.

(B to C) RMP (B) and evoked APs (C) of MCH neurons after 13-week feeding.

(D) Initial body weight at 6 weeks of age. **(E to F)** Body weight (E) and cumulative caloric intake (F) during the feeding period. **(G)** Food efficiency over 13-week

feeding. **(H)** White adipose tissue (WAT) mass (sum of gonadal, inguinal and

retroperitoneal pads) after 13-week feeding. **(I)** Representative H&E-stained adipocytes from gonadal fat pads. **(J to K)** Cumulative distribution (J) and mean adipocyte area (K). **(L)** Liver mass after 13-week feeding. **(M)** Representative H&E-stained images of the liver. **(N to O)** Cumulative distribution of liver lipid droplet size (N) and percent lipid area (O).

(E, G-H, L) Tukey's multiple comparison: * $p < 0.05$ f/f chow vs f/f WD. (N)

Bonferroni multiple comparison: * $p < 0.05$. (I, M) Scale bar = 200 μm .

Comparison of these female mice found no effect of KO on BW at baseline and throughout chow feeding (Figure 3.15D,E). When fed with WD, *f/f* mice gained more BW compared to those fed chow, whereas BW of KO mice on different diets did not statistically differ (Figure 3.15E). There was no difference in food intake among the groups, however, WD increased food efficiency only in *f/f* mice (Figure 3.15F-G). Thus, differences in energy expenditure may underlie the WD-induced weight gain, which is absent in KO mice.

Consistent with the BW results, WD significantly increased adiposity in female *f/f* mice compared to those fed chow, which was absent in KO mice (Figures 3.15H and 3.16A-C). Nevertheless, adipocyte size was similar between WD groups (Figure 3.15I-K). WD also increased liver mass in *f/f* but not KO mice (Figure 3.15L). Histological assessment showed hepatosteatosis after WD feeding, which was worse in *f/f* than KO mice (Figures 3.15M-O). EP2R deletion did not alter other organ weights (Figures 3.16D-G). Together, these results indicate that EP2R KO in MCH neurons may protect female mice from DIO. However, the protective effect is less prominent than in males, and may not rely on MCH neuron depolarization, unveiling an interesting sex difference.

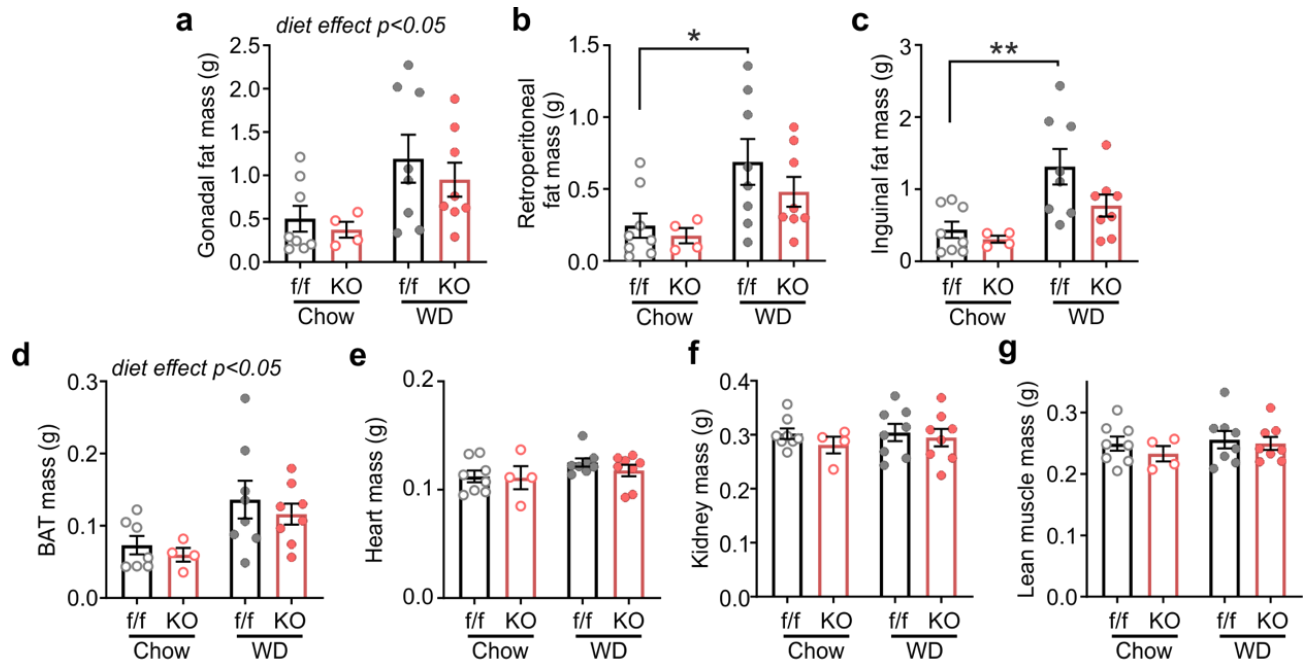


Figure 3.16. Organ profile of female f/f and KO mice after chow or WD feeding.

(A to G) Weight of various organs from female control (f/f) and MCH-EP2R KO mice (KO) following 13-week chow or WD, including gonadal fat (A), retroperitoneal fat (B), inguinal fat (C), brown adipose tissue (BAT; D), heart (E), kidneys (F), and lean muscle mass (G).

Tukey's multiple comparison: * $p < 0.05$, ** $p < 0.01$.

3.4. Discussion

The present study demonstrates that HFD-induced hypothalamic inflammation can directly stimulate neurons that promote weight gain. Specifically, prolonged consumption of WD significantly increases the intrinsic excitability of MCH neurons through the inflammatory mediator PGE₂ in male rodents. The onset of the WD-induced excitation of MCH neurons preceded significant weight gain, suggesting that it is not secondary to obesity. It is likely due to dietary fat, not sugar, as two types of HFD with differing sugar content depolarized MCH neurons, whereas a low-fat/ high-sucrose diet did not do so. The membrane depolarization is mediated by PGE₂ activating EP2R, which downregulates Na⁺/K⁺-ATPase function. This is mediated by PKA, which can directly phosphorylate Na⁺/K⁺-ATPase to decrease its affinity for intracellular Na⁺²⁹⁵. Moreover, EP2R can induce oxidative stress^{296,297}, which could inhibit Na⁺/K⁺-ATPase²⁹⁸. Thus, we identified a novel role of Na⁺/K⁺-ATPase as a regulator of the central energy balance circuitry through modulation of MCH neuron excitability.

PGE₂ is a well-known orchestrator of sickness syndrome during disease states²⁸², however, our study reveals a novel, non-canonical role of PGE₂ in DIO. MCH neurons respond bidirectionally to PGE₂, indicating that they can sense a spectrum of inflammation to dynamically modulate energy state in opposing directions. On one hand, higher concentrations of PGE₂ hyperpolarize MCH neurons. This could occur during high-grade inflammation causing sickness syndrome. In support of this, inhibition of MCH neurons has been implicated in

lipopolysaccharide-induced anorexia and weight loss ²⁸⁶. Conversely, prolonged WD depolarizes MCH neurons, which is blocked by COX-2 inhibitors. COX-2 synthesizes a host of prostanoids, some of which can modulate Na⁺/K⁺-ATPase activity, such as PGE₂, PGF_{2α} and PGI₂ ²⁹⁹. However, we found that the EP2R-specific antagonist completely reversed the WD effect, indicating that other prostanoids are unlikely to be involved. Low concentrations of PGE₂ also depolarize MCH neurons via EP2R, supporting the notion that HFD-induced low-grade inflammation stimulates MCH neurons to promote positive energy balance.

MCH neurons promote a net positive energy balance by mediating the motivational aspect of feeding ¹⁶⁸ and sleep ^{187,188,300,301}, while suppressing physical activity ¹⁸³ and metabolic rate ¹⁶². While many of these functions can be attributed to the MCH peptide, MCH neurons express several co-transmitters including GABA, glutamate, nesfatin-1 and CART ^{172,173,187}. Changes in neuronal excitability could affect the release of these co-transmitters from MCH neurons, which are known to have distinct roles in energy and glucose homeostasis, and sleep ^{174,175,187}. Furthermore, MCH neurons modulate memory and mood ^{191,192,302}. Therefore, it is possible that the PGE₂-EP2R-MCH axis is also involved in sleep, cognitive and mood dysfunction associated with HFD intake ^{303–307}.

Our previous study showed that prolonged WD consumption in male rats induces persistent increases in excitatory synaptic contacts to MCH neurons ³⁰⁸. This synaptic effect was present at week 4 but not week 1 of WD, which aligns with the time course of intrinsic depolarization in the present study. Taken

together, chronic HFD intake results in both intrinsic and synaptic plasticity converging to maintain elevated excitability of MCH neurons in males.

The causal role of PGE₂ and MCH neurons in DIO is clearly demonstrated by the leanness of mice with conditional deletion of EP2R in MCH neurons, which is reminiscent of the lean phenotype of MCH-ablated or MCH-deficient rodents^{158,163,174}. KO mice had less lipid deposition in white adipose tissue and liver than controls, which is likely due to the observed hypophagia and attenuation of MCH-mediated autonomic control over the metabolism in these organs³⁰⁹. While EP2R deletion in MCH neurons conferred some protection against DIO in both males and females, the effect was more modest in females. This may be because female mice did not exhibit the same excitation of MCH neuron or voracious weight gain as males in general. Hypothalamic inflammation in female mice may be more mild, perhaps even undetectable, consistent with previous reports^{310,311}. Alternatively, there may be another mechanism by which EP2R signaling alters the output of MCH neurons without changes in RMP that could explain the partial protection of KO females. This sexual divergence in the role of MCH EP2R in obesity warrants future investigation.

In conclusion, we identified novel roles of hypothalamic PGE₂ and Na⁺/K⁺-ATPase in the energy balance circuitry that contributes to DIO. Furthermore, our study indicates that MCH neurons can act as inflammation sensors, dynamically and bidirectionally responding to varying levels of inflammation, regulating a wide spectrum of energy balance outcomes.

Chapter 4 – High-fat diet induces time-dependent synaptic plasticity of the lateral hypothalamus

Adapted from

Victoria Linehan* & Lisa Z. Fang*, et al., High-fat diet induces time-dependent synaptic plasticity of the lateral hypothalamus. *Molecular Metabolism* **36**, 100977 (2020). doi: <https://doi.org/10.1016/j.molmet.2020.100977>

*denotes equal contribution

4.1. *Introduction*

The global incidence of obesity is increasing, leading to a concomitant rise in its associated comorbidities, including type II diabetes, cardiovascular disease, and some cancers. Most prevalent is diet-induced obesity (DIO), which is typically caused by an overconsumption of energy-dense foods without a sufficient increase in energy expenditure to compensate.

DIO is associated with functional and structural changes in the hypothalamic neuronal circuitry controlling energy balance. For instance, synaptic remodeling occurs within the arcuate nucleus of rodent models of DIO, characterized by a change in the number of excitatory and inhibitory synaptic contacts to neuropeptide Y and proopiomelanocortin neurons^{140,312}. These changes are thought to be a homeostatic negative feedback mechanism underlying counter-regulatory responses to elevated caloric intake and fat mass. On the other hand, high-fat diet (HFD), commonly used in DIO models, can drive caloric overconsumption through a positive feedback mechanism involving the reward system³¹³. These functionally opposing negative and positive feedback mechanisms are likely to be dynamically regulated during the development and maintenance phases of DIO.

The hypothalamic energy balance circuitry is comprised of several nuclei, including the arcuate nucleus, lateral hypothalamus (LH), ventromedial hypothalamus and paraventricular nucleus³¹⁴. Moreover, the LH is uniquely connected to the reward system to mediate the motivation to work for food and other rewards³¹⁵. Within the LH, orexin (ORX) and melanin-concentrating

hormone (MCH) neurons are two distinct peptidergic cell types that underlie these functions. These cell populations are known for their complementary and partially antagonistic roles in energy balance and reward³¹⁶ through reciprocal connections to related brain regions^{317–320}.

Both ORX and MCH neurons are orexigenic, as acute application of these neuropeptides induces food intake^{184,199}. Yet, ORX-induced food intake and weight gain diminishes with prolonged infusion³²¹ whereas chronic administration of MCH induces sustained hyperphagia and obesity^{161,322}, suggesting differential roles in long-term energy balance. ORX neurons are activated by HFD³²³, food-associated cues^{214,324,325} and other highly salient stimuli^{326,327}. Furthermore, postnatal ablation of ORX neurons results in reduced food intake²⁰³, while their ablation in adulthood results in a modest increase in food intake³¹⁷, suggesting that age may be a factor in energy balance mechanisms. ORX signaling also promotes arousal and motivation to seek and consume palatable food²¹⁴, while increasing metabolism, sympathetic activation and locomotor activity^{201,328}. In sum, despite promoting acute food intake, the net result of ORX signalling is negative energy balance and resistance to DIO³²⁹. Thus, previous studies overall indicate that ORX neurons play an integrated role in goal-directed behaviors where motivational activation is matched by arousal and physical activity. In contrast, MCH neurons promote positive energy balance and a higher body weight. Activation of these neurons promotes the preference and consumption of food according to its nutrient values³³⁰. MCH stimulates food intake, particularly palatable, calorie-dense food^{322,331}, while promoting energy conservation through

reduced metabolism and locomotor activity^{163,332}. Together, these studies delineate the complementary roles of ORX and MCH in different aspects of food intake control and opposing effects on overall energy balance.

The activity of ORX and MCH neurons is regulated by excitatory and inhibitory synaptic inputs, whose functional properties change during development in a cell-type specific manner. While excitatory synapses to ORX neurons functionally mature before adolescence (prior to weaning), MCH neurons take much longer to reach the adult level³³³. How these age-dependent synaptic properties interact with prolonged HFD exposure remains obscure. Therefore, the present study investigated the synaptic effects of HFD on ORX and MCH neurons in rats from adolescence to adulthood. Our study provides novel insights into the impact of HFD on the regulatory mechanisms involved in energy homeostasis. This has important implications in our society today, given the abundance of palatable energy-dense foods that are widely available starting from a very young age.

4.2. *Methods*

4.2.1. *Animals*

All experiments were conducted following the guidelines of Canadian Council of Animal Care and were approved by Memorial University's Institutional Animal Care Committee. Male Sprague-Dawley rats (Charles River, Saint Constant, Canada or Memorial University breeding colony) and C57BL/6NCrl (Charles River, Saint Constant, Canada) were fed ad libitum with a standard

chow (LabDiet autoclavable rodent diet 5010, 12.7% in fat) or a palatable HFD (TestDiet AIN-76A Western Diet, 40.1% in fat).

4.2.2. *Electrophysiology*

Following the feeding period, rats were deeply anesthetized with isoflurane and the brain was removed. Acute 250- μm slices of the hypothalamus were generated using a vibratome (VT-1000, Leica Microsystems) in cold artificial cerebrospinal fluid (ACSF; composition: (in mM): 126 NaCl, 2.5 KCl, 1.2 NaH_2PO_4 , 1.2 MgCl_2 , 2 CaCl_2 , 18 NaHCO_3 and 2.5 glucose) bubbled with 95% O_2 /5% CO_2 . Slices were incubated at 32-34°C for 30 minutes and then left at room temperature until experiments were performed. For whole cell patch clamp recordings, hemisected slices were placed in a recording chamber perfused with ACSF at 1-2 mL/min, 32°C. Glass pipette recording electrodes had a tip resistance of 3-5 $\text{M}\Omega$ when filled with internal solution (in mM): 123 K-gluconate, 2 MgCl_2 , 8 KCl, 0.2 EGTA, 10 HEPES, 5 $\text{Na}_2\text{-ATP}$, 0.3 Na-GTP, and 2.7 biocytin. Whole cell series/access resistance was 5-20 $\text{M}\Omega$, which was monitored throughout the recording by applying a 20-mV, 50-ms square pulse every minute. Multiclamp 700B and pClamp 9 or 10 software (Molecular Devices, Sunnyvale, CA) were used to collect data. Signals were filtered at 1 kHz and digitized at 5-10 kHz.

All voltage clamp recordings were performed at a holding potential of -70 mV. Action potential-independent miniature excitatory postsynaptic currents

(mEPSC) were isolated using tetrodotoxin (1 μ M; Alomone Labs, Jerusalem, Israel) and picrotoxin (50 μ M; Sigma, Oakville, Canada) in the bath.

4.2.3. *Identification of ORX and MCH neurons*

ORX and MCH neurons can be distinguished with high accuracy among other neurons in the LH based on a unique set of electrophysiological responses to negative and positive current injections (600 ms, incremental steps from -200 to +200 pA)^{220,289}. Briefly, ORX neurons display an H-current and a rebound depolarization following relief from hyperpolarization, which is capped by action potentials in some cells. They also fire spontaneously and display a uniphasic afterhyperpolarizing potential. MCH neurons are typically not spontaneously active but, upon positive current injections, display action potentials with uniphasic afterhyperpolarizing potential and spike adaptation. These cells also show no H-current and no rebound during or following hyperpolarization, respectively.

Post-hoc immunohistochemistry was performed on a subset of cells labeled with biocytin during patch clamp recording. Following experiments, brain slices were fixed in 10% formalin for at least 12 hours. Subsequently, slices were incubated with goat anti-ORX-A IgG (1:2000; SC8070, Santa Cruz Biotechnology, Dallas, TX, USA) and rabbit anti-MCH IgG (1:1000-2000; H-070-47, Phoenix Pharmaceuticals, Burlingame, CA, USA) for 3 days at 4°C. Then appropriate secondary antibodies and Alexa 350-conjugated streptavidin (1:500; Jackson ImmunoResearch, West Grove, PA, USA) were applied for 3 hours at

room temperature or overnight at 4°C. Colocalization of biocytin with either ORX-A or MCH was assessed using an epifluorescence microscope.

4.2.4. *Double immunohistochemistry*

Three-week old rats were fed for 4 weeks with chow (4wCtrl) or HFD (4wHFD), and six-week old rats were fed HFD for 1 week (1wHFD). After the feeding period, rats were deeply anesthetized with isoflurane and transcardially perfused with 4% paraformaldehyde (PFA). Brains were removed, post-fixed overnight in 4% PFA, and serially cryoprotected in 15% then 30% sucrose in PBS. 16- μ m sections containing the hypothalamus were collected using a cryostat (CM 3050S, Leica Microsystems). For immunofluorescence, tissue sections were incubated overnight at 4°C in guinea pig anti-vGluT2 (1:500; 135 404, Synaptic Systems, Goettingen, Germany) and either goat anti-proMCH IgG (1:500; sc14509, Santa Cruz Biotechnology, Dallas, TX, USA) or goat anti-ORX-A IgG (1:500; sc8070, Santa Cruz Biotechnology, Dallas, TX, USA). The next day, sections were incubated in Cy3-conjugated anti-guinea pig IgG (1:500; 706-165-148, Jackson ImmunoResearch, West Grove, PA, USA) and AlexaFluor 488-conjugated anti-goat IgG (1:500; A11055, Invitrogen) for 2 hours at room temperature. Slides were coverslipped using Dako fluorescence mounting medium (Agilent Technologies, Inc., Santa Clara, CA, USA) and stored at 4°C until imaging.

4.2.5. *Confocal imaging and analysis*

Neurons immunopositive for ORX-A or MCH with clear nuclei were randomly selected for imaging within the LH dorsal to the fornix. 5- μm z-stacks (5 sections at 1 μm intervals) were taken at 60X (1.42 NA) magnification using a laser-scanning confocal microscope (Fluoview FV1000, Olympus Corporation), and Z-projected images were generated. The following steps were performed using ImageJ by experimenters blind to the experimental groups. First, a pilot study was conducted to determine an appropriate threshold for positive vGluT2 by testing a series of thresholds on a random set of vGluT2-stained sections, followed by visual comparison of the resulting binary images to the original. Next, a threshold was applied separately to grayscale images of neuropeptides or vGluT2 to generate binary images. The threshold for vGluT2 was set at 10% of the pixel intensity distribution based on the pilot study. Lastly, the binary images were merged and the number of vGluT2 puncta directly apposed to MCH or ORX neuron somata were counted.

4.2.6. *Data analysis*

MiniAnalysis software (Synaptosoft, Inc.) was used to measure the frequency and amplitude of mEPSCs. Data are expressed as mean \pm SEM. The number of cells (n) and animals (N) used are indicated in the corresponding figure legend. Unpaired t-tests, one-way and two-way ANOVAs were performed using Prism 7 (GraphPad Software) to assess statistical differences between

groups and to test the effect of diet. If ANOVA indicated significance, a Sidak multiple comparisons test was performed. $p < 0.05$ was considered significant.

4.3. *Results*

A previous study in the lab has demonstrated that ORX neurons undergo dynamic synaptic plasticity in response to HFD feeding¹⁴⁸. Their response is dependent on the duration of the diet, as 1 week of HFD reveals a long-term depression (LTD) of glutamatergic synapses, which is absent by 4 weeks of HFD. Given the role of ORX neurons in feeding, this may represent an immediate compensatory response to prevent overconsumption, which is eventually lost as HFD prolongs.

On the other hand, as shown in Chapter 3, MCH neurons display a robust intrinsic activation, which is absent at 1 week but present after 4 weeks of HFD. As MCH neurons promote weight gain, cells may initially resist depolarization, opposing weight gain, which wanes as HFD persists.

Together, these duration-dependent changes seem to support the development of obesity if HFD is present for a longer period. We therefore asked if other properties of ORX and MCH neurons follow suit. To this end we assessed how spontaneous excitatory transmission is altered after 1 and 4 weeks of HFD feeding. Importantly, these cells have been reported to display age-dependent changes in excitability³³³, thus we age-matched animals such that they were 7 weeks old at the end of their respective feeding periods, corresponding to adulthood.

4.3.1. *Orexin neurons*

In ORX neurons, 1 week of HFD feeding induced an increase in mEPSC amplitude (Fig. 4.1A-B). However, these changes are transient, as the mean mEPSC amplitude returned to Ctrl levels by 4 weeks of feeding (Fig. 4.1A-B).

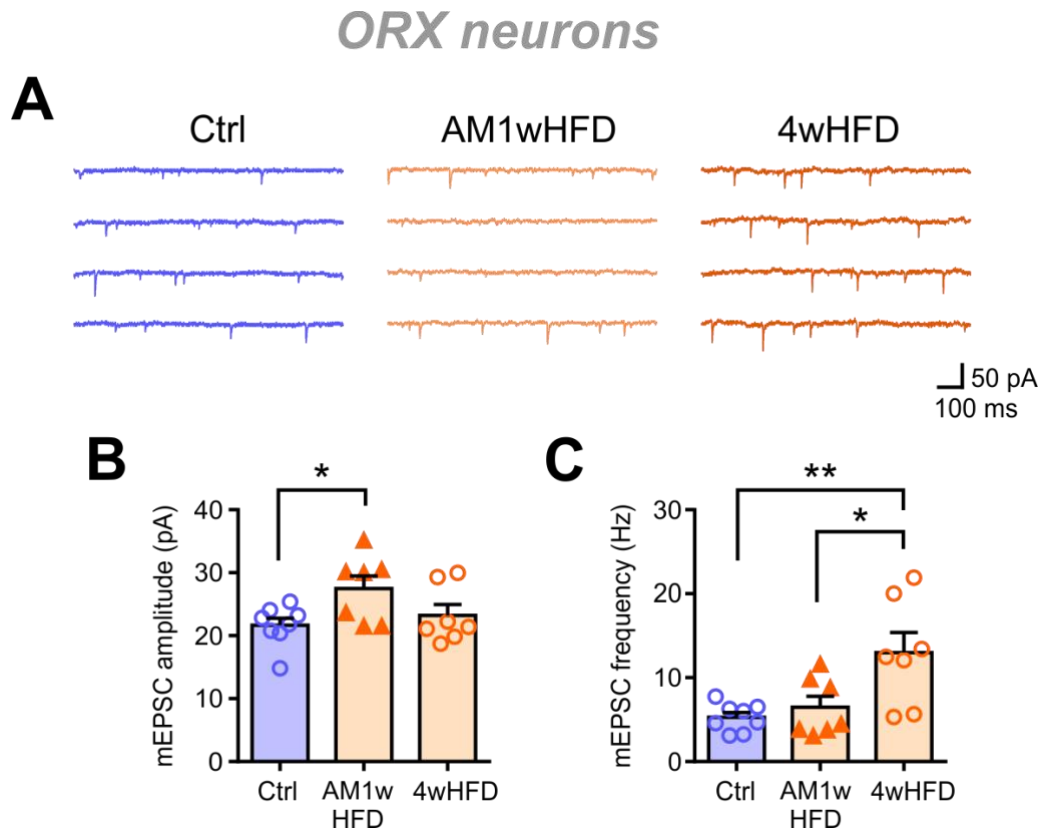


Figure 4.1. Acute HFD feeding induces an increase in spontaneous excitatory transmission to ORX neurons.

Feeding periods were staggered so that all rats were 7-week old at the time of assessment. (A) Representative mEPSC recordings from ORX neurons of rats fed a control chow diet (Ctrl), or HFD for 1 week (AM1wHFD) and 4 weeks (4wHFD). (B-C) ORX neurons from age-matched 1-week HFD group (AM1wHFD) show a larger mEPSC amplitude (B) but no change in mEPSC frequency compared to Ctrl (C). By 4 weeks (4wHFD), there was a significant increase in mEPSC frequency. One-way ANOVA: mEPSC amplitude (B),

$p=0.0255$; mEPSC frequency (C), $p=0.0058$. * $p<0.05$, ** $p<0.01$, Sidak's multiple comparison test. $n=7-10$ cells, $N=4-7$ rats.

Analysis of mEPSC frequency revealed a different time course of the HFD effect. In contrast to the early change in mEPSC amplitude, mEPSC frequency was not affected by 1 week of HFD but was significantly increased by 4 weeks (Fig. 4.1A, C). The published article³⁰⁸ addresses the possible mechanisms underlying the mEPSC amplitude changes, while the remainder of this chapter (adapted from the article) will focus on the change in frequency.

One possible explanation for the increase in mEPSC frequency observed could be an increase in the number of excitatory synaptic contacts. To test this hypothesis, a confocal analysis was performed to assess the number of excitatory terminals in contact with ORX neurons. There was no change in the number of vGluT2 puncta in apposition with ORX neurons at 1 or 4 weeks (Fig. 4.2A-D). Together, these results suggest that increased mEPSC frequency after 4 weeks of HFD may not involve synaptic remodeling at ORX neuron somata, although possible remodeling at the dendrites cannot be excluded.

ORX neurons

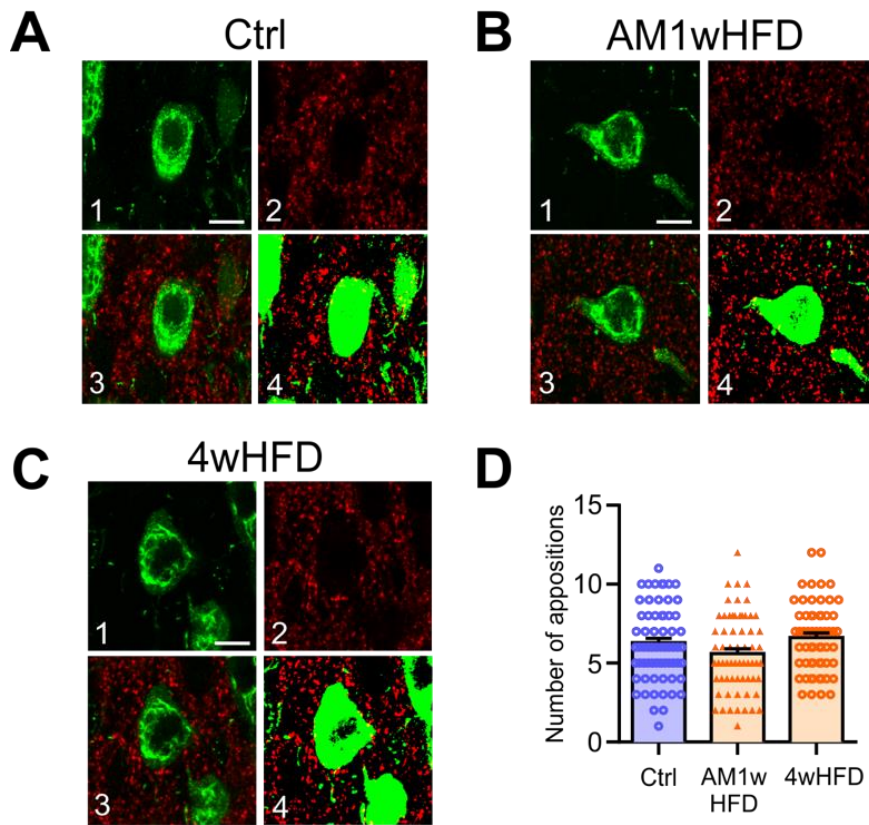


Figure 4.2. HFD does not influence the number of excitatory synapses to ORX neuron somata.

(A-C) Representative immunofluorescence images of the lateral hypothalamus. Images show confocal images of ORX-A⁺ neurons (green; A1, B1, C1), vGluT2⁺ glutamatergic puncta (red; A2, B2, C2), the merged confocal image containing both channels (A3, B3, C3), and the merged binary image used for analysis, generated by applying a threshold to individual channels (A4, B4, C4). Scale bar = 10 μ m. (D) No difference in the number of vGluT2⁺ appositions to ORX neuron somata is found among feeding groups (One-way ANOVA, $p=0.0526$). $n=59-65$ neurons from 2-4 slices per rat, $N=3-4$ rats per diet condition

Overall, our data indicate that ORX neurons experience acute increases in excitatory inputs during short-term HFD feeding (1-4 weeks), which is not mediated by synaptic remodelling at the level of the soma. The transient nature of HFD-induced changes suggests that ORX neurons functionally adapt to the diet after prolonged feeding.

4.3.2. Melanin-concentrating hormone neurons

In MCH neurons, HFD had no effect on the mEPSC amplitude (Fig. 4.3A-B) after either 1 or 4 weeks of feeding. In contrast, the frequency of mEPSCs in MCH neurons showed time-dependent effects of HFD, such that frequency was significantly higher after 4 weeks of HFD feeding compared to control and 1 week of HFD (Fig. 4.3A, C).

MCH neurons

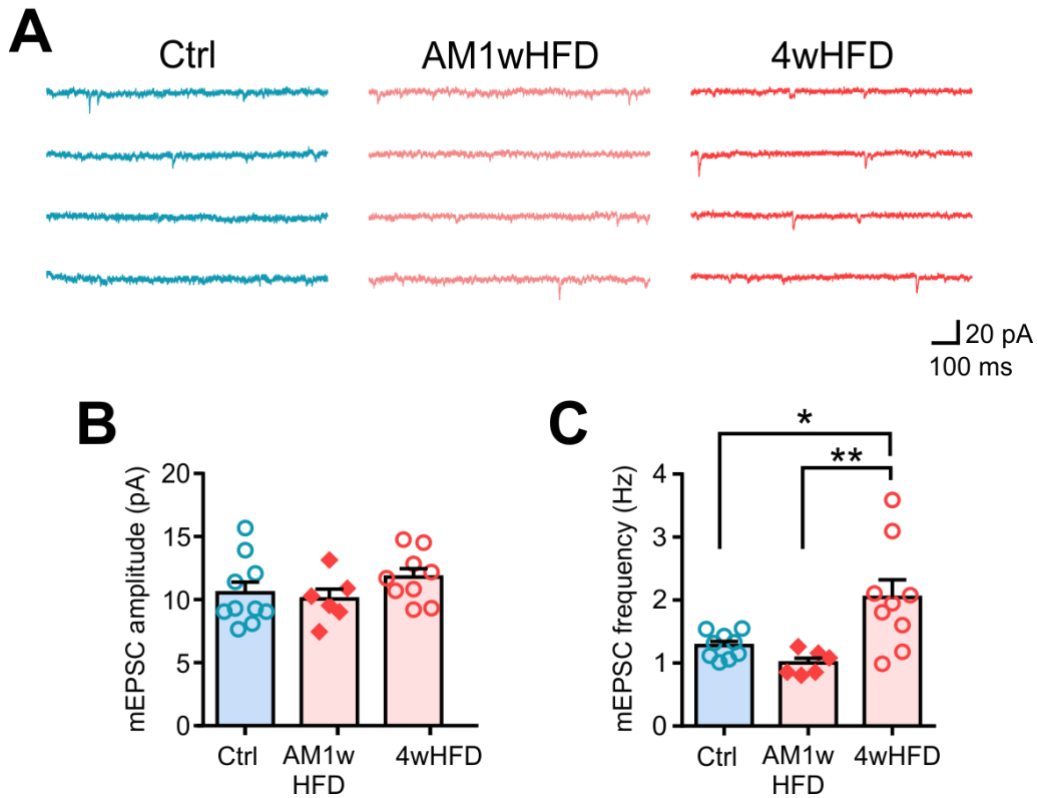


Figure 4.3. Chronic HFD persistently increases excitatory transmission to MCH neurons.

Feeding periods were staggered so that all rats were 7-week old at the time of assessment. (A) Representative mEPSC recordings of MCH neurons from rats fed a chow control (Ctrl) or HFD for 1 week (AM1wHFD) and 4 weeks (4wHFD). (B) HFD feeding does not affect mEPSC amplitude in MCH neurons (One-way ANOVA, $p=0.3180$). (C) HFD induces a delayed increase in mEPSC frequency (One-way ANOVA, $p=0.0029$). For (A-B): $n=6-9$ cells, $N=4-6$ rats. * $p<0.05$, ** $p<0.01$, Sidak's multiple comparison test.

This led us to ask whether there was a concomitant change to the number of excitatory contacts on MCH neurons. To test this, a confocal immunofluorescence analysis was performed to assess the number of excitatory terminals in contact with MCH neurons. We found that the number of vGluT2-immunopositive excitatory terminals in apposition with MCH neuron somata was significantly increased after 4 weeks but not after 1 week of HFD feeding (Fig. 4.4A-D), matching the changes in mEPSC that we observed. These results together suggest that prolonged HFD induces a delayed increase in the number of excitatory synaptic contacts to MCH neurons.

MCH neurons

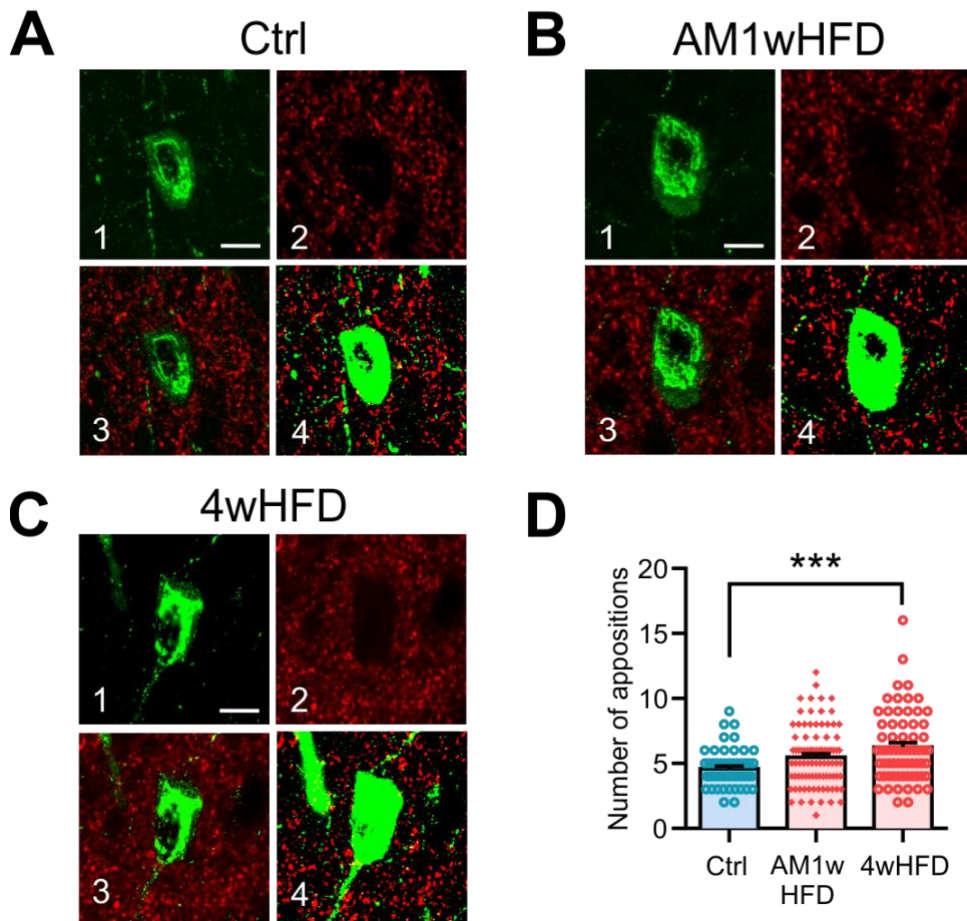


Figure 4.4. HFD induces a delayed increase in the number of excitatory synaptic contacts to MCH neurons.

(A-C) Representative immunohistochemical images of the lateral hypothalamus of rats that were fed for the indicated time. Images show an example of confocal immunofluorescence for MCH+ neurons (green; A1, B1, C1), vGluT2+ puncta (red; A2, B2, C2), the merged confocal image containing both channels (A3, B3, C3), and the merged binary image used for analysis (A4, B4, C4). Scale bar = 10

μm . (F) Four weeks of HFD feeding induced an increase in the number of vGluT2+ puncta apposed to the somata of MCH neurons (One-way ANOVA, $p=0.0005$).

$n=52-90$ neurons from 2-4 slices per rat, $N = 3-4$ rats per diet condition.

*** $p<0.001$, Sidak's multiple comparison test.

4.4. Discussion

The present study demonstrates that ORX and MCH neurons undergo synaptic plasticity during HFD in a mechanistically-distinct, cell-type dependent manner. On one hand, ORX neurons display early but transient changes in excitatory transmission in response to HFD feeding. On the other hand, MCH neurons show a delayed increase in excitatory transmission with the onset at 4 weeks of HFD, still preceding the onset of a significant weight gain. These differential effects of HFD may underlie the complementary and partially antagonistic roles of these cells in energy balance. The mechanism by which HFD induces synaptic remodeling remains unclear; however, metabolic and hormonal changes associated with HFD may be involved. For example, leptin, insulin, endocannabinoids and brain-derived neurotrophic factor have been shown to mediate HFD-induced synaptic remodeling in various brain regions^{312,334,335}. ORX and MCH neurons directly receive widely distributed afferents from overlapping and discrete brain areas, including many nuclei in the hypothalamus, other subcortical and cortical areas, and the midbrain³¹⁷ that are involved in energy balance, reward and sleep/wake control. Some of these direct inputs are indeed glutamatergic^{336–339}. It remains unknown whether all of the above or only selective pathways are sensitive to HFD, and whether the same synapses undergo dynamic plasticity over the course of HFD or whether different sets of synapses show plasticity at different time points.

ORX neurons display an acute increase in excitatory transmission. Glutamatergic synaptic activity has been shown to underlie basal excitability of

ORX neurons³⁴⁰. Thus, increased excitatory drive along with known upregulation of ORX mRNA by short-term HFD exposure³⁴¹ will likely lead to an increased release of ORX peptide. Released ORX may stimulate downstream targets in the reward system such as the ventral tegmental area³⁴², which is also known to undergo rapid synaptic plasticity in response to palatable food consumption³⁴³. In this light, these plastic changes may influence the rewarding value of palatable diet and reinforce further consumption by promoting motivation and food seeking. In fact, non-food rewards, such as cocaine, have been demonstrated to induce synaptic alterations to ORX neurons^{344,345}, suggesting that these cells respond with synaptic plasticity to rewarding stimuli in general.

By week 4, the change in mEPSC amplitude normalizes, while mEPSC frequency increases in ORX neurons. Although not included in this adapted chapter, the published article demonstrates that the increase in mEPSC frequency does not accompany any change in paired-pulse ratio (PPR)³⁰⁸, suggesting that the presynaptic release probability is unchanged. This would suggest that there is instead a change in the number of active excitatory synapses, although, this was not supported by a confocal analysis that found no change in the number of excitatory terminals in apposition with ORX neurons. The possibility of synaptic remodeling at the dendrites cannot be excluded as our confocal analysis was limited to somatic contacts. However, a similar confocal analysis had successfully detected changes in the number of vGluT2-expressing terminals making somatic contact with ORX neurons in obese mice³³⁴. Alternatively, structural components of synapses can exist but be functionally

quiescent³⁴⁶, which could dissociate electrophysiological and immunohistochemical results. Furthermore, the discrepancy may be partially explained if only a subpopulation of ORX neurons responds to HFD. For example, ORX neurons have been subdivided into two groups based on electrophysiological properties³⁴⁷, which display differential responses to glucose³⁴⁸ and sleep deprivation³⁴⁹. As these subpopulations cannot be segregated immunohistochemically, changes in one subpopulation may be masked by a lack of change in other ORX subtypes.

Also, we may not have detected differences in synaptic contacts due to technical limitations, such as ORX-A not labelling the full extent of the cell body. However, the aforementioned study that successfully detected differences in axosomatic contacts to ORX neurons used the very same antibody. In future studies, perhaps the ORX-A antibody could be used in conjunction with a plasma membrane marker to ensure accurate detection of puncta that are apposed to the soma.

Contrastingly, there is a significant increase in the number of excitatory terminals apposing MCH neurons after 4 weeks of feeding, suggesting that synaptic remodeling has occurred. Importantly, these changes occur before the onset of excess weight gain (around 5 weeks of HFD). Although not presented in this adapted chapter, the published article also investigates excitatory transmission after 11 weeks of HFD feeding, which is summarized in Figure 4.5. At this more chronic timepoint, mEPSC frequency in MCH neurons is increased compared to 4 weeks of HFD³⁰⁸. The progressive amplification of the magnitude

of mEPSCs with longer HFD feeding suggests that the observed effects are unlikely to be a result of obesity. Although not explicitly tested, given the role of MCH in positive energy balance, our data suggest that the timing of the onset and continuance of elevated excitatory drive to MCH neurons may contribute to the development and maintenance of DIO.

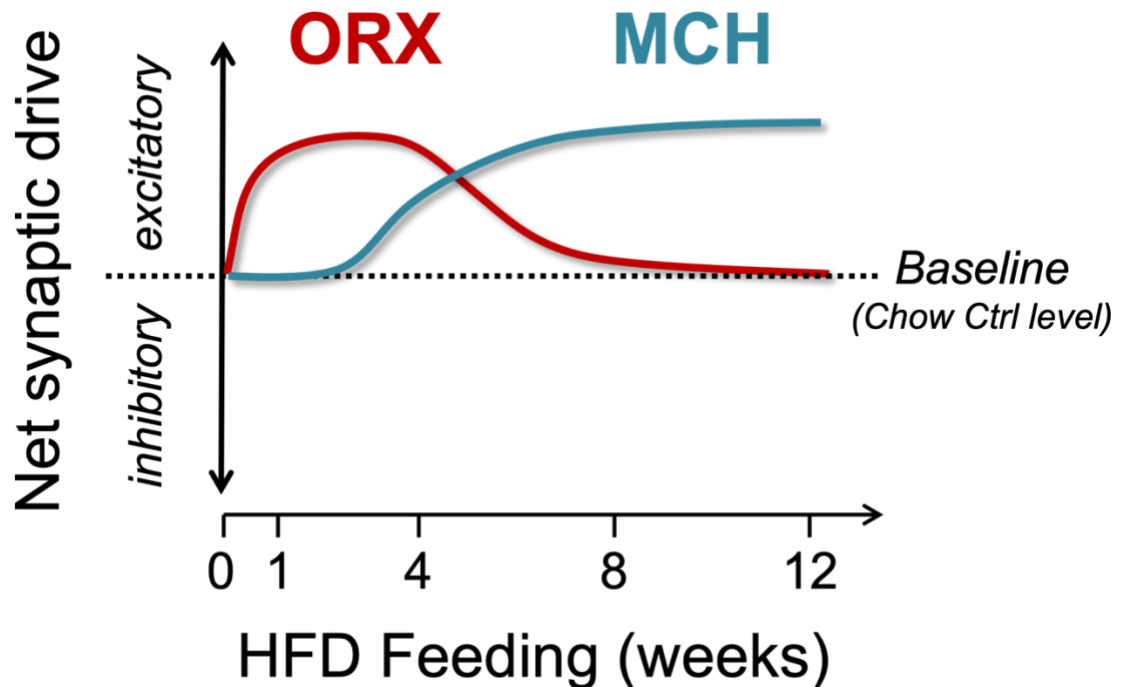


Figure 4.5. Net change in synaptic properties of adult ORX and MCH neurons over the course of HFD feeding

A schematic summarizing the time course of synaptic changes in ORX and MCH neurons due to HFD. In ORX neurons, excitatory synaptic transmission increases during the acute phase (from 1 day to 4 weeks) but returns to chow Ctrl levels (baseline) by week 11 of HFD. Thus, the synaptic drive to ORX neurons is excitatory in the early phase of HFD, which normalizes with prolonged feeding. In MCH neurons, as HFD exposure persists, the excitatory synaptic drive starts to increase by week 4 and continues to increase with prolonged feeding. Thus, the synaptic drive follows the changes in excitatory transmission.

Previous studies have shown that ORX and MCH neurons undergo various forms of synaptic plasticity during obese states or HFD feeding. For example, DIO or leptin-deficiency changes the expression of cannabinoid receptors on excitatory and inhibitory synaptic terminals, resulting in altered endocannabinoid-dependent control of ORX neurons^{334,350}. Leptin deficient mice also display altered endocannabinoid-mediated synaptic inhibition in perifornical neurons, about half of which were identified as MCH neurons³⁵¹. Furthermore, HFD impairs thermosensitivity of ORX neurons²⁸⁹ and leptin-induced inhibition of excitatory transmission to MCH and ORX neurons³⁴³. Time-dependent plasticity has also been observed, where excitatory synapses to ORX neurons are primed for long-term depression after 1 week of HFD feeding, but not after 4 weeks¹⁴⁸. Therefore, HFD can also induce other plastic and metaplastic changes that could collectively shape the synaptic inputs that regulate the excitability of these neurons.

4.5. *Conclusion*

The present study is the first to investigate time-dependent HFD-induced changes in spontaneous synaptic transmission in lateral hypothalamic cell populations. Over the course of HFD feeding, we found that synaptic plasticity was differentially altered in ORX and MCH neurons, which was coincident with the duration of feeding. As energy balance is coordinated by many neuronal populations, synaptic plasticity in ORX and MCH neurons are unlikely to be the sole determinant of the response to HFD but may nevertheless impact the overall

activity and output of the feeding circuitry. In the short-term, ORX neurons receive an increased excitatory drive and may mediate the rewarding aspect of HFD consumption²¹⁴. In the long-term, reversal of the excitatory effects on ORX neurons may provide a permissive condition for weight gain³²⁹, while a delayed increase in excitatory inputs to MCH neurons could contribute to the development and maintenance of DIO^{163,332}. These complex, time-dependent changes in synaptic plasticity suggest that the HFD effects on feeding-related neurons are dynamic and not necessarily static. When comparing studies or choosing appropriate timing, either for investigation or for weight loss interventions, it is important to consider the effects of feeding duration.

Chapter 5 – Summary and discussion

5.1. *Summary of main findings*

Energy homeostasis is maintained by a complex network of neurons. This dissertation provides evidence that exposure to a HFD elevates the body weight set point through a coordinated effort between homeostatic and hedonic systems, in part mediated by the ORX and MCH systems (Figure 5.1). Acute HFD induces synaptic adaptations in ORX neurons that promote hedonic feeding, and this initial hyperphagia supports the subsequent development of obesity. As significant weight gain begins, inflammatory signalling coincides with synaptic and intrinsic changes in MCH neurons. Obesity can be mitigated by blocking PGE₂ inflammatory signalling in MCH neurons during HFD feeding, suggesting that the PGE₂-EP2R-MCH axis described in this dissertation may play a significant role in determining the body weight set point. This represents a novel neuronal mechanism by which hypothalamic inflammation can contribute to weight gain.

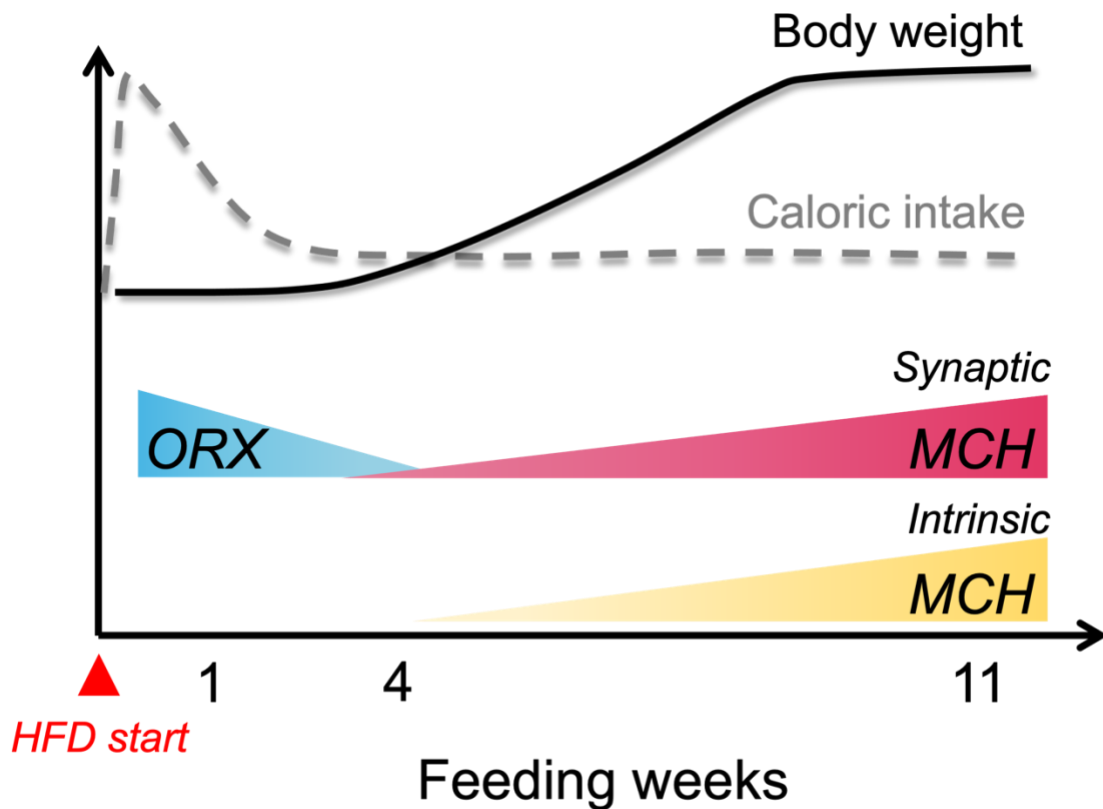


Figure 5.1. Summary figure depicting the time course of ORX and MCH neuron activation with body weight and food intake changes.

ORX neurons are transiently active during acute (1 week) HFD feeding, likely driving early hyperphagia that supports the development of obesity. As ORX activation subsides, MCH activation begins, preceding significant weight gain. As HFD becomes chronic, the magnitude of MCH activation increases, contributing to both the development and maintenance of obesity.

5.2. Discussion

5.2.1. Reversal of obesity

The set point theory suggests that a shift in set point would induce a counterregulatory response as the body avidly defends the newly established body weight. Chapter 2 of this thesis supports the set point theory, as switching the diet from HFD to chow results in a transient hypophagia and initial rapid weight loss that both decay and return to a steady-state over time, which is clearly seen in Figures 2.5, 2.6, and 2.8. This may underscore why it is difficult to lose weight long-term.

MCH neuron depolarization induced by 4 weeks of HFD is reversible when rats are returned to chow for 4 weeks. As weight loss becomes more difficult with prolonged HFD, I speculate that the RMP changes to MCH neurons will become irreversible, or a dietary intervention longer than 4 weeks of chow would be required to reverse the RMP depolarization. Indeed, even after significant weight loss, there are reports of stable DIO-induced changes in the energy balance circuitry. For example, dietary fat typically inhibits AgRP neurons, however, over the course of DIO this response desensitizes. This desensitization persists even when mice have lost weight²⁵⁷, overall supporting orexigenic function.

In Chapters 3 and 4, the magnitude of the intrinsic and synaptic effects on MCH neurons increased as HFD became more chronic. This perhaps means that a dieting intervention at early time points, before MCH neuron adaptations become stable, would be more efficacious at inducing weight loss. This is in line with our findings in Chapter 2, as a prolonged history of HFD makes it

considerably harder to reverse the set point from high to low level in adulthood. This is seemingly consistent with humans, as obesity in childhood impairs future weight loss in adulthood³⁵².

5.2.2. The search for a molecular/cellular correlate of set point

Manipulation of certain neuronal circuits and cell types can prevent DIO in rodents as shown in this thesis and other reports^{239,353–355}, which may be indicative of the role of these neurons in determining the set point.

Chronic diet-induced neuroinflammation could cause the body weight set point to deviate, as suppression of hypothalamic inflammation is protective against DIO^{65,67,69}. In support of this, a glucagon-like peptide 1 receptor (GLP1R) agonist-mediated reduction in body weight was associated with a decrease in hypothalamic microgliosis and SOCS3, a suppressor of leptin and insulin signalling³⁵⁶.

In Chapter 3, we highlight EP2R signalling in MCH neurons as a driver of obesity. It is tempting to speculate that this mechanism in part establishes a higher body weight set point during HFD feeding. Consistent with the idea of a flexible set point, MCH neuron depolarization can be reversed by dieting, which follows a similar time course to the resolution of ARC gliosis induced by dieting³⁵⁷.

5.2.3. Timeline of obesity development vs maintenance

Although we surmise that the increased excitatory drive to ORX neurons after short-term HFD induces the initial hyperphagia, we know that ORX neurons

also play a strong role in energy expenditure^{329,358}. There is a report that 1 day of HFD feeding increases energy expenditure in rodents^{359,360}, which returned to levels of chow-fed only controls at 3 weeks, before further decreasing by 7 weeks³⁶⁰. This matches our general time course of mEPSC changes on ORX neurons. At 11 weeks of feeding, the reversal of excitatory drive to ORX neurons coupled with an increase in MCH neuron excitability is consistent with a decreased energy expenditure.

In a calcium imaging study in freely behaving mice, it was shown that eating is less likely to happen when ORX neurons are active, and food consumption rapidly decreases ORX neuron activity³⁶¹. This natural behavior of ORX neurons supports a primary function in foraging behavior accompanying energy expenditure rather than consummatory behavior. Interestingly, we have previously demonstrated that ORX neurons undergo an age-dependent decrease in mIPSC amplitude, which is attenuated when animals are fed HFD³⁰⁸. This may represent a net increase in inhibitory drive to ORX neurons during HFD feeding, which may favor overeating. In addition to the role of ORX neuron activity in the development of obesity, inhibition of these neurons may be permissive for obesity maintenance as well.

MCH neuron activation is persistent as HFD prolongs, suggesting their involvement in the development and maintenance of obesity. This is further supported by the reversal of RMP when HFD is removed, and the resultant lean phenotype when MCH neuron activation is suppressed by deletion of EP2R in Chapter 3. The parallel time course of synaptic and intrinsic plasticity of MCH

neurons is unlikely to be a coincidence and leads us to ask whether PGE₂ could also mediate the synaptic effects. PGE₂-EP4R signalling in microglia promotes DIO by internalization of anorectic POMC projections³⁶². Increased microglial phagocytic function would not explain the increase in synaptic contacts we see to MCH neurons, however, due to vast heterogeneity of microglial function³⁶³, it is possible that microglial PGE₂ contributes to the synaptic plasticity seen in the LH. Energy status can also affect astrocytic ensheathment of neurons^{364,365}, and astrocytes surrounding MCH and ORX neurons are known to undergo remodelling upon homeostatic challenge³⁶⁶. Therefore, it is possible PGE₂ has undescribed roles in synaptic remodelling.

5.2.4. Sex differences in obesity

As only Chapter 3 addressed the important issue of sex, I will discuss possible implications of sex differences in our other findings here.

In animal models, females typically develop a more mild obesity^{251,367-371}. This milder phenotype is attributed to a higher energy expenditure during HFD challenge compared to males^{370,372}. Consistent with this, BAT mass and activity is greater in HFD-fed females³⁷³. As ORX can enhance BAT thermogenesis²⁰⁷, perhaps the increased excitatory drive to ORX neurons is sustained throughout the course of HFD feeding in females. Also, as weight gain is more gradual in HFD-fed females³⁷⁰, one might also expect a delayed time course for MCH neuron plasticity since the majority of these changes occurred just prior to the onset of significant weight gain in males.

Critically, studies report a marked absence of HFD-induced hypothalamic inflammation in female rodents^{310,311,374}. These studies, however, examined either bulk hypothalamic content or specifically the ARC, which could have obfuscated meaningful differences in discrete hypothalamic nuclei.

One study did not observe microgliosis in the LH of HFD-fed female rats³⁷⁴, however, a preliminary study in our lab shows an increase in the density of microglia marked by ionized calcium binding adaptor molecule 1 (Iba1) in the LH of female mice [data not shown]. This difference could be a result of a species divergence, the hypothalamic nucleus examined, variable feeding paradigms, or a combination of these factors. It is plausible, however, that the degree of hypothalamic inflammation is higher in males than in females, and thus more easily detectable. This could also explain why the effect of the MCH-specific EP2R KO is more subtle in females. In support of this, male neutrophils have increased COX2 and PGE₂ synthesis in response to an acute inflammatory insult *in vitro*³⁷⁵. As well, estradiol inhibits LPS-induced microglial activation and reduces levels of COX2 and PGE₂ in murine cells^{376–378}. Whether estradiol plays a similar role during a low-grade chronic inflammation, such as that seen during DIO, remains unknown.

5.2.5. *Inflammation – cause vs result?*

Is inflammation a cause or a result of obesity? There is substantial preclinical evidence that inflammation causes obesity, as many studies demonstrate that upregulation of inflammatory factors is sufficient to induce

weight gain, and suppression is protective against obesity. This is much less clear in humans, as brain imaging and post-mortem studies can only confirm the presence or absence of inflammation, and not the time course.

Perhaps the strongest evidence that inflammation is not a result of obesity is the absence of hypothalamic microgliosis in genetic models of obesity (*ob/ob*, *db/db*, and MC4R KO mice), despite their elevated body weight. Only after these mice were exposed to HFD did microgliosis appear³⁷⁹. However, additional studies are needed to confirm this, as microgliosis is not the only indicator of inflammation. Curiously, there is a report of hippocampal inflammation in *ob/ob* mice, as measured by gene expression analysis³⁸⁰. Therefore, it is premature to state that inflammation is not a result of obesity, although it appears that it is certainly a result of overnutrition.

It is worth mentioning that inflammation itself is not always negative, and in fact, acute inflammation is needed to resolve conditions such as tissue injury³⁸¹. Surprisingly, an acute inflammatory response in adipose tissue is needed for WAT remodelling after HFD exposure, as suppression leads to ectopic lipid accumulation³⁸². Therefore, inflammation plays a dual role, with acute states being essential for adaptive function, and chronic states resulting in impairment and dysfunction.

5.2.6. Circuit-level considerations

MCH and ORX neurons exist in local microcircuits and can bidirectionally communicate³⁸³, dynamically influencing the other's activity. As such, perhaps

the coincident enhancement in excitatory transmission to both cell types after 4 weeks of HFD is due to increased ORX neuron glutamatergic output. The enhanced excitatory drive to MCH neurons is due to an increase in synaptic contacts, but it is unknown whether glutamatergic terminals of ORX neurons directly contribute to this. Likewise, MCH neurons are known to be glutamatergic [refs], but it is not known whether they release glutamate at synapses with ORX neurons.

5.2.7. Putative upstream targets

Possible sources of glutamatergic afferents to MCH neurons include the lateral orbitofrontal cortex (IOFC), VH, and lateral PBN. Although the IOFC becomes disinhibited during DIO¹³⁹, the identity of the LH cells as their potential projection target is unknown. On the other hand, a subpopulation of VH cells synapse directly on to ORX neurons³⁸⁴. As HFD has been shown to enhance VH glutamatergic input to the NAc³⁸⁵, it is possible that excitatory drive to ORX neurons is similarly enhanced. Lastly, the lateral PBN provides glutamatergic innervation to the LH, exclusively to ORX neurons located supraforinally³⁸⁶. However, the functional implication of this synapse has not been explored. Other sources of glutamatergic innervation include the DH³⁸⁷ and amygdala³³⁸, which undergo extensive remodelling after HFD or obesity^{388–392}. Using viral-mediated circuit mapping and electrophysiology, we can start to elucidate the upstream brain areas implicated in the HFD-induced synaptic plasticity of the LH.

5.2.8. Downstream targets of MCH and ORX

A major downstream target of MCH and ORX neurons is the mesolimbic system. ORX neurons potentiate dopamine release in the NAc³⁹³ which is rewarding. Thus, increased output from ORX neurons during acute HFD feeding may promote hedonic consumption through increasing dopamine release in the NAc²¹¹. This increased dopaminergic tone is then progressively lost as MCH neuron activity peaks during prolonged HFD feeding.

In accordance with this, MCH suppresses dopamine release in the NAc³⁹⁴, therefore, one would expect chronic MCH neuron activation during DIO to reduce dopaminergic transmission. Reduced dopamine transmission in the NAc is indeed the case in models of genetic and dietary obesity^{395,396}. Consumption of palatable foods like HFD increases dopamine release^{313,397}, which may inherently contribute to overconsumption³⁹⁸ as this would transiently rectify the hypodopaminergic state during obesity.

Another major brain area for MCH and ORX action is the hippocampus, which likely mediates impairments in cognition and memory seen during obesity³⁹⁹. As discussed, the role of MCH in the hippocampus is inconclusive^{191,192,400–402}, but may be partially explained by MCH subpopulations¹⁹². As presented in this thesis, we observed variability in the RMP of MCH neurons after HFD feeding, with some seemingly unresponsive cells, which would support the notion of subpopulations.

Interestingly, Ox1R signalling was found to mediate impairments in hippocampal plasticity and pattern separation induced by 8 weeks of HFD

feeding⁴⁰³. As increased excitatory synaptic transmission to ORX neurons reverses between 4 and 11 weeks of feeding, it would be interesting to determine whether the HFD-induced cognitive impairments are still ORX-mediated at more chronic time points. If they are, this would suggest an enhanced ORX tone independent of depolarization or increased excitatory drive to ORX neurons.

5.2.9. Cell-level considerations

5.2.9.1. Cell specificity

It is notable that the direct effect of HFD on intrinsic excitability is at least somewhat specific to MCH neurons, sparing ORX neurons that share the same environmental milieu. We identified that this specificity is not conferred by the presence of EP2R, as ORX neurons express this receptor (Figure 5.2). Instead, this is likely at the level of Na⁺/K⁺-ATPase. Unlike MCH neurons, Na⁺/K⁺-ATPase in ORX neurons contribute minimally to the RMP as assessed by ouabain [data not shown], therefore modulation of their function is unlikely to result in significant changes to membrane potential.

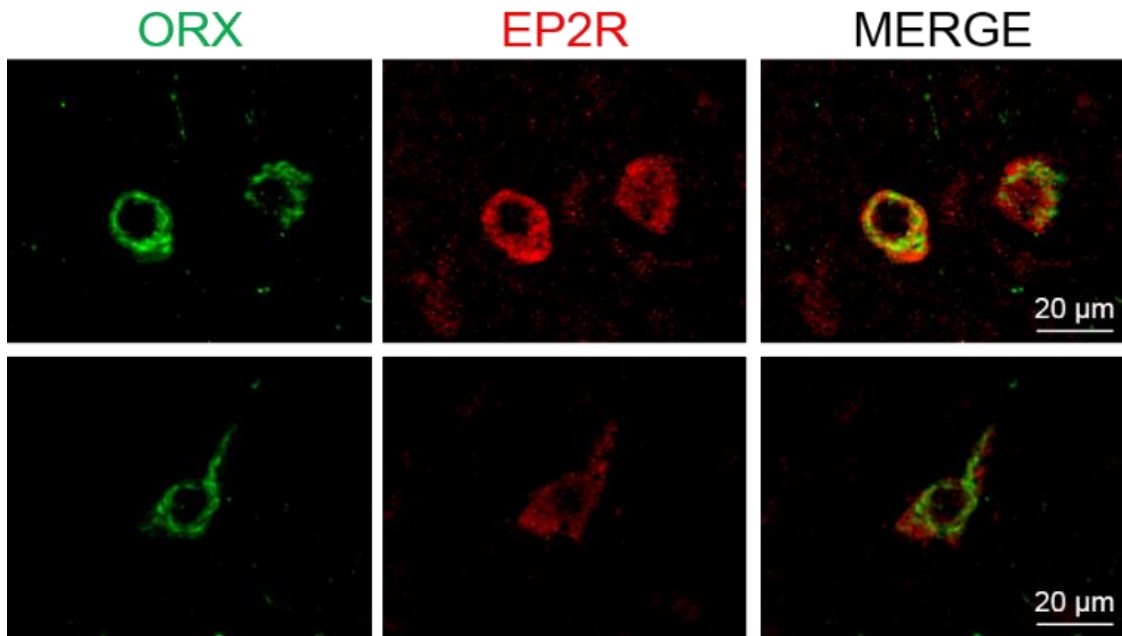


Figure 5.2. ORX neurons express EP2R.

Representative double immunofluorescence images of ORX (green) and EP2R (red) expression in the lateral hypothalamus. Scale bar = 20 μm

Curiously, ORX neurons are activated by intracerebroventricular administration of PGE₂, as assessed by c-Fos expression⁴⁰⁴, demonstrating that PGE₂ *can* recruit ORX neurons. However, this is likely independent of EP2R and Na⁺/K⁺-ATPase signalling. As well, the concentration used elicited fever in animals, therefore the level of PGE₂ was likely higher than that seen during DIO.

5.2.9.2. *MCH neuron subpopulations*

As previously described, MCH neurons are not neurochemically homogeneous. MCH+/CART+ and MCH+/CART- cells have distinct anatomical locations, as well as projection targets⁴⁰⁵. Anecdotally though, it appears that all MCH+ neurons were also EP2R+, making all MCH neurons capable of engaging PGE₂-EP2R signalling. However, as MCH+/CART- neurons project caudally, they may be implicated in the control of energy expenditure or sleep, while rostral-projecting MCH+/CART+ cells could be more important in the regulation of feeding behavior and memory⁴⁰⁵. Future studies investigating the discrete roles of these subpopulations will aid in disentangling the functional consequence.

Also, CART is not the sole co-transmitter in MCH neurons. The majority of MCH neurons are also glutamatergic, expressing vGlut2, with a small proportion (<10%) expressing the vesicular glutamate transporter 3 (vGlut3)¹⁷². vGlut3 might function to enhance co-transmitter loading and release⁴⁰⁶, therefore, vGlut3+ MCH neurons may have enhanced co-transmitter release. However, the functional implication would depend on the identity of the co-transmitter(s) present at that terminal. For example, some MCH neurons also contain

enkephalin and nociceptin¹⁷², which are involved in pain and stress^{407,408}, thus enhanced release of these peptides would likely differ from the MCH peptide in terms of behavioral consequences.

5.2.9.3. *ORX neuron subpopulations*

There are two electrophysiologically-distinct ORX neuron subtypes that have been described. These two subtypes can be discriminated by their response to a hyperpolarizing current. H-type ORX neurons exhibit a delayed firing while D-type ORX neurons display immediate firing following a hyperpolarization³⁴⁷.

H-type cells receive more excitatory inputs in comparison to D-type cells. Given that the LS, amygdala, and bed nucleus of the stria terminalis (BNST) comprise some of the heaviest glutamatergic inputs to ORX neurons^{409,410}, H-type cells may be preferentially involved in mediating stress behaviors. Meanwhile, sleep deprivation exclusively excites D-type ORX neurons³⁴⁹, implicating them in the regulation of sleep/wake. Both types are sensitive to glucose, however, H-types exhibit a prolonged response³⁴⁸. This could mean that H- and D-type cells play divergent roles in energy balance.

The studies in Chapters 3 and 4 did not segregate ORX neurons into subtypes. The data does not seem to support the idea that HFD has distinct effects on these subtypes, however, as the observed responses to HFD did not

show an obvious bimodal pattern in either RMP or mEPSC measures. Despite this, parsing these two groups may reveal subtype-specific effects of HFD.

5.2.10. *Perspective on obesity treatment and prevention*

5.2.10.1. *Anti-inflammatory pharmacotherapies*

Despite the evidence for the contribution of both peripheral and central inflammation to obesity, pharmacotherapies that target inflammatory factors have not been tested in clinical trials. A retrospective study determined that individuals with type II diabetes were >2x more likely to lose weight when they were prescribed aspirin⁴¹¹, a non-steroidal anti-inflammatory drug (NSAID) that inhibits the synthesis of COX enzymes. However, meta-analyses examining anti-TNF α drugs show no change or an increase in weight and BMI post-therapy. Although, these findings are compromised by all participants having a chronic inflammatory disease⁴¹².

Despite the disappointing lack of human studies, hesitation in implementing chronic non-inflammatory drugs to treat human obesity is warranted. Inflammation is *necessary* for normal physiological function⁴¹³, and individuals that chronically use immunosuppressive drugs or NSAIDs are at an increased risk for adverse renal and cardiovascular events^{414,415}, and hepatotoxicity^{416,417}. Therefore, it is uncertain whether the risks associated with anti-inflammatory treatment would outweigh the risks of not pursuing treatment.

5.2.10.2. *Dietary intervention and supplementation*

Outside of caloric restriction, several other dietary interventions have been proposed to aid in reducing weight and treating obesity^{418–420}. One of the most popular is a Mediterranean style diet, which emphasizes high consumption of plants, nuts and olive oil, and low consumption of dairy and red meat⁴²¹. This type of diet has been associated with weight loss and other metabolic-related improvements in individuals with obesity^{420,422,423}.

Others have taken to mimicking the beneficial effects of caloric restriction at the cellular level using certain compounds termed “caloric restriction mimetics”. Resveratrol, a naturally occurring dietary compound, has been found to reverse obesity in mice⁴²⁴ and significantly improve the metabolic profile of humans over the course of 30 days⁴²⁵. However, in both the case of the Mediterranean style diet and caloric restriction mimetics, the long-term efficacy has not been assessed. Further, as with any large lifestyle change, the proclivity to adhere to the regimen typically wanes with time⁴²⁶.

5.2.10.3. *Deep brain stimulation*

Deep brain stimulation (DBS) is a neuromodulation therapy that has significantly improved the lives of those with movement disorders, and show promise in treating psychiatric disorders⁴²⁷. DBS has been used to treat obesity in rare cases but has had inconsistent effects⁴²⁸. This may be due to differences in where the device is implanted and variations in the stimulation protocol used. Notably, two subjects that had previously undergone bariatric surgery but

regained all weight lost showed significant improvements in control of food intake and had substantially reduced body weight after 6 months of NAc DBS⁴²⁹. This finding, although preliminary, is exciting especially for those with obesity that was unsuccessfully treated with other interventions.

A caveat of these devices is their indiscriminate impact on neighboring cells and circuits. Therefore, it is not unusual to have undesirable side effects that accompany DBS. Some of those reported for obesity DBS studies include manic symptoms, nausea, difficulties falling asleep, and seizure⁴³⁰. Due to the small sample size and limited studies, this probably does not capture the full range of adverse side effects.

Presently, there are ongoing clinical trials examining the effect of DBS on obesity, which will aid in clarifying the efficacy of these treatments and will help better inform future treatment parameters.

5.2.10.4. *Development of novel therapies*

In the face of steadily increasing rates of obesity, we only have imperfect therapies. Even the most efficacious pharmacotherapy induced >25% weight loss in only *a third* of the patients taking the highest dose²⁹. Additionally, 50% of patients that underwent bariatric surgery report regaining a significant amount of weight⁴³¹. Although neuromodulation therapies seem promising, the inconsistent outcome and many unknown variables leave us very far away from an approved DBS treatment. Therefore, we are in dire need of novel therapeutic options and druggable targets.

With the wealth of preclinical studies that successfully achieve weight loss, the (not-so) simple solution is to make more targeted therapies that suppress inflammation or modulate activity in an intended region, or even intended circuit or cell type. However, targeting the CNS is especially difficult due to the challenge of bypassing the BBB. there is no standard way to target specific cells or circuits in humans. Therefore, the feasibility of such treatments in humans is unknown, and if possible, may be decades away. Despite this, recent advancements in small molecule targeting strategies, such as antibody- and peptide-mediated targeting⁴³², and nanoparticle delivery⁴³³ offer a hopeful outlook that such therapies are not just science fiction.

5.2.11. *Limitations and challenges*

5.2.11.1. *Diet*

Another challenge with the current state of preclinical studies is the use of various diets. Although many DIO mouse models use diets high in fat, varying compositions of fat, fat source, and other macronutrient constituents can make comparisons between studies difficult. Additionally, the typical American or European diet contains ~36-40% fat⁴³⁴, which makes the popularly used 60% HFD supraphysiological and perhaps less relevant than the ~40% HFDs in studying DIO. Although WD and 45FD both contain ~40% fat, the source of fat and fatty acid composition differs (Table 5.1). Specifically, WD contains more SFAs, while 45FD contains more polyunsaturated fat. From our studies, this difference does not seemingly impact body weight gain (Chapter 2) or MCH

neuron depolarization (Chapter 3), however, only mice fed WD showed an attenuated hypophagia upon switching to chow after repeated dieting cycles. This suggests that a previous history of SFA may alter the homeostatic response to favor positive energy balance. This is quite plausible as SFAs induce hypothalamic inflammation and promote weight gain, while polyunsaturated fatty acids are not associated with hypothalamic inflammation and promote weight loss^{435,436}.

Diets high in fat are known to alter glucose homeostasis and insulin and leptin sensitivity⁴³⁷, therefore it is possible that the depolarizing effect of WD on MCH neurons is instead a result of resistance to these hormones. Although this is unlikely as we were able to completely block the depolarization effect by inhibiting PGE₂ synthesis or signaling, we must still consider this possibility. MCH neurons are known to be glucose-excited²⁸⁷, however HFD impairs glucose uptake in the brain⁴³⁹. This likely results in decreased levels of glucose locally in the hypothalamus, which would inhibit MCH neurons. HFD is also known to induce hyperleptinemia and hyperinsulinemia, and while MCH expression is inhibited by leptin¹⁸⁴, a subpopulation of MCH neurons is excited by insulin¹⁸³. While enhanced insulin activity at MCH neurons is a plausible alternate explanation, insulin receptor inactivation in MCH neurons had virtually no effect on BW or fat pad mass of HFD-fed mice¹⁸³, in contrast to the lean phenotype of mice lacking EP2R from MCH neurons in Chapter 3. Therefore, hyperinsulinemia itself is not a plausible mechanism to explain the phenotype we see.

Table 5.1. Fatty acid composition of WD and 45FD.

Fatty acid	% Diet Composition	
	WD	45FD
Saturated	62.4	31.4
Monounsaturated	30.7	35.5
Polyunsaturated	6.9	33.1

Further, all of the rodent diets used in this thesis have been formulated for optimal rodent health, which is not an accurate reflection of American dietary patterns. A relatively new diet called “Total Western Diet” (TWD) has been formulated to best mimic the American diet⁴³⁸. Identification of any differences that emerge in body weight regulation using TWD in comparison to the well-described HFDs in the literature will be pertinent in the future.

On a final note, mouse physiology does not necessarily translate to human physiology. These experiments are hugely important as proof of principle and for informing future translational studies, however, human practice should not be informed by mouse data alone.

5.3. *Conclusion*

It is worth acknowledging that obesity is a multifactorial problem. Therapies must be combined with an adequate education of nutrition and food choices, access to healthcare⁴⁴⁰, food security⁴³⁶, and reformed food policies⁴⁴². Therefore, as advancements in science progress, so must education, healthcare, and policy reform to best treat and prevent obesity.

The primary focus of this dissertation is to assess the impact of HFD on physiological and neuronal function, and to inform novel therapeutic targets. To this end, we have provided evidence that homeostatic and hedonic systems work in tandem to coordinate a shift in body weight set point. We deciphered changes in neuronal activity that may underlie the development and maintenance phases of obesity. Lastly, we identified a long-sought link between HFD-induced

hypothalamic inflammation and weight gain, which could be targeted in the treatment of obesity. This work as a whole adds depth to the current understanding of the neuronal control of energy balance, and will hopefully aid in the ultimate goal of combatting obesity.

References

1. Obesity and overweight <https://www.who.int/news-room/fact-sheets/detail/obesity-and-overweight>.
2. Dai, H., Alsalhe, T.A., Chalghaf, N., Riccò, M., Bragazzi, N.L., and Wu, J. (2020). The global burden of disease attributable to high body mass index in 195 countries and territories, 1990–2017: An analysis of the Global Burden of Disease Study. *PLoS Med* 17, e1003198. 10.1371/journal.pmed.1003198.
3. Mahase, E. (2023). Global cost of overweight and obesity will hit \$4.32tn a year by 2035, report warns. *BMJ*, p523. 10.1136/bmj.p523.
4. Costa-Font, J., and Mas, N. (2016). ‘Globesity’? The effects of globalization on obesity and caloric intake. *Food Policy* 64, 121–132. 10.1016/j.foodpol.2016.10.001.
5. Hall, K.D., Ayuketah, A., Brychta, R., Cai, H., Cassimatis, T., Chen, K.Y., Chung, S.T., Costa, E., Courville, A., Darcey, V., et al. (2019). Ultra-Processed Diets Cause Excess Calorie Intake and Weight Gain: An Inpatient Randomized Controlled Trial of Ad Libitum Food Intake. *Cell Metabolism* 30, 67-77.e3. 10.1016/j.cmet.2019.05.008.
6. Brownson, R.C., Boehmer, T.K., and Luke, D.A. (2005). DECLINING RATES OF PHYSICAL ACTIVITY IN THE UNITED STATES: What Are the Contributors? *Annu. Rev. Public Health* 26, 421–443. 10.1146/annurev.publhealth.26.021304.144437.
7. Wareham, N.J., Van Sluijs, E.M.F., and Ekelund, U. (2005). Physical activity and obesity prevention: a review of the current evidence. *Proc. Nutr. Soc.* 64, 229–247. 10.1079/PNS2005423.
8. Bell, A.C., Ge, K., and Popkin, B.M. (2002). The Road to Obesity or the Path to Prevention: Motorized Transportation and Obesity in China. *Obesity Research* 10, 277–283. 10.1038/oby.2002.38.
9. Stamatakis, E., Ekelund, U., and Wareham, N.J. (2007). Temporal trends in physical activity in England: The Health Survey for England 1991 to 2004. *Preventive Medicine* 45, 416–423. 10.1016/j.ypmed.2006.12.014.
10. Newby, P., Muller, D., Hallfrisch, J., Qiao, N., Andres, R., and Tucker, K.L. (2003). Dietary patterns and changes in body mass index and waist circumference in adults,. *The American Journal of Clinical Nutrition* 77, 1417–1425. 10.1093/ajcn/77.6.1417.

11. Duffey, K.J., Gordon-Larsen, P., Steffen, L.M., Jacobs, D.R., and Popkin, B.M. (2009). Regular Consumption from Fast Food Establishments Relative to Other Restaurants Is Differentially Associated with Metabolic Outcomes in Young Adults. *The Journal of Nutrition* 139, 2113–2118. 10.3945/jn.109.109520.
12. Thorp, A.A., Owen, N., Neuhaus, M., and Dunstan, D.W. (2011). Sedentary Behaviors and Subsequent Health Outcomes in Adults. *American Journal of Preventive Medicine* 41, 207–215. 10.1016/j.amepre.2011.05.004.
13. Hu, F.B. (2003). Television Watching and Other Sedentary Behaviors in Relation to Risk of Obesity and Type 2 Diabetes Mellitus in Women. *JAMA* 289, 1785. 10.1001/jama.289.14.1785.
14. Vandelanotte, C., Sugiyama, T., Gardiner, P., and Owen, N. (2009). Associations of Leisure-Time Internet and Computer Use With Overweight and Obesity, Physical Activity and Sedentary Behaviors: Cross-Sectional Study. *J Med Internet Res* 11, e28. 10.2196/jmir.1084.
15. Patel, S.R., and Hu, F.B. (2008). Short Sleep Duration and Weight Gain: A Systematic Review. *Obesity* 16, 643–653. 10.1038/oby.2007.118.
16. Patel, S.R., Malhotra, A., White, D.P., Gottlieb, D.J., and Hu, F.B. (2006). Association between Reduced Sleep and Weight Gain in Women. *American Journal of Epidemiology* 164, 947–954. 10.1093/aje/kwj280.
17. Taheri, S., Lin, L., Austin, D., Young, T., and Mignot, E. (2004). Short Sleep Duration Is Associated with Reduced Leptin, Elevated Ghrelin, and Increased Body Mass Index. *PLoS Med* 1, e62. 10.1371/journal.pmed.0010062.
18. Bellicha, A., Van Baak, M.A., Battista, F., Beaulieu, K., Blundell, J.E., Busetto, L., Carraça, E.V., Dicker, D., Encantado, J., Ermolao, A., et al. (2021). Effect of exercise training on weight loss, body composition changes, and weight maintenance in adults with overweight or obesity: An overview of 12 systematic reviews and 149 studies. *Obesity Reviews* 22, e13256. 10.1111/obr.13256.
19. Kim, J.Y. (2021). Optimal Diet Strategies for Weight Loss and Weight Loss Maintenance. *Journal of Obesity & Metabolic Syndrome* 30, 20–31. 10.7570/jomes20065.
20. Leung, A.W.Y., Chan, R.S.M., Sea, M.M.M., and Woo, J. (2017). An Overview of Factors Associated with Adherence to Lifestyle Modification Programs for Weight Management in Adults. *IJERPH* 14, 922. 10.3390/ijerph14080922.

21. Del Corral, P., Chandler-Laney, P.C., Casazza, K., Gower, B.A., and Hunter, G.R. (2009). Effect of Dietary Adherence with or without Exercise on Weight Loss: A Mechanistic Approach to a Global Problem. *The Journal of Clinical Endocrinology & Metabolism* 94, 1602–1607. 10.1210/jc.2008-1057.
22. Dulloo, A.G., and Montani, J.-P. (2015). Pathways from dieting to weight regain, to obesity and to the metabolic syndrome: an overview: Dieting and cardiometabolic risks. *Obes Rev* 16, 1–6. 10.1111/obr.12250.
23. Wilding, J.P.H., Batterham, R.L., Calanna, S., Davies, M., Van Gaal, L.F., Lingvay, I., McGowan, B.M., Rosenstock, J., Tran, M.T.D., Wadden, T.A., et al. (2021). Once-Weekly Semaglutide in Adults with Overweight or Obesity. *N Engl J Med* 384, 989–1002. 10.1056/NEJMoa2032183.
24. O’Neil, P.M., Birkenfeld, A.L., McGowan, B., Mosenzon, O., Pedersen, S.D., Wharton, S., Carson, C.G., Jepsen, C.H., Kabisch, M., and Wilding, J.P.H. (2018). Efficacy and safety of semaglutide compared with liraglutide and placebo for weight loss in patients with obesity: a randomised, double-blind, placebo and active controlled, dose-ranging, phase 2 trial. *The Lancet* 392, 637–649. 10.1016/S0140-6736(18)31773-2.
25. Frias, J.P., Nauck, M.A., Van, J., Benson, C., Bray, R., Cui, X., Milicevic, Z., Urva, S., Haupt, A., and Robins, D.A. (2020). Efficacy and tolerability of tirzepatide, a dual glucose-dependent insulinotropic peptide and glucagon-like peptide-1 receptor agonist in patients with type 2 diabetes: A 12-week, randomized, double-blind, placebo-controlled study to evaluate different dose-escalation regimens. *Diabetes Obes Metab* 22, 938–946. 10.1111/dom.13979.
26. Wilding, J.P.H., Batterham, R.L., Davies, M., Van Gaal, L.F., Kandler, K., Konakli, K., Lingvay, I., McGowan, B.M., Oral, T.K., Rosenstock, J., et al. (2022). Weight regain and cardiometabolic effects after withdrawal of semaglutide: The STEP 1 trial extension. *Diabetes Obesity Metabolism* 24, 1553–1564. 10.1111/dom.14725.
27. McCartney, M. (2023). Semaglutide: should the media slim down its enthusiasm? *BMJ*, p624. 10.1136/bmj.p624.
28. Lu, Y., Liu, Y., and Krumholz, H.M. (2022). Racial and Ethnic Disparities in Financial Barriers Among Overweight and Obese Adults Eligible for Semaglutide in the United States. *JAHA* 11, e025545. 10.1161/JAHA.121.025545.
29. Jastreboff, A.M., Aronne, L.J., Ahmad, N.N., Wharton, S., Connery, L., Alves, B., Kiyosue, A., Zhang, S., Liu, B., Bunck, M.C., et al. (2022). Tirzepatide

Once Weekly for the Treatment of Obesity. *N Engl J Med* 387, 205–216. 10.1056/NEJMoa2206038.

30. Gloy, V.L., Briel, M., Bhatt, D.L., Kashyap, S.R., Schauer, P.R., Mingrone, G., Bucher, H.C., and Nordmann, A.J. (2013). Bariatric surgery versus non-surgical treatment for obesity: a systematic review and meta-analysis of randomised controlled trials. *BMJ* 347, f5934–f5934. 10.1136/bmj.f5934.
31. Cheng, J., Gao, J., Shuai, X., Wang, G., and Tao, K. (2016). The comprehensive summary of surgical versus non-surgical treatment for obesity: a systematic review and meta-analysis of randomized controlled trials. *Oncotarget* 7, 39216–39230. 10.18632/oncotarget.9581.
32. Jakobsen, G.S., Småstuen, M.C., Sandbu, R., Nordstrand, N., Hofsø, D., Lindberg, M., Hertel, J.K., and Hjelmæsæth, J. (2018). Association of Bariatric Surgery vs Medical Obesity Treatment With Long-term Medical Complications and Obesity-Related Comorbidities. *JAMA* 319, 291. 10.1001/jama.2017.21055.
33. Di Angelantonio, E., Bhupathiraju, S.N., Wormser, D., Gao, P., Kaptoge, S., De Gonzalez, A.B., Cairns, B.J., Huxley, R., Jackson, C.L., Joshy, G., et al. (2016). Body-mass index and all-cause mortality: individual-participant-data meta-analysis of 239 prospective studies in four continents. *The Lancet* 388, 776–786. 10.1016/S0140-6736(16)30175-1.
34. Saper, C.B., Chou, T.C., and Elmquist, J.K. (2002). The Need to Feed. *Neuron* 36, 199–211. 10.1016/S0896-6273(02)00969-8.
35. Müller, M.J., Bosy-Westphal, A., and Heymsfield, S.B. (2010). Is there evidence for a set point that regulates human body weight? *F1000 Med Rep* 2. 10.3410/M2-59.
36. Mela, D.J. (2006). Eating for pleasure or just wanting to eat? Reconsidering sensory hedonic responses as a driver of obesity. *Appetite* 47, 10–17. 10.1016/j.appet.2006.02.006.
37. Lee, P.C., and Dixon, J.B. (2017). Food for Thought: Reward Mechanisms and Hedonic Overeating in Obesity. *Curr Obes Rep* 6, 353–361. 10.1007/s13679-017-0280-9.
38. Martin, L.E., Holsen, L.M., Chambers, R.J., Bruce, A.S., Brooks, W.M., Zarcone, J.R., Butler, M.G., and Savage, C.R. (2010). Neural Mechanisms Associated With Food Motivation in Obese and Healthy Weight Adults. *Obesity* 18, 254–260. 10.1038/oby.2009.220.

39. Brown, R.M., Kupchik, Y.M., Spencer, S., Garcia-Keller, C., Spanswick, D.C., Lawrence, A.J., Simonds, S.E., Schwartz, D.J., Jordan, K.A., Jhou, T.C., et al. (2017). Addiction-like Synaptic Impairments in Diet-Induced Obesity. *Biological Psychiatry* 81, 797–806. 10.1016/j.biopsych.2015.11.019.
40. Matikainen-Ankney, B.A., Legaria, A.A., Pan, Y., Vachez, Y.M., Murphy, C.A., Schaefer, R.F., McGrath, Q.J., Wang, J.G., Bluiitt, M.N., Ankney, K.C., et al. (2023). Nucleus Accumbens D1 Receptor–Expressing Spiny Projection Neurons Control Food Motivation and Obesity. *Biological Psychiatry* 93, 512–523. 10.1016/j.biopsych.2022.10.003.
41. Liu, S., Globa, A.K., Mills, F., Naef, L., Qiao, M., Bamji, S.X., and Borgland, S.L. (2016). Consumption of palatable food primes food approach behavior by rapidly increasing synaptic density in the VTA. *Proc. Natl. Acad. Sci. U.S.A.* 113, 2520–2525. 10.1073/pnas.1515724113.
42. LeCheminant, J.D., Heden, T., Smith, J., and Covington, N.K. (2009). Comparison of energy expenditure, economy, and pedometer counts between normal weight and overweight or obese women during a walking and jogging activity. *Eur J Appl Physiol* 106, 675–682. 10.1007/s00421-009-1059-9.
43. DeLany, J.P., Kelley, D.E., Hames, K.C., Jakicic, J.M., and Goodpaster, B.H. (2013). High energy expenditure masks low physical activity in obesity. *Int J Obes* 37, 1006–1011. 10.1038/ijo.2012.172.
44. Elbelt, U., Schuetz, T., Hoffmann, I., Pirlich, M., Strasburger, C.J., and Lochs, H. (2010). Differences of energy expenditure and physical activity patterns in subjects with various degrees of obesity. *Clinical Nutrition* 29, 766–772. 10.1016/j.clnu.2010.05.003.
45. Johannsen, D.L., Welk, G.J., Sharp, R.L., and Flakoll, P.J. (2008). Differences in Daily Energy Expenditure in Lean and Obese Women: The Role of Posture Allocation. *Obesity* 16, 34–39. 10.1038/oby.2007.15.
46. Stenkula, K.G., and Erlanson-Albertsson, C. (2018). Adipose cell size: importance in health and disease. *American Journal of Physiology-Regulatory, Integrative and Comparative Physiology* 315, R284–R295. 10.1152/ajpregu.00257.2017.
47. Virtue, S., and Vidal-Puig, A. (2008). It's Not How Fat You Are, It's What You Do with It That Counts. *PLoS Biol* 6, e237. 10.1371/journal.pbio.0060237.
48. Choi, T.-Y., Ahmadi, N., Sourayanezhad, S., Zeb, I., and Budoff, M.J. (2013). Relation of vascular stiffness with epicardial and pericardial adipose tissues,

- and coronary atherosclerosis. *Atherosclerosis* 229, 118–123. 10.1016/j.atherosclerosis.2013.03.003.
49. Iacobellis, G., and Bianco, A.C. (2011). Epicardial adipose tissue: emerging physiological, pathophysiological and clinical features. *Trends in Endocrinology & Metabolism* 22, 450–457. 10.1016/j.tem.2011.07.003.
50. Byrne, C.D. (2013). Ectopic fat, insulin resistance and non-alcoholic fatty liver disease. *Proc. Nutr. Soc.* 72, 412–419. 10.1017/S0029665113001249.
51. Rohm, T.V., Meier, D.T., Olefsky, J.M., and Donath, M.Y. (2022). Inflammation in obesity, diabetes, and related disorders. *Immunity* 55, 31–55. 10.1016/j.immuni.2021.12.013.
52. Duan, Y., Zeng, L., Zheng, C., Song, B., Li, F., Kong, X., and Xu, K. (2018). Inflammatory Links Between High Fat Diets and Diseases. *Front. Immunol.* 9, 2649. 10.3389/fimmu.2018.02649.
53. Le Chatelier, E., Nielsen, T., Qin, J., Prifti, E., Hildebrand, F., Falony, G., Almeida, M., Arumugam, M., Batto, J.-M., Kennedy, S., et al. (2013). Richness of human gut microbiome correlates with metabolic markers. *Nature* 500, 541–546. 10.1038/nature12506.
54. Rosenbaum, M., Knight, R., and Leibel, R.L. (2015). The gut microbiota in human energy homeostasis and obesity. *Trends in Endocrinology & Metabolism* 26, 493–501. 10.1016/j.tem.2015.07.002.
55. Ravussin, Y., Koren, O., Spor, A., LeDuc, C., Gutman, R., Stombaugh, J., Knight, R., Ley, R.E., and Leibel, R.L. (2012). Responses of Gut Microbiota to Diet Composition and Weight Loss in Lean and Obese Mice. *Obesity* 20, 738–747. 10.1038/oby.2011.111.
56. Kim, K.-A., Gu, W., Lee, I.-A., Joh, E.-H., and Kim, D.-H. (2012). High Fat Diet-Induced Gut Microbiota Exacerbates Inflammation and Obesity in Mice via the TLR4 Signaling Pathway. *PLoS ONE* 7, e47713. 10.1371/journal.pone.0047713.
57. Milanski, M., Degasperi, G., Coope, A., Morari, J., Denis, R., Cintra, D.E., Tsukumo, D.M.L., Anhe, G., Amaral, M.E., Takahashi, H.K., et al. (2009). Saturated Fatty Acids Produce an Inflammatory Response Predominantly through the Activation of TLR4 Signaling in Hypothalamus: Implications for the Pathogenesis of Obesity. *J. Neurosci.* 29, 359–370. 10.1523/JNEUROSCI.2760-08.2009.

58. Rocha, D.M., Caldas, A.P., Oliveira, L.L., Bressan, J., and Hermsdorff, H.H. (2016). Saturated fatty acids trigger TLR4-mediated inflammatory response. *Atherosclerosis* 244, 211–215. 10.1016/j.atherosclerosis.2015.11.015.
59. Lancaster, G.I., Langley, K.G., Berglund, N.A., Kammoun, H.L., Reibe, S., Estevez, E., Weir, J., Mellett, N.A., Pernes, G., Conway, J.R.W., et al. (2018). Evidence that TLR4 Is Not a Receptor for Saturated Fatty Acids but Mediates Lipid-Induced Inflammation by Reprogramming Macrophage Metabolism. *Cell Metabolism* 27, 1096-1110.e5. 10.1016/j.cmet.2018.03.014.
60. Hildebrandt, X., Ibrahim, M., and Peltzer, N. (2023). Cell death and inflammation during obesity: “Know my methods, WAT(son).” *Cell Death Differ* 30, 279–292. 10.1038/s41418-022-01062-4.
61. Lindhorst, A., Raulien, N., Wieghofer, P., Eilers, J., Rossi, F.M.V., Bechmann, I., and Gericke, M. (2021). Adipocyte death triggers a pro-inflammatory response and induces metabolic activation of resident macrophages. *Cell Death Dis* 12, 579. 10.1038/s41419-021-03872-9.
62. Zatterale, F., Longo, M., Naderi, J., Raciti, G.A., Desiderio, A., Miele, C., and Beguinot, F. (2020). Chronic Adipose Tissue Inflammation Linking Obesity to Insulin Resistance and Type 2 Diabetes. *Front. Physiol.* 10, 1607. 10.3389/fphys.2019.01607.
63. De Souza, C.T., Araujo, E.P., Bordin, S., Ashimine, R., Zollner, R.L., Boschero, A.C., Saad, M.J.A., and Velloso, L.A. (2005). Consumption of a fat-rich diet activates a proinflammatory response and induces insulin resistance in the hypothalamus. *Endocrinology* 146, 4192–4199. 10.1210/en.2004-1520.
64. Guillemot-Legris, O., and Muccioli, G.G. (2017). Obesity-Induced Neuroinflammation: Beyond the Hypothalamus. *Trends in Neurosciences* 40, 237–253. 10.1016/j.tins.2017.02.005.
65. Valdearcos, M., Douglass, J.D., Robblee, M.M., Dorfman, M.D., Stifler, D.R., Bennett, M.L., Gerritse, I., Fasnacht, R., Barres, B.A., Thaler, J.P., et al. (2017). Microglial Inflammatory Signaling Orchestrates the Hypothalamic Immune Response to Dietary Excess and Mediates Obesity Susceptibility. *Cell Metabolism* 26, 185-197.e3. 10.1016/j.cmet.2017.05.015.
66. Lee, C.H., Kim, H.J., Lee, Y.-S., Kang, G.M., Lim, H.S., Lee, S., Song, D.K., Kwon, O., Hwang, I., Son, M., et al. (2018). Hypothalamic Macrophage Inducible Nitric Oxide Synthase Mediates Obesity-Associated Hypothalamic Inflammation. *Cell Reports* 25, 934-946.e5. 10.1016/j.celrep.2018.09.070.

67. Zhang, X., Zhang, G., Zhang, H., Karin, M., Bai, H., and Cai, D. (2008). Hypothalamic IKK β /NF- κ B and ER stress link overnutrition to energy imbalance and obesity. *Cell* 135, 61–73. 10.1016/j.cell.2008.07.043.
68. Thaler, J.P., Yi, C.-X., Schur, E.A., Guyenet, S.J., Hwang, B.H., Dietrich, M.O., Zhao, X., Sarruf, D.A., Izgur, V., Maravilla, K.R., et al. (2012). Obesity is associated with hypothalamic injury in rodents and humans. *J Clin Invest* 122, 153–162. 10.1172/JCI59660.
69. Douglass, J.D., Dorfman, M.D., Fasnacht, R., Shaffer, L.D., and Thaler, J.P. (2017). Astrocyte IKK β /NF- κ B signaling is required for diet-induced obesity and hypothalamic inflammation. *Molecular Metabolism* 6, 366–373. 10.1016/j.molmet.2017.01.010.
70. van de Sande-Lee, S., Melhorn, S.J., Rachid, B., Rodovalho, S., De-Lima-Junior, J.C., Campos, B.M., Pedro, T., Beltramini, G.C., Chaim, E.A., Pareja, J.C., et al. (2020). Radiologic evidence that hypothalamic gliosis is improved after bariatric surgery in obese women with type 2 diabetes. *Int J Obes* 44, 178–185. 10.1038/s41366-019-0399-8.
71. Kreutzer, C., Peters, S., Schulte, D.M., Fangmann, D., Türk, K., Wolff, S., van Eimeren, T., Ahrens, M., Beckmann, J., Schafmayer, C., et al. (2017). Hypothalamic Inflammation in Human Obesity Is Mediated by Environmental and Genetic Factors. *Diabetes* 66, 2407–2415. 10.2337/db17-0067.
72. Moraes, J.C., Coope, A., Morari, J., Cintra, D.E., Roman, E.A., Pauli, J.R., Romanatto, T., Carvalheira, J.B., Oliveira, A.L.R., Saad, M.J., et al. (2009). High-Fat Diet Induces Apoptosis of Hypothalamic Neurons. *PLoS ONE* 4, e5045. 10.1371/journal.pone.0005045.
73. Hanuscheck, N., Thalman, C., Domingues, M., Schmaul, S., Muthuraman, M., Hetsch, F., Ecker, M., Endle, H., Oshaghi, M., Martino, G., et al. (2022). Interleukin-4 receptor signaling modulates neuronal network activity. *J Exp Med* 219, e20211887. 10.1084/jem.20211887.
74. Kawasaki, Y., Zhang, L., Cheng, J.-K., and Ji, R.-R. (2008). Cytokine Mechanisms of Central Sensitization: Distinct and Overlapping Role of Interleukin-1 β , Interleukin-6, and Tumor Necrosis Factor- α in Regulating Synaptic and Neuronal Activity in the Superficial Spinal Cord. *J. Neurosci.* 28, 5189–5194. 10.1523/JNEUROSCI.3338-07.2008.
75. Luo, H., Liu, H.-Z., Zhang, W.-W., Matsuda, M., Lv, N., Chen, G., Xu, Z.-Z., and Zhang, Y.-Q. (2019). Interleukin-17 Regulates Neuron-Glial Communications, Synaptic Transmission, and Neuropathic Pain after Chemotherapy. *Cell Reports* 29, 2384–2397.e5. 10.1016/j.celrep.2019.10.085.

76. Reis, W.L., Yi, C.-X., Gao, Y., Tschöp, M.H., and Stern, J.E. (2015). Brain Innate Immunity Regulates Hypothalamic Arcuate Neuronal Activity and Feeding Behavior. *Endocrinology* 156, 1303–1315. 10.1210/en.2014-1849.
77. Obradovic, M., Sudar-Milovanovic, E., Soskic, S., Essack, M., Arya, S., Stewart, A.J., Gojobori, T., and Isenovic, E.R. (2021). Leptin and Obesity: Role and Clinical Implication. *Front. Endocrinol.* 12, 585887. 10.3389/fendo.2021.585887.
78. Tokarz, V.L., MacDonald, P.E., and Klip, A. (2018). The cell biology of systemic insulin function. *Journal of Cell Biology* 217, 2273–2289. 10.1083/jcb.201802095.
79. Banks, W.A., Kastin, A.J., Huang, W., Jaspan, J.B., and Maness, L.M. (1996). Leptin enters the brain by a saturable system independent of insulin. *Peptides* 17, 305–311. 10.1016/0196-9781(96)00025-3.
80. Banks, W.A., Jaspan, J.B., and Kastin, A.J. (1997). Selective, Physiological Transport of Insulin Across the Blood-Brain Barrier: Novel Demonstration by Species-Specific Radioimmunoassays. *Peptides* 18, 1257–1262. 10.1016/S0196-9781(97)00198-8.
81. De Luca, C., Kowalski, T.J., Zhang, Y., Elmquist, J.K., Lee, C., Kilimann, M.W., Ludwig, T., Liu, S.-M., and Chua, S.C. (2005). Complete rescue of obesity, diabetes, and infertility in db/db mice by neuron-specific LEPR-B transgenes. *J. Clin. Invest.* 115, 3484–3493. 10.1172/JCI24059.
82. Kleinridders, A., Ferris, H.A., Cai, W., and Kahn, C.R. (2014). Insulin Action in Brain Regulates Systemic Metabolism and Brain Function. *Diabetes* 63, 2232–2243. 10.2337/db14-0568.
83. Wondmkun, Y.T. (2020). Obesity, Insulin Resistance, and Type 2 Diabetes: Associations and Therapeutic Implications. *DMSO Volume 13*, 3611–3616. 10.2147/DMSO.S275898.
84. Pretz, D., Le Foll, C., Rizwan, M.Z., Lutz, T.A., and Tups, A. (2021). Hyperleptinemia as a contributing factor for the impairment of glucose intolerance in obesity. *FASEB j.* 35. 10.1096/fj.202001147R.
85. Bruun, J.M., Helge, J.W., Richelsen, B., and Stallknecht, B. (2006). Diet and exercise reduce low-grade inflammation and macrophage infiltration in adipose tissue but not in skeletal muscle in severely obese subjects. *American Journal of Physiology-Endocrinology and Metabolism* 290, E961–E967. 10.1152/ajpendo.00506.2005.

86. Cai, D., Yuan, M., Frantz, D.F., Melendez, P.A., Hansen, L., Lee, J., and Shoelson, S.E. (2005). Local and systemic insulin resistance resulting from hepatic activation of IKK- β and NF- κ B. *Nat Med* 11, 183–190. 10.1038/nm1166.
87. Hotamisligil, G.S., Shargill, N.S., and Spiegelman, B.M. (1993). Adipose Expression of Tumor Necrosis Factor- α : Direct Role in Obesity-Linked Insulin Resistance. *Science* 259, 87–91. 10.1126/science.7678183.
88. Hanada, T., and Yoshimura, A. (2002). Regulation of cytokine signaling and inflammation. *Cytokine & Growth Factor Reviews* 13, 413–421. 10.1016/S1359-6101(02)00026-6.
89. Kievit, P., Howard, J.K., Badman, M.K., Balthasar, N., Coppari, R., Mori, H., Lee, C.E., Elmquist, J.K., Yoshimura, A., and Flier, J.S. (2006). Enhanced leptin sensitivity and improved glucose homeostasis in mice lacking suppressor of cytokine signaling-3 in POMC-expressing cells. *Cell Metabolism* 4, 123–132. 10.1016/j.cmet.2006.06.010.
90. Jais, A., and Brüning, J.C. (2022). Arcuate Nucleus-Dependent Regulation of Metabolism—Pathways to Obesity and Diabetes Mellitus. *Endocrine Reviews* 43, 314–328. 10.1210/endrev/bnab025.
91. Groppe, E., Shanabrough, M., Borok, E., Xu, A.W., Janoschek, R., Buch, T., Plum, L., Balthasar, N., Hampel, B., Waisman, A., et al. (2005). Agouti-related peptide-expressing neurons are mandatory for feeding. *Nat Neurosci* 8, 1289–1291. 10.1038/nn1548.
92. Krashes, M.J., Koda, S., Ye, C., Rogan, S.C., Adams, A.C., Cusher, D.S., Maratos-Flier, E., Roth, B.L., and Lowell, B.B. (2011). Rapid, reversible activation of AgRP neurons drives feeding behavior in mice. *J. Clin. Invest.* 121, 1424–1428. 10.1172/JCI46229.
93. Aponte, Y., Atasoy, D., and Sternson, S.M. (2011). AGRP neurons are sufficient to orchestrate feeding behavior rapidly and without training. *Nat Neurosci* 14, 351–355. 10.1038/nn.2739.
94. Zhan, C., Zhou, J., Feng, Q., Zhang, J., Lin, S., Bao, J., Wu, P., and Luo, M. (2013). Acute and Long-Term Suppression of Feeding Behavior by POMC Neurons in the Brainstem and Hypothalamus, Respectively. *J. Neurosci.* 33, 3624–3632. 10.1523/JNEUROSCI.2742-12.2013.
95. Belgardt, B.F., Okamura, T., and Brüning, J.C. (2009). Hormone and glucose signalling in POMC and AgRP neurons: PI3K and K_{ATP} in the arcuate nucleus. *The Journal of Physiology* 587, 5305–5314. 10.1113/jphysiol.2009.179192.

96. Engström Ruud, L., Pereira, M.M.A., De Solis, A.J., Fenselau, H., and Brüning, J.C. (2020). NPY mediates the rapid feeding and glucose metabolism regulatory functions of AgRP neurons. *Nat Commun* 11, 442. 10.1038/s41467-020-14291-3.
97. Tong, Q., Ye, C.-P., Jones, J.E., Elmquist, J.K., and Lowell, B.B. (2008). Synaptic release of GABA by AgRP neurons is required for normal regulation of energy balance. *Nat Neurosci* 11, 998–1000. 10.1038/nn.2167.
98. Challis, B.G., Coll, A.P., Yeo, G.S.H., Pinnock, S.B., Dickson, S.L., Thresher, R.R., Dixon, J., Zahn, D., Rochford, J.J., White, A., et al. (2004). Mice lacking pro-opiomelanocortin are sensitive to high-fat feeding but respond normally to the acute anorectic effects of peptide-YY₃₋₃₆. *Proc. Natl. Acad. Sci. U.S.A.* 101, 4695–4700. 10.1073/pnas.0306931101.
99. Lau, J., Farzi, A., Qi, Y., Heilbronn, R., Mietzsch, M., Shi, Y.-C., and Herzog, H. (2018). CART neurons in the arcuate nucleus and lateral hypothalamic area exert differential controls on energy homeostasis. *Molecular Metabolism* 7, 102–118. 10.1016/j.molmet.2017.10.015.
100. Baldini, G., and Phelan, K.D. (2019). The melanocortin pathway and control of appetite-progress and therapeutic implications. *Journal of Endocrinology* 241, R1–R33. 10.1530/JOE-18-0596.
101. Shah, B.P., Vong, L., Olson, D.P., Koda, S., Krashes, M.J., Ye, C., Yang, Z., Fuller, P.M., Elmquist, J.K., and Lowell, B.B. (2014). MC4R-expressing glutamatergic neurons in the paraventricular hypothalamus regulate feeding and are synaptically connected to the parabrachial nucleus. *Proc. Natl. Acad. Sci. U.S.A.* 111, 13193–13198. 10.1073/pnas.1407843111.
102. Farooqi, I.S., Keogh, J.M., Yeo, G.S.H., Lank, E.J., Cheetham, T., and O’Rahilly, S. (2003). Clinical Spectrum of Obesity and Mutations in the Melanocortin 4 Receptor Gene. *N Engl J Med* 348, 1085–1095. 10.1056/NEJMoa022050.
103. Garfield, A.S., Li, C., Madara, J.C., Shah, B.P., Webber, E., Steger, J.S., Campbell, J.N., Gavrilova, O., Lee, C.E., Olson, D.P., et al. (2015). A neural basis for melanocortin-4 receptor–regulated appetite. *Nat Neurosci* 18, 863–871. 10.1038/nn.4011.
104. Atasoy, D., Betley, J.N., Su, H.H., and Sternson, S.M. (2012). Deconstruction of a neural circuit for hunger. *Nature* 488, 172–177. 10.1038/nature11270.
105. Wang, L., Suyama, S., Lee, S.A., Ueta, Y., Seino, Y., Sharp, G.W.G., and Yada, T. (2022). Fasting inhibits excitatory synaptic input on paraventricular

- oxytocin neurons via neuropeptide Y and Y1 receptor, inducing rebound hyperphagia, and weight gain. *Front. Nutr.* 9, 994827. 10.3389/fnut.2022.994827.
106. Inada, K., Tsujimoto, K., Yoshida, M., Nishimori, K., and Miyamichi, K. (2022). Oxytocin signaling in the posterior hypothalamus prevents hyperphagic obesity in mice. *eLife* 11, e75718. 10.7554/eLife.75718.
107. Romanov, R.A., Zeisel, A., Bakker, J., Girach, F., Hellysaz, A., Tomer, R., Alpár, A., Mulder, J., Clotman, F., Keimpema, E., et al. (2017). Molecular interrogation of hypothalamic organization reveals distinct dopamine neuronal subtypes. *Nat Neurosci* 20, 176–188. 10.1038/nn.4462.
108. Oldfield, B.J., Giles, M.E., Watson, A., Anderson, C., Colvill, L.M., and McKinley, M.J. (2002). The neurochemical characterisation of hypothalamic pathways projecting polysynaptically to brown adipose tissue in the rat. *Neuroscience* 110, 515–526. 10.1016/S0306-4522(01)00555-3.
109. Li, M.M., Madara, J.C., Steger, J.S., Krashes, M.J., Balthasar, N., Campbell, J.N., Resch, J.M., Conley, N.J., Garfield, A.S., and Lowell, B.B. (2019). The Paraventricular Hypothalamus Regulates Satiety and Prevents Obesity via Two Genetically Distinct Circuits. *Neuron* 102, 653-667.e6. 10.1016/j.neuron.2019.02.028.
110. Betley, J.N., Xu, S., Cao, Z.F.H., Gong, R., Magnus, C.J., Yu, Y., and Sternson, S.M. (2015). Neurons for hunger and thirst transmit a negative-valence teaching signal. *Nature* 521, 180–185. 10.1038/nature14416.
111. Fu, O., Iwai, Y., Narukawa, M., Ishikawa, A.W., Ishii, K.K., Murata, K., Yoshimura, Y., Touhara, K., Misaka, T., Minokoshi, Y., et al. (2019). Hypothalamic neuronal circuits regulating hunger-induced taste modification. *Nat Commun* 10, 4560. 10.1038/s41467-019-12478-x.
112. Jennings, J.H., Rizzi, G., Stamatakis, A.M., Ung, R.L., and Stuber, G.D. (2013). The Inhibitory Circuit Architecture of the Lateral Hypothalamus Orchestrates Feeding. *Science* 341, 1517–1521. 10.1126/science.1241812.
113. Lerma-Cabrera, J.M., Carvajal, F., De La Torre, L., De La Fuente, L., Navarro, M., Thiele, T.E., and Cubero, I. (2012). Control of food intake by MC4-R signaling in the lateral hypothalamus, nucleus accumbens shell and ventral tegmental area: Interactions with ethanol. *Behavioural Brain Research* 234, 51–60. 10.1016/j.bbr.2012.06.006.
114. Morgan, D.A., McDaniel, L.N., Yin, T., Khan, M., Jiang, J., Acevedo, M.R., Walsh, S.A., Ponto, L.L.B., Norris, A.W., Lutter, M., et al. (2015). Regulation

- of Glucose Tolerance and Sympathetic Activity by MC4R Signaling in the Lateral Hypothalamus. *Diabetes* 64, 1976–1987. 10.2337/db14-1257.
115. Cui, H., Sohn, J.-W., Gautron, L., Funahashi, H., Williams, K.W., Elmquist, J.K., and Lutter, M. (2012). Neuroanatomy of melanocortin-4 receptor pathway in the lateral hypothalamic area. *J. Comp. Neurol.* 520, 4168–4183. 10.1002/cne.23145.
116. Woodworth, H.L., Beekly, B.G., Batchelor, H.M., Bugescu, R., Perez-Bonilla, P., Schroeder, L.E., and Leininger, G.M. (2017). Lateral Hypothalamic Neurotensin Neurons Orchestrate Dual Weight Loss Behaviors via Distinct Mechanisms. *Cell Reports* 21, 3116–3128. 10.1016/j.celrep.2017.11.068.
117. Pei, H., Patterson, C.M., Sutton, A.K., Burnett, K.H., Myers, M.G., and Olson, D.P. (2019). Lateral Hypothalamic Mc3R-Expressing Neurons Modulate Locomotor Activity, Energy Expenditure, and Adiposity in Male Mice. *Endocrinology* 160, 343–358. 10.1210/en.2018-00747.
118. Stamatakis, A.M., Van Swieten, M., Basiri, M.L., Blair, G.A., Kantak, P., and Stuber, G.D. (2016). Lateral Hypothalamic Area Glutamatergic Neurons and Their Projections to the Lateral Habenula Regulate Feeding and Reward. *J. Neurosci.* 36, 302–311. 10.1523/JNEUROSCI.1202-15.2016.
119. Jennings, J.H., Ung, R.L., Resendez, S.L., Stamatakis, A.M., Taylor, J.G., Huang, J., Veleta, K., Kantak, P.A., Aita, M., Shilling-Scriver, K., et al. (2015). Visualizing Hypothalamic Network Dynamics for Appetitive and Consummatory Behaviors. *Cell* 160, 516–527. 10.1016/j.cell.2014.12.026.
120. Patterson, C.M., Wong, J.-M.T., Leininger, G.M., Allison, M.B., Mabrouk, O.S., Kasper, C.L., Gonzalez, I.E., Mackenzie, A., Jones, J.C., Kennedy, R.T., et al. (2015). Ventral Tegmental Area Neurotensin Signaling Links the Lateral Hypothalamus to Locomotor Activity and Striatal Dopamine Efflux in Male Mice. *Endocrinology* 156, 1692–1700. 10.1210/en.2014-1986.
121. Mota, C.M.D. (2022). Melanin-concentrating hormone neurons affect adipose tissues and modulate weight gain. *The Journal of Physiology* 600, 727–728. 10.1113/JP282373.
122. Ma, X., Zubcevic, L., Brüning, J.C., Ashcroft, F.M., and Burdakov, D. (2007). Electrical Inhibition of Identified Anorexigenic POMC Neurons by Orexin/Hypocretin. *J. Neurosci.* 27, 1529–1533. 10.1523/JNEUROSCI.3583-06.2007.
123. Al-Massadi, O., Quiñones, M., Clasadonte, J., Hernandez-Bautista, R., Romero-Picó, A., Folgueira, C., Morgan, D.A., Kalló, I., Heras, V., Senra, A., et al. (2019). MCH Regulates SIRT1/FoxO1 and Reduces POMC Neuronal

- Activity to Induce Hyperphagia, Adiposity, and Glucose Intolerance. *Diabetes* 68, 2210–2222. 10.2337/db19-0029.
124. Wu, Z., Kim, E.R., Sun, H., Xu, Y., Mangieri, L.R., Li, D.-P., Pan, H.-L., Xu, Y., Arenkiel, B.R., and Tong, Q. (2015). GABAergic Projections from Lateral Hypothalamus to Paraventricular Hypothalamic Nucleus Promote Feeding. *J. Neurosci.* 35, 3312–3318. 10.1523/JNEUROSCI.3720-14.2015.
125. Noble, E.E., Hahn, J.D., Konanur, V.R., Hsu, T.M., Page, S.J., Cortella, A.M., Liu, C.M., Song, M.Y., Suarez, A.N., Szujewski, C.C., et al. (2018). Control of Feeding Behavior by Cerebral Ventricular Volume Transmission of Melanin-Concentrating Hormone. *Cell Metab* 28, 55-68.e7. 10.1016/j.cmet.2018.05.001.
126. O'Connor, E.C., Kremer, Y., Lefort, S., Harada, M., Pascoli, V., Rohner, C., and Lüscher, C. (2015). Accumbal D1R Neurons Projecting to Lateral Hypothalamus Authorize Feeding. *Neuron* 88, 553–564. 10.1016/j.neuron.2015.09.038.
127. Walle, R., Petitbon, A., Fois, G.R., Contini, A., Ortore, R., Oummadi, A., De Smedt-Peyrusse, V., de Kerchove d'Exaerde, A., Giros, B., Chaouloff, F., et al. (2022). The ventral striatum contributes to energy balance (Neuroscience) 10.1101/2022.05.05.490599.
128. Gabriella, I., Tseng, A., Sanchez, K.O., Shah, H., and Stanley, B.G. (2022). Stimulation of GABA Receptors in the Lateral Septum Rapidly Elicits Food Intake and Mediates Natural Feeding. *Brain Sciences* 12, 848. 10.3390/brainsci12070848.
129. Xu, Y., Jiang, Z., Li, H., Cai, J., Jiang, Y., Otiz-Guzman, J., Xu, Y., Arenkiel, B.R., and Tong, Q. (2023). Lateral septum as a melanocortin downstream site in obesity development. *Cell Reports* 42, 112502. 10.1016/j.celrep.2023.112502.
130. Campos, C.A., Bowen, A.J., Han, S., Wisse, B.E., Palmiter, R.D., and Schwartz, M.W. (2017). Cancer-induced anorexia and malaise are mediated by CGRP neurons in the parabrachial nucleus. *Nat Neurosci* 20, 934–942. 10.1038/nn.4574.
131. Campos, C.A., Bowen, A.J., Schwartz, M.W., and Palmiter, R.D. (2016). Parabrachial CGRP Neurons Control Meal Termination. *Cell Metabolism* 23, 811–820. 10.1016/j.cmet.2016.04.006.
132. Xu, Y., Wu, Z., Sun, H., Zhu, Y., Kim, E.R., Lowell, B.B., Arenkiel, B.R., Xu, Y., and Tong, Q. (2013). Glutamate Mediates the Function of Melanocortin

- Receptor 4 on Sim1 Neurons in Body Weight Regulation. *Cell Metabolism* 18, 860–870. 10.1016/j.cmet.2013.11.003.
133. Touzani, K., Ferssiwi, A., and Velley, L. (1990). Localization of lateral hypothalamic neurons projecting to the medial part of the parabrachial area of the rat. *Neuroscience Letters* 114, 17–21. 10.1016/0304-3940(90)90421-5.
134. Grill, H.J., and Hayes, M.R. (2009). The nucleus tractus solitarius: a portal for visceral afferent signal processing, energy status assessment and integration of their combined effects on food intake. *Int J Obes* 33, S11–S15. 10.1038/ijo.2009.10.
135. Chen, J., Cheng, M., Wang, L., Zhang, L., Xu, D., Cao, P., Wang, F., Herzog, H., Song, S., and Zhan, C. (2020). A Vagal-NTS Neural Pathway that Stimulates Feeding. *Current Biology* 30, 3986-3998.e5. 10.1016/j.cub.2020.07.084.
136. Roman, C.W., Derkach, V.A., and Palmiter, R.D. (2016). Genetically and functionally defined NTS to PBN brain circuits mediating anorexia. *Nat Commun* 7, 11905. 10.1038/ncomms11905.
137. Aklan, I., Sayar Atasoy, N., Yavuz, Y., Ates, T., Coban, I., Koksalar, F., Filiz, G., Topcu, I.C., Oncul, M., Dilsiz, P., et al. (2020). NTS Catecholamine Neurons Mediate Hypoglycemic Hunger via Medial Hypothalamic Feeding Pathways. *Cell Metabolism* 31, 313-326.e5. 10.1016/j.cmet.2019.11.016.
138. Lau, B.K., Murphy-Royal, C., Kaur, M., Qiao, M., Bains, J.S., Gordon, G.R., and Borgland, S.L. (2021). Obesity-induced astrocyte dysfunction impairs heterosynaptic plasticity in the orbitofrontal cortex. *Cell Reports* 36, 109563. 10.1016/j.celrep.2021.109563.
139. Seabrook, L.T., Naef, L., Baimel, C., Judge, A.K., Kenney, T., Ellis, M., Tayyab, T., Armstrong, M., Qiao, M., Floresco, S.B., et al. (2023). Disinhibition of the orbitofrontal cortex biases decision-making in obesity. *Nat Neurosci* 26, 92–106. 10.1038/s41593-022-01210-6.
140. Horvath, T.L., Sarman, B., García-Cáceres, C., Enriori, P.J., Sotonyi, P., Shanabrough, M., Borok, E., Argente, J., Chowen, J.A., Perez-Tilve, D., et al. (2010). Synaptic input organization of the melanocortin system predicts diet-induced hypothalamic reactive gliosis and obesity. *Proc. Natl. Acad. Sci. U.S.A.* 107, 14875–14880. 10.1073/pnas.1004282107.
141. Dietrich, M.O., and Horvath, T.L. (2013). Hypothalamic control of energy balance: insights into the role of synaptic plasticity. *Trends in Neurosciences* 36, 65–73. 10.1016/j.tins.2012.12.005.

142. Wei, W., Pham, K., Gammons, J.W., Sutherland, D., Liu, Y., Smith, A., Kaczorowski, C.C., and O'Connell, K.M.S. (2015). Diet composition, not calorie intake, rapidly alters intrinsic excitability of hypothalamic AgRP/NPY neurons in mice. *Sci Rep* 5, 16810. 10.1038/srep16810.
143. Baver, S.B., Hope, K., Guyot, S., Bjørbaek, C., Kaczorowski, C., and O'Connell, K.M.S. (2014). Leptin modulates the intrinsic excitability of AgRP/NPY neurons in the arcuate nucleus of the hypothalamus. *J Neurosci* 34, 5486–5496. 10.1523/JNEUROSCI.4861-12.2014.
144. Banerjee, J., Dorfman, M.D., Fasnacht, R., Douglass, J.D., Wyse-Jackson, A.C., Barria, A., and Thaler, J.P. (2022). CX3CL1 Action on Microglia Protects from Diet-Induced Obesity by Restoring POMC Neuronal Excitability and Melanocortin System Activity Impaired by High-Fat Diet Feeding. *Int J Mol Sci* 23, 6380. 10.3390/ijms23126380.
145. Paeger, L., Pippow, A., Hess, S., Paehler, M., Klein, A.C., Husch, A., Pouzat, C., Brüning, J.C., and Kloppenburg, P. (2017). Energy imbalance alters Ca²⁺ handling and excitability of POMC neurons. *Elife* 6, e25641. 10.7554/eLife.25641.
146. Jais, A., Paeger, L., Sotelo-Hitschfeld, T., Bremser, S., Prinzensteiner, M., Klemm, P., Mykytiuk, V., Widdershooven, P.J.M., Vesting, A.J., Grzelka, K., et al. (2020). PNOARC Neurons Promote Hyperphagia and Obesity upon High-Fat-Diet Feeding. *Neuron* 106, 1009-1025.e10. 10.1016/j.neuron.2020.03.022.
147. Rossi, M.A., Basiri, M.L., McHenry, J.A., Kosyk, O., Otis, J.M., van den Munkhof, H.E., Bryois, J., Hübel, C., Breen, G., Guo, W., et al. (2019). Obesity remodels activity and transcriptional state of a lateral hypothalamic brake on feeding. *Science* 364, 1271–1274. 10.1126/science.aax1184.
148. Linehan, V., Fang, L.Z., and Hirasawa, M. (2018). Short-term high-fat diet primes excitatory synapses for long-term depression in orexin neurons: High-fat diet unmasks LTD in orexin neurons. *J Physiol* 596, 305–316. 10.1113/JP275177.
149. Anand, B.K., and Brobeck, J.R. (1951). Localization of a "Feeding Center" in the Hypothalamus of the Rat. *Experimental Biology and Medicine* 77, 323–325. 10.3181/00379727-77-18766.
150. Levitt, D.R., and Teitelbaum, P. (1975). Somnolence, akinesia, and sensory activation of motivated behavior in the lateral hypothalamic syndrome. *Proc. Natl. Acad. Sci. U.S.A.* 72, 2819–2823. 10.1073/pnas.72.7.2819.

151. Lytle, L.D., and Campbell, B.A. (1975). Effects of lateral hypothalamic lesions on consummatory behavior in developing rats. *Physiology & Behavior* *15*, 323–331. 10.1016/0031-9384(75)90100-6.
152. Morrison, S.D., Barnett, R.J., and Mayer, J. (1958). Localization of Lesions in the Lateral Hypothalamus of Rats With Induced Adipsia and Aphagia. *American Journal of Physiology-Legacy Content* *193*, 230–234. 10.1152/ajplegacy.1958.193.1.230.
153. Ungerstedt, U. (1970). C 16: Is Interruption of the Nigro-Striatal Dopamine System Producing the “Lateral Hypothalamus Syndrome”? *Acta Physiologica Scandinavica* *80*, 35A-36A. 10.1111/j.1748-1716.1970.tb04858.x.
154. Bernardis, L.L., and Bellinger, L.L. (1996). The lateral hypothalamic area revisited: Ingestive behavior. *Neuroscience & Biobehavioral Reviews* *20*, 189–287. 10.1016/0149-7634(95)00015-1.
155. Grossman, S.P., Dacey, D., Halaris, A.E., Collier, T., and Routtenberg, A. (1978). Aphagia and Adipsia After Preferential Destruction of Nerve Cell Bodies in Hypothalamus. *Science* *202*, 537–539. 10.1126/science.705344.
156. Pissios, P., Bradley, R.L., and Maratos-Flier, E. (2006). Expanding the Scales: The Multiple Roles of MCH in Regulating Energy Balance and Other Biological Functions. *Endocrine Reviews* *27*, 606–620. 10.1210/er.2006-0021.
157. Sanchez, M., Baker, B.I., and Celis, M. (1997). Melanin-Concentrating Hormone (MCH) Antagonizes the Effects of α -MSH and Neuropeptide E-I on Grooming and Locomotor Activities in the Rat. *Peptides* *18*, 393–396. 10.1016/S0196-9781(96)00327-0.
158. Shimada, M., Tritos, N.A., Lowell, B.B., Flier, J.S., and Maratos-Flier, E. (1998). Mice lacking melanin-concentrating hormone are hypophagic and lean. *Nature* *396*, 670–674. 10.1038/25341.
159. Ludwig, D.S., Tritos, N.A., Mastaitis, J.W., Kulkarni, R., Kokkotou, E., Elmquist, J., Lowell, B., Flier, J.S., and Maratos-Flier, E. (2001). Melanin-concentrating hormone overexpression in transgenic mice leads to obesity and insulin resistance. *J. Clin. Invest.* *107*, 379–386. 10.1172/JCI10660.
160. Subramanian, K.S., Lauer, L.T., Hayes, A.M.R., Décarie-Spain, L., McBurnett, K., Nourbash, A.C., Donohue, K.N., Kao, A.E., Bashaw, A.G., Burdakov, D., et al. (2023). Hypothalamic melanin-concentrating hormone neurons integrate food-motivated appetitive and consummatory processes in rats. *Nat Commun* *14*, 1755. 10.1038/s41467-023-37344-9.

161. Della-Zuana, O., Presse, F., Ortola, C., Duhault, J., Nahon, J., and Levens, N. (2002). Acute and chronic administration of melanin-concentrating hormone enhances food intake and body weight in Wistar and Sprague–Dawley rats. *Int J Obes* 26, 1289–1295. 10.1038/sj.ijo.0802079.
162. Izawa, S., Yoneshiro, T., Kondoh, K., Nakagiri, S., Okamatsu-Ogura, Y., Terao, A., Minokoshi, Y., Yamanaka, A., and Kimura, K. (2021). Melanin-concentrating hormone-producing neurons in the hypothalamus regulate brown adipose tissue and thus contribute to energy expenditure. *J Physiol*. 10.1113/JP281241.
163. Alon, T., and Friedman, J.M. (2006). Late-onset leanness in mice with targeted ablation of melanin concentrating hormone neurons. *J Neurosci* 26, 389–397. 10.1523/JNEUROSCI.1203-05.2006.
164. Tan, C.P., Sano, H., Iwaasa, H., Pan, J., Sailer, A.W., Hreniuk, D.L., Feighner, S.D., Palyha, O.C., Pong, S.-S., Figueroa, D.J., et al. (2002). Melanin-Concentrating Hormone Receptor Subtypes 1 and 2: Species-Specific Gene Expression. *Genomics* 79, 785–792. 10.1006/geno.2002.6771.
165. Hamamoto, A., Kobayashi, Y., and Saito, Y. (2015). Identification of amino acids that are selectively involved in Gi/o activation by rat melanin-concentrating hormone receptor 1. *Cellular Signalling* 27, 818–827. 10.1016/j.cellsig.2015.01.008.
166. Chee, M.J.S., Pissios, P., and Maratos-Flier, E. (2013). Neurochemical characterization of neurons expressing melanin-concentrating hormone receptor 1 in the mouse hypothalamus. *J. Comp. Neurol.* 521, 2208–2234. 10.1002/cne.23273.
167. Rossi, M., Choi, S.J., O’Shea, D., Miyoshi, T., Ghatei, M.A., and Bloom, S.R. (1997). Melanin-Concentrating Hormone Acutely Stimulates Feeding, But Chronic Administration Has No Effect on Body Weight. *Endocrinology* 138, 351–355. 10.1210/endo.138.1.4887.
168. Mul, J.D., la Fleur, S.E., Toonen, P.W., Afrasiab-Middelmann, A., Binnekade, R., Schetters, D., Verheij, M.M.M., Sears, R.M., Homberg, J.R., Schoffelmeer, A.N.M., et al. (2011). Chronic loss of melanin-concentrating hormone affects motivational aspects of feeding in the rat. *PLoS One* 6, e19600. 10.1371/journal.pone.0019600.
169. Elias, C.F., Sita, L.V., Zambon, B.K., Oliveira, E.R., Vasconcelos, L.A.P., and Bittencourt, J.C. (2008). Melanin-concentrating hormone projections to areas involved in somatomotor responses. *Journal of Chemical Neuroanatomy* 35, 188–201. 10.1016/j.jchemneu.2007.10.002.

170. An, S., Cutler, G., Zhao, J.J., Huang, S.-G., Tian, H., Li, W., Liang, L., Rich, M., Bakleh, A., Du, J., et al. (2001). Identification and characterization of a melanin-concentrating hormone receptor. *Proc. Natl. Acad. Sci. U.S.A.* *98*, 7576–7581. 10.1073/pnas.131200698.
171. Chee, M.J.S., Pissios, P., Prasad, D., and Maratos-Flier, E. (2014). Expression of Melanin-Concentrating Hormone Receptor 2 Protects Against Diet-Induced Obesity in Male Mice. *Endocrinology* *155*, 81–88. 10.1210/en.2013-1738.
172. Mickelsen, L.E., Kolling, F.W., Chimileski, B.R., Fujita, A., Norris, C., Chen, K., Nelson, C.E., and Jackson, A.C. (2017). Neurochemical Heterogeneity Among Lateral Hypothalamic Hypocretin/Orexin and Melanin-Concentrating Hormone Neurons Identified Through Single-Cell Gene Expression Analysis. *eNeuro* *4*. 10.1523/ENEURO.0013-17.2017.
173. Chee, M.J.S., Arrigoni, E., and Maratos-Flier, E. (2015). Melanin-concentrating hormone neurons release glutamate for feedforward inhibition of the lateral septum. *J Neurosci* *35*, 3644–3651. 10.1523/JNEUROSCI.4187-14.2015.
174. Schneeberger, M., Tan, K., Nectow, A.R., Parolari, L., Caglar, C., Azevedo, E., Li, Z., Domingos, A., and Friedman, J.M. (2018). Functional analysis reveals differential effects of glutamate and MCH neuropeptide in MCH neurons. *Mol Metab* *13*, 83–89. 10.1016/j.molmet.2018.05.001.
175. Whiddon, B.B., and Palmiter, R.D. (2013). Ablation of neurons expressing melanin-concentrating hormone (MCH) in adult mice improves glucose tolerance independent of MCH signaling. *J Neurosci* *33*, 2009–2016. 10.1523/JNEUROSCI.3921-12.2013.
176. Sankhe, A.S., Bordeleau, D., Alfonso, D.I.M., Wittman, G., and Chee, M.J. (2023). Loss of glutamatergic signalling from MCH neurons reduced anxiety-like behaviours in novel environments. *J Neuroendocrinology* *35*. 10.1111/jne.13222.
177. Alberto, C.O., Trask, R.B., and Hirasawa, M. (2011). Dopamine Acts as a Partial Agonist for 2A Adrenoceptor in Melanin-Concentrating Hormone Neurons. *Journal of Neuroscience* *31*, 10671–10676. 10.1523/JNEUROSCI.6245-10.2011.
178. Van Den Pol, A.N., Acuna-Goycolea, C., Clark, K.R., and Ghosh, P.K. (2004). Physiological Properties of Hypothalamic MCH Neurons Identified with Selective Expression of Reporter Gene after Recombinant Virus Infection. *Neuron* *42*, 635–652. 10.1016/S0896-6273(04)00251-X.

179. Parsons, M.P., Burt, J., Cranford, A., Alberto, C., Zipperlen, K., and Hirasawa, M. (2012). Nociceptin Induces Hypophagia in the Perifornical and Lateral Hypothalamic Area. *PLoS ONE* 7, e45350. 10.1371/journal.pone.0045350.
180. Li, Y., and van den Pol, A.N. (2006). Differential Target-Dependent Actions of Coexpressed Inhibitory Dynorphin and Excitatory Hypocretin/Orexin Neuropeptides. *J. Neurosci.* 26, 13037–13047. 10.1523/JNEUROSCI.3380-06.2006.
181. Yao, Y., Fu, L.-Y., Zhang, X., and Van Den Pol, A.N. (2012). Vasopressin and oxytocin excite MCH neurons, but not other lateral hypothalamic GABA neurons. *American Journal of Physiology-Regulatory, Integrative and Comparative Physiology* 302, R815–R824. 10.1152/ajpregu.00452.2011.
182. Burdakov, D., Gerasimenko, O., and Verkhatsky, A. (2005). Physiological Changes in Glucose Differentially Modulate the Excitability of Hypothalamic Melanin-Concentrating Hormone and Orexin Neurons *In Situ*. *J. Neurosci.* 25, 2429–2433. 10.1523/JNEUROSCI.4925-04.2005.
183. Hausen, A.C., Ruud, J., Jiang, H., Hess, S., Varbanov, H., Kloppenburg, P., and Brüning, J.C. (2016). Insulin-Dependent Activation of MCH Neurons Impairs Locomotor Activity and Insulin Sensitivity in Obesity. *Cell Rep* 17, 2512–2521. 10.1016/j.celrep.2016.11.030.
184. Qu, D., Ludwig, D.S., Gammeltoft, S., Piper, M., Pelleymounter, M.A., Cullen, M.J., Mathes, W.F., Przypek, J., Kanarek, R., and Maratos-Flier, E. (1996). A role for melanin-concentrating hormone in the central regulation of feeding behaviour. *Nature* 380, 243–247. 10.1038/380243a0.
185. Leininger, G.M., Jo, Y.-H., Leshan, R.L., Louis, G.W., Yang, H., Barrera, J.G., Wilson, H., Opland, D.M., Faouzi, M.A., Gong, Y., et al. (2009). Leptin Acts via Leptin Receptor-Expressing Lateral Hypothalamic Neurons to Modulate the Mesolimbic Dopamine System and Suppress Feeding. *Cell Metabolism* 10, 89–98. 10.1016/j.cmet.2009.06.011.
186. Konadhode, R.R., Pelluru, D., Blanco-Centurion, C., Zayachkivsky, A., Liu, M., Uhde, T., Glen, W.B., Van Den Pol, A.N., Mulholland, P.J., and Shiromani, P.J. (2013). Optogenetic Stimulation of MCH Neurons Increases Sleep. *Journal of Neuroscience* 33, 10257–10263. 10.1523/JNEUROSCI.1225-13.2013.
187. Jogo, S., Glasgow, S.D., Herrera, C.G., Ekstrand, M., Reed, S.J., Boyce, R., Friedman, J., Burdakov, D., and Adamantidis, A.R. (2013). Optogenetic identification of a rapid eye movement sleep modulatory circuit in the hypothalamus. *Nat Neurosci* 16, 1637–1643. 10.1038/nn.3522.

188. Tsunematsu, T., Ueno, T., Tabuchi, S., Inutsuka, A., Tanaka, K.F., Hasuwa, H., Kilduff, T.S., Terao, A., and Yamanaka, A. (2014). Optogenetic manipulation of activity and temporally controlled cell-specific ablation reveal a role for MCH neurons in sleep/wake regulation. *J Neurosci* 34, 6896–6909. 10.1523/JNEUROSCI.5344-13.2014.
189. Bittencourt, J.C., Presse, F., Arias, C., Peto, C., Vaughan, J., Nahon, J.-L., Vale, W., and Sawchenko, P.E. (1992). The melanin-concentrating hormone system of the rat brain: An immuno- and hybridization histochemical characterization. *J. Comp. Neurol.* 319, 218–245. 10.1002/cne.903190204.
190. Liu, J.-J., Tsien, R.W., and Pang, Z.P. (2022). Hypothalamic melanin-concentrating hormone regulates hippocampus-dorsolateral septum activity. *Nat Neurosci* 25, 61–71. 10.1038/s41593-021-00984-5.
191. Kosse, C., and Burdakov, D. (2019). Natural hypothalamic circuit dynamics underlying object memorization. *Nat Commun* 10, 2505. 10.1038/s41467-019-10484-7.
192. Izawa, S., Chowdhury, S., Miyazaki, T., Mukai, Y., Ono, D., Inoue, R., Ohmura, Y., Mizoguchi, H., Kimura, K., Yoshioka, M., et al. (2019). REM sleep-active MCH neurons are involved in forgetting hippocampus-dependent memories. *Science* 365, 1308–1313. 10.1126/science.aax9238.
193. Noble, E.E., Wang, Z., Liu, C.M., Davis, E.A., Suarez, A.N., Stein, L.M., Tsan, L., Terrill, S.J., Hsu, T.M., Jung, A.-H., et al. (2019). Hypothalamus-hippocampus circuitry regulates impulsivity via melanin-concentrating hormone. *Nat Commun* 10, 4923. 10.1038/s41467-019-12895-y.
194. He, X., Li, Y., Zhang, N., Huang, J., Ming, X., Guo, R., Hu, Y., Ji, P., and Guo, F. (2022). Melanin-concentrating hormone promotes anxiety and intestinal dysfunction via basolateral amygdala in mice. *Front. Pharmacol.* 13, 906057. 10.3389/fphar.2022.906057.
195. García-Fuster, M.J., Parks, G.S., Clinton, S.M., Watson, S.J., Akil, H., and Civelli, O. (2012). The melanin-concentrating hormone (MCH) system in an animal model of depression-like behavior. *European Neuropsychopharmacology* 22, 607–613. 10.1016/j.euroneuro.2011.12.001.
196. Nambu, T., Sakurai, T., Mizukami, K., Hosoya, Y., Yanagisawa, M., and Goto, K. (1999). Distribution of orexin neurons in the adult rat brain. *Brain Research* 827, 243–260. 10.1016/S0006-8993(99)01336-0.
197. Sakurai, T., Moriguchi, T., Furuya, K., Kajiwara, N., Nakamura, T., Yanagisawa, M., and Goto, K. (1999). Structure and Function of Human

- Prepro-orexin Gene. *Journal of Biological Chemistry* 274, 17771–17776. 10.1074/jbc.274.25.17771.
198. Marcus, J.N., Aschkenasi, C.J., Lee, C.E., Chemelli, R.M., Saper, C.B., Yanagisawa, M., and Elmquist, J.K. (2001). Differential expression of orexin receptors 1 and 2 in the rat brain. *J. Comp. Neurol.* 435, 6–25. 10.1002/cne.1190.
199. Sakurai, T., Amemiya, A., Ishii, M., Matsuzaki, I., Chemelli, R.M., Tanaka, H., Williams, S.C., Richardson, J.A., Kozlowski, G.P., Wilson, S., et al. (1998). Orexins and Orexin Receptors: A Family of Hypothalamic Neuropeptides and G Protein-Coupled Receptors that Regulate Feeding Behavior. *Cell* 92, 573–585. 10.1016/S0092-8674(00)80949-6.
200. Yamanaka, A., Sakurai, T., Katsumoto, T., Masashi Yanagisawa, and Goto, K. (1999). Chronic intracerebroventricular administration of orexin-A to rats increases food intake in daytime, but has no effect on body weight. *Brain Research* 849, 248–252. 10.1016/S0006-8993(99)01905-8.
201. Inutsuka, A., Inui, A., Tabuchi, S., Tsunematsu, T., Lazarus, M., and Yamanaka, A. (2014). Concurrent and robust regulation of feeding behaviors and metabolism by orexin neurons. *Neuropharmacology* 85, 451–460. 10.1016/j.neuropharm.2014.06.015.
202. Hara, J., Yanagisawa, M., and Sakurai, T. (2005). Difference in obesity phenotype between orexin-knockout mice and orexin neuron-deficient mice with same genetic background and environmental conditions. *Neuroscience Letters* 380, 239–242. 10.1016/j.neulet.2005.01.046.
203. Hara, J., Beuckmann, C.T., Nambu, T., Willie, J.T., Chemelli, R.M., Sinton, C.M., Sugiyama, F., Yagami, K., Goto, K., Yanagisawa, M., et al. (2001). Genetic Ablation of Orexin Neurons in Mice Results in Narcolepsy, Hypophagia, and Obesity. *Neuron* 30, 345–354. 10.1016/S0896-6273(01)00293-8.
204. Schuld, A., Hebebrand, J., Geller, F., and Pollmächer, T. (2000). Increased body-mass index in patients with narcolepsy. *The Lancet* 355, 1274–1275. 10.1016/S0140-6736(05)74704-8.
205. Hagan, J.J., Leslie, R.A., Patel, S., Evans, M.L., Wattam, T.A., Holmes, S., Benham, C.D., Taylor, S.G., Routledge, C., Hemmati, P., et al. (1999). Orexin A activates locus coeruleus cell firing and increases arousal in the rat. *Proc. Natl. Acad. Sci. U.S.A.* 96, 10911–10916. 10.1073/pnas.96.19.10911.

206. Lubkin, M., and Stricker-Krongrad, A. (1998). Independent Feeding and Metabolic Actions of Orexins in Mice. *Biochemical and Biophysical Research Communications* 253, 241–245. 10.1006/bbrc.1998.9750.
207. Tupone, D., Madden, C.J., Cano, G., and Morrison, S.F. (2011). An Orexinergic Projection from Perifornical Hypothalamus to Raphe Pallidus Increases Rat Brown Adipose Tissue Thermogenesis. *J. Neurosci.* 31, 15944–15955. 10.1523/JNEUROSCI.3909-11.2011.
208. Ciriello, J., McMurray, J.C., Babic, T., and De Oliveira, C.V.R. (2003). Collateral axonal projections from hypothalamic hypocretin neurons to cardiovascular sites in nucleus ambiguus and nucleus tractus solitarius. *Brain Research* 991, 133–141. 10.1016/j.brainres.2003.08.016.
209. Zheng, H., Patterson, L.M., and Berthoud, H.-R. (2005). Orexin-A projections to the caudal medulla and orexin-induced c-Fos expression, food intake, and autonomic function. *J. Comp. Neurol.* 485, 127–142. 10.1002/cne.20515.
210. Barson, J.R. (2020). Orexin/hypocretin and dysregulated eating: Promotion of foraging behavior. *Brain Research* 1731, 145915. 10.1016/j.brainres.2018.08.018.
211. Castro, D.C., Terry, R.A., and Berridge, K.C. (2016). Orexin in Rostral Hotspot of Nucleus Accumbens Enhances Sucrose ‘Liking’ and Intake but Scopolamine in Caudal Shell Shifts ‘Liking’ Toward ‘Disgust’ and ‘Fear.’ *Neuropsychopharmacol* 41, 2101–2111. 10.1038/npp.2016.10.
212. Meffre, J., Sicre, M., Diarra, M., Marchessaux, F., Paleressompouille, D., and Ambroggi, F. (2019). Orexin in the Posterior Paraventricular Thalamus Mediates Hunger-Related Signals in the Nucleus Accumbens Core. *Current Biology* 29, 3298-3306.e4. 10.1016/j.cub.2019.07.069.
213. España, R.A., Oleson, E.B., Locke, J.L., Brookshire, B.R., Roberts, D.C.S., and Jones, S.R. (2010). The hypocretin-orexin system regulates cocaine self-administration via actions on the mesolimbic dopamine system. *European Journal of Neuroscience* 31, 336–348. 10.1111/j.1460-9568.2009.07065.x.
214. Harris, G.C., Wimmer, M., and Aston-Jones, G. (2005). A role for lateral hypothalamic orexin neurons in reward seeking. *Nature* 437, 556–559. 10.1038/nature04071.
215. Chou, T.C., Lee, C.E., Lu, J., Elmquist, J.K., Hara, J., Willie, J.T., Beuckmann, C.T., Chemelli, R.M., Sakurai, T., Yanagisawa, M., et al. (2001). Orexin (Hypocretin) Neurons Contain Dynorphin. *J. Neurosci.* 21, RC168–RC168. 10.1523/JNEUROSCI.21-19-j0003.2001.

216. Muschamp, J.W., Hollander, J.A., Thompson, J.L., Voren, G., Hassinger, L.C., Onvani, S., Kamenecka, T.M., Borgland, S.L., Kenny, P.J., and Carlezon, W.A. (2014). Hypocretin (orexin) facilitates reward by attenuating the antireward effects of its cotransmitter dynorphin in ventral tegmental area. *Proc. Natl. Acad. Sci. U.S.A.* *111*. 10.1073/pnas.1315542111.
217. Baimel, C., Lau, B.K., Qiao, M., and Borgland, S.L. (2017). Projection-Target-Defined Effects of Orexin and Dynorphin on VTA Dopamine Neurons. *Cell Reports* *18*, 1346–1355. 10.1016/j.celrep.2017.01.030.
218. Matzeu, A., Kallupi, M., George, O., Schweitzer, P., and Martin-Fardon, R. (2018). Dynorphin Counteracts Orexin in the Paraventricular Nucleus of the Thalamus: Cellular and Behavioral Evidence. *Neuropsychopharmacol.* *43*, 1010–1020. 10.1038/npp.2017.250.
219. Yamanaka, A., Beuckmann, C.T., Willie, J.T., Hara, J., Tsujino, N., Mieda, M., Tominaga, M., Yagami, K., Sugiyama, F., Goto, K., et al. (2003). Hypothalamic Orexin Neurons Regulate Arousal According to Energy Balance in Mice. *Neuron* *38*, 701–713. 10.1016/S0896-6273(03)00331-3.
220. Linehan, V., Trask, R.B., Briggs, C., Rowe, T.M., and Hirasawa, M. (2015). Concentration-dependent activation of dopamine receptors differentially modulates GABA release onto orexin neurons. *Eur J Neurosci* *42*, 1976–1983. 10.1111/ejn.12967.
221. Linehan, V., Rowe, T.M., and Hirasawa, M. (2019). Dopamine modulates excitatory transmission to orexin neurons in a receptor subtype-specific manner. *American Journal of Physiology-Regulatory, Integrative and Comparative Physiology* *316*, R68–R75. 10.1152/ajpregu.00150.2018.
222. Li, Y., and Van Den Pol, A.N. (2005). Direct and Indirect Inhibition by Catecholamines of Hypocretin/Orexin Neurons. *J. Neurosci.* *25*, 173–183. 10.1523/JNEUROSCI.4015-04.2005.
223. Tsujino, N., Yamanaka, A., Ichiki, K., Muraki, Y., Kilduff, T.S., Yagami, K., Takahashi, S., Goto, K., and Sakurai, T. (2005). Cholecystokinin Activates Orexin/Hypocretin Neurons through the Cholecystokinin A Receptor. *J. Neurosci.* *25*, 7459–7469. 10.1523/JNEUROSCI.1193-05.2005.
224. Tsunematsu, T., Fu, L.-Y., Yamanaka, A., Ichiki, K., Tanoue, A., Sakurai, T., and Van Den Pol, A.N. (2008). Vasopressin Increases Locomotion through a V1a Receptor in Orexin/Hypocretin Neurons: Implications for Water Homeostasis. *J. Neurosci.* *28*, 228–238. 10.1523/JNEUROSCI.3490-07.2008.

225. Leininger, G.M., Opland, D.M., Jo, Y.-H., Faouzi, M., Christensen, L., Cappellucci, L.A., Rhodes, C.J., Gnegy, M.E., Becker, J.B., Pothos, E.N., et al. (2011). Leptin Action via Neurotensin Neurons Controls Orexin, the Mesolimbic Dopamine System and Energy Balance. *Cell Metabolism* 14, 313–323. 10.1016/j.cmet.2011.06.016.
226. Parsons, M.P., and Hirasawa, M. (2010). ATP-Sensitive Potassium Channel-Mediated Lactate Effect on Orexin Neurons: Implications for Brain Energetics during Arousal. *Journal of Neuroscience* 30, 8061–8070. 10.1523/JNEUROSCI.5741-09.2010.
227. Dauvilliers, Y., and Barateau, L. (2017). Narcolepsy and Other Central Hypersomnias: CONTINUUM: Lifelong Learning in Neurology 23, 989–1004. 10.1212/CON.0000000000000492.
228. Seifinejad, A., Ramosaj, M., Shan, L., Li, S., Possovre, M.-L., Pfister, C., Fronczek, R., Garrett-Sinha, L.A., Frieser, D., Honda, M., et al. (2023). Epigenetic silencing of selected hypothalamic neuropeptides in narcolepsy with cataplexy. *Proc. Natl. Acad. Sci. U.S.A.* 120, e2220911120. 10.1073/pnas.2220911120.
229. Chemelli, R.M., Willie, J.T., Sinton, C.M., Elmquist, J.K., Scammell, T., Lee, C., Richardson, J.A., Williams, S.C., Xiong, Y., Kisanuki, Y., et al. (1999). Narcolepsy in orexin Knockout Mice. *Cell* 98, 437–451. 10.1016/S0092-8674(00)81973-X.
230. Mieda, M., Willie, J.T., Hara, J., Sinton, C.M., Sakurai, T., and Yanagisawa, M. (2004). Orexin peptides prevent cataplexy and improve wakefulness in an orexin neuron-ablated model of narcolepsy in mice. *Proc. Natl. Acad. Sci. U.S.A.* 101, 4649–4654. 10.1073/pnas.0400590101.
231. Schwartz, M.D., Nguyen, A.T., Warriar, D.R., Palmerston, J.B., Thomas, A.M., Morairty, S.R., Neylan, T.C., and Kilduff, T.S. (2016). Locus Coeruleus and Tubero-mammillary Nuclei Ablations Attenuate Hypocretin/Orexin Antagonist-Mediated REM Sleep. *eNeuro* 3, ENEURO.0018-16.2016. 10.1523/ENEURO.0018-16.2016.
232. Mochizuki, T., Arrigoni, E., Marcus, J.N., Clark, E.L., Yamamoto, M., Honer, M., Borroni, E., Lowell, B.B., Elmquist, J.K., and Scammell, T.E. (2011). Orexin receptor 2 expression in the posterior hypothalamus rescues sleepiness in narcoleptic mice. *Proc. Natl. Acad. Sci. U.S.A.* 108, 4471–4476. 10.1073/pnas.1012456108.
233. Feng, H., Wen, S.-Y., Qiao, Q.-C., Pang, Y.-J., Wang, S.-Y., Li, H.-Y., Cai, J., Zhang, K.-X., Chen, J., Hu, Z.-A., et al. (2020). Orexin signaling modulates synchronized excitation in the sublaterodorsal tegmental nucleus

- to stabilize REM sleep. *Nat Commun* 11, 3661. 10.1038/s41467-020-17401-3.
234. Grafe, L.A., Eacret, D., Luz, S., Gotter, A.L., Renger, J.J., Winrow, C.J., and Bhatnagar, S. (2017). Orexin 2 receptor regulation of the hypothalamic–pituitary–adrenal (HPA) response to acute and repeated stress. *Neuroscience* 348, 313–323. 10.1016/j.neuroscience.2017.02.038.
235. Gilbert, P.A., and Khokhar, S. (2008). Changing dietary habits of ethnic groups in Europe and implications for health: *Nutrition Reviews*©, Vol. 66, No. 4. *Nutrition Reviews* 66, 203–215. 10.1111/j.1753-4887.2008.00025.x.
236. Keeseey, R.E., and Hirvonen, M.D. (1997). Body weight set-points: determination and adjustment. *J Nutr* 127, 1875S-1883S. 10.1093/jn/127.9.1875S.
237. Speakman, J.R., Levitsky, D.A., Allison, D.B., Bray, M.S., de Castro, J.M., Clegg, D.J., Clapham, J.C., Dulloo, A.G., Gruer, L., Haw, S., et al. (2011). Set points, settling points and some alternative models: theoretical options to understand how genes and environments combine to regulate body adiposity. *Dis Model Mech* 4, 733–745. 10.1242/dmm.008698.
238. National Research Council (US) Committee on Diet and Health (1989). *Diet and Health: Implications for Reducing Chronic Disease Risk* (National Academies Press (US)).
239. Luchtman, D.W., Chee, M.J.S., Doslikova, B., Marks, D.L., Baracos, V.E., and Colmers, W.F. (2015). Defense of Elevated Body Weight Setpoint in Diet-Induced Obese Rats on Low Energy Diet Is Mediated by Loss of Melanocortin Sensitivity in the Paraventricular Hypothalamic Nucleus. *PLoS ONE* 10, e0139462. 10.1371/journal.pone.0139462.
240. Guo, J., Jou, W., Gavrilova, O., and Hall, K.D. (2009). Persistent diet-induced obesity in male C57BL/6 mice resulting from temporary obesigenic diets. *PLoS One* 4, e5370. 10.1371/journal.pone.0005370.
241. Levin, B.E., and Keeseey, R.E. (1998). Defense of differing body weight set points in diet-induced obese and resistant rats. *American Journal of Physiology-Regulatory, Integrative and Comparative Physiology* 274, R412–R419. 10.1152/ajpregu.1998.274.2.R412.
242. Johannsen, D.L., Knuth, N.D., Huizenga, R., Rood, J.C., Ravussin, E., and Hall, K.D. (2012). Metabolic Slowing with Massive Weight Loss despite Preservation of Fat-Free Mass. *The Journal of Clinical Endocrinology & Metabolism* 97, 2489–2496. 10.1210/jc.2012-1444.

243. McNay, D.E.G., and Speakman, J.R. (2013). High fat diet causes rebound weight gain. *Molecular Metabolism* 2, 103–108. 10.1016/j.molmet.2012.10.003.
244. Briggs, D.I., Lockie, S.H., Wu, Q., Lemus, M.B., Stark, R., and Andrews, Z.B. (2013). Calorie-restricted weight loss reverses high-fat diet-induced ghrelin resistance, which contributes to rebound weight gain in a ghrelin-dependent manner. *Endocrinology* 154, 709–717. 10.1210/en.2012-1421.
245. Bray, G.A., Paeratakul, S., and Popkin, B.M. (2004). Dietary fat and obesity: a review of animal, clinical and epidemiological studies. *Physiology & Behavior* 83, 549–555. 10.1016/j.physbeh.2004.08.039.
246. Butler, M.J., and Eckel, L.A. (2018). Eating as a motivated behavior: modulatory effect of high fat diets on energy homeostasis, reward processing and neuroinflammation. *Integr Zool* 13, 673–686. 10.1111/1749-4877.12340.
247. Blasio, A., Rice, K.C., Sabino, V., and Cottone, P. (2014). Characterization of a shortened model of diet alternation in female rats: effects of the CB1 receptor antagonist rimonabant on food intake and anxiety-like behavior. *Behavioural Pharmacology* 25, 609–617. 10.1097/FBP.000000000000059.
248. Dore, R., Valenza, M., Wang, X., Rice, K.C., Sabino, V., and Cottone, P. (2014). The inverse agonist of CB₁ receptor SR141716 blocks compulsive eating of palatable food: CB system and compulsive eating. *Addiction Biology* 19, 849–861. 10.1111/adb.12056.
249. Hu, S., Wang, L., Yang, D., Li, L., Togo, J., Wu, Y., Liu, Q., Li, B., Li, M., Wang, G., et al. (2018). Dietary Fat, but Not Protein or Carbohydrate, Regulates Energy Intake and Causes Adiposity in Mice. *Cell Metabolism* 28, 415-431.e4. 10.1016/j.cmet.2018.06.010.
250. Sárvári, A.K., Van Hauwaert, E.L., Markussen, L.K., Gammelmark, E., Marcher, A.-B., Ebbesen, M.F., Nielsen, R., Brewer, J.R., Madsen, J.G.S., and Mandrup, S. (2021). Plasticity of Epididymal Adipose Tissue in Response to Diet-Induced Obesity at Single-Nucleus Resolution. *Cell Metabolism* 33, 437-453.e5. 10.1016/j.cmet.2020.12.004.
251. Casimiro, I., Stull, N.D., Tersey, S.A., and Mirmira, R.G. (2021). Phenotypic sexual dimorphism in response to dietary fat manipulation in C57BL/6J mice. *J Diabetes Complications* 35, 107795. 10.1016/j.jdiacomp.2020.107795.
252. Heinonen, I., Rinne, P., Ruohonen, S.T., Ruohonen, S., Ahotupa, M., and Savontaus, E. (2014). The effects of equal caloric high fat and western diet

- on metabolic syndrome, oxidative stress and vascular endothelial function in mice. *Acta Physiol (Oxf)* 211, 515–527. 10.1111/apha.12253.
253. Sousa, L.G.O. de, Marshall, A.G., Norman, J.E., Fuqua, J.D., Lira, V.A., Rutledge, J.C., and Bodine, S.C. (2021). The effects of diet composition and chronic obesity on muscle growth and function. *J Appl Physiol* (1985) 130, 124–138. 10.1152/jappphysiol.00156.2020.
254. Guo, J., and Hall, K.D. (2011). Predicting Changes of Body Weight, Body Fat, Energy Expenditure and Metabolic Fuel Selection in C57BL/6 Mice. *PLoS ONE* 6, e15961. 10.1371/journal.pone.0015961.
255. He, M.-Q., Wang, J.-Y., Wang, Y., Sui, J., Zhang, M., Ding, X., Zhao, Y., Chen, Z.-Y., Ren, X.-X., and Shi, B.-Y. (2020). High-fat diet-induced adipose tissue expansion occurs prior to insulin resistance in C57BL/6J mice. *Chronic Diseases and Translational Medicine* 6, 198–207. 10.1016/j.cdtm.2020.06.003.
256. Carlin, J., Hill-Smith, T.E., Lucki, I., and Reyes, T.M. (2013). Reversal of dopamine system dysfunction in response to high-fat diet: High-Fat Diet and Dopamine: Recovery. *Obesity* 21, 2513–2521. 10.1002/oby.20374.
257. Beutler, L.R., Corpuz, T.V., Ahn, J.S., Kosar, S., Song, W., Chen, Y., and Knight, Z.A. (2020). Obesity causes selective and long-lasting desensitization of AgRP neurons to dietary fat. *eLife* 9, e55909. 10.7554/eLife.55909.
258. Thaiss, C.A., Itav, S., Rothschild, D., Meijer, M.T., Levy, M., Moresi, C., Dohnalová, L., Braverman, S., Rozin, S., Malitsky, S., et al. (2016). Persistent microbiome alterations modulate the rate of post-dieting weight regain. *Nature* 540, 544–551. 10.1038/nature20796.
259. Rossi, H.L., Luu, A.K.S., Kothari, S.D., Kuburas, A., Neubert, J.K., Caudle, R.M., and Reiber, A. (2013). Effects of diet-induced obesity on motivation and pain behavior in an operant assay. *Neuroscience* 235, 87–95. 10.1016/j.neuroscience.2013.01.019.
260. Mustaca, A.E., Bentosela, M., and Papini, M.R. (2000). Consummatory Successive Negative Contrast in Mice. *Learning and Motivation* 31, 272–282. 10.1006/lmot.2000.1055.
261. Austen, J.M., Strickland, J.A., and Sanderson, D.J. (2016). Memory-dependent effects on palatability in mice. *Physiology & Behavior* 167, 92–99. 10.1016/j.physbeh.2016.09.001.

262. Chow, C.C., and Hall, K.D. (2014). Short and long-term energy intake patterns and their implications for human body weight regulation. *Physiol Behav* 134, 60–65. 10.1016/j.physbeh.2014.02.044.
263. Maric, T., Woodside, B., and Luheshi, G.N. (2014). The effects of dietary saturated fat on basal hypothalamic neuroinflammation in rats. *Brain Behav Immun* 36, 35–45. 10.1016/j.bbi.2013.09.011.
264. Gao, Y., Bielohuby, M., Fleming, T., Grabner, G.F., Foppen, E., Bernhard, W., Guzmán-Ruiz, M., Layritz, C., Legutko, B., Zinser, E., et al. (2017). Dietary sugars, not lipids, drive hypothalamic inflammation. *Mol Metab* 6, 897–908. 10.1016/j.molmet.2017.06.008.
265. Smith, D.L., Yang, Y., Nagy, T.R., Patki, A., Vasselli, J.R., Zhang, Y., Dickinson, S.L., and Allison, D.B. (2018). Weight Cycling Increases Longevity Compared with Sustained Obesity in Mice. *Obesity (Silver Spring)* 26, 1733–1739. 10.1002/oby.22290.
266. Simonds, S.E., Pryor, J.T., and Cowley, M.A. (2018). Repeated weight cycling in obese mice causes increased appetite and glucose intolerance. *Physiol Behav* 194, 184–190. 10.1016/j.physbeh.2018.05.026.
267. Anderson, E.K., Gutierrez, D.A., Kennedy, A., and Hasty, A.H. (2013). Weight cycling increases T-cell accumulation in adipose tissue and impairs systemic glucose tolerance. *Diabetes* 62, 3180–3188. 10.2337/db12-1076.
268. Barbosa-da-Silva, S., Fraulob-Aquino, J.C., Lopes, J.R., Mandarim-de-Lacerda, C.A., and Aguila, M.B. (2012). Weight cycling enhances adipose tissue inflammatory responses in male mice. *PLoS One* 7, e39837. 10.1371/journal.pone.0039837.
269. Delahanty, L.M., Pan, Q., Jablonski, K.A., Aroda, V.R., Watson, K.E., Bray, G.A., Kahn, S.E., Florez, J.C., Perreault, L., Franks, P.W., et al. (2014). Effects of Weight Loss, Weight Cycling, and Weight Loss Maintenance on Diabetes Incidence and Change in Cardiometabolic Traits in the Diabetes Prevention Program. *Diabetes Care* 37, 2738–2745. 10.2337/dc14-0018.
270. Kakinami, L., Knäuper, B., and Brunet, J. (2020). Weight cycling is associated with adverse cardiometabolic markers in a cross-sectional representative US sample. *J Epidemiol Community Health*, jech-2019-213419. 10.1136/jech-2019-213419.
271. Venditti, E.M., Wing, R.R., Jakicic, J.M., Butler, B.A., and Marcus, M.D. (1996). Weight cycling, psychological health, and binge eating in obese women. *Journal of Consulting and Clinical Psychology* 64, 400–405. 10.1037/0022-006X.64.2.400.

272. Keramati, M., and Gutkin, B. (2014). Homeostatic reinforcement learning for integrating reward collection and physiological stability. *eLife* 3, e04811. 10.7554/eLife.04811.
273. Almeida, M.C., Vizin, R.C.L., and Carrettiero, D.C. (2015). Current understanding on the neurophysiology of behavioral thermoregulation. *Temperature (Austin)* 2, 483–490. 10.1080/23328940.2015.1095270.
274. Hall, K.D., Hammond, R.A., and Rahmandad, H. (2014). Dynamic interplay among homeostatic, hedonic, and cognitive feedback circuits regulating body weight. *Am J Public Health* 104, 1169–1175. 10.2105/AJPH.2014.301931.
275. Levin, B.E., and Dunn-Meynell, A.A. (2002). Defense of body weight depends on dietary composition and palatability in rats with diet-induced obesity. *Am J Physiol Regul Integr Comp Physiol* 282, R46-54. 10.1152/ajpregu.2002.282.1.R46.
276. Rosenbaum, J.L., Frayo, R.S., Melhorn, S.J., Cummings, D.E., and Schur, E.A. (2019). Effects of multiple cycles of weight loss and regain on the body weight regulatory system in rats. *American Journal of Physiology-Endocrinology and Metabolism* 317, E863–E870. 10.1152/ajpendo.00110.2019.
277. Sampey, B.P., Vanhooose, A.M., Winfield, H.M., Freerman, A.J., Muehlbauer, M.J., Fueger, P.T., Newgard, C.B., and Makowski, L. (2011). Cafeteria Diet Is a Robust Model of Human Metabolic Syndrome With Liver and Adipose Inflammation: Comparison to High-Fat Diet. *Obesity* 19, 1109–1117. 10.1038/oby.2011.18.
278. Lang, P., Hasselwander, S., Li, H., and Xia, N. (2019). Effects of different diets used in diet-induced obesity models on insulin resistance and vascular dysfunction in C57BL/6 mice. *Sci Rep* 9, 19556. 10.1038/s41598-019-55987-x.
279. Lauderdale, D., and Rathouz, P. (2000). Body mass index in a US national sample of Asian Americans: effects of nativity, years since immigration and socioeconomic status. *Int J Obes* 24, 1188–1194. 10.1038/sj.ijo.0801365.
280. Lee, M.-L., Matsunaga, H., Sugiura, Y., Hayasaka, T., Yamamoto, I., Ishimoto, T., Imoto, D., Suematsu, M., Iijima, N., Kimura, K., et al. (2021). Prostaglandin in the ventromedial hypothalamus regulates peripheral glucose metabolism. *Nat Commun* 12, 2330. 10.1038/s41467-021-22431-6.
281. Valdearcos, M., Douglass, J.D., Robblee, M.M., Dorfman, M.D., Stifler, D.R., Bennett, M.L., Gerritse, I., Fasnacht, R., Barres, B.A., Thaler, J.P., et al.

- (2018). Microglial Inflammatory Signaling Orchestrates the Hypothalamic Immune Response to Dietary Excess and Mediates Obesity Susceptibility. *Cell Metab* 27, 1356. 10.1016/j.cmet.2018.04.019.
282. Saper, C.B., Romanovsky, A.A., and Scammell, T.E. (2012). Neural circuitry engaged by prostaglandins during the sickness syndrome. *Nat Neurosci* 15, 1088–1095. 10.1038/nn.3159.
283. Timper, K., and Brüning, J.C. (2017). Hypothalamic circuits regulating appetite and energy homeostasis: pathways to obesity. *Disease Models & Mechanisms* 10, 679–689. 10.1242/dmm.026609.
284. Wang, Y., Ziogas, D.C., Biddinger, S., and Kokkotou, E. (2010). You deserve what you eat: lessons learned from the study of the melanin-concentrating hormone (MCH)-deficient mice. *Gut* 59, 1625–1634. 10.1136/gut.2010.210526.
285. Guyon, A., Banisadr, G., Rovère, C., Cervantes, A., Kitabgi, P., Melik-Parsadaniantz, S., and Nahon, J.-L. (2005). Complex effects of stromal cell-derived factor-1 α on melanin-concentrating hormone neuron excitability: SDF-1 α modulation of neuronal excitability. *European Journal of Neuroscience* 21, 701–710. 10.1111/j.1460-9568.2005.03890.x.
286. Le Thuc, O., Cansell, C., Bourourou, M., Denis, R.G., Stobbe, K., Devaux, N., Guyon, A., Cazareth, J., Heurteaux, C., Rostène, W., et al. (2016). Central CCL2 signaling onto MCH neurons mediates metabolic and behavioral adaptation to inflammation. *EMBO Rep* 17, 1738–1752. 10.15252/embr.201541499.
287. Kong, D., Vong, L., Parton, L.E., Ye, C., Tong, Q., Hu, X., Choi, B., Brüning, J.C., and Lowell, B.B. (2010). Glucose stimulation of hypothalamic MCH neurons involves K(ATP) channels, is modulated by UCP2, and regulates peripheral glucose homeostasis. *Cell Metab* 12, 545–552. 10.1016/j.cmet.2010.09.013.
288. Johansson, J.U., Pradhan, S., Lokteva, L.A., Woodling, N.S., Ko, N., Brown, H.D., Wang, Q., Loh, C., Cekanaviciute, E., Buckwalter, M., et al. (2013). Suppression of inflammation with conditional deletion of the prostaglandin E2 EP2 receptor in macrophages and brain microglia. *J Neurosci* 33, 16016–16032. 10.1523/JNEUROSCI.2203-13.2013.
289. Belanger-Willoughby, N., Linehan, V., and Hirasawa, M. (2016). Thermosensing mechanisms and their impairment by high-fat diet in orexin neurons. *Neuroscience* 324, 82–91. 10.1016/j.neuroscience.2016.03.003.

290. Galarraga, M., Campión, J., Muñoz-Barrutia, A., Boqué, N., Moreno, H., Martínez, J.A., Milagro, F., and Ortiz-de-Solórzano, C. (2012). Adiposoft: automated software for the analysis of white adipose tissue cellularity in histological sections. *Journal of Lipid Research* 53, 2791–2796. 10.1194/jlr.D023788.
291. Piao, D., Ritchey, J.W., Holyoak, G.R., Wall, C.R., Sultana, N., Murray, J.K., and Bartels, K.E. (2018). *In vivo* percutaneous reflectance spectroscopy of fatty liver development in rats suggests that the elevation of the scattering power is an early indicator of hepatic steatosis. *J. Innov. Opt. Health Sci.* 11, 1850019. 10.1142/S1793545818500190.
292. Munakata, M., Fujimoto, M., Jin, Y.H., and Akaike, N. (1998). Characterization of electrogenic Na/K pump in rat neostriatal neurons. *Brain Res* 800, 282–293. 10.1016/s0006-8993(98)00533-2.
293. Verdonck, F., Volders, P.G.A., Vos, M.A., and Sipido, K.R. (2003). Increased Na⁺ concentration and altered Na/K pump activity in hypertrophied canine ventricular cells. *Cardiovasc Res* 57, 1035–1043. 10.1016/s0008-6363(02)00734-4.
294. Kreydiyyeh, S.I., Riman, S., Serhan, M., and Kassardjian, A. (2007). TNF- α modulates hepatic Na⁺-K⁺ ATPase activity via PGE₂ and EP₂ receptors. *Prostaglandins Other Lipid Mediat* 83, 295–303. 10.1016/j.prostaglandins.2007.02.003.
295. Einholm, A.P., Nielsen, H.N., Holm, R., Toustrup-Jensen, M.S., and Vilsen, B. (2016). Importance of a Potential Protein Kinase A Phosphorylation Site of Na⁺,K⁺-ATPase and Its Interaction Network for Na⁺ Binding. *J Biol Chem* 291, 10934–10947. 10.1074/jbc.M115.701201.
296. Kosuge, Y., Nango, H., Kasai, H., Yanagi, T., Mawatari, T., Nishiyama, K., Miyagishi, H., Ishige, K., and Ito, Y. (2020). Generation of Cellular Reactive Oxygen Species by Activation of the EP₂ Receptor Contributes to Prostaglandin E₂-Induced Cytotoxicity in Motor Neuron-Like NSC-34 Cells. *Oxid Med Cell Longev* 2020, 6101838. 10.1155/2020/6101838.
297. Liang, X., Wang, Q., Hand, T., Wu, L., Breyer, R.M., Montine, T.J., and Andreasson, K. (2005). Deletion of the prostaglandin E₂ EP₂ receptor reduces oxidative damage and amyloid burden in a model of Alzheimer's disease. *J Neurosci* 25, 10180–10187. 10.1523/JNEUROSCI.3591-05.2005.
298. Alharbi, Y., Kapur, A., Felder, M., Barroilhet, L., Stein, T., Pattnaik, B.R., and Patankar, M.S. (2019). Plumbagin-induced oxidative stress leads to inhibition of Na⁺/K⁺-ATPase (NKA) in canine cancer cells. *Sci Rep* 9, 11471. 10.1038/s41598-019-47261-x.

299. Karmazyn, M., Tuana, B.S., and Dhalla, N.S. (1981). Effect of prostaglandins on rat heart sarcolemmal ATPases. *Can J Physiol Pharmacol* 59, 1122–1127. 10.1139/y81-173.
300. Blanco-Centurion, C., Liu, M., Konadhode, R.P., Zhang, X., Pelluru, D., van den Pol, A.N., and Shiromani, P.J. (2016). Optogenetic activation of melanin-concentrating hormone neurons increases non-rapid eye movement and rapid eye movement sleep during the night in rats. *Eur J Neurosci* 44, 2846–2857. 10.1111/ejn.13410.
301. Vetrivelan, R., Kong, D., Ferrari, L.L., Arrigoni, E., Madara, J.C., Bandaru, S.S., Lowell, B.B., Lu, J., and Saper, C.B. (2016). Melanin-concentrating hormone neurons specifically promote rapid eye movement sleep in mice. *Neuroscience* 336, 102–113. 10.1016/j.neuroscience.2016.08.046.
302. Borowsky, B., Durkin, M.M., Ogozalek, K., Marzabadi, M.R., DeLeon, J., Lagu, B., Heurich, R., Lichtblau, H., Shaposhnik, Z., Daniewska, I., et al. (2002). Antidepressant, anxiolytic and anorectic effects of a melanin-concentrating hormone-1 receptor antagonist. *Nat Med* 8, 825–830. 10.1038/nm741.
303. Duthheil, S., Ota, K.T., Wohleb, E.S., Rasmussen, K., and Duman, R.S. (2016). High-Fat Diet Induced Anxiety and Anhedonia: Impact on Brain Homeostasis and Inflammation. *Neuropsychopharmacology* 41, 1874–1887. 10.1038/npp.2015.357.
304. Luppi, M., Cerri, M., Martelli, D., Tupone, D., Del Vecchio, F., Di Cristoforo, A., Perez, E., Zamboni, G., and Amici, R. (2014). Waking and sleeping in the rat made obese through a high-fat hypercaloric diet. *Behav Brain Res* 258, 145–152. 10.1016/j.bbr.2013.10.014.
305. Panagiotou, M., Meijer, J.H., and Deboer, T. (2018). Chronic high-caloric diet modifies sleep homeostasis in mice. *Eur J Neurosci* 47, 1339–1352. 10.1111/ejn.13932.
306. Vagena, E., Ryu, J.K., Baeza-Raja, B., Walsh, N.M., Syme, C., Day, J.P., Houslay, M.D., and Baillie, G.S. (2019). A high-fat diet promotes depression-like behavior in mice by suppressing hypothalamic PKA signaling. *Transl Psychiatry* 9, 141. 10.1038/s41398-019-0470-1.
307. Parent, M.B., Higgs, S., Cheke, L.G., and Kanoski, S.E. (2022). Memory and eating: A bidirectional relationship implicated in obesity. *Neuroscience & Biobehavioral Reviews* 132, 110–129. 10.1016/j.neubiorev.2021.10.051.

308. Linehan, V., Fang, L.Z., Parsons, M.P., and Hirasawa, M. (2020). High-fat diet induces time-dependent synaptic plasticity of the lateral hypothalamus. *Mol Metab* 36, 100977. 10.1016/j.molmet.2020.100977.
309. Imbernon, M., Beiroa, D., Vázquez, M.J., Morgan, D.A., Veyrat-Durebex, C., Porteiro, B., Díaz-Arteaga, A., Senra, A., Busquets, S., Velásquez, D.A., et al. (2013). Central melanin-concentrating hormone influences liver and adipose metabolism via specific hypothalamic nuclei and efferent autonomic/JNK1 pathways. *Gastroenterology* 144, 636-649.e6. 10.1053/j.gastro.2012.10.051.
310. Lainez, N.M., Jonak, C.R., Nair, M.G., Ethell, I.M., Wilson, E.H., Carson, M.J., and Coss, D. (2018). Diet-Induced Obesity Elicits Macrophage Infiltration and Reduction in Spine Density in the Hypothalamus of Male but Not Female Mice. *Front. Immunol.* 9, 1992. 10.3389/fimmu.2018.01992.
311. Morselli, E., Fuente-Martin, E., Finan, B., Kim, M., Frank, A., Garcia-Caceres, C., Navas, C.R., Gordillo, R., Neinast, M., Kalainayakan, S.P., et al. (2014). Hypothalamic PGC-1 α Protects Against High-Fat Diet Exposure by Regulating ER α . *Cell Reports* 9, 633–645. 10.1016/j.celrep.2014.09.025.
312. Pinto, S., Roseberry, A.G., Liu, H., Diano, S., Shanabrough, M., Cai, X., Friedman, J.M., and Horvath, T.L. (2004). Rapid Rewiring of Arcuate Nucleus Feeding Circuits by Leptin. *Science* 304, 110–115. 10.1126/science.1089459.
313. Rada, P., Avena, N.M., Barson, J.R., Hoebel, B.G., and Leibowitz, S.F. (2012). A High-Fat Meal, or Intraperitoneal Administration of a Fat Emulsion, Increases Extracellular Dopamine in the Nucleus Accumbens. *Brain Sciences* 2, 242–253. 10.3390/brainsci2020242.
314. Schwartz, M.W., Woods, S.C., Porte, D., Seeley, R.J., and Baskin, D.G. (2000). Central nervous system control of food intake. *Nature* 404, 661–671. 10.1038/35007534.
315. Kenny, P.J. (2011). Common cellular and molecular mechanisms in obesity and drug addiction. *Nat Rev Neurosci* 12, 638–651. 10.1038/nrn3105.
316. Barson, J.R., Morganstern, I., and Leibowitz, S.F. (2013). Complementary Roles of Orexin and Melanin-Concentrating Hormone in Feeding Behavior. *International Journal of Endocrinology* 2013, 1–10. 10.1155/2013/983964.
317. González, J.A., Iordanidou, P., Strom, M., Adamantidis, A., and Burdakov, D. (2016). Awake dynamics and brain-wide direct inputs of hypothalamic MCH and orexin networks. *Nat Commun* 7, 11395. 10.1038/ncomms11395.

318. González, J.A., Jensen, L.T., Fugger, L., and Burdakov, D. (2012). Convergent inputs from electrically and topographically distinct orexin cells to locus coeruleus and ventral tegmental area: Properties of mouse orexin cells innervating LC and VTA. *European Journal of Neuroscience* 35, 1426–1432. 10.1111/j.1460-9568.2012.08057.x.
319. Bittencourt, J.C. (2011). Anatomical organization of the melanin-concentrating hormone peptide family in the mammalian brain. *General and Comparative Endocrinology* 172, 185–197. 10.1016/j.ygcen.2011.03.028.
320. Muroya, S., Funahashi, H., Yamanaka, A., Kohno, D., Uramura, K., Nambu, T., Shibahara, M., Kuramochi, M., Takigawa, M., Yanagisawa, M., et al. (2004). Orexins (hypocretins) directly interact with neuropeptide Y, POMC and glucose-responsive neurons to regulate Ca²⁺ signaling in a reciprocal manner to leptin: orexigenic neuronal pathways in the mediobasal hypothalamus. *Eur J Neurosci* 19, 1524–1534. 10.1111/j.1460-9568.2004.03255.x.
321. Haynes, A.C., Jackson, B., Overend, P., Buckingham, R.E., Wilson, S., Tadayyon, M., and Arch, J.R.S. (1999). Effects of single and chronic intracerebroventricular administration of the orexins on feeding in the rat. *Peptides* 20, 1099–1105. 10.1016/S0196-9781(99)00105-9.
322. Gomori, A., Ishihara, A., Ito, M., Mashiko, S., Matsushita, H., Yumoto, M., Ito, M., Tanaka, T., Tokita, S., Moriya, M., et al. (2003). Chronic intracerebroventricular infusion of MCH causes obesity in mice. *American Journal of Physiology-Endocrinology and Metabolism* 284, E583–E588. 10.1152/ajpendo.00350.2002.
323. Chang, G.-Q., Karatayev, O., Davydova, Z., and Leibowitz, S.F. (2004). Circulating Triglycerides Impact on Orexigenic Peptides and Neuronal Activity in Hypothalamus. *Endocrinology* 145, 3904–3912. 10.1210/en.2003-1582.
324. Petrovich, G.D., Hobin, M.P., and Reppucci, C.J. (2012). Selective Fos induction in hypothalamic orexin/hypocretin, but not melanin-concentrating hormone neurons, by a learned food-cue that stimulates feeding in sated rats. *Neuroscience* 224, 70–80. 10.1016/j.neuroscience.2012.08.036.
325. Choi, D.L., Davis, J.F., Fitzgerald, M.E., and Benoit, S.C. (2010). The role of orexin-A in food motivation, reward-based feeding behavior and food-induced neuronal activation in rats. *Neuroscience* 167, 11–20. 10.1016/j.neuroscience.2010.02.002.
326. Moorman, D.E., James, M.H., Kilroy, E.A., and Aston-Jones, G. (2016). Orexin/hypocretin neuron activation is correlated with alcohol seeking and

- preference in a topographically specific manner. *Eur J Neurosci* 43, 710–720. 10.1111/ejn.13170.
327. Plaza-Zabala, A., Maldonado, R., and Berrendero, F. (2012). The Hypocretin/Orexin System: Implications for Drug Reward and Relapse. *Mol Neurobiol* 45, 424–439. 10.1007/s12035-012-8255-z.
328. Shirasaka, T., Nakazato, M., Matsukura, S., Takasaki, M., and Kannan, H. (1999). Sympathetic and cardiovascular actions of orexins in conscious rats. *American Journal of Physiology-Regulatory, Integrative and Comparative Physiology* 277, R1780–R1785. 10.1152/ajpregu.1999.277.6.R1780.
329. Zink, A.N., Bunney, P.E., Holm, A.A., Billington, C.J., and Kotz, C.M. (2018). Neuromodulation of orexin neurons reduces diet-induced adiposity. *Int J Obes* 42, 737–745. 10.1038/ijo.2017.276.
330. Domingos, A.I., Sordillo, A., Dietrich, M.O., Liu, Z.-W., Tellez, L.A., Vaynshteyn, J., Ferreira, J.G., Ekstrand, M.I., Horvath, T.L., De Araujo, I.E., et al. (2013). Hypothalamic melanin concentrating hormone neurons communicate the nutrient value of sugar. *eLife* 2, e01462. 10.7554/eLife.01462.
331. Clegg, D.J., Air, E.L., Woods, S.C., and Seeley, R.J. (2002). Eating Elicited by Orexin-A, But Not Melanin-Concentrating Hormone, Is Opioid Mediated. *Endocrinology* 143, 2995–3000. 10.1210/endo.143.8.8977.
332. Mul, J.D., Yi, C.-X., van den Berg, S.A.A., Ruiter, M., Toonen, P.W., van der Elst, M.C.J., Voshol, P.J., Ellenbroek, B.A., Kalsbeek, A., la Fleur, S.E., et al. (2010). Pmch expression during early development is critical for normal energy homeostasis. *Am J Physiol Endocrinol Metab* 298, E477–488. 10.1152/ajpendo.00154.2009.
333. Linehan, V., and Hirasawa, M. (2018). Electrophysiological Properties of Melanin-Concentrating Hormone and Orexin Neurons in Adolescent Rats. *Front. Cell. Neurosci.* 12, 70. 10.3389/fncel.2018.00070.
334. Cristino, L., Busetto, G., Imperatore, R., Ferrandino, I., Palomba, L., Silvestri, C., Petrosino, S., Orlando, P., Bentivoglio, M., Mackie, K., et al. (2013). Obesity-driven synaptic remodeling affects endocannabinoid control of orexinergic neurons. *Proc. Natl. Acad. Sci. U.S.A.* 110. 10.1073/pnas.1219485110.
335. Stranahan, A.M., Norman, E.D., Lee, K., Cutler, R.G., Telljohann, R.S., Egan, J.M., and Mattson, M.P. (2008). Diet-induced insulin resistance impairs hippocampal synaptic plasticity and cognition in middle-aged rats. *Hippocampus* 18, 1085–1088. 10.1002/hipo.20470.

336. Henny, P., and Jones, B.E. (2006). Innervation of orexin/hypocretin neurons by GABAergic, glutamatergic or cholinergic basal forebrain terminals evidenced by immunostaining for presynaptic vesicular transporter and postsynaptic scaffolding proteins. *J. Comp. Neurol.* 499, 645–661. 10.1002/cne.21131.
337. Niu, J.-G., Yokota, S., Tsumori, T., Qin, Y., and Yasui, Y. (2010). Glutamatergic lateral parabrachial neurons innervate orexin-containing hypothalamic neurons in the rat. *Brain Research* 1358, 110–122. 10.1016/j.brainres.2010.08.056.
338. Niu, J.-G., Yokota, S., Tsumori, T., Oka, T., and Yasui, Y. (2012). Projections from the anterior basomedial and anterior cortical amygdaloid nuclei to melanin-concentrating hormone-containing neurons in the lateral hypothalamus of the rat. *Brain Research* 1479, 31–43. 10.1016/j.brainres.2012.08.011.
339. Bochorishvili, G., Nguyen, T., Coates, M.B., Viar, K.E., Stornetta, R.L., and Guyenet, P.G. (2014). The orexinergic neurons receive synaptic input from C1 cells in rats: C1 Cell Input to Orexinergic Neurons. *J. Comp. Neurol.* 522, 3834–3846. 10.1002/cne.23643.
340. Li, Y., Gao, X.-B., Sakurai, T., and Van Den Pol, A.N. (2002). Hypocretin/Orexin Excites Hypocretin Neurons via a Local Glutamate Neuron—A Potential Mechanism for Orchestrating the Hypothalamic Arousal System. *Neuron* 36, 1169–1181. 10.1016/S0896-6273(02)01132-7.
341. Wortley, K.E., Chang, G.-Q., Davydova, Z., and Leibowitz, S.F. (2003). Orexin gene expression is increased during states of hypertriglyceridemia. *American Journal of Physiology-Regulatory, Integrative and Comparative Physiology* 284, R1454–R1465. 10.1152/ajpregu.00286.2002.
342. Terrill, S.J., Hyde, K.M., Kay, K.E., Greene, H.E., Maske, C.B., Knierim, A.E., Davis, J.F., and Williams, D.L. (2016). Ventral tegmental area orexin 1 receptors promote palatable food intake and oppose postingestive negative feedback. *American Journal of Physiology-Regulatory, Integrative and Comparative Physiology* 311, R592–R599. 10.1152/ajpregu.00097.2016.
343. Liu, J.-J., Bello, N.T., and Pang, Z.P. (2017). Presynaptic Regulation of Leptin in a Defined Lateral Hypothalamus–Ventral Tegmental Area Neurocircuitry Depends on Energy State. *J. Neurosci.* 37, 11854–11866. 10.1523/JNEUROSCI.1942-17.2017.
344. Yeoh, J.W., James, M.H., Jobling, P., Bains, J.S., Graham, B.A., and Dayas, C.V. (2012). Cocaine potentiates excitatory drive in the perifornical/lateral hypothalamus: Cocaine-induced plasticity in the perifornical/lateral

- hypothalamic area. *The Journal of Physiology* 590, 3677–3689. 10.1113/jphysiol.2012.230268.
345. Rao, Y., Mineur, Y.S., Gan, G., Wang, A.H., Liu, Z.-W., Wu, X., Suyama, S., De Lecea, L., Horvath, T.L., Picciotto, M.R., et al. (2013). Repeated *in vivo* exposure of cocaine induces long-lasting synaptic plasticity in hypocretin/orexin-producing neurons in the lateral hypothalamus in mice: Cocaine-induced synaptic plasticity in hypocretin neurons. *The Journal of Physiology* 591, 1951–1966. 10.1113/jphysiol.2012.246983.
346. Chang, C.Y., Jiang, X., Moulder, K.L., and Mennerick, S. (2010). Rapid Activation of Dormant Presynaptic Terminals by Phorbol Esters. *J. Neurosci.* 30, 10048–10060. 10.1523/JNEUROSCI.1159-10.2010.
347. Schöne, C., Venner, A., Knowles, D., Karnani, M.M., and Burdakov, D. (2011). Dichotomous cellular properties of mouse orexin/hypocretin neurons: Cellular dichotomy in the orexin system. *The Journal of Physiology* 589, 2767–2779. 10.1113/jphysiol.2011.208637.
348. Williams, R.H., Alexopoulos, H., Jensen, L.T., Fugger, L., and Burdakov, D. (2008). Adaptive sugar sensors in hypothalamic feeding circuits. *Proc. Natl. Acad. Sci. U.S.A.* 105, 11975–11980. 10.1073/pnas.0802687105.
349. Briggs, C., Bowes, S.C., Semba, K., and Hirasawa, M. (2019). Sleep deprivation-induced pre- and postsynaptic modulation of orexin neurons. *Neuropharmacology* 154, 50–60. 10.1016/j.neuropharm.2018.12.025.
350. Becker, T.M., Favero, M., Di Marzo, V., Cristino, L., and Busetto, G. (2017). Endocannabinoid-dependent disinhibition of orexinergic neurons: Electrophysiological evidence in leptin-knockout obese mice. *Molecular Metabolism* 6, 594–601. 10.1016/j.molmet.2017.04.005.
351. Jo, Y.-H., Chen, Y.-J.J., Chua, S.C., Talmage, D.A., and Role, L.W. (2005). Integration of Endocannabinoid and Leptin Signaling in an Appetite-Related Neural Circuit. *Neuron* 48, 1055–1066. 10.1016/j.neuron.2005.10.021.
352. Morales, E., Torres-Castillo, N., and Garaulet, M. (2021). Infancy and Childhood Obesity Grade Predicts Weight Loss in Adulthood: The ONTIME Study. *Nutrients* 13, 2132. 10.3390/nu13072132.
353. Zhang, X., and Van Den Pol, A.N. (2016). Hypothalamic arcuate nucleus tyrosine hydroxylase neurons play orexigenic role in energy homeostasis. *Nat Neurosci* 19, 1341–1347. 10.1038/nn.4372.

354. Sweeney, P., Chen, C., Rajapakse, I., and Cone, R.D. (2021). Network dynamics of hypothalamic feeding neurons. *Proc. Natl. Acad. Sci. U.S.A.* *118*, e2011140118. 10.1073/pnas.2011140118.
355. Livneh, Y., Sugden, A.U., Madara, J.C., Essner, R.A., Flores, V.I., Sugden, L.A., Resch, J.M., Lowell, B.B., and Andermann, M.L. (2020). Estimation of Current and Future Physiological States in Insular Cortex. *Neuron* *105*, 1094-1111.e10. 10.1016/j.neuron.2019.12.027.
356. Liao, T., Zhang, S., Yuan, X., Mo, W., Wei, F., Zhao, S., Yang, W., Liu, H., and Rong, X. (2020). Liraglutide Lowers Body Weight Set Point in DIO Rats and its Relationship with Hypothalamic Microglia Activation. *Obesity* *28*, 122–131. 10.1002/oby.22666.
357. Berkseth, K.E., Guyenet, S.J., Melhorn, S.J., Lee, D., Thaler, J.P., Schur, E.A., and Schwartz, M.W. (2014). Hypothalamic Gliosis Associated With High-Fat Diet Feeding Is Reversible in Mice: A Combined Immunohistochemical and Magnetic Resonance Imaging Study. *Endocrinology* *155*, 2858–2867. 10.1210/en.2014-1121.
358. Wang, J., Osaka, T., and Inoue, S. (2001). Energy expenditure by intracerebroventricular administration of orexin to anesthetized rats. *Neuroscience Letters* *315*, 49–52. 10.1016/S0304-3940(01)02322-9.
359. Azzout-Marniche, D., Chaumontet, C., Nadkarni, N.A., Piedcoq, J., Fromentin, G., Tomé, D., and Even, P.C. (2014). Food intake and energy expenditure are increased in high-fat-sensitive but not in high-carbohydrate-sensitive obesity-prone rats. *American Journal of Physiology-Regulatory, Integrative and Comparative Physiology* *307*, R299–R309. 10.1152/ajpregu.00065.2014.
360. Bjursell, M., Gerdin, A.-K., Lelliott, C.J., Egecioglu, E., Elmgren, A., Törnell, J., Oscarsson, J., and Bohlooly-Y, M. (2008). Acutely reduced locomotor activity is a major contributor to Western diet-induced obesity in mice. *American Journal of Physiology-Endocrinology and Metabolism* *294*, E251–E260. 10.1152/ajpendo.00401.2007.
361. González, J.A., Jensen, L.T., Iordanidou, P., Strom, M., Fugger, L., and Burdakov, D. (2016). Inhibitory Interplay between Orexin Neurons and Eating. *Current Biology* *26*, 2486–2491. 10.1016/j.cub.2016.07.013.
362. Niraula, A., Fasnacht, R.D., Ness, K.M., Frey, J.M., Cuschieri, S.A., Dorfman, M.D., and Thaler, J.P. (2023). Prostaglandin PGE2 Receptor EP4 Regulates Microglial Phagocytosis and Increases Susceptibility to Diet-Induced Obesity. *Diabetes* *72*, 233–244. 10.2337/db21-1072.

363. Tan, Y.-L., Yuan, Y., and Tian, L. (2020). Microglial regional heterogeneity and its role in the brain. *Mol Psychiatry* 25, 351–367. 10.1038/s41380-019-0609-8.
364. Varela, L., Stutz, B., Song, J.E., Kim, J.G., Liu, Z.-W., Gao, X.-B., and Horvath, T.L. (2021). Hunger-promoting AgRP neurons trigger an astrocyte-mediated feed-forward autoactivation loop in mice. *J Clin Invest* 131. 10.1172/JCI144239.
365. MacDonald, A.J., Holmes, F.E., Beall, C., Pickering, A.E., and Ellacott, K.L.J. (2020). Regulation of food intake by astrocytes in the brainstem dorsal vagal complex. *Glia* 68, 1241–1254. 10.1002/glia.23774.
366. Briggs, C., Hirasawa, M., and Semba, K. (2018). Sleep Deprivation Distinctly Alters Glutamate Transporter 1 Apposition and Excitatory Transmission to Orexin and MCH Neurons. *J. Neurosci.* 38, 2505–2518. 10.1523/JNEUROSCI.2179-17.2018.
367. O raha, J., Enriquez, R.F., Herzog, H., and Lee, N.J. (2022). Sex-specific changes in metabolism during the transition from chow to high-fat diet feeding are abolished in response to dieting in C57BL/6J mice. *Int J Obes* 46, 1749–1758. 10.1038/s41366-022-01174-4.
368. Gelineau, R.R., Arruda, N.L., Hicks, J.A., Monteiro De Pina, I., Hatzidis, A., and Seggio, J.A. (2017). The behavioral and physiological effects of high-fat diet and alcohol consumption: Sex differences in C57BL6/J mice. *Brain Behav* 7, e00708. 10.1002/brb3.708.
369. Pettersson, U.S., Waldén, T.B., Carlsson, P.-O., Jansson, L., and Phillipson, M. (2012). Female Mice are Protected against High-Fat Diet Induced Metabolic Syndrome and Increase the Regulatory T Cell Population in Adipose Tissue. *PLoS ONE* 7, e46057. 10.1371/journal.pone.0046057.
370. Maric, I., Krieger, J.-P., Van Der Velden, P., Borchers, S., Asker, M., Vujicic, M., Wernstedt Asterholm, I., and Skibicka, K.P. (2022). Sex and Species Differences in the Development of Diet-Induced Obesity and Metabolic Disturbances in Rodents. *Front. Nutr.* 9, 828522. 10.3389/fnut.2022.828522.
371. Hong, J., Stubbins, R.E., Smith, R.R., Harvey, A.E., and Núñez, N.P. (2009). Differential susceptibility to obesity between male, female and ovariectomized female mice. *Nutr J* 8, 11. 10.1186/1475-2891-8-11.
372. Eckel, L.A., and Moore, S.R. (2004). Diet-induced hyperphagia in the rat is influenced by sex and exercise. *American Journal of Physiology-Regulatory, Integrative and Comparative Physiology* 287, R1080–R1085. 10.1152/ajpregu.00424.2004.

373. Choi, D.K., Oh, T.S., Choi, J.-W., Mukherjee, R., Wang, X., Liu, H., and Yun, J.W. (2011). Gender Difference in Proteome of Brown Adipose Tissues between Male and Female Rats Exposed to a High Fat Diet. *Cell Physiol Biochem* 28, 933–948. 10.1159/000335807.
374. Butler, M.J., Perrini, A.A., and Eckel, L.A. (2020). Estradiol treatment attenuates high fat diet-induced microgliosis in ovariectomized rats. *Hormones and Behavior* 120, 104675. 10.1016/j.yhbeh.2020.104675.
375. Pace, S., Rossi, A., Krauth, V., Dehm, F., Troisi, F., Bilancia, R., Weinigel, C., Rummler, S., Werz, O., and Sautebin, L. (2017). Sex differences in prostaglandin biosynthesis in neutrophils during acute inflammation. *Sci Rep* 7, 3759. 10.1038/s41598-017-03696-8.
376. Smith, J.A., Das, A., Butler, J.T., Ray, S.K., and Banik, N.L. (2011). Estrogen or Estrogen Receptor Agonist Inhibits Lipopolysaccharide Induced Microglial Activation and Death. *Neurochem Res* 36, 1587–1593. 10.1007/s11064-010-0336-7.
377. Baker, A.E., Brautigam, V.M., and Watters, J.J. (2004). Estrogen Modulates Microglial Inflammatory Mediator Production via Interactions with Estrogen Receptor β . *Endocrinology* 145, 5021–5032. 10.1210/en.2004-0619.
378. Vegeto, E., Bonincontro, C., Pollio, G., Sala, A., Viappiani, S., Nardi, F., Brusadelli, A., Viviani, B., Ciana, P., and Maggi, A. (2001). Estrogen Prevents the Lipopolysaccharide-Induced Inflammatory Response in Microglia. *J. Neurosci.* 21, 1809–1818. 10.1523/JNEUROSCI.21-06-01809.2001.
379. Gao, Y., Ottaway, N., Schriever, S.C., Legutko, B., García-Cáceres, C., De La Fuente, E., Mergen, C., Bour, S., Thaler, J.P., Seeley, R.J., et al. (2014). Hormones and diet, but not body weight, control hypothalamic microglial activity: Hypothalamic Microglia in Obesity. *Glia* 62, 17–25. 10.1002/glia.22580.
380. Jin, Z., Kim, K.E., Shin, H.J., Jeong, E.A., Park, K.-A., Lee, J.Y., An, H.S., Choi, E.B., Jeong, J.H., Kwak, W., et al. (2020). Hippocampal Lipocalin 2 Is Associated With Neuroinflammation and Iron-Related Oxidative Stress in ob/ob Mice. *Journal of Neuropathology & Experimental Neurology* 79, 530–541. 10.1093/jnen/nlaa017.
381. Koh, T.J., and DiPietro, L.A. (2011). Inflammation and wound healing: the role of the macrophage. *Expert Rev. Mol. Med.* 13, e23. 10.1017/S1462399411001943.

382. Wernstedt Asterholm, I., Tao, C., Morley, T.S., Wang, Q.A., Delgado-Lopez, F., Wang, Z.V., and Scherer, P.E. (2014). Adipocyte Inflammation Is Essential for Healthy Adipose Tissue Expansion and Remodeling. *Cell Metabolism* 20, 103–118. 10.1016/j.cmet.2014.05.005.
383. Guan, J.-L., Uehara, K., Lu, S., Wang, Q.-P., Funahashi, H., Sakurai, T., Yanagizawa, M., and Shioda, S. (2002). Reciprocal synaptic relationships between orexin- and melanin-concentrating hormone-containing neurons in the rat lateral hypothalamus: a novel circuit implicated in feeding regulation. *Int J Obes* 26, 1523–1532. 10.1038/sj.ijo.0802155.
384. Hsu, T.M., Hahn, J.D., Konanur, V.R., Noble, E.E., Suarez, A.N., Thai, J., Nakamoto, E.M., and Kanoski, S.E. (2015). Hippocampus ghrelin signaling mediates appetite through lateral hypothalamic orexin pathways. *eLife* 4, e11190. 10.7554/eLife.11190.
385. Tsai, S.-F., Hsu, P.-L., Chen, Y.-W., Hossain, M.S., Chen, P.-C., Tzeng, S.-F., Chen, P.-S., and Kuo, Y.-M. (2022). High-fat diet induces depression-like phenotype via astrocyte-mediated hyperactivation of ventral hippocampal glutamatergic afferents to the nucleus accumbens. *Mol Psychiatry* 27, 4372–4384. 10.1038/s41380-022-01787-1.
386. Arima, Y., Yokota, S., and Fujitani, M. (2019). Lateral parabrachial neurons innervate orexin neurons projecting to brainstem arousal areas in the rat. *Sci Rep* 9, 2830. 10.1038/s41598-019-39063-y.
387. Siegel, A., and Tassoni, J.P. (1971). Differential Efferent Projections from the Ventral and Dorsal Hippocampus of the Cat. *Brain Behav Evol* 4, 185–200. 10.1159/000125433.
388. Grillo, C.A., Piroli, G.G., Junor, L., Wilson, S.P., Mott, D.D., Wilson, M.A., and Reagan, L.P. (2011). Obesity/hyperleptinemic phenotype impairs structural and functional plasticity in the rat hippocampus. *Physiology & Behavior* 105, 138–144. 10.1016/j.physbeh.2011.02.028.
389. Hao, S., Dey, A., Yu, X., and Stranahan, A.M. (2016). Dietary obesity reversibly induces synaptic stripping by microglia and impairs hippocampal plasticity. *Brain, Behavior, and Immunity* 51, 230–239. 10.1016/j.bbi.2015.08.023.
390. Hardaway, J.A., Halladay, L.R., Mazzone, C.M., Pati, D., Bloodgood, D.W., Kim, M., Jensen, J., DiBerto, J.F., Boyt, K.M., Shiddapur, A., et al. (2019). Central Amygdala Prepronociceptin-Expressing Neurons Mediate Palatable Food Consumption and Reward. *Neuron* 102, 1037-1052.e7. 10.1016/j.neuron.2019.03.037.

391. Schepers, J., Gebhardt, C., Bracke, A., Eiffler, I., and Von Bohlen Und Halbach, O. (2020). Structural and functional consequences in the amygdala of leptin-deficient mice. *Cell Tissue Res* 382, 421–426. 10.1007/s00441-020-03266-x.
392. Ip, C.K., Zhang, L., Farzi, A., Qi, Y., Clarke, I., Reed, F., Shi, Y.-C., Enriquez, R., Dayas, C., Graham, B., et al. (2019). Amygdala NPY Circuits Promote the Development of Accelerated Obesity under Chronic Stress Conditions. *Cell Metabolism* 30, 111-128.e6. 10.1016/j.cmet.2019.04.001.
393. Thomas, C.S., Mohammadkhani, A., Rana, M., Qiao, M., Baimel, C., and Borgland, S.L. (2022). Optogenetic stimulation of lateral hypothalamic orexin/dynorphin inputs in the ventral tegmental area potentiates mesolimbic dopamine neurotransmission and promotes reward-seeking behaviours. *Neuropsychopharmacol.* 47, 728–740. 10.1038/s41386-021-01196-y.
394. Pissios, P., Frank, L., Kennedy, A.R., Porter, D.R., Marino, F.E., Liu, F.-F., Pothos, E.N., and Maratos-Flier, E. (2008). Dysregulation of the Mesolimbic Dopamine System and Reward in MCH^{-/-} Mice. *Biological Psychiatry* 64, 184–191. 10.1016/j.biopsych.2007.12.011.
395. Geiger, B.M., Haburcak, M., Avena, N.M., Moyer, M.C., Hoebel, B.G., and Pothos, E.N. (2009). Deficits of mesolimbic dopamine neurotransmission in rat dietary obesity. *Neuroscience* 159, 1193–1199. 10.1016/j.neuroscience.2009.02.007.
396. Geiger, B.M., Frank, L.E., Caldera-siu, A.D., Stiles, L., and Pothos, E.N. (2007). Deficiency of central dopamine in multiple obesity models. *Appetite* 49, 293. 10.1016/j.appet.2007.03.075.
397. Jones, S.R., and Fordahl, S.C. (2021). Bingeing on High-Fat Food Enhances Evoked Dopamine Release and Reduces Dopamine Uptake in the Nucleus Accumbens. *Obesity* 29, 721–730. 10.1002/oby.23122.
398. Blum, K., Thanos, P.K., and Gold, M.S. (2014). Dopamine and glucose, obesity, and reward deficiency syndrome. *Front. Psychol.* 5. 10.3389/fpsyg.2014.00919.
399. Loprinzi, P.D., and Frith, E. (2018). Obesity and episodic memory function. *J Physiol Sci* 68, 321–331. 10.1007/s12576-018-0612-x.
400. Pachoud, B., Adamantidis, A., Ravassard, P., Luppi, P.-H., Grisar, T., Lakaye, B., and Salin, P.-A. (2010). Major Impairments of Glutamatergic Transmission and Long-Term Synaptic Plasticity in the Hippocampus of Mice Lacking the Melanin-Concentrating Hormone Receptor-1. *Journal of Neurophysiology* 104, 1417–1425. 10.1152/jn.01052.2009.

401. Mutlu-Burnaz, O., Yulug, B., Oncul, M., Celik, E., Atasoy, N.S., Cankaya, S., Hanoglu, L., and Velioglu, H.A. (2022). Chemogenetic inhibition of MCH neurons does not alter memory performance in mice. *Biomedicine & Pharmacotherapy* 155, 113771. 10.1016/j.biopha.2022.113771.
402. Adamantidis, A., and De Lecea, L. (2009). A role for Melanin-Concentrating Hormone in learning and memory. *Peptides* 30, 2066–2070. 10.1016/j.peptides.2009.06.024.
403. Forte, N., Boccella, S., Tunisi, L., Fernández-Rilo, A.C., Imperatore, R., Iannotti, F.A., De Risi, M., Iannotta, M., Piscitelli, F., Capasso, R., et al. (2021). Orexin-A and endocannabinoids are involved in obesity-associated alteration of hippocampal neurogenesis, plasticity, and episodic memory in mice. *Nat Commun* 12, 6137. 10.1038/s41467-021-26388-4.
404. Takahashi, Y., Zhang, W., Sameshima, K., Kuroki, C., Matsumoto, A., Sunanaga, J., Kono, Y., Sakurai, T., Kanmura, Y., and Kuwaki, T. (2013). Orexin neurons are indispensable for prostaglandin E₂-induced fever and defence against environmental cooling in mice: Orexin neurons in PGE₂ and cooling-induced thermogenesis. *The Journal of Physiology* 591, 5623–5643. 10.1113/jphysiol.2013.261271.
405. Cvetkovic, V., Brischoux, F., Jacquemard, C., Fellmann, D., Griffond, B., and Risold, P.-Y. (2004). Characterization of subpopulations of neurons producing melanin-concentrating hormone in the rat ventral diencephalon. *J Neurochem* 91, 911–919. 10.1111/j.1471-4159.2004.02776.x.
406. Gras, C., Amilhon, B., Lepicard, È.M., Poirel, O., Vinatier, J., Herbin, M., Dumas, S., Tzavara, E.T., Wade, M.R., Nomikos, G.G., et al. (2008). The vesicular glutamate transporter VGLUT3 synergizes striatal acetylcholine tone. *Nat Neurosci* 11, 292–300. 10.1038/nn2052.
407. Corder, G., Castro, D.C., Bruchas, M.R., and Scherrer, G. (2018). Endogenous and Exogenous Opioids in Pain. *Annu. Rev. Neurosci.* 41, 453–473. 10.1146/annurev-neuro-080317-061522.
408. Bali, A., Randhawa, P.K., and Jaggi, A.S. (2015). Stress and opioids: Role of opioids in modulating stress-related behavior and effect of stress on morphine conditioned place preference. *Neuroscience & Biobehavioral Reviews* 51, 138–150. 10.1016/j.neubiorev.2014.12.018.
409. Yoshida, K., McCormack, S., España, R.A., Crocker, A., and Scammell, T.E. (2006). Afferents to the orexin neurons of the rat brain. *J. Comp. Neurol.* 494, 845–861. 10.1002/cne.20859.

410. Sakurai, T., Nagata, R., Yamanaka, A., Kawamura, H., Tsujino, N., Muraki, Y., Kageyama, H., Kunita, S., Takahashi, S., Goto, K., et al. (2005). Input of Orexin/Hypocretin Neurons Revealed by a Genetically Encoded Tracer in Mice. *Neuron* 46, 297–308. 10.1016/j.neuron.2005.03.010.
411. Boaz, M., Lisy, L., Zandman-Goddard, G., and Wainstein, J. (2009). The effect of anti-inflammatory (aspirin and/or statin) therapy on body weight in Type 2 diabetic individuals: EAT, a retrospective study. *Diabetic Medicine* 26, 708–713. 10.1111/j.1464-5491.2009.02747.x.
412. Singh, S., Facciorusso, A., Singh, A.G., Castele, N.V., Zarrinpar, A., Prokop, L.J., Grunvald, E.L., Curtis, J.R., and Sandborn, W.J. (2018). Obesity and response to anti-tumor necrosis factor- α agents in patients with select immune-mediated inflammatory diseases: A systematic review and meta-analysis. *PLoS ONE* 13, e0195123. 10.1371/journal.pone.0195123.
413. Nathan, C., and Ding, A. (2010). Nonresolving Inflammation. *Cell* 140, 871–882. 10.1016/j.cell.2010.02.029.
414. Ruiz, R., and Kirk, A.D. (2015). Long-Term Toxicity of Immunosuppressive Therapy. In *Transplantation of the Liver* (Elsevier), pp. 1354–1363. 10.1016/B978-1-4557-0268-8.00097-X.
415. Vonkeman, H.E., and Van De Laar, M.A.F.J. (2010). Nonsteroidal Anti-Inflammatory Drugs: Adverse Effects and Their Prevention. *Seminars in Arthritis and Rheumatism* 39, 294–312. 10.1016/j.semarthrit.2008.08.001.
416. Aithal, G.P., and Day, C.P. (2007). Nonsteroidal Anti-Inflammatory Drug-Induced Hepatotoxicity. *Clinics in Liver Disease* 11, 563–575. 10.1016/j.cld.2007.06.004.
417. Tran-Minh, M.-L., Sousa, P., Maillet, M., Allez, M., and Gornet, J.-M. (2017). Hepatic complications induced by immunosuppressants and biologics in inflammatory bowel disease. *WJH* 9, 613. 10.4254/wjh.v9.i13.613.
418. Sumithran, P., and Proietto, J. (2008). Ketogenic diets for weight loss: A review of their principles, safety and efficacy. *Obesity Research & Clinical Practice* 2, 1–13. 10.1016/j.orcp.2007.11.003.
419. Varady, K.A., Cienfuegos, S., Ezpeleta, M., and Gabel, K. (2022). Clinical application of intermittent fasting for weight loss: progress and future directions. *Nat Rev Endocrinol* 18, 309–321. 10.1038/s41574-022-00638-x.
420. Shai, I., Schwarzfuchs, D., Henkin, Y., Shahar, D.R., Witkow, S., Greenberg, I., Golan, R., Fraser, D., Bolotin, A., Vardi, H., et al. (2008). Weight Loss with

- a Low-Carbohydrate, Mediterranean, or Low-Fat Diet. *N Engl J Med* 359, 229–241. 10.1056/NEJMoa0708681.
421. Widmer, R.J., Flammer, A.J., Lerman, L.O., and Lerman, A. (2015). The Mediterranean Diet, its Components, and Cardiovascular Disease. *The American Journal of Medicine* 128, 229–238. 10.1016/j.amjmed.2014.10.014.
422. Richard, C., Couture, P., Desroches, S., and Lamarche, B. (2013). Effect of the mediterranean diet with and without weight loss on markers of inflammation in men with metabolic syndrome: Effect of the MedDiet with and Without WL. *Obesity* 21, 51–57. 10.1002/oby.20239.
423. Huo, R., Du, T., Xu, Y., Xu, W., Chen, X., Sun, K., and Yu, X. (2015). Effects of Mediterranean-style diet on glycemic control, weight loss and cardiovascular risk factors among type 2 diabetes individuals: a meta-analysis. *Eur J Clin Nutr* 69, 1200–1208. 10.1038/ejcn.2014.243.
424. Baur, J.A., Pearson, K.J., Price, N.L., Jamieson, H.A., Lerin, C., Kalra, A., Prabhu, V.V., Allard, J.S., Lopez-Lluch, G., Lewis, K., et al. (2006). Resveratrol improves health and survival of mice on a high-calorie diet. *Nature* 444, 337–342. 10.1038/nature05354.
425. Timmers, S., Konings, E., Bilet, L., Houtkooper, R.H., van de Weijer, T., Goossens, G.H., Hoeks, J., van der Krieken, S., Ryu, D., Kersten, S., et al. (2011). Calorie Restriction-like Effects of 30 Days of Resveratrol Supplementation on Energy Metabolism and Metabolic Profile in Obese Humans. *Cell Metabolism* 14, 612–622. 10.1016/j.cmet.2011.10.002.
426. Burgess, E., Hassmén, P., and Pumpa, K.L. (2017). Determinants of adherence to lifestyle intervention in adults with obesity: a systematic review: Adherence to lifestyle intervention in obesity. *Clin Obes* 7, 123–135. 10.1111/cob.12183.
427. Lozano, A.M., Lipsman, N., Bergman, H., Brown, P., Chabardes, S., Chang, J.W., Matthews, K., McIntyre, C.C., Schlaepfer, T.E., Schulder, M., et al. (2019). Deep brain stimulation: current challenges and future directions. *Nat Rev Neurol* 15, 148–160. 10.1038/s41582-018-0128-2.
428. Formolo, D.A., Gaspar, J.M., Melo, H.M., Eichwald, T., Zepeda, R.J., Latini, A., Okun, M.S., and Walz, R. (2019). Deep Brain Stimulation for Obesity: A Review and Future Directions. *Front. Neurosci.* 13, 323. 10.3389/fnins.2019.00323.
429. Shivacharan, R.S., Rolle, C.E., Barbosa, D.A.N., Cunningham, T.N., Feng, A., Johnson, N.D., Safer, D.L., Bohon, C., Keller, C., Buch, V.P., et al.

- (2022). Pilot study of responsive nucleus accumbens deep brain stimulation for loss-of-control eating. *Nat Med* 28, 1791–1796. 10.1038/s41591-022-01941-w.
430. Contreras López, W.O., Navarro, P.A., and Crispín, S. (2022). Effectiveness of Deep Brain Stimulation in Reducing Body Mass Index and Weight: A Systematic Review. *Stereotact Funct Neurosurg* 100, 75–85. 10.1159/000519158.
431. Magro, D.O., Geloneze, B., Delfini, R., Pareja, B.C., Callejas, F., and Pareja, J.C. (2008). Long-term Weight Regain after Gastric Bypass: A 5-year Prospective Study. *OBES SURG* 18, 648–651. 10.1007/s11695-007-9265-1.
432. Zhao, Z., Ukidve, A., Kim, J., and Mitragotri, S. (2020). Targeting Strategies for Tissue-Specific Drug Delivery. *Cell* 181, 151–167. 10.1016/j.cell.2020.02.001.
433. Hajal, C., Offeddu, G.S., Shin, Y., Zhang, S., Morozova, O., Hickman, D., Knutson, C.G., and Kamm, R.D. (2022). Engineered human blood–brain barrier microfluidic model for vascular permeability analyses. *Nat Protoc* 17, 95–128. 10.1038/s41596-021-00635-w.
434. Speakman, J.R. (2019). Use of high-fat diets to study rodent obesity as a model of human obesity. *Int J Obes* 43, 1491–1492. 10.1038/s41366-019-0363-7.
435. Moussavi, N., Gavino, V., and Receveur, O. (2008). Could the Quality of Dietary Fat, and Not Just Its Quantity, Be Related to Risk of Obesity? *Obesity* 16, 7–15. 10.1038/oby.2007.14.
436. Cintra, D.E., Ropelle, E.R., Moraes, J.C., Pauli, J.R., Morari, J., De Souza, C.T., Grimaldi, R., Stahl, M., Carnevalheira, J.B., Saad, M.J., et al. (2012). Unsaturated Fatty Acids Revert Diet-Induced Hypothalamic Inflammation in Obesity. *PLoS ONE* 7, e30571. 10.1371/journal.pone.0030571.
437. Buettner, R., Schölmerich, J., and Bollheimer, L.C. (2007). High-fat Diets: Modeling the Metabolic Disorders of Human Obesity in Rodents*. *Obesity* 15, 798–808. 10.1038/oby.2007.608.
438. Hintze, K.J., Benninghoff, A.D., Cho, C.E., and Ward, R.E. (2018). Modeling the Western Diet for Preclinical Investigations. *Advances in Nutrition* 9, 263–271. 10.1093/advances/nmy002.
439. Jais, A., Solas, M., Backes, H., Chaurasia, B., Kleinridders, A., Theurich, S., Mauer, J., Steculorum, S.M., Hampel, B., Goldau, J., et al. (2016). Myeloid-

Cell-Derived VEGF Maintains Brain Glucose Uptake and Limits Cognitive Impairment in Obesity. *Cell* 165, 882–895. 10.1016/j.cell.2016.03.033.

440. Wolfenden, L., Ezzati, M., Larijani, B., and Dietz, W. (2019). The challenge for global health systems in preventing and managing obesity. *Obesity Reviews* 20, 185–193. 10.1111/obr.12872.
441. Dhurandhar, E.J. (2016). The food-insecurity obesity paradox: A resource scarcity hypothesis. *Physiology & Behavior* 162, 88–92. 10.1016/j.physbeh.2016.04.025.
442. Hawkes, C., Smith, T.G., Jewell, J., Wardle, J., Hammond, R.A., Friel, S., Thow, A.M., and Kain, J. (2015). Smart food policies for obesity prevention. *The Lancet* 385, 2410–2421. 10.1016/S0140-6736(14)61745-1.

Appendices

7.1. Supplementary material for Chapter 2

Supplementary Table 7.1. Statistics for Figures 2.1 – 2.10

Note that weeks indicated are the age of mice unless stated otherwise.

Figure	Statistical test	P value	F, t, r ²
Figure 2.1			
2.1A	2way RM	Time: <0.0001	Time: F(2.143, 62.15) = 547.8
	ANOVA	%Fat diet: <0.0001 Interaction: <0.0001	%Fat diet: F(3, 29) = 18.74 Interaction: F(36, 348) = 12.90
2.1B	2way RM	Time: <0.0001	Time: F(7.306, 216.7) = 11.55
	ANOVA	%Fat diet: <0.0001 Interaction: 0.0042	%Fat diet: F(3, 356) = 25.20 Interaction: F(36, 356) = 1.800
2.1C	2way RM	Time: 0.1263	Time: F(5.157, 249.5) = 1.741
	ANOVA	%Fat diet: <0.0001 Interaction: 0.0005	%Fat diet: F(3, 29) = 18.45 Interaction: F(33, 319) = 2.115
2.1D	2way RM	Time: <0.0001	Time: F(7.871, 233.5) = 13.05
	ANOVA	%Fat diet: <0.0001 Interaction: 0.0194	%Fat diet: F(3, 356) = 13.41 Interaction: F(36, 356) = 1.592
2.1E	1way ANOVA	0.0007	F(3, 13) = 11.18
2.1F	1way ANOVA	0.0002	F(3, 13) = 14.83
2.1G	1way ANOVA	0.0040	F(3, 13) = 7.353

2.1H	1way ANOVA	0.5645	F(3, 12) = 0.7098
2.1I	1way ANOVA	0.0586	F(3, 13) = 3.208
2.1J	1way ANOVA	0.1360	F(3, 13) = 2.208
2.1K	Kruskal-Wallis test	0.1393	N/A
2.1L	1way ANOVA	0.1684	F(3, 13) = 1.969
Figure 2.2			
2.2A	2way RM ANOVA (weeks 4-7.5)	Time: <0.0001 Diet: 0.0819 Interaction: 0.0401	Time: F(6, 102) = 83.04 Diet: F(1, 17) = 3.418 Interaction: F(6, 102) = 2.299
	2way RM ANOVA (weeks 8-23)	Time: <0.0001 Diet: <0.0001 Interaction: <0.0001	Time: F(31, 763) = 510.8 Diet: F(2, 25) = 28.75 Interaction: F(62, 763) = 53.81
	2way RM ANOVA (weeks 24-28)	Time: <0.0001 Diet: <0.0001 Interaction: 0.6044	Time: F(11, 179) = 31.36 Diet: F(1, 17) = 58.84 Interaction: F(11, 179) = 0.8359
2.2B	2way RM ANOVA (weeks 5-8)	Time: <0.0001 Diet: 0.0484 Interaction: 0.9309	Time: F(3, 51) = 12.77 Diet: F(1, 17) = 4.522 Interaction: F(3, 51) = 0.1474
	2way RM ANOVA (weeks 9-23)	Time: <0.0001 Diet: <0.0001 Interaction: <0.0001	Time: F(14, 347) = 6.284 Diet: F(2, 25) = 70.81 Interaction: F(28, 347) = 2.787

	2way RM ANOVA (weeks 24-28)	Time: 0.0377 Diet: 0.9963 Interaction: 0.0239	Time: $F(4, 65) = 2.708$ Diet: $F(1, 17) = 0.001834$ Interaction: $F(4, 65) = 3.021$
2.2C	2way RM ANOVA (weeks 5-8)	Time: 0.4120 Diet: 0.9136 Interaction: 0.9301	Time: $F(3, 15) = 1.019$ Diet: $F(1, 5) = 0.01301$ Interaction: $F(3, 15) = 0.1469$
	2way RM ANOVA (weeks 9-23)	Time: 0.2651 Diet: 0.0374 Interaction: 0.2459	Time: $F(13, 166) = 1.226$ Diet: $F(2, 13) = 4.275$ Interaction: $F(26, 166) = 1.197$
	2way RM ANOVA (weeks 24-28)	Time: 0.5747 Diet: 0.3210 Interaction: 0.6809	Time: $F(4, 20) = 0.7417$ Diet: $F(1, 5) = 1.212$ Interaction: $F(4, 20) = 0.5795$
2.2D	2way RM ANOVA (weeks 5-8)	Time: <0.0001 Diet: 0.0461 Interaction: 0.9305	Time: $F(3, 51) = 11.05$ Diet: $F(1, 17) = 4.628$ Interaction: $F(3, 51) = 0.1480$
	2way RM ANOVA (weeks 9-23)	Time: <0.0001 Diet: <0.0001 Interaction: 0.0003	Time: $F(14, 341) = 5.278$ Diet: $F(2, 25) = 53.95$ Interaction: $F(28, 341) = 2.279$
	2way RM ANOVA (weeks 24-28)	Time: 0.0579 Diet: 0.8216 Interaction: 0.0350	Time: $F(4, 65) = 2.412$ Diet: $F(1, 17) = 0.05241$ Interaction: $F(4, 65) = 2.758$

2.2E	2way RM ANOVA (weeks 4-26)	Time: <0.0001 Diet: <0.0001 Interaction: <0.0001	Time: F(3.301, 92.35) = 996.6 Diet: F(3, 28) = 47.52 Interaction: F(129, 1203) = 47.43
	2way RM ANOVA (weeks 27-30)	Time: <0.0001 Diet: <0.0001 Interaction: 0.0013	Time: F(2.825, 62.16) = 22.57 Diet: F(2, 22) = 58.01 Interaction: F(16, 176) = 2.584
2.2F	2way RM ANOVA (weeks 5-26)	Time: <0.0001 Diet: <0.0001 Interaction: <0.0001	Time: F(7.109, 218.4) = 19.61 Diet: F(3, 645) = 38.98 Interaction: F(63, 645) = 6.764
	2way RM ANOVA (weeks 27-30)	Time: 0.7128 Diet: 0.2104 Interaction: 0.1158	Time: F(2.261, 72.34) = 0.3769 Diet: F(2, 96) = 1.584 Interaction: F(6, 96) = 1.759
2.2G	2way RM ANOVA (weeks 5-26)	Time: <0.0001 Diet: 0.0860 Interaction: <0.0001	Time: F(4.160, 40.56) = 11.26 Diet: F(3, 12) = 2.790 Interaction: (60, 195) = 4.692
	2way RM ANOVA (weeks 27-30)	Time: 0.2830 Diet: 0.0561 Interaction: 0.5990	Time: F(1.814, 15.12) = 1.364 Diet: F(2, 9) = 4.037 Interaction: F(6, 25) = 0.7723
2.2H	2way RM ANOVA (weeks 5-26)	Time: <0.0001 Diet: <0.0001 Interaction: <0.0001	Time: F(7.671, 263.1) = 19.91 Diet: F(3, 686) = 20.52 Interaction: F(60, 686) = 4.090

	2way RM ANOVA (weeks 27-30)	Time: 0.3223 Diet: 0.0867 Interaction: 0.1373	Time: $F(2.534, 76.64) = 1.172$ Diet: $F(2, 121) = 2.496$ Interaction: $F(8, 121) = 1.581$
2.2I	1way ANOVA	<0.0001	$F(7, 64) = 24.81$
2.2J	2way ANOVA	Age: <0.0001 Diet: 0.0014 Interaction: 0.5756	$F(1, 36) = 22.95$ Diet: $F(1, 36) = 11.96$ Interaction: $F(1, 36) = 0.3192$
2.2K	2way ANOVA	Age: <0.0001 Diet: 0.0125 Interaction: <0.0001	Age: $F(1, 59) = 76.74$ Diet: $F(2, 59) = 4.729$ Interaction: $F(2, 59) = 15.86$
Figure 2.3			
2.3A	Unpaired t-test	0.0117	$t = 2.750$
2.3B	Welch's t-test	0.0009	$t = 4.597$
2.3C	Unpaired t-test	0.1025	$t = 1.704$
Figure 2.4			
2.4A	2way RM ANOVA	Time: <0.0001 Diet: 0.0316 Interaction: 0.0002	Time: $F(2.780, 16.68) = 165.8$ Diet: $F(2, 6) = 6.489$ Interaction: $F(12, 36) = 4.494$
2.4B	1way ANOVA	0.7107	$F = 0.3566$
Figure 2.5			
2.5A	2way RM ANOVA	Time: <0.0001 Diet: 0.0001	Time: $F(2.457, 76.16) = 259.3$ Diet: $F(3, 31) = 9.400$

	(weeks 4-16)	Interaction: <0.0001	Interaction: F(66, 682) = 17.41
	2way RM ANOVA (weeks 16.43-32)	Time: <0.0001 Diet: <0.0001 Interaction: <0.0001	Time: F(2.999, 48.57) = 66.99 Diet: F(1, 17) = 44.76 Interaction: F(31, 502) = 20.43
2.5B	2way RM ANOVA (weeks 5-17)	Time: <0.0001 Diet: <0.0001 Interaction: <0.0001	Time: F(6.613, 205) = 29.01 Diet: F(3, 31) = 13.40 Interaction: F(33, 341) = 7.529
	2way RM ANOVA (weeks 18-32)	Time: <0.0001 Diet: 0.3173 Interaction: <0.0001	Time: F(4.870, 80.70) = 11.63 Diet: F(1, 17) = 1.061 Interaction: F(14, 232) = 9.816
2.5C	2way RM ANOVA (weeks 5-17)	Time: 0.0691 Diet: 0.0223 Interaction: <0.0001	Time: F(3.191, 31.91) = 2.560 Diet: F(3, 10) = 5.026 Interaction: F(33, 110) = 5.863
	2way RM ANOVA (weeks 18-32)	Time: 0.0070 Diet: 0.2552 Interaction: <0.0001	Time: F(3.102, 15.51) = 5.789 Diet: F(1, 5) = 1.650 Interaction: F(13, 65) = 7.416
2.5D	2way RM ANOVA (weeks 5-17)	Time: <0.0001 Diet: <0.0001 Interaction: <0.0001	Time: F(6.338, 196.5) = 29.08 Diet: F(3, 31) = 19.56 Interaction: F(33, 341) = 11.42
	2way RM ANOVA	Time: <0.0001 Diet: 0.0523	Time: F(5.301, 94.19) = 12.22 Diet: (1, 231) = 3.805

	(weeks 18-32)	Interaction: <0.0001	Interaction: F(13, 231) = 14.75
2.5E	1way ANOVA	0.0553	F = 3.359
2.5F	1way ANOVA	0.0091	F = 9.889
2.5G	1way ANOVA	0.4293	F = 0.8824
2.5H	Simple linear regression	0.0111	R ² = 0.2698
Figure 2.6			
2.6A	2way RM ANOVA (weeks 4-16)	Time: <0.0001 Diet: <0.0001 Interaction: <0.0001	Time: F(3.2, 113.1) = 498.6 Diet: F(3, 39) = 43.33 Interaction: F(72, 848) = 37.47
	2way RM ANOVA (weeks 16.43 – 32)	Time: <0.0001 Diet: <0.0001 Interaction: <0.0001	Time: F(2.488, 56.59) = 123.6 Diet: F(2, 24) = 50.87 Interaction: F(62, 705) = 19.65
2.6B	2way RM ANOVA (weeks 5-16)	Time: <0.0001 Diet: <0.0001 Interaction: <0.0001	Time: F(5.993, 232.6) = 35.51 Diet: F(3, 427) = 36.59 Interaction: F(33, 427) = 11.67
	2way RM ANOVA (weeks 17-32)	Time: <0.0001 Diet: 0.2371 Interaction: <0.0001	Time: F(4.765, 111.5) = 20.40 Diet: F(2, 24) = 1.529 Interaction: F(30, 351) = 10.47
2.6C	2way RM ANOVA	Time: 0.0119 Diet: 0.9532	Time: F(3.146, 31.46) = 4.214 Diet: F(3, 14) = 0.1093

	(weeks 5-16)	Interaction: <0.0001	Interaction: $F(33, 110) = 7.580$
	2way RM ANOVA (weeks 17-32)	Time: <0.0001 Diet: 0.9290 Interaction: <0.0001	Time: $F(3.927, 35.04) = 26.16$ Diet: $F(2, 9) = 0.07424$ Interaction: $F(26, 116) = 18.99$
2.6D	2way RM ANOVA (weeks 5-16)	Time: <0.0001 Diet: <0.0001 Interaction: <0.0001	Time: $F(5.331, 184.2) = 33.32$ Diet: $F(3, 380) = 25.04$ Interaction: $F(33, 380) = 10.59$
	2way RM ANOVA (weeks 17-32)	Time: <0.0001 Diet: 0.4610 Interaction: <0.0001	Time: $F(4.430, 112.8) = 22.81$ Diet: $F(2, 26) = 0.7979$ Interaction: $F(26, 331) = 11.26$
2.6E	1way ANOVA	0.0029	$F = 7.244$
2.6F	1way ANOVA	0.0137	$F = 6.497$
2.6G	1way ANOVA	0.0002	$F = 11.47$
2.6H	Simple linear regression	0.5229	$R^2 = 0.01228$
Figure 2.7			
2.7A	Simple linear regression 45FD vs. WD	0.0432	$F(1, 50) = 4.304$
2.7B	Simple linear regression	0.9301	$F(1, 21) = 0.007875$

	45FD vs. WD (8w feeding)		
2.7C	Simple linear regression 45FD vs. WD (24w feeding)	0.0051	F(1, 12) = 11.65
Figure 2.8			
2.8A	2way RM ANOVA	Time: <0.0001 Diet: <0.0001 Interaction: <0.0001	Time: F(56, 1424) = 398.9 Diet: F(2, 26) = 26.01 Interaction: F(112, 1424) = 18.63
2.8B	2way RM ANOVA	Time: <0.0001 Diet: 0.0760 Interaction: <0.0001	Time: F(27, 692) = 34.82 Diet: F(2, 26) = 2.850 Interaction: F(54, 692) = 12.11
2.8C	2way RM ANOVA	Time: <0.0001 Diet: 0.1892 Interaction: <0.0001	Time: F(25, 200) = 8.157 Diet: F(2, 8) = 2.065 Interaction: F(50, 200) = 4.452
2.8D	2way RM ANOVA	Time: <0.0001 Diet: 0.0265 Interaction: <0.0001	Time: F(25, 643) = 30.39 Diet: F(2, 26) = 4.187 Interaction: F(50, 643) = 13.52
2.8E	2way RM ANOVA	Time: <0.0001 Diet: <0.0001 Interaction: <0.0001	Time: F(56, 1801) = 970.1 Diet: F(2, 33) = 81.97 Interaction: F(112, 1801) = 45.35

2.8F	2way RM ANOVA	Time: <0.0001 Diet: <0.0001 Interaction: <0.0001	Time: F(8.638, 247.3) = 39.52 Diet: F(2, 29) = 14.04 Interaction: F(54, 773) = 17.83
2.8G	2way RM ANOVA	Time: <0.0001 Diet: 0.5771 Interaction: <0.0001	Time: F(5.794, 57.94) = 10.43 Diet: F(2, 10) = 0.2733 Interaction: F(50, 250) = 9.695
2.8H	2way RM ANOVA	Time: <0.0001 Diet: <0.0001 Interaction: <0.0001	Time: F(9.747, 352.1) = 40.33 Diet: F(2, 903) = 15.55 Interaction: F(50, 903) = 20.52
Figure 2.9			
2.9A	2way RM ANOVA	Time: <0.0001 Switch: 0.4568 Interaction: 0.0043	Time: F(3, 81) = 38.66 Switch: F(2, 27) = 0.8067 Interaction: F(6, 81) = 3.461
2.9B	2way RM ANOVA	Time: 0.0413 Switch: 0.0448 Interaction: 0.2946	Time: F(3, 27) = 3.148 Switch: F(2, 9) = 4.471 Interaction: F(6, 27) = 1.291
2.9C	2way RM ANOVA	Time: <0.0001 Switch: 0.0964 Interaction: 0.0009	Time: F(3, 81) = 22.93 Switch: F(2, 27) = 2.555 Interaction: F(6, 81) = 4.273
2.9D	2way RM ANOVA	Time: <0.0001 Switch: 0.0661 Interaction: 0.0695	Time: F(4, 108) = 59.97 Switch: F(2, 27) = 3.009 Interaction: F(8, 108) = 1.886

2.9E	2way RM ANOVA	Time: <0.0001 Switch: 0.3060 Interaction: 0.2942	Time: F(2.149, 19.34) = 53.06 Switch: F(2, 9) = 1.354 Interaction: F(8, 36) = 1.261
2.9F	2way RM ANOVA	Time: <0.0001 Switch: 0.5406 Interaction: 0.1082	Time: F(1.575, 42.52) = 44.95 Switch: F(2, 27) = 0.9402 Interaction: F(8, 108) = 1.693
2.9G	2way RM ANOVA	Time: <0.0001 Switch: 0.0033 Interaction: 0.0001	Time: F(1.599, 71.97) = 76.02 Switch: F(2, 45) = 6.523 Interaction: (4, 90) = 6.359
2.9H	2way RM ANOVA	Time: <0.0001 Switch: 0.0085 Interaction: 0.0002	Time: F(1.812, 27.18) = 20.64 Switch: F(2, 15) = 6.663 Interaction: F(6, 45) = 5.686
2.9I	2way RM ANOVA	Time: <0.0001 Switch: <0.0001 Interaction: <0.0001	Time: F(2.321, 104.5) = 46.42 Switch: F(2, 45) = 25.77 Interaction: F(6, 135) = 6.641
2.9J	2way RM ANOVA	Time: <0.0001 Switch: 0.0007 Interaction: <0.0001	Time: F(3.058, 137.6) = 65.76 Switch: F(2, 45) = 8.484 Interaction: F(8, 180) = 7.012
2.9K	2way RM ANOVA	Time: <0.0001 Switch: 0.2167 Interaction: <0.0001	Time: F(3.069, 44.50) = 62.28 Switch: F(2, 15) = 1.696 Interaction: F(8, 58) = 6.998

2.9L	2way RM ANOVA	Time: <0.0001 Switch: <0.0001 Interaction: <0.0001	Time: F(2.693, 121.2) = 92.11 Switch: F(2, 45) = 13.26 Interaction: F(8, 180) = 13.39
Figure 2.10			
2.10A	3way RM ANOVA	Pre vs post BW: <0.0001 HFD: 0.1896 Type of dieting: 0.0278 Pre vs post BW x HFD: 0.0008 Pre vs post BW x Type of dieting: 0.5961 Type of dieting x HFD: 0.6373 Pre vs post BW x HFD x Type of dieting: 0.7675	Pre vs post BW: F(1, 37) = 206.9 HFD: F(1, 37) = 1.786 Type of dieting: F(1, 37) = 5.243 Pre vs post BW x HFD: F(1, 37) = 13.30 Pre vs post BW x Type of dieting: F(1, 37) = 0.2858 Type of dieting x HFD: F(1, 37) = 0.2260 Pre vs post BW x HFD x Type of dieting: F(1, 37) = 0.08869
2.10B	2way ANOVA	HFD: 0.0008 Type of dieting: 0.5961 Interaction: 0.7675	HFD: F(1, 37) = 13.30 Type of dieting: F(1, 37) = 0.2858 Interaction: F(1, 37) = 0.08869
2.10C	2way ANOVA	HFD: <0.0001 Type of dieting: 0.2251	HFD: F(1, 39) = 29.87 Type of dieting: F(1, 39) = 1.519

		Interaction: 0.0056	Interaction: $F(1, 39) = 8.616$
2.10D	2way ANOVA	HFD: 0.9709 Type of dieting: 0.0114 Interaction: 0.8030	HFD: $F(1, 39) = 0.001350$ Type of dieting: $F(1, 39) = 7.048$ Interaction: $F(1, 39) = 0.06310$
2.10E	2way ANOVA	HFD: 0.4026 Type of dieting: 0.0617 Interaction: 0.0719	HFD: $F(1, 38) = 0.7165$ Type of dieting: $F(1, 38) = 3.708$ Interaction: $F(1, 38) = 3.428$
2.10F	2way ANOVA	HFD: 0.0676 Type of dieting: 0.0009 Interaction: 0.2385	HFD: $F(1, 39) = 3.533$ Type of dieting: $F(1, 39) = 12.92$ Interaction: $F(1, 39) = 1.433$
2.10G	2way ANOVA	HFD: 0.1835 Type of dieting: 0.7651 Interaction: 0.4871	HFD: $F(1, 39) = 1.834$ Type of dieting: $F(1, 39) = 0.09052$ Interaction: $F(1, 39) = 0.4923$
2.10H	2way ANOVA	HFD: 0.9292 Type of dieting: 0.2317 Interaction: 0.4631	HFD: $F(1, 39) = 0.007998$ Type of dieting: $F(1, 39) = 1.476$ Interaction: $F(1, 39) = 0.5492$

7.2. Supplementary material for Chapter 3

Supplementary Table 7.2. Statistics for Figures 3.2 – 3.16

Figure	Sample size cells (n)/animals (N)	Test	p value	F, t
Figure 3.2				
3.2B	1C n/N = 33/19 1W n/N = 21/14 2C n/N = 34/3 2W n/N = 46/5 4C n/N = 18/9	2way ANOVA	Diet: <0.0001 Time: 0.3200 Interaction: <0.0001	diet: F(1,246)=29.12 time: F(3,246)=1.175 interaction: F(3,246)=7.349
3.2C	4W n/N = 19/10 11C n/N = 37/13 11W n/N = 46/16	2way ANOVA	Diet: 0.0010 Time: <0.0001 Interaction: 0.1208	Diet: F(1,246)=11.11 Time: F(3,246)=10.31 Interaction: F(3,246)=1.959
3.2D		2way ANOVA	Diet: 0.0002 Time: <0.0001 Interaction: 0.0208	Diet: F(1,246)=14.64 Time: F(3,246)=9.190 Interaction: F(3,246)=3.309
3.2E	4C n/N = 18/9 4W n/N = 19/10 8C n/N = 28/5 4W/4C n/N = 36/7	1way ANOVA	<0.0001	F(3,97)=10.40
3.2F	Rat chow n/N = 43/17 Rat WD n/N = 46/16 Rat HFMS n/N = 10/6 Mouse chow n/N = 21/10 Mouse WD n/N = 22/12 Mouse LFHS n/N = 8/6	1way ANOVA	Rats: <0.0001 Mice: 0.0478	Rats: F(2,96)=20.84 Mice: F(2,48)=3.242
3.2G	Rat chow n/N = 39/13	1way ANOVA	Rats: 0.9095	Rats: F(2,62)=0.09503

	Rat WD n/N = 13/5 Rat HFHS n/N = 13/4 Mouse chow n/N = 25/9 Mouse WD n/N = 30/13 Mouse LFHS n/N = 5/2		Mice: 0.8013	Mice: F(2,56)=0.2224
--	--	--	--------------	----------------------

Figure 3.3

3.3A	1 week Chow n/N = 33/19 1 week WD n/N = 21/14	2way RM ANOVA	Diet: 0.7500 Driving current: <0.0001 Interaction: 0.8540	Diet: F(1,52)=0.1026 Driving current: F(3,156)=496.8 Interaction: F(3,156)=0.2601
	2 week Chow n/N = 34/3 2 week WD n/N = 46/5	2way RM ANOVA	Diet: 0.1271 Driving current: <0.0001 Interaction: 0.1931	Diet: F(1,78)=2.379 Driving current: F(3,234)=839.9 Interaction: F(3,234)=1.588
	4 week Chow n/N = 18/9 4 week WD n/N = 19/10	2way RM ANOVA	Diet: 0.0050 Driving current: <0.0001 Interaction: 0.5041	Diet: F(1,35)=8.978 Driving current: F(3,105)=286.8 Interaction: F(3,105)=0.7864
	11 week Chow n/N = 37/13 11 week WD n/N = 46/16	2way RM ANOVA	Diet: 0.0314 Driving current: <0.0001 Interaction: 0.2042	Diet: F(1,81)=4.797 Driving current: F(3,243)=101.7 Interaction: F(3,243)=1.542
3.3B	1 week Chow n/N = 33/19 1 week WD n/N = 21/14	2way RM ANOVA	Diet: 0.7656 Driving current: <0.0001 Interaction: 0.8887	Diet: F(1,52)=0.08980 Driving current: F(3,156)=73.92 Interaction: F(3,156)=0.2110

	2 week Chow n/N = 34/3 2 week WD n/N = 46/5	2way RM ANOVA	Diet: 0.1646 Driving current: <0.0001 Interaction: <0.0001	Diet: F(1,78)=1.968 Driving current: F(3,234)=263.2 Interaction: F(3,234)=14.99
	4 week Chow n/N = 18/9 4 week WD n/N = 19/10	2way RM ANOVA	Diet: 0.0009 Driving current: <0.0001 Interaction: 0.0057	Diet: F(1,35)=13.19 Driving current: F(3,105)=86.86 Interaction: F(3,105)=4.422
	11 week Chow n/N = 37/13 11 week WD n/N = 46/16	2way RM ANOVA	Diet: 0.0007 Driving current: <0.0001 Interaction: 0.0003	Diet: F(1,81)=12.47 Driving current: F(3,243)=211.3 Interaction: F(3,243)=6.443

Figure 3.4

3.4B	Chow n/N = 16/8 WD n/N = 18/9	Two-tailed unpaired t- test	0.0401	t=2.140; df=32
3.4C		Two-tailed unpaired t- test	0.9309	t=0.08741; df=32
3.4D		Two-tailed unpaired t- test	0.1409	t=1.510; df=32
3.4E		Two-tailed unpaired t- test	0.8695	t=0.1656; df=32
3.4F		Two-tailed unpaired t- test	0.1119	t=1.635; df=32
3.4G		Two-tailed unpaired t- test	0.3519	t=0.9446; df=32

Figure 3.5

3.5A	Chow N = 20 WD N = 25	2way RM ANOVA	Diet: <0.0001	Diet: F(1,43)=35.68
-------------	--------------------------	------------------	------------------	---------------------

			Time: <0.0001 Interaction: <0.0001	Time: F(11,473)=5232 Interaction: F(11,473)=41.68
3.5B	Chow N = 20 WD N = 23	2way RM ANOVA	Diet: <0.0001 Time: <0.0001 Interaction: 0.0117	Diet: F(1,41)=103.0 Time: F(2.180,89.38)=240.8 Interaction: F(10,410)=2.317
3.5C	Chow N = 5 HFMS N = 5	2way RM ANOVA	Diet: 0.0223 Time: <0.0001 Interaction: <0.0001	Diet: F(1,8)=7.979 Time: F(8,64)=627.6 Interaction: F(8,64)=7.653
3.5D	Chow N = 5 HFMS N = 4	2way RM ANOVA	Diet: 0.0053 Time: <0.0001 Interaction: <0.0001	Diet: F(1,7)=15.91 Time: F(6,42)=12.07 Interaction: F(6,42)=7.803
3.5E	Chow N =11 LFHS N = 7 WD N =15	2way RM ANOVA	Diet: <0.0001 Time: <0.0001 Interaction: <0.0001	Diet: F(2,30)=136.9 Time: F(12,360)=669.8 Interaction: F(24,360)=80.75
3.5F	Chow N =3 LFHS N = 2 WD N = 4	2way RM ANOVA	Diet: 0.0005 Time: 0.0196 Interaction: 0.0080	Diet: F(2,6)=34.98 Time: F(11,66)=2.284 Interaction: F(22,66)=2.178

Figure 3.6

3.6A	TTX chow n/N = 30/4 TTX WD n/N = 33/3 Syn block chow n/N = 4/3 Syn block WD n/N = 8/4	2way ANOVA	Diet: <0.0001 Treatment: 0.1084 Interaction: 0.0037	Diet: F(1,66)=39.10 Treatment: F(1,66)=2.649 Interaction: F(1,66)=9.076
3.6C	Chow n/N = 6/3 WD n/N = 8/4	2way RM ANOVA	Diet: 0.1670 Ouabain: <0.0001	Diet: F(1,12)=2.165 Ouabain: F(1,12)=140.8

			Interaction: 0.0045	Interaction: F(1,12)=12.16
3.6D	Untreated chow n/N = 6/3 Untreated WD n/N = 8/4 Syn block chow n/N = 4/3 Syn block WD n/N = 8/4	2way ANOVA	Diet: 0.0002 Treatment: 0.5513 Interaction: 0.5638	Diet: F(1,22)=19.16 Treatment: F(1,22)=0.3662 Interaction: F(1,22)=0.3434
3.6E	Chow n/N = 5/3 WD n/N = 8/3	2way RM ANOVA	Diet: 0.0156 Holding potential: 0.3262 Interaction: 0.7159	Diet: F(1,11)=8.167 Holding potential: F(3,33)=1.197 Interaction: F(3,33)=0.4544
3.6F	Chow n/N = 11/4 WD n/N = 10/5	2way RM ANOVA	Diet: 0.0937 Ext-free K+: <0.0001 Interaction: 0.0014	Diet: F(1,19)=3.114 Ext-free K+: F(1,19)=88.98 Interaction: F(1,19)=13.86
3.6G		Two-tailed unpaired t- test	0.0014	t=3.723; df=19
3.6H	10 mM Na chow n/N = 18/9 10 mM Na WD n/N = 19/10 40 mM Na chow n/N = 15/5 40 mM Na WD n/N = 13/7	2way ANOVA	Diet: 0.0041 [Na+]i: <0.0001 Interaction: 0.3483	Diet: F(1,61)=8.909 [Na+]i: F(1,61)=33.78 Interaction: F(1,61)=0.8933

Figure 3.7

3.7A	Chow n/N = 71/26 WD n/N = 63/27	Two-tailed unpaired t- test	0.4689	t=0.7264; df=132
-------------	--	-----------------------------------	--------	------------------

3.7B	Chow n/N = 71/26	Least squares linear regression	0.8946	r ² =0.0002358
3.7C	WD n/N = 63/27	Least squares linear regression	0.7048	r ² =0.001677
3.7D	Chow n/N = 5/3	2way RM ANOVA	Treatment: 0.0001 Holding potential: <0.0001 Interaction: 0.4844	Treatment: F(1,8)=46.82 Holding potential: F(3,24)=36.40 Interaction: F(3,24)=0.8418
3.7E	WD n/N = 8/3	2way RM ANOVA	Treatment: 0.0107 Holding potential: <0.0001 Interaction: 0.9762	Treatment: F(1,14)=8.650 Holding potential: F(3,42)=49.53 Interaction: F(3,42)=0.06890
3.7F	10 mM Na chow n/N = 18/9 10 mM Na WD n/N = 19/10 40 mM Na chow n/N = 15/5 40 mM Na WD n/N = 13/7	2way RM ANOVA	Treatment: <0.0001 Driving current: <0.0001 Interaction: 0.0423	Treatment: F(3,61)=8.984 Driving current: F(3,183)=396.2 Interaction: F(9,183)=1.993

Figure 3.8

3.8B	Untreated Ctrl n/N = 29/8 10 ⁻¹¹ n/N = 21/3 10 ⁻¹⁰ n/N = 40/11 10 ⁻⁹ n/N = 26/6 10 ⁻⁸ n/N = 7/2 10 ⁻⁶ n/N = 11/2	1way ANOVA	<0.0001	F(7,153)=15.63
-------------	--	------------	---------	----------------

	10 ⁻⁵ n/N = 18/4 10 ⁻⁴ n/N = 9/3			
3.8C	Untreated n/N = 14/5 +10 μ M PGE2 n/N = 18/4 +EP1 antag n/N = 25/4 +EP2 antag n/N = 17/4 +EP3 antag n/N = 15/3 +EP4 antag n/N = 17/3	1way ANOVA	<0.0001	F(5,100)=8.517
3.8D	Untreated n/N = 14/5 10 μ M PGE2 n/N = 18/4 +EP3 antag n/N = 15/3	2way RM ANOVA	Treatment: 0.0363 Driving current: <0.0001 Interaction: 0.1195	Treatment: F(2,44)=3.578 Driving current: F(3,132)=196.1 Interaction: F(6,132)=1.727
3.8E	Untreated n/N = 15/7 100 pM PGE2 n/N = 16/6 +EP1 antag n/N = 12/3 +EP2 antag n/N = 12/4 +EP3 antag n/N = 14/4 +EP4 antag n/N = 14/3 +EP2 agonist n/N = 15/3	1way ANOVA	<0.0001	F(6,91)=7.274
3.8F	Untreated n/N = 15/6 100 pM PGE2 n/N = 16/6 +EP2 antag n/N = 12/4	2way RM ANOVA	Treatment: 0.0004 Driving current: <0.0001 Interaction: 0.4580	Treatment: F(2,40)=9.479 Driving current: F(1,411,56.45)=393.7 Interaction: F(6,120)=0.9562

Figure 3.9

3.9A (left)	Chow untreated n/N = 37/13 +COX inhib n/N = 22/9	Two-tailed unpaired t-test	0.1800	t=1.357; df=57
3.9A (right)	WD untreated n/N = 27/8 +COX inhib n/N = 25/7 +COX1 inhib n/N = 18/4 +COX2 inhib n/N = 18/6	1way ANOVA	<0.0001	F(3,87)=9.142
3.9B (left)	Chow untreated n/N= 15/6 +EP2 antag n/N = 13/4	Two-tailed unpaired t-test	0.1312	t=1.559; df=26
3.9B (right)	WD untreated n/N = 26/10 +EP1/3/4 antag n/N = 9/4 +EP2 antag n/N = 13/4	1way ANOVA	0.0351	F(2,45)=3.612
3.9D	Chow untreated n/N = 9/4 +COX inhib n/N = 9/8 WD untreated n/N = 9/6 +COX inhib n/N = 9/7	2way ANOVA	Diet: <0.0001 COX inhibitor: 0.0091 Interaction: 0.0025	Diet: F(1,32)=31.72 COX inhibitor: F(1,32)=7.705 Interaction: F(1,32)=10.73
3.9F	Chow untreated n/N = 9/4 +PGE2 n/N = 9/8 WD untreated n/N = 9/7 +PGE2 n/N = 9/6	2way ANOVA	Diet: 0.0591 PGE2: 0.0660 Interaction: 0.0002	Diet: F(1,32)=3.830 PGE2: F(1,32)=3.623 Interaction: F(1,32)=17.76

Figure 3.10

3.10A	Chow untreated n/N = 15/6 WD untreated n/N = 19/10 Chow + INDO n/N = 11/2 WD + INDO n/N = 16/3	2way ANOVA	Diet: 0.0002 Treatment: 0.0029 Interaction: 0.6508	Diet: F(1,58)=15.56 Treatment: F(1,58)=9.663 Interaction: F(1,58)=0.2071
3.10B	WD n/N = 25/6 WD+H89 n/N = 24/7	Two-tailed unpaired t-test	0.0095	t=2.703; df=47

Figure 3.11

3.11A	WT untreated n/N = 10/3 WT+But n/N = 13/3 KO untreated n/N = 7/3 KO+But n/N = 10/3	2way ANOVA	Genotype: 0.1698 Drug: 0.0074 Interaction: 0.0036	Genotype: F(1,36)=1.963 Drug: F(1,36)=8.065 Interaction: F(1,36)=9.719
3.11B		2way RM ANOVA	Group: <0.0001 Driving current: <0.0001 Interaction: <0.0001	Group: F(3,36)=35.27 Driving current: F(3,108)=35.27 Interaction: F(9,108)=20.36

Figure 3.12

3.12B	Ctrl n/N = 8/4 But n/N = 8/3	Two-tailed unpaired t-test	0.2934	t=1.092; df=14
3.12C		2way RM ANOVA	Treatment: 0.6065	Treatment: F(1,14)=0.2776

			Driving current: 0.4033 Interaction: 0.0180	Driving current: F(1.746, 24.44)=0.9102 Interaction: F(3, 42)=3.745
Figure 3.13				
3.13B	f/f chow n/N = 19/4 f/f WD n/N = 21/4 KO chow n/N = 20/3 KO WD n/N = 22/3 f/f chow n/N = 19/4 f/f WD n/N = 21/4 KO chow n/N = 19/3 KO WD n/N = 22/3	2way ANOVA	Genotype: 0.0013 Diet: 0.3405 Interaction: 0.0011	Genotype: F(1, 78)=11.08 Diet: F(1, 78)=0.9196 Interaction: F(1, 78)=11.58
3.13C		2way RM ANOVA	Group: 0.0630 Driving current: <0.0001 Interaction: 0.0488	Group: F(3, 77)=2.535 Driving current: F(1.246, 95.97)=87.66 Interaction: F(9, 231)=1.930
3.13D	f/f N = 19 KO N = 21	Two-tailed unpaired t-test	0.1067	T=1.652; df=38
3.13E	f/f chow N = 11 f/f WD N = 8 KO chow N = 9 KO WD N = 12	2way RM ANOVA	Group: <0.0001 Time: <0.0001 Interaction: <0.0001	Group: F(3, 36)=29.70 Time: F(13, 468)=465.3 Interaction: F(39, 468)=26.73
3.13F	f/f chow N = 10	2way RM ANOVA	Group: 0.0445	Group: F(3, 26)=3.091

	f/f WD N = 7 KO chow N = 4 KO WD N = 9		Time: <0.0001 Interaction: <0.0001	Time: F(12, 312)=4154 Interaction: F(36, 312)=4.277
3.13G		2way ANOVA	Genotype: 0.1303 Diet:<0.0001 Interaction: 0.4993	Genotype: F(1,26)=2.440 Diet: F(1,26)=72.93 Interaction: F(1,26)=0.4694
3.13H	f/f chow N = 10 f/f WD N = 7 KO chow N = 9 KO WD N = 9	2way ANOVA	Genotype: 0.0068 Diet: <0.0001 Interaction: 0.0097	Genotype: F(1, 31)=8.424 Diet: F(1, 31)=52.63 Interaction: F(1, 31)=7.587
3.13J	f/f N = 7 KO N = 3	2way RM ANOVA	Genotype: 0.0207 Adipocyte area: <0.0001 Interaction: <0.0001	Genotype: F(1,8)=8.25 Adipocyte area: F(1.412,11.37)=459.9 Interaction: F(20,160)=8.964
3.13K		Two-tailed unpaired t- test	0.0206	t=2.877, df=8
3.13L	f/f chow N = 9 f/f WD N = 7 KO chow N = 9 KO WD N = 9	2way ANOVA	Genotype: 0.0098 Diet: 0.0017 Interaction: 0.0323	Genotype: F(1, 30)=7.598 Diet: F(1, 30)=11.85 Interaction: F(1, 30)=5.042
3.13N	f/f N = 7 KO N = 3	2way RM ANOVA	Genotype: 0.0891 Lipid droplet size: <0.0001 Interaction: <0.0001	Genotype: F(1,8)=3.744 Lipid droplet size: F(99,792)=133.1 Interaction: (99,792)=4.846
3.13O		Two-tailed unpaired t- test	0.0228	t=2.810, df=8

Figure 3.14

3.14A	f/f chow N = 10 f/f WD N = 7 KO chow N = 9 KO WD N = 9	2way ANOVA	Genotype: 0.0775 Diet: <0.0001 Interaction: 0.0488	Genotype: F(1, 31)=3.333 Diet: F(1, 31)=49.36 Interaction F(1, 31)=4.206
3.14B	f/f chow N = 10 f/f WD N = 7 KO chow N = 9 KO WD N = 9	2way ANOVA	Genotype: 0.0016 Diet: <0.0001 Interaction: 0.0055	Genotype: F(1, 31)=11.94 Diet: F(1, 31)=30.93 Interaction: F(1, 31)=8.904
3.14C	f/f chow N = 10 f/f WD N = 7 KO chow N = 9 KO WD N = 9	2way ANOVA	Genotype: 0.0012 Diet: <0.0001 Interaction: 0.0117	Genotype: F(1, 31)=12.77 Diet: F(1, 31)=37.86 Interaction: F(1, 31)=7.171
3.14D	f/f chow N = 10 f/f WD N = 7 KO chow N = 8 KO WD N = 9	2way ANOVA	Genotype: 0.9549 Diet: <0.0001 Interaction: 0.3417	Genotype: F(1, 30)=0.003255 Diet: F(1, 30)=22.56 Interaction F(1, 30)=0.9333
3.14E	f/f chow N = 9 f/f WD N = 7 KO chow N = 8 KO WD N = 9	2way ANOVA	Genotype: 0.8089 Diet: 0.2076 Interaction: 0.1445	Genotype: F(1, 29)=0.05960 Diet: F(1, 29)=1.661 Interaction: F(1, 29)=2.249
3.14F	f/f chow N = 9 f/f WD N = 7 KO chow N = 9 KO WD N = 8	2way ANOVA	Genotype: 0.9908 Diet: 0.1598 Interaction: 0.6385	Genotype: F(1, 29)=0.0001348 Diet: F(1, 29)=2.081 Interaction: F(1, 29)=0.2254
3.14G	f/f chow N = 10 f/f WD N = 7 KO chow N = 9 KO WD N = 9	2way ANOVA	Genotype: 0.3614 Diet: 0.1717 Interaction: 0.3105	Genotype: F(1, 31)=0.8582 Diet: F(1, 31)=1.958 Interaction: F(1, 31)=1.063
3.14H	f/f chow N = 10 f/f WD N = 7	2way ANOVA	Genotype: 0.0632 Diet: 0.0746	Genotype: F(1, 31)=3.712 Diet: F(1, 31)=3.404

	KO chow N = 9 KO WD N = 9		Interaction: 0.0166	Interaction: F(1, 31)=6.417
Figure 3.15				
3.15B	f/f chow n/N = 22/7 f/f WD n/N = 20/4 KO chow n/N = 24/3 KO WD n/N = 22/5	2way ANOVA	Genotype: 0.5648 Diet: 0.0277 Interaction: 0.9747	Genotype: F(1, 84)=0.3341 Diet: F(1, 84)=5.023 Interaction: F(1, 84)=0.001011
3.15C		2way RM ANOVA	Group: 0.5605 Driving current: <0.0001 Interaction: 0.7790	Group: F(3, 84)=0.6903 Driving current: F(3, 252)=60.88 Interaction: F(9, 252)=0.6207
3.15D	f/f N = 17 KO N = 15	Two-tailed unpaired t-test	0.8059	t=0.2480; df=30
3.15E	f/f chow N = 7 f/f WD N = 10 KO chow N = 6 KO WD N = 9	2way RM ANOVA	Group: 0.0068 Time: <0.0001 Interaction: <0.0001	Group: F(3, 28)=4.987 Time: F(11, 308)=125.7 Interaction: F(33, 308)=3.948
3.15F	f/f chow N = 6 f/f WD N = 9 KO chow N = 5 KO WD N = 5	2way RM ANOVA	Group: 0.9928 Time: <0.0001 Interaction: 0.6829	Group: F(3, 21)=0.02990 Time: F(12, 252)=608.6 Interaction: F(36, 252)=0.8706
3.15G		2way ANOVA	Genotype: 0.6828 Diet: 0.0025	Genotype: F(1,21)=0.1717 Diet: F(1,21)=11.75

			Interaction: 0.3652	Interaction: F(1,21)=0.8566
3.15H	f/f chow N = 8 f/f WD N = 8 KO chow N = 4 KO WD N = 8	2way ANOVA	Genotype: 0.2229 Diet: 0.0041 Interaction: 0.5405	Genotype: F(1, 24)=1.566 Diet: F(1, 24)=10.09 Interaction: F(1, 24)=0.3855
3.15J	f/f N = 3 KO N = 3	2way RM ANOVA	Genotype: 0.6278 Adipocyte area: <0.0001 Interaction: 0.9873	Genotype: F(1,4)=0.2749 Adipocyte area: F(39, 156)=45.45 Interaction: F(39, 156)=0.5382
3.15K		Two-tailed unpaired t-test	0.6337	t=0.5150, df=4
3.15L	f/f chow N = 8 f/f WD N = 8 KO chow N = 4 KO WD N = 8	2way ANOVA	Genotype: 0.2602 Diet: 0.0025 Interaction: 0.3154	Genotype: F(1, 24)=1.330 Diet: F(1, 24)=11.43 Interaction: F(1, 24)=1.051
3.15N	f/f N = 3 KO N = 3	2way RM ANOVA	Genotype: 0.0494 Lipid droplet size: <0.0001 Interaction: <0.0001	Genotype: F(1,4)=7.771 Lipid droplet size: F(178, 712)=62.09 Interaction: (178, 712)=3.239
3.15O		Two-tailed unpaired t-test	0.4494	t=0.8376, df=4

Figure 3.16

3.16A	f/f chow N = 8 f/f WD N = 8 KO chow N = 4 KO WD N = 8	2way ANOVA	Genotype: 0.4218 Diet: 0.0096 Interaction: 0.8002	Genotype: F(1, 24)=0.6679 Diet: F(1, 24)=7.931 Interaction: F(1, 24)=0.06547
3.16B	f/f chow N = 8 f/f WD N = 8 KO chow N = 4	2way ANOVA	Genotype: 0.2839 Diet: 0.0069	Genotype: F(1, 24)=1.201 Diet: F(1, 24)=8.717

	KO WD N = 8		Interaction: 0.5937	Interaction: F(1, 24)=0.2924
3.16C	f/f chow N = 8 f/f WD N = 8 KO chow N = 4 KO WD N = 8	2way ANOVA	Genotype: 0.0887 Diet: 0.0016 Interaction: 0.2896	Genotype: F(1, 24)=3.147 Diet: F(1, 24)=12.63 Interaction: F(1, 24)=1.173
3.16D	f/f chow N = 7 f/f WD N = 8 KO chow N = 4 KO WD N = 8	2way ANOVA	Genotype: 0.4153 Diet: 0.0069 Interaction: 0.8687	Genotype: F(1, 23)=0.6882 Diet: F(1, 23)=8.787 Interaction: F(1, 23)=0.02795
3.16E	f/f chow N = 8 f/f WD N = 8 KO chow N = 4 KO WD N = 8	2way ANOVA	Genotype: 0.4795 Diet: 0.1154 Interaction: 0.6103	Genotype: F(1, 24)=0.5160 Diet: F(1, 24)=2.668 Interaction: F(1, 24)=0.2667
3.16F	f/f chow N = 8 f/f WD N = 8 KO chow N = 4 KO WD N = 8	2way ANOVA	Genotype: 0.1850 Diet: 0.6445 Interaction: 0.5908	Genotype: F(1, 24)=1.862 Diet: F(1, 24)=0.2183 Interaction: F(1, 24)=0.2970
3.16G	f/f chow N = 8 f/f WD N = 8 KO chow N = 4 KO WD N = 8	2way ANOVA	Genotype: 0.9465 Diet: 0.7303 Interaction: 0.6057	Genotype: F(1, 24)=0.004599 Diet: F(1, 24)=0.1216 Interaction: F(1, 24)=0.2737
3.16H	f/f chow N = 8 f/f WD N = 8 KO chow N = 4 KO WD N = 8	2way ANOVA	Genotype: 0.2151 Diet: 0.4496 Interaction: 0.8235	Genotype: F(1, 24)=1.622 Diet: F(1, 24)=0.5908 Interaction: F(1, 24)=0.05088

7.3. Ethics clearance

Your Annual Report has been approved

Subject: Your Annual Report has been approved
From: ambakwe@mun.ca
Date: 5/11/2023, 1:22 PM
To: "Hirasawa Michiru(Principal Investigator)" <michiru@mun.ca>
CC: ambakwe@mun.ca



Dear: Dr. Michiru Hirasawa, Faculty of Medicine\Division of BioMedical Sciences

Researcher Portal File No.: 20211649
Animal Care File: 18-02-MH
Entitled: (18-02-MH) Effect of diet on the hypothalamic function
Related Awards:

Awards File No	Title	Status	
20171018	Mechanism for high fat diet-induced activation of MCH neurons and its role in obesity	Active	1. Research Initiatives & Services (RIS) – St. John's and Grenfell Campuses
20192001	Prostaglandin-E2-mediated activation of melanin-concentrating hormone neurons in diet-induced obesity	Active	1. Research Initiatives & Services (RIS) – St. John's and Grenfell Campuses
20192507	Material Transfer Agreement	Active	1. Research Initiatives & Services (RIS) – St. John's and Grenfell Campuses

Approval Date: May 01, 2021
Next Annual Report Due: May 01, 2024
Ethics Clearance Expires: May 01, 2024

Your Annual Report was reviewed by the ACC and approved.

Animal use records will be compiled and reported to the Canadian Council on Animal Care.

NOTE: You can access a copy of this email at any time under the "Shared Communications" section of the Logs tab of your file in the [Memorial Researcher Portal](#).

Please note that approval of the protocol or amendment does not guarantee space for animal housing or procedures. Coordination with Animal Care & Veterinary Resources is required prior to ordering animals.

Your Annual Report has been approved

Sincerely,

ANULIKA MBAKWE


ACC Coordinator | Department of Animal Care & Veterinary Resources (ACVR)

Animal Resource Centre (ARC) | Room H-1A100 |


Memorial University of Newfoundland | Research

T: 709-864-3763 | ambakwe@mun.ca | www.mun.ca/acs

7.4. Copyright permissions



[Home](#)
[Help](#)
[Live Chat](#)
[Lisa Fang](#)



High-fat diet-induced elevation of body weight set point in male mice

Author: Michiru Hirasawa, Oishi Hawlader, Josué A. Lily Vidal, et al

Publication: Obesity

Publisher: John Wiley and Sons

Date: Feb 21, 2023

© 2023 The Obesity Society.

Order Completed

Thank you for your order.

This Agreement between Memorial University of Newfoundland – Lisa Fang (“You”) and John Wiley and Sons (“John Wiley and Sons”) consists of your license details and the terms and conditions provided by John Wiley and Sons and Copyright Clearance Center.

Your confirmation email will contain your order number for future reference.

License Number	5563350491572
License date	Jun 06, 2023

[Printable Details](#)

Licensed Content

Licensed Content Publisher	John Wiley and Sons
Licensed Content Publication	Obesity
Licensed Content Title	High-fat diet-induced elevation of body weight set point in male mice
Licensed Content Author	Michiru Hirasawa, Oishi Hawlader, Josué A. Lily Vidal, et al
Licensed Content Date	Feb 21, 2023
Licensed Content Volume	31
Licensed Content Issue	4
Licensed Content Pages	11

Order Details

Type of use	Dissertation/Thesis
Requestor type	Author of this Wiley article
Format	Print and electronic
Portion	Full article
Will you be translating?	No

About Your Work

Title	Adaptations in physiological and neuronal function during diet-induced obesity
Institution name	Memorial University of Newfoundland
Expected presentation date	Aug 2023

Additional Data

Requestor Location

Requestor Location	Memorial University of Newfoundland 300 Prince Philip Drive Room H4334 Memorial University St. John's, NL A1B 3X6 Canada Attn: Memorial University of Newfoundland
--------------------	--

Tax Details

Publisher Tax ID	EU826007151
------------------	-------------

Price

Total	0.00 CAD
-------	----------

Would you like to purchase the full text of this article? If so, please continue on to the content ordering system located here: [Purchase PDF](#)
If you click on the buttons below or close this window, you will not be able to return to the content ordering system.

CLOSE WINDOW

Total: 0.00 CAD

ORDER MORE

© 2023 Copyright - All Rights Reserved | Copyright Clearance Center, Inc. | Privacy statement | Data Security and Privacy | For California Residents | Terms and Conditions
Comments? We would like to hear from you. E-mail us at customer-care@copyright.com

PNAS authors do not need to obtain permission in the following cases:

1. to use their original figures or tables in their future works;
2. to make copies of their articles for their own personal use, including classroom use, or for the personal use of colleagues, provided those copies are not for sale and are not distributed in a systematic way;
3. to include their articles as part of their dissertations; or
4. to use all or part of their articles in printed compilations of their own works.

The full journal reference must be cited and, for articles published in volumes 90–105 (1993–2008), "Copyright (copyright year) National Academy of Sciences" must be included as a copyright note.



High-fat diet induces time-dependent synaptic plasticity of the lateral hypothalamus

Author: Victoria Linehan, Lisa Z. Fang, Matthew P. Parsons, Michiru Hirasawa

Publication: Molecular Metabolism

Publisher: Elsevier

Date: June 2020

© 2020 The Authors. Published by Elsevier GmbH.

Journal Author Rights

Please note that, as the author of this Elsevier article, you retain the right to include it in a thesis or dissertation, provided it is not published commercially. Permission is not required, but please ensure that you reference the journal as the original source. For more information on this and on your other retained rights, please visit: <https://www.elsevier.com/about/our-business/policies/copyright#Author-rights>

BACK

CLOSE WINDOW

7.5. Diet composition information

Product Data

DIO SERIES DIETS



The "Original" High Fat Diets for Diet Induced Obesity

Formulas

Product #	D12450B		D12451		D12492	
	gm%	kcal%	gm%	kcal%	gm%	kcal%
Protein	19.2	20	24	20	26.2	20
Carbohydrate	67.3	70	41	35	26.3	20
Fat	4.3	10	24	45	34.9	60
Total		100		100		100
	kcal/gm	3.85	4.73	100	5.24	100
Ingredient	gm	kcal	gm	kcal	gm	kcal
Casein, 80 Mesh	200	800	200	800	200	800
L-Cystine	3	12	3	12	3	12
Corn Starch	315	1260	72.8	291	0	0
Maltodextrin 10	35	140	100	400	125	500
Sucrose	350	1400	172.8	691	68.8	275.2
Cellulose, BW200	50	0	50	0	50	0
Soybean Oil	25	225	25	225	25	225
Lard*	20	180	177.5	1598	245	2205
Mineral Mix S10026	10	0	10	0	10	0
DiCalcium Phosphate	13	0	13	0	13	0
Calcium Carbonate	5.5	0	5.5	0	5.5	0
Potassium Citrate, 1 H2O	16.5	0	16.5	0	16.5	0
Vitamin Mix V10001	10	40	10	40	10	40
Choline Bitartrate	2	0	2	0	2	0
FD&C Yellow Dye #5	0.05	0				
FD&C Red Dye #40			0.05	0		
FD&C Blue Dye #1					0.05	0
Total	1055.05	4057	858.15	4057	773.85	4057

Formulated by E. A. Ulman, Ph.D., Research Diets, Inc., 8/26/98 and 3/1 1/99.

*Typical analysis of cholesterol in lard = 0.95 mg/gram. D12450B -

Cholesterol (mg)/4057 kcal = 19
Cholesterol (mg)/kg = 18

D12451 -
Cholesterol (mg)/4057 kcal = 168.6

Cholesterol (mg)/kg = 196.5

D12492 -
Cholesterol (mg)/4057 kcal = 232.8

Cholesterol (mg)/kg = 300.8



Research Diets, Inc.
20 Jules Lane
New Brunswick, NJ 08901
Tel: 732.247.2390
Fax: 732.247.2340
info@researchdiets.com

Copyright © 2006 Research Diets, Inc. All rights reserved. DIO-1500



Rodent Diets with 25 or 45 kcal% Fat (from Mostly Lard)

Formulated by:
Research Diets, Inc.
July 2011

Product #	D11071701		D12451	
	25 kcal% Fat		45 kcal% Fat	
	gm (%)	kcal (%)	gm (%)	kcal (%)
Protein	21	20	24	20
Carbohydrate	57	55	41	35
Fat	12	25	24	45
Total		100		100
kcal/gm	4.19		4.73	
Ingredient	gm	kcal	gm	kcal
Casein, 80 Mesh	200	800	200	800
L-Cystine	3	12	3	12
Corn Starch	272.0	1088	72.8	291
Maltodextrin 10	100.0	400	100.0	400
Sucrose	172.8	691	172.8	691
Cellulose, BW200	50	0	50	0
Soybean Oil	25	225	25	225
Lard	89	801	177.5	1598
Mineral Mix S10026	10.0	0	10.0	0
DiCalcium Phosphate	13.0	0	13.0	0
Calcium Carbonate	5.5	0	5.5	0
Potassium Citrate, 1 H2O	16.5	0	16.5	0
Vitamin Mix V10001	10	40	10	40
Choline Bitartrate	2	0	2	0
FD&C Yellow Dye #5	0.025	0	0	0
FD&C Red Dye #40	0.025	0	0.05	0
FD&C Blue Dye #1	0	0	0	0
Total	968.850	4057	858.150	4057

Research Diets, Inc.
20 Jules Lane
New Brunswick, NJ 08901 USA
info@researchdiets.com

NystromC01.for.xls





Product Data - D12079B

Report ▶ Repeat ▶ Revise

Description

RD Western Diet

Used in Research

Obesity
Diabetes
Osteoporosis
Hypertension
Atherosclerosis
Metabolic Syndrome

Packaging

Product is packed in 12.5 kg box.
Each box is identified with the product name, description, lot number and expiration date.

Lead Time

5-7 business days.

Gamma-Irradiation

Yes. Add 10 days to delivery time.

Form

Pellet, Powder, Liquid

Shelf Life

Most diets require storage in a cool dry environment. Stored correctly they should last 6 months.

Control Diets

Custom diets available on request.

Formula

Product # D12079B	gm%	kcal%
Protein	20	17
Carbohydrate	50	43
Fat	21	41
Total kcal/gm	4.7	100

Ingredient	gm	kcal
Casein, 80 Mesh	195	780
DL-Methionine	3	12
Corn Starch	50	200
Maltodextrin 10	100	400
Sucrose	341	1364
Cellulose	50	0
Milk Fat, Anhydrous*	200	1800
Corn Oil	10	90
Mineral Mix S10001	35	0
Calcium Carbonate	4	0
Vitamin Mix V10001	10	40
Choline Bitartrate	2	0
Cholesterol, USP*	1.5	0
Ethoxyquin	0.04	0
Total	1001.54	4686

*Anhydrous milk fat typically contains approximately 0.3% cholesterol.

On this basis, D12079B contains approximately 0.21% cholesterol.

Formulated by E. A. Ulman, Ph.D., Research Diets, Inc., October 12, 1995.

Diet formulated to match Teklad Western Diet #TD88137, except that 1% Corn Oil replaces 1% Butter Fat.



Where NutriPhenomics Begins



Prolab® RMH 3000

5P00*

DESCRIPTION

Prolab® Rat/Mouse/Hamster 3000 is formulated primarily for growth and reproduction in Lab Rats. This diet is formulated using managed formulation, delivering Constant Nutrition®. This is paired with the selection of highest quality ingredients to assure minimal inherent biological variation in long-term studies.

Features and Benefits

- [Managed Formulation delivers Constant Nutrition®](#)
- High quality animal protein added to create a superior balance of amino acids for optimum performance
- Supports optimum growth and efficient reproduction performance of rats, hamsters and mice
- Formulated to feed rats, hamsters and many mouse strains

Product Forms Available

- Oval pellet, 3/8" x 5/8" x 1" Catalog # 0001495

Other Versions Available

- 5P75 Prolab® IsoPro® RMH 3000, Catalog # 0006972
Vacuum Packaged 6.5# Boxes
- 5P76 Prolab® IsoPro® RMH 3000, 25 lb 0006973

GUARANTEED ANALYSIS

Crude protein not less than	22.00%
Crude fat not less than	5.00%
Crude fiber not more than	5.00%
Moisture not more than	9.00%
Ash not more than	12.00%

INGREDIENTS

Whole wheat, dehulled soybean meal, wheat middlings, ground corn, fish meal, porcine animal fat preserved with BHA and citric acid, dehydrated alfalfa meal, calcium carbonate, soybean oil, brewers dried yeast, dicalcium phosphate, salt, DL-methionine, L-lysine, choline chloride, menadione dimethylpyrimidinol bisulfite (source of Vitamin K), magnesium oxide, ferrous sulfate, pyridoxine hydrochloride, cholecalciferol, vitamin A acetate, biotin, dl-alpha tocopheryl acetate (form of Vitamin E), vitamin B12 supplement, riboflavin supplement, thiamine mononitrate, zinc oxide, calcium pantothenate, folic acid, nicotinic acid, manganous oxide, ferrous carbonate, copper sulfate, zinc sulfate, calcium iodate, cobalt carbonate, sodium selenite.

FEEDING DIRECTIONS

Feed ad libitum to rodents. Plenty of fresh, clean water should be available to the animals at all times.

Rats- All rats will eat varying amounts of feed depending on their genetic origin. Larger strains will eat up to 30 grams per day. Smaller strains will eat up to 15 grams per day. Feeders in rat cages should be designed to hold two to three days supply of feed at one time.

Mice- Adult mice will eat up to 5 grams of pelleted ration daily. Some of the larger strains may eat as much as 8 grams per day per animal. Feed should be available on a free choice basis in wire feeders above the floor of the cage.

Hamsters- Adults will eat up to 14 grams per day.

For information regarding shelf life please visit www.labdiet.com.

CHEMICAL COMPOSITION¹

Nutrients²

Protein, %	22.5
Arginine, %	1.40
Cystine, %	0.40
Glycine, %	1.10
Histidine, %	0.56
Isoleucine, %	0.89
Leucine, %	1.64
Lysine, %	1.29
Methionine, %	0.58
Phenylalanine, %	1.00
Tyrosine, %	0.64
Threonine, %	0.81
Tryptophan, %	0.28
Valine, %	1.03
Serine, %	1.10
Aspartic Acid, %	2.27
Glutamic Acid, %	5.00
Alanine, %	1.19
Proline, %	1.48
Taurine, %	0.03
Fat (ether extract), %	5.5
Fat (acid hydrolysis), %	6.9
Cholesterol, ppm	193
Linoleic Acid, %	1.65
Linolenic Acid, %	0.19
Arachidonic Acid, %	0.02
Omega-3 Fatty Acids, %	0.38
Total Saturated Fatty Acids, %	1.55
Total Monounsaturated Fatty Acids, %	1.63
Fiber (Crude), %	4.2
Neutral Detergent Fiber ³ , %	15.6
Acid Detergent Fiber ⁴ , %	5.2
Nitrogen-Free Extract (by difference), %	51.4
Starch, %	31.3
Sucrose, %	1.41
Total Digestible Nutrients, %	77.4
Gross Energy, kcal/gm	4.18
Physiological Fuel Value⁵, kcal/gm	3.45
Metabolizable Energy, kcal/gm	3.14
Minerals	
Ash, %	6.4
Calcium, %	1.09
Phosphorus, %	0.79
Phosphorus (non-phytate), %	0.47
Potassium, %	0.94
Magnesium, %	0.24
Sulfur, %	0.29
Sodium, %	0.23
Chloride, %	0.40
Fluorine, ppm	17

Iron, ppm	360
Zinc, ppm	120
Manganese, ppm	97
Copper, ppm	14
Cobalt, ppm	0.41
Iodine, ppm	0.99
Chromium (added), ppm	0.01
Selenium, ppm	0.41

Vitamins

Carotene, ppm	1.2
Vitamin K, ppm	1.9
Thiamin, ppm	9.8
Riboflavin, ppm	14
Niacin, ppm	60
Pantothenic Acid, ppm	13
Choline Chloride, ppm	2000
Folic Acid, ppm	1.2
Pyridoxine, ppm	8.3
Biotin, ppm	0.40
B ₁₂ , mcg/kg	77
Vitamin A, IU/gm	18
Vitamin D ₃ (added), IU/gm	2.5
Vitamin E, IU/kg	75
Ascorbic Acid, mg/gm	0.0

Calories provided by:

Protein, %	26.073
Fat (ether extract), %	14.341
Carbohydrates, %	59.586

*Product Code

1. Formulation based on calculated values from the latest ingredient analysis information. Since nutrient composition of natural ingredients varies and some nutrient loss will occur due to manufacturing processes, analysis will differ accordingly.

2. Nutrients expressed as percent of ration except where otherwise indicated. Moisture content is assumed to be 10.0% for the purpose of calculations.

3. NDF = approximately cellulose, hemicellulose and lignin.

4. ADF = approximately cellulose and lignin.

5. Physiological Fuel Value (kcal/gm) = Sum of decimal fractions of protein, fat and carbohydrate (use Nitrogen Free Extract) x 4,9,4 kcal/gm respectively.

NOTE: When assayed, actual levels may vary from calculated values.

LabDiet®
www.labdiet.com